Nuclear Power Plant Fire Modeling Application Guide (NPP FIRE MAG)

Second Draft Report for Comment

U.S.NRC

United States Nuclear Regulatory Commission

Protecting People and the Environment

EPRI | ELECTRIC POWER
RESEARCH INSTITUTE

AVAILABILITY OF REFERENCE MATERIALS
IN NRC PUBLICATIONS

NRC Reference Material

As of November 1999, you may electronically access NUREG-series publications and other NRC records at the NRC's Public Electronic Reading Room at http://www.nrc.gov/reading-rm.html. Public records include NUREG-series publications; *Federal Register* notices; applicant, licensee, and vendor documents and correspondence; NRC correspondence and internal memoranda; bulletins and information notices; inspection and investigative reports; licensee event reports; and Commission papers and their attachments.

NRC publications in the NUREG series, NRC regulations, and *Title 10, Energy* in the Code of *Federal Regulations* may also be purchased from one of these two sources:
1. The Superintendent of Documents
   U.S. Government Printing Office
   Mail Stop SSOP
   Washington, DC 20402-0001
   Internet: bookstore.gpo.gov
   Telephone: 202-512-1800
   Fax: 202-512-2250
2. The National Technical Information Service
   Springfield, VA 22161-0002
   www.ntis.gov
   1-800-553-6847 or, locally, 703-605-6000

A single copy of each NRC draft report for comment is available free, to the extent of supply, upon written request as follows:
Address: Office of the Chief Information Officer,
            Reproduction and Distribution
              Services Section
            U.S. Nuclear Regulatory Commission
            Washington, DC 20555-0001
E-mail: DISTRIBUTION@nrc.gov
Facsimile: 301-415-2289

Some of the NUREG-series publications posted under http://www.nrc.gov/reading-rm/doc-collections/nuregs are updated periodically and may differ from the last printed version. Although references to material found on a website bear the date the material was accessed, the material available on the date cited may subsequently be removed from the site.

Non-NRC Reference Material

Documents available from public and special technical libraries include all open literature items, such as books, journal articles, and transactions, *Federal Register* notices, Federal and State legislation, and congressional reports. Such documents as theses, dissertations, foreign reports and translations, and non-NRC conference proceedings may be purchased from their sponsoring organization.

Copies of industry codes and standards used in a substantive manner in the NRC regulatory process are maintained at:

> The NRC Technical Library
> Two White Flint North
> 11545 Rockville Pike
> Rockville, MD 20852-2738

These standards are available for reference by the public. Codes and standards are usually copyrighted and may be purchased from their originating organization, or, if they are American National Standards, from:

> American National Standards Institute
> 11 West 42nd Street
> New York, NY 10036-8002
> www.ansi.org
> 212-642-4900

Legally binding regulatory requirements are stated only in laws; NRC regulations; licenses, including technical specifications; or orders, not in NUREG-series publications. The views expressed in contractor-prepared publications in this series are not necessarily those of the NRC.

The NUREG series comprises (1) technical and administrative reports and books prepared by the staff (NUREG-XXXX) or agency contractors (NUREG/CR-XXXX), (2) proceedings of conferences (NUREG/CP-XXXX), (3) reports resulting from international agreements (NUREG/IA-XXXX), (4) brochures (NUREG/BR-XXXX), and (5) compilations of legal decisions and orders of the Commission and Atomic and Safety Licensing Boards and of Directors' decisions under Section 2.206 of the NRC's regulations (NUREG-0750).

Nuclear Power Plant Fire Modeling Application Guide

NUREG-1934   EPRI 1023259

Second Draft Report for Comment

July 2011

U.S. Nuclear Regulatory Commission   Electric Power Research Institute (EPRI)
Office of Nuclear Regulatory Research (RES) 3412 Hillview Avenue
Washington, DC 20555-0001   Palo Alto, CA 94303

U.S. NRC-RES Project Manager   EPRI Project Manager
M.H. Salley   R. Wachowiak

COMMENTS ON DRAFT REPORT

Any interested party may submit comments on this report for consideration by NRC staff. Comments may be accompanied by additional relevant information or supporting data. Please specify the report number "NUREG-1934, draft" in your comments and send them to the following address by August 31, 2011:

Chief, Rulemaking and Directives Branch
U.S. Nuclear Regulatory Commission
Mail Stop TWB-05-B01
Washington, DC 20555-0001

Comments may be submitted electronically using the NRC's website:
http://www.nrc.gov//public-involve/doc-comment/form.html

For any questions about the material in this report, please contact:

David Stroup
CSB-4C07M
U.S. Nuclear Regulatory Commission
Washington, DC 20555-0001
Phone: 301-251-7609
E-mail: david.stroup@nrc.gov

ORDERING INFORMATION

Requests for copies of this report should be directed to EPRI Orders and Conferences, 1355 Willow Way, Suite 278, Concord, CA 94520, (800) 313-3774, press 2 or internally x5379, (925) 609-9169, (925) 609-1310 (fax).

Electric Power Research Institute, EPRI, and TOGETHER...SHAPING THE FUTURE OF ELECTRICITY are registered service marks of the Electric Power Research Institute, Inc.

CITATIONS

This report was prepared by:

U.S. Nuclear Regulatory Commission,
Office of Nuclear Regulatory Research (RES)
Washington, DC 20555-0001

Principal Investigator:
D. Stroup

National Institute of Standards and
Technology
Building Fire Research Laboratory (BFRL)
100 Bureau Drive, Stop 8600
Gaithersburg, MD 20899-8600

Principal Investigators:
K. McGrattan
R. Peacock

University of Maryland

Principle Investigator:
J. Milke

Electric Power Research Institute (EPRI)
3412 Hillview Avenue
Palo Alto, CA 94303

Principal Investigator:
R. Wachowiak

Science Applications International Corp (SAIC)
1671 Dell Ave, Suite 100
Campbell, CA 95008

Principal Investigators:
F. Joglar
D. Birk
B. Najafi

Hughes Associates, Inc.

Principal Investigator:
S. Hunt

Westinghouse

Principal Investigator:
C. Worrell

ERIN Engineering

Principal Investigator:
K. Zee

The report is a corporate document that should be cited in the literature in the following manner:

Nuclear Power Plant Fire Modeling Application Guide (NPP FIRE MAG), U.S. Nuclear Regulatory Commission, Office of Nuclear Regulatory Research (RES), Washington, DC, 2010 and Electric Power Research Institute (EPRI), Palo Alto, CA, NUREG-1934 and EPRI 1023259.

ABSTRACT

There is a movement to introduce risk-informed and performance-based (RI/PB) analyses into fire protection engineering practice, both domestically and worldwide. This movement exists in both the general fire protection and the nuclear power plant (NPP) fire protection communities. The U.S. Nuclear Regulatory Commission (NRC) has used risk-informed insights as a part of its regulatory decision making since the 1990s.

In 2001, the National Fire Protection Association (NFPA) issued NFPA 805, *Performance-Based Standard for Fire Protection for Light-Water Reactor Electric Generating Plants, 2001 Edition.* In July 2004, the NRC amended its fire protection requirements in Title 10, Section 50.48 of the *Code of Federal Regulations* (10 CFR 50.48) to permit existing reactor licensees to voluntarily adopt fire protection requirements contained in NFPA 805 as an alternative to the existing deterministic fire protection requirements. In addition, the NPP fire protection community has been using RI/PB approaches and insights to support fire protection decision making in general.

One key element in RI/PB fire protection is the availability of verified and validated (V&V) fire models that can reliably estimate the effects of fires. The U.S. NRC, together with the Electric Power Research Institute (EPRI) and the National Institute of Standards and Technology (NIST), conducted a research project to verify and validate five fire models that have been used for NPP applications. The results of this effort are documented in a seven-volume NUREG report, NUREG-1824 (EPRI 1011999), *Verification & Validation of Selected Fire Models for Nuclear Power Plant Applications.*

This report describes the implications of the V&V results for fire model users and reviewers. The features and limitations of the five fire models documented in NUREG-1824 are discussed relative to NPP fire hazard. Finally, the report provides information on the use of fire models in support of NFPA 805, NRC fire protection inspection oversight programs, and other commercial NPP applications.

CONTENTS

FIGURES

TABLES

REPORT SUMMARY

Background

Since the 1990s, when the NRC adopted the policy of using risk-informed methods to make regulatory decisions whenever possible, the nuclear power industry has been moving from prescriptive rules and practices toward the use of risk information to supplement decision making. Several initiatives have furthered this transition within the fire protection field, including risk-informed, performance-based fire protection programs (FPPs) compliant with Title 10, Section 50.48(c) of the *Code of Federal Regulations* (10 CFR 50.48(c)) and FPP change evaluation under the existing Title 10 Section 50.48 and Regulatory Guide 1.189. RI/PB fire protection often relies on fire modeling to estimate the effects of fires.

Objectives

- To provide guidance on the application of fire models to NPP hazard
- To provide guidance on fire hazard and risk assessment

Approach

The project team developed fire scenarios of interest in NPPs. The five fire models used in the Verification and Validation (V&V) study (NUREG-1824, EPRI 1011999)—(1) NRC's Fire Dynamics Tools (FDTs), (2) EPRI's Fire-Induced Vulnerability Evaluation Revision 1 (FIVE-Rev1), (3) the National Institute of Standards and Technology's (NIST) Consolidated Model of Fire Growth and Smoke Transport (CFAST), (4) Electricité de France's (EdF) MAGIC, and (5) NIST's Fire Dynamics Simulator (FDS)—were used to develop this report. Finally, the project team developed guidance on the selection and application of each model and treatment of uncertainty and/or sensitivity as part of the fire modeling analysis.

Results

The results of this effort are presented in a step-by-step process for using fire modeling in nuclear power plant applications. The recommended methodology consists of six steps: (1) define fire modeling goals, (2) characterize fire scenarios, (3) select fire models, (4) calculate fire-generated conditions, (5) conduct sensitivity and uncertainty analyses, and (6) document the results.

EPRI Perspective

The use of fire models to support regulatory decision making requires a good understanding of their limitations and predictive capabilities, and also presents challenges that should be addressed if the fire protection community is to realize the full benefit of fire modeling and performance-based fire protection. EPRI, with NRC support, will continue to provide training to the fire protection community, using this document to promote fire modeling and gain feedback on how the results of this work may affect known applications of fire modeling. In the long term, model improvement and additional experiments should be considered.

This report supersedes EPRI 10002981, *Fire Modeling Guide for Nuclear Power Plant Applications*, August 2002, as guidance for fire modeling practitioners in nuclear power plants (NPPs). The report has benefited from the insights gained since 2002 on the predictive capability of selected fire models in improving confidence in the use of fire modeling in NPP decision making.

PREFACE

This report is the fifth in a series designed to assist those responsible for performing and reviewing fire modeling in nuclear power plant applications.

In August 2002, EPRI published EPRI 1002981, *Fire Modeling Guide for Nuclear Power Plant Applications*. This report offered step-by-step guidance that analysts could follow when using fire modeling to support nuclear power plant algebraic models. It also included FIVE Rev 1, an Excel-based library of fire models previously documented by EPRI, and additional models from fire protection literature.

In December 2004, the NRC published NUREG-1805, *Fire Dynamics Tools (FDTs) Quantitative Fire Hazard Analysis Methods for the U.S. Nuclear Regulatory Commission Fire Protection Inspection Program*. This report provided an introduction to the principles of fire dynamics, and included an Excel-based library of fire models comparable to EPRI FIVE Rev 1.

In a follow-up effort as a part of the NRC/RES-EPRI Memorandum of Understanding, NRC/RES and EPRI jointly conducted a verification and validation of selected fire models for use in nuclear power plant fire modeling to gain insight into the predictive capabilities of these models. The results of this work were published in NUREG-1824 (EPRI 1011999), *Verification and Validation of Selected Fire Models for Nuclear Power Plant Applications*, May 2007. Using, in part, the findings of this work, the NRC conducted a Phenomena Identification and Ranking Table (PIRT) study to evaluate the current state of knowledge for fire modeling for NPP applications. The results of this work were published in NUREG/CR-6978, *A Phenomena Identification and Ranking Table (PIRT) Exercise for Nuclear Power Plant Fire Modeling Applications*, November 2008.

ACKNOWLEDGEMENTS

LIST OF ACRONYMS

AGA	American Gas Association
AHJ	Authority Having Jurisdiction
ASET	Advanced Science and Engineering Technologies
ASME	American Society of Mechanical Engineers
ASTM	American Society for Testing and Materials
BE	Benchmark Exercise
BFRL	Building and Fire Research Laboratory
BRE	Building Research Establishment
BWR	Boiling Water Reactor
CAROLFIRE	Cable Response to Live Fire
CDF	Core Damage Frequency
CFAST	Consolidated Fire Growth and Smoke Transport Model
CFD	Computational Fluid Dynamics
CFR	*Code of Federal Regulations*
CHRISTIFIRE	Cable Heat Release, Ignition, and Spread in Tray Installations during Fire
CSR	Cable Spreading Room
ECCS	Emergency Core Cooling Systems
EdF	Electricité de France
EPRI	Electric Power Research Institute
ERFBS	Electrical Raceway Fire Barrier System
FDS	Fire Dynamics Simulator
FDT^s	Fire Dynamics Tools (NUREG-1805)
FHA	Fire Hazard Analysis
FIVE-Rev1	Fire-Induced Vulnerability Evaluation, Revision 1
FFT	Fast Fourier Transform
FM/SNL	Factory Mutual & Sandia National Laboratories
FPA	Foote, Pagni, and Alvares
FPRA	Fire probabilistic risk assessment
FRA	Fire Risk Analysis
GRS	Gesellschaft für Anlagen- und Reaktorsicherheit (Germany)
HGL	Hot Gas Layer
HRR	Heat Release Rate
HRRPUA	Heat release rate per unit area
IAFSS	International Association of Fire Safety Science
iBMB	Institut für Baustoffe, Massivbau und Brandschutz
ICFMP	International Collaborative Fire Model Project
IEEE	Institute of Electrical and Electronics Engineers
IPEEE	Individual Plant Examination of External Events
LERF	Large Early Release Frequency
LES	Large eddy simulation
LFS	Limiting fire scenarios
LLNL	Lawrence Livermore National Laboratory
LOL	Low oxygen limit
MCC	Motor Control Center
MCR	Main Control Room
MEFS	Maximum expected fire scenarios

MOVs	Motor-operated valves
MQH	McCaffrey, Quintiere, and Harkleroad
MOU	Memorandum of Understanding
NBS	National Bureau of Standards (now NIST)
NFPA	National Fire Protection Association
NIST	National Institute of Standards and Technology
NPP	Nuclear Power Plant
NRC	U.S. Nuclear Regulatory Commission
NRR	Office of Nuclear Reactor Regulation (NRC)
PE	Polyethylene
PMMA	Polymethyl-Methacrylate
PRA	Probabilistic Risk Assessment
PVC	Polyvinyl chloride
PWR	Pressurized Water Reactor
RCP	Reactor Coolant Pump
RES	Office of Nuclear Regulatory Research (NRC)
RI/PB	Risk-Informed, Performance-Based
RIS	Regulatory Issue Summary
RTE	Radiation Transport Equation
RTI	Response Time Index
SBDG	Stand-By Diesel Generator
SDP	Significance Determination Process
SFPE	Society of Fire Protection Engineers
SNL	Sandia National Laboratory
SWGR	Switchgear Room
THIEF	Thermally-Induced Electrical Failure
TP	Thermoplastic
TS	Thermoset
UL	Underwriters Laboratory
V&V	Verification & Validation
XPE	Cross-linked polyethylene and neoprene

1
INTRODUCTION

1.1 Background

In 2001, the National Fire Protection Association (NFPA) issued the first edition of NFPA 805, *Performance-Based Standard for Fire Protection for Light-Water Reactor Electric Generating Plants*, 2001 Edition[1]. Effective July 16, 2004, the Nuclear Regulatory Commission (NRC) amended its fire protection requirements in Title 10, Section 50.48(c) of the *Code of Federal Regulations* (10 CFR 50.48(c)) to permit existing reactor licensees to voluntarily adopt fire protection requirements contained in NFPA 805 following a performance-based approach as an alternative to the existing deterministic fire protection requirements. One important element in a performance-based approach is the estimation of fire hazard using mathematical fire models. Fire modeling is one possible approach that can be used for this purpose, according to NFPA 805, to demonstrate compliance with the regulatory requirements noted in 10 CFR 50.48(c). NFPA 805 also allows the use of a fire probabilistic risk assessment (Fire PRA) in regulatory applications. Fire modeling is used in Fire PRAs to determine the effects of fire hazard so that the associated risk can be quantified.

As part of its fire modeling requirements, NFPA 805 states that "fire models shall be verified and validated" (section 2.4.1.2.3) and that "only fire models that are acceptable to the authority having jurisdiction (AHJ) shall be used in fire modeling calculations" (section 2.4.1.2.1). This is an important requirement because the verification and validation (V&V) of fire models is intended to ensure the correctness, suitability, and overall quality of the method. Specifically, verification is the process used to determine whether a model correctly represents the developer's conceptual description (i.e., whether it was "built" correctly), while validation is used to determine whether a model is a suitable representation of the real world and is capable of reproducing phenomena of interest (i.e., whether the correct model was "built").

In 2007, the NRC's Office of Nuclear Regulatory Research (RES) and the Electric Power Research Institute (EPRI) as a part of the NRC/RES-EPRI Memorandum of Understanding (MOU) completed a collaborative project for the V&V of five select fire modeling tools to support the implementation of the voluntary fire protection rule that adopts NFPA 805 as a Risk-Informed/Performance-Based (RI/PB) alternative. The results of this study are documented in NUREG-1824 (EPRI 1011999), "Verification and Validation of Selected Fire Models for Nuclear Power Plant Applications." The National Institute of Standards and Technology (NIST) was also an important partner in developing this publication, providing extensive fire modeling and experimentation expertise. The V&V effort is intended to increase the confidence of reviewers who evaluate fire models used in NRC inspection oversight programs, such as the Fire Protection Significance Determination Process (SDP).

---

[1] All references in this chapter to NFPA 805 are specific to the 2001 edition of the standard, which is the code of record (COR) required by 10 CFR 50.48(c).

This report builds on the V&V research described earlier by incorporating the results into a set of guidelines and recommendations for conducting fire modeling studies in support of NFPA 805, Fire PRAs, Fire Protection SDPs, and/or other commercial nuclear industry applications. When the NRC Advisory Commission on Reactor Safeguards (ACRS) issued a letter to Luis Reyes, Executive Director for Operations, recommended publication of NUREG-1824 (EPRI 1011999), they identified two major items to be included in the user's guide (Wallis, 2006). Specifically, the ACRS recommended that the user's guide include:

- Estimates of the ranges of normalized parameters to be expected in nuclear plant applications
- Quantitative estimates of the uncertainties associated with each model's predictions, preferably in the form of probability distributions

The ACRS indicated that quantitative estimates of the "intrinsic model uncertainty" would be a valuable input in risk-informed as well as non-risk-informed applications. Chapters 2 and 3 address the first ACRS recommendation. Chapter 4 specifically addresses developing the V&V results into quantitative estimates of model uncertainty which is the second ACRS recommendation. Finally, the appendices contain examples which illustrate the entire process for several NPP scenarios.

1.2 Objective

The objective of this guide is to describe the process of conducting a fire modeling analysis principally for commercial nuclear power plant (NPP) applications. The process described in this guide addresses most of the technical elements relevant to fire modeling analysis, such as the selection and definition of fire scenarios and the determination and implementation of input values, sensitivity analysis, uncertainty quantification, and documentation. In addition, requirements associated with fire modeling analyses and analytical fire modeling tools in NFPA 805 are addressed through generic guidance, recommended best practices, and example applications.

1.3 Scope

1.3.1 User Capabilities

This guide should be used as a complement to, not a substitute for, "user's manuals" for specific fire modeling tools, fire dynamics textbooks, technical references, education and training. This guide only compiles information and organizes it procedurally for NPP applications. Analysts are encouraged to review the references made throughout the guide for in-depth coverage of the advantages and the range of applicability of specific models or assumptions. Once a fire scenario has been selected, this guide will help the fire model user define the necessary modeling parameters, select an appropriate model, and properly interpret the fire modeling results. Since all models are merely approximations of reality, this guide also provides useful insights for translating real configurations into modeling scenarios. Due to the technical nature of this guide, users with the following areas of expertise will benefit the most from it:

- General knowledge of the behavior of compartment fires
- General knowledge of basic engineering principles, specifically thermodynamics, heat transfer, and fluid mechanics
- Ability to understanding the basis of mathematical models involving algebraic and differential equations

This guide focuses on the capabilities of the models selected for V&V. However, some generic guidance is also provided, and most of the discussion is applicable to any fire model of the respective type (algebraic model, zone model, or computational fluid dynamics (CFD) model). Five specific models are discussed in this guide:

(1) The NRC's Fire Dynamics Tools (FDT^S), NUREG-1805 and Supplements

(2) EPRI's Fire-Induced Vulnerability Evaluation, Revision 1 (FIVE-Rev1)

(3) NIST's Consolidated Model of Fire Growth and Smoke Transport (CFAST) Version (6)

(4) Electricite de France's (EdF) MAGIC code Version (4.1.1)

(5) NIST's Fire Dynamics Simulator (FDS) Version (5)

1.3.2 Training Resources

For individuals seeking to enhance or update their expertise in the areas noted in section 1.3.1, there are several resources available, including academic courses, short courses, and written materials. The following three U.S. institutions have established undergraduate and/or graduate degree programs in fire protection engineering:

- California Polytechnic Institute, San Luis Obispo (http://fpe.calpoly.edu/)
- University of Maryland (http://www.fpe.umd.edu)
- Worcester Polytechnic Institute (http://www.wpi.edu/Academics/Depts/Fire/)

Information on academic institutions with degree programs or single classes in fire protection engineering can also be found at:

http://www.careersinfireprotectionengineering.com/career_types.htm

A background in engineering fundamentals is essential for fire modelers, especially in the areas of fluid mechanics, thermodynamics, and heat transfer. These subjects are offered at virtually any academic institution with programs in fire protection, mechanical, aerospace, civil, and chemical engineering. While general courses provide basic background discussions, courses involving fire applications are preferable, and would be provided by the institutions offering courses or degree programs in fire protection engineering.

In addition to the academic programs, short courses in fire behavior and fire modeling are available through professional and industry associations, such as the Society of Fire Protection Engineers (SFPE) (http://www.sfpe.org) and the Electric Power Research Institute (http://www.epri.com).

Key written references on fire behavior and fire modeling include:

ASTM E1355–05a (2005), "ASTM Standard Guide for Evaluating the Predictive Capability of Deterministic fire Models," American Society for Testing and Materials, West Conshohocken, PA, 2005.

Buchanan, A. H. (2001), *Structural Design for Fire Safety*, John Wiley and Sons, LTD, Chichester, England, 2001.

Babrauskas, V., *Ignition Handbook*, Fire Science Publishers/Society of Fire Protection Engineers, Issaquah WA (2003).

Drysdale, D., An Introduction to Fire Dynamics, 2nd Ed., John Wiley, 2002.

Karlsson, B. and Quintiere, J., Enclosure Fire Dynamics, CRC Press, 1999

Quintiere, J.G., Principles of Fire Behavior, Delmar Publishers, 1998.

Quintiere,J.G., Fundamentals of Fire Phenomena, John Wiley, 2006.

Fire Protection Handbook, National Fire Protection Association, 20th Ed., A.E. Cote, (Editor) 2008.

M.H. Salley and R.P. Kassawara, "Verification and Validation of Selected Fire Models for Nuclear Power Plant Applications," NUREG-1824, EPRI 1011999, Nuclear Regulatory Commission, 2007.

SFPE Handbook of Fire Protection Engineering, 4th Ed., P.DiNenno, (Editor), National Fire Protection Association, 2008.

SFPE, "SFPE Engineering Guide to Assessing Flame Radiation to External Targets from Pool Fires," SFPE Engineering Guide, Society of Fire Protection Engineers, Bethesda, MD, March 1999.

SFPE, "SFPE Engineering Guide to Fire Exposures to Structural Elements," SFPE Engineering Guide, Society of Fire Protection Engineers, Bethesda, MD, November, 2005.

SFPE, "SFPE Engineering Guide to Piloted Ignition of Solid Materials Under Radiant Exposure," SFPE Engineering Guide, Society of Fire Protection Engineers, Bethesda, MD, January, 2002.

SFPE, "SFPE Engineering Guide to Predicting Room of Origin Fire Hazards," SFPE Engineering Guide, Society of Fire Protection Engineers, Bethesda, MD, November, 2007.

1.4 Fire Modeling Theory

Fire development in compartments is often divided into phases depending on the dominant processes at any given stage of development. Ignition is dictated by the characteristics of the fuel item being ignited (i.e., ignition temperature, geometry, orientation, and thermophysical properties[2]) and the strength of the ignition source. Once the flames are sustained on a burning fuel item, a smoke plume develops; transporting mass and heat vertically as a result of the buoyancy of the smoke (see Figure 1-1). The plume will entrain air as it rises, thereby causing the smoke to cool and become diluted; as a result, the quantity of smoke being transported will increase with increasing elevation. After a smoke plume strikes the ceiling, the smoke travels

---

[2] Thermophysical properties include thermal conductivity, specific heat, and density.

horizontally under the ceiling in a relatively thin layer, referred to as a ceiling jet. As the ceiling jet travels, the smoke cools with increasing distance from the plume impingement point, in part because of air entrainment into the ceiling jet as well as heat losses from the ceiling jet to the solid ceiling boundary.

In an ideal situation, once the ceiling jet reaches the enclosing walls, a Hot Gas Layer[3] (HGL) develops. As a result of the continuing supply of smoke mass and heat via the plume, the HGL becomes deeper, and its temperature increases. Other properties of the smoke in the HGL also increase (including concentration of gas species and solid particulates).

Radiant heat from the HGL to other combustibles not involved in the fire increases their temperature. Similarly, the temperature of non-burning combustibles will also increase as a result of receiving thermal radiation from the burning item(s). As the other combustibles reach their respective ignition temperatures, they will also ignite. In some cases, the ignition of many other combustibles in the space caused by heating from the HGL occurs within a very short time span. This is commonly referred to as flashover.

Several aspects of fire behavior may be of interest when applying fire models, depending on the purpose of the modeling application. Analysts may seek to determine the effects associated with heating of targets submerged in smoke or receiving radiant heat from the flames, the response of ceiling-mounted detectors or sprinklers to the fire environment, or other phenomena.

---

[3] Hot Gas Layer or HGL is also called "smoke layer" or "hot upper layer" in other publications in fire protection engineering.
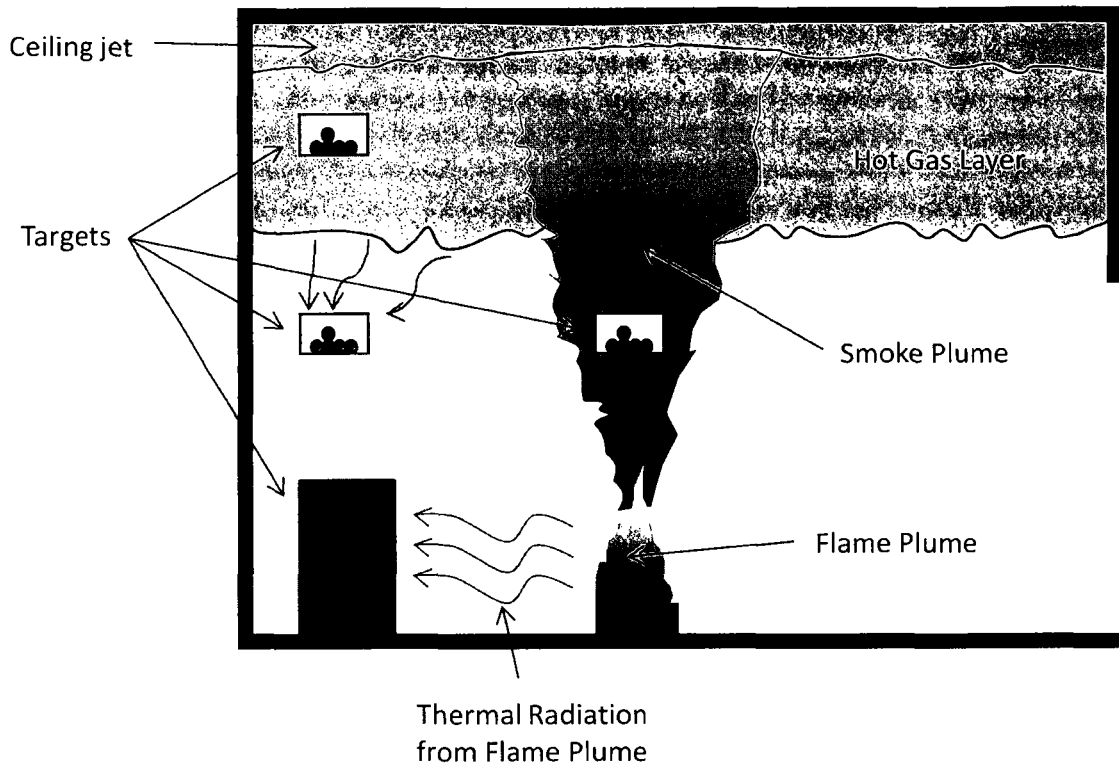
Figure 1-1. Characteristics of compartment fires.

The aspects of fire behavior that may be of interest in such analyses include:

- Rate of smoke production
- Rate of smoke filling
- Properties of the ceiling jet
- Properties of the HGL
- Target response to incident heat flux via either thermal radiation or convection

A detailed review of each of these aspects is provided in texts on fire dynamics. A brief review of each is provided here.

Rate of smoke production

Smoke is defined as a combination of the gaseous and solid particulates resulting from the combustion process, plus the air that is entrained into the flame and/or smoke plume. Consequently, the rate of smoke production at a particular height in the plume is the combination of the generation rate of combustion products and air entrainment rate into the flame and/or smoke plume between the top of the fuel and the height of interest. In most cases, the air entrainment rate greatly exceeds the generation rate of combustion products. Hence, the correlations used to estimate the rate of smoke production are usually taken from experimental research on entrained air.

Rate of smoke filling

The rate of smoke filling is dependent on the rate of smoke production, the heat release rate, floor area and height of the space, and time from ignition. For a fire with a steady heat release rate, the rate of smoke filling in a compartment will decrease with time due to a decrease in the smoke production rate, which decreases as the height available to entrain air decreases when the HGL deepens.

Properties of the ceiling jet

The ceiling jet transports smoke and heat horizontally away from the region of plume impact with the ceiling. The response of ceiling-mounted fire detectors or sprinklers is governed primarily by their interaction with a ceiling jet. The temperature and concentration of smoke in a ceiling jet is principally dependent on the height of the space, distance between the impact point of the smoke plume and the ceiling, and the heat release rate of the fire.

Properties of the HGL

As smoke and heat are transported to the HGL via the smoke and fire plumes, the properties of the HGL will change. The principal properties of interest include the depth, temperature and gas concentrations in the HGL. The magnitude of the properties depends on the heat release rate of the fire, geometry of the space, ventilation openings (permitting material from the HGL to leave the space, providing air to the fire, and/or causing a stirring action), yields of combustion products, and the elapsed time after ignition. These changes can be tracked by considering the conservation of energy, mass, and species relative to the HGL.

Target response to incident heat flux via either thermal radiation or convection

The targets' temperature will increase as a result of receiving heat via either thermal radiation or convection. Radiation heat transfer is dependent on the intensity of thermal radiation emitted by a source, the size of the source, and the proximity of the target to the source. For this application, the flame height, the portion of heat released from the fire as radiation, and the distance separating the target from the flame are the dominant parameters. Convection heat transfer occurs whenever the target is submerged in the smoke plume or HGL.

1.4.1 Algebraic Models

Algebraic models may be standalone equations found in literature or may be contained within spreadsheets (such as the NRC's FDT^s), and can help give a general understanding of one of the fire environment phenomena. These equations are typically closed-form algebraic expressions, many of which were developed as correlations from empirical data. In some cases, they may take the form of a first-order ordinary differential equation, and, when used properly, can provide an estimate of fire variables, such as HGL temperature, heat flux from flames or the HGL, smoke production rate, depth of the HGL, and the actuation time for detectors.

Introduction

Algebraic models are helpful because they require minimal computational time and a limited number of input variables. When applying the results of the algebraic models, users need to be aware that the development of most equations involved assumptions to simplify the analysis. Other than for very simple situations, algebraic models are useful primarily as screening tools (i.e., to provide a rough approximation to an analysis, perhaps as a check of an aspect of the results of the computer-based models), and are also applicable when only one phenomenon can be treated in isolation: for instance, plume or ceiling jet correlations are not applicable if there is a significant HGL unless they are modified to account for this effect.

1.4.2 Zone Models

A zone model, such as the Consolidated Fire and Smoke Transport Model (CFAST) or MAGIC, calculates fire environment variables using control volumes, or zones, of a space. The zones correspond to a cooler lower layer and an HGL, as depicted in Figure 1-2. The fundamental idea behind a zone model is that each zone is well-mixed and that all fire environment variables (temperature, smoke concentration, etc.) are therefore uniform throughout the zone. Conditions in each zone are calculated by applying conservation equations and the ideal gas law. The variables in each zone change as a function of time and rely on the initial conditions specified by the user. It is assumed that there is a well-defined boundary separating the two zones, though this boundary may move up or down throughout the simulation.
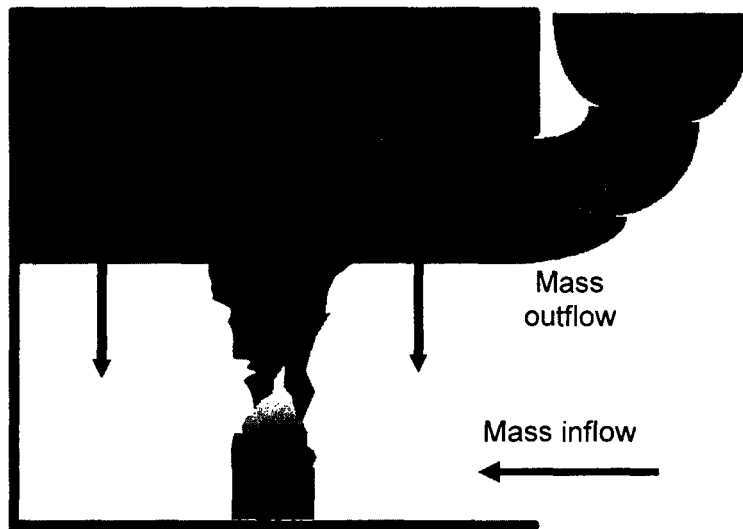
Figure 1-2. A two-zone enclosure fire with an HGL above and a cool lower layer below.

Zone models are most applicable in situations involving simple geometries or where spatial resolution within a compartment is not important. The preparation of input for a zone model, the computation time, and the amount of output data generated are slightly more extensive than a simple algebraic model; however, the overall computational time cost is still low.

Zone models can easily analyze conditions resulting from fires involving single compartments or compartments with adjacent spaces, and are often used to compute the HGL temperature, HGL composition, and target heat fluxes. They are also capable of modeling some effects of natural and mechanical ventilation in both horizontal and vertical directions. Some zone models allow the user to select a thermal plume model, which may assist in better characterization of a known fire scenario, while others assume an axisymmetric smoke plume. Other features of a zone model may include a user-specified one-zone assumption or multiple fire plumes.

Simulations of spaces with complex ceilings or numerous compartments can be challenging with a zone model. Because zone models assume uniform conditions in the HGL and lower layer, results cannot be distinguished for a location situated in the upper part of the space over another, nor is an analysis of different fire locations in the compartment possible.

Because of the uniform layer assumption, applying zone models to characterize large horizontal flow paths is challenging, and greater errors are obtained with increasing deviation from parallelepiped geometries. These limitations result from the conflict between the assumptions of the model and actual fire phenomena, such as the cooling of an HGL with continued mixing in ambient air. As the layer cools, the HGL assumption is no longer applicable. Due to the zone approach, smoke transport time lags are not considered in the simulation, which is an acceptable approximation in relatively small spaces but may lead to significant error in large-volume spaces or spaces with large aspect ratios.

Smoke production, fire plume dynamics, ceiling jet characteristics, heat transfer, and ventilation flows are all algebraic models embedded within zone models. Other parameters that can be calculated with a zone model include thermal behavior, detection response, and suppression response. The output of a zone model is typically simple to understand and is generally presented through an automatic user interface.

1.4.3 CFD Models

A CFD model is often useful when trying to determine fire variables at a specific location or when there are geometric features that are expected to play a significant role in the results beyond what is calculated in a zone model approximation. A typical CFD model consists of a preprocessor, a solver, and a postprocessor. CFD models can provide a detailed analysis in both simple and complex geometries.

CFD models essentially apply a series of conservation and state equations across multiple cell boundaries in a space. The number of cell boundaries depends on the mesh size, which breaks the geometry into three-dimensional subvolumes called cells. Solutions to partial derivatives of the conservation equations are updated as a function of time within each numerical grid cell, with the solutions in all cells, collectively describing the fire environment within the geometry at the cell resolution.

The number of grid cells defines the type of mesh. A fine mesh is made up of numerous grid cells. Since the equations are applied at each cell's boundaries, a more detailed distribution of fire parameters is characterized. A coarse mesh is made up of fewer grid cells and can result in

Introduction

less accurate results. The type of mesh and number of grid cells should be based on the geometry and the desired results. If a more detailed simulation is needed, then a finer mesh should be used. Be aware that a finer mesh significantly increases the computational running time of the model as well as the quantity of output data.

CFD models have much better spatial fidelity than zone models, being able to distinguish conditions in one part of the space from another. Because of the appreciable amount of time and effort required to apply CFD models as compared to zone models or algebraic models, CFD models are generally applied when:

- Spatial resolution is important, either relative to the locations of fuel packages or targets.
- Large compartments relative to the fire size are involved.
- Compartments have complex geometries, flow connections, or numerous obstructions in the upper part of the compartment.
- Large numbers of compartments are within the area of interest and the presence of each compartment is expected to affect the fire environment in the area of interest.

An example of a CFD fire simulation of a fire experiment is shown in Figure 1-3. The purpose of the calculation was to simulate an experiment that was part of the validation study described in NUREG-1824 (EPRI 1011999). In the experiment, a pan fire was placed in a relatively small compartment, and temperatures and heat fluxes were measured at various locations. The CFD simulation is able to describe the changing behavior of the fire as it interacts with its surroundings.
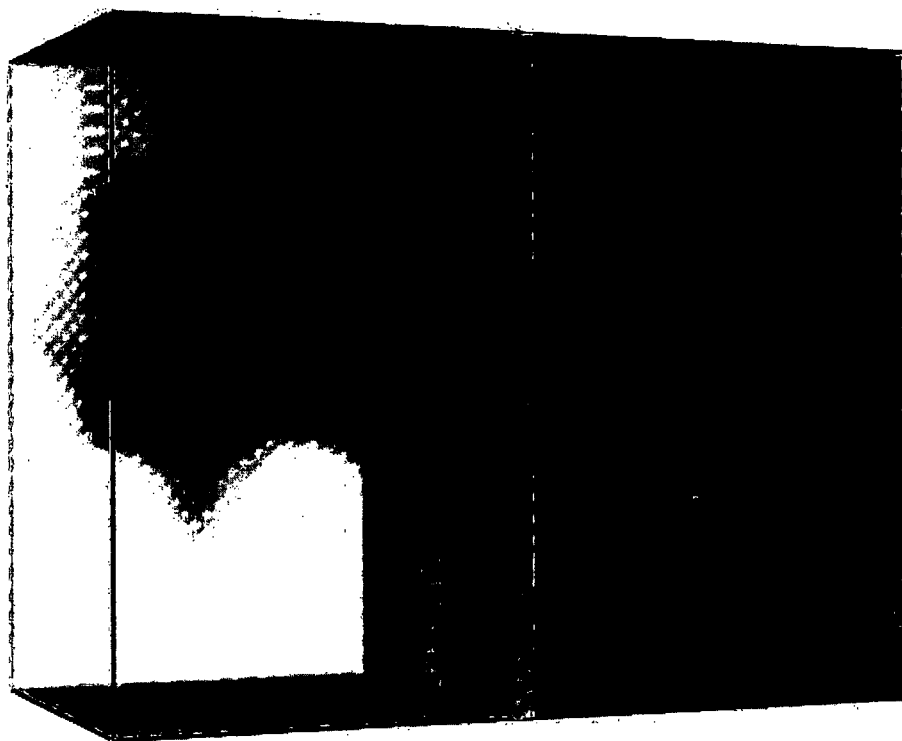
Time: 670.0

Figure 1-3. A CFD visualization of compartment fire experiment.

While CFD models provide a detailed analysis of a space, they are costly to create, simulate and maintain. The input files created in the preprocessing stage require a significant effort to create. The user must understand the code syntax and the implications and assumptions embedded in the model. A firm understanding of fire dynamics is important in providing input data that is relevant to the application. Most CFD models have default values that must be recognized and adjusted as necessary if the simulation is going to be accurate. The relevance of the default values needs to be confirmed for any application. User manuals and technical references for each CFD model outline such values and may provide recommended ranges for the parameters.

Depending on the complexity of the scenario and the computer computational power, the solver within the model can take a few hours to weeks to complete all the calculations. This time cost depends on the measured parameters, the size of the geometry, and the mesh size of the calculations. Outputs of field models are visualized through a post-processing program. The CFD model developed at NIST, Fire Dynamics Simulator (FDS), employs the program "Smokeview" to represent distributions of temperature, mass, heat flux, burning rate, etc. throughout the geometry. These parameters can be described through point locations, isocontours, or vector diagrams. Output data may also be stored in a comma-separated value file format that can be read by a standard spreadsheet program.

1.4.4 V&V

The use of fire models to support fire protection decision making requires a good understanding of their limitations and predictive capabilities. NFPA 805 states that fire models shall only be applied within the limitations of the given model and shall be verified and validated.

Verification is the process of determining that a model preserves the laws of science and math, thereby assessing whether it was "built" correctly. In this assessment, the theoretical basis of the model is reviewed to confirm that the scientific and mathematical foundation of the model is correct, that is, that the laws of physics and chemistry are upheld and proper numerical techniques are employed.

Validation is the process of determining that a model is a suitable representation of the real world and is thus capable of reproducing the phenomena of interest. Validating a model requires that the output of subroutines or the entire model provide predictions that compare reasonably well with experimental data.

As noted in Section 1.1, the NRC RES and the EPRI conducted a collaborative project for V&V of the five selected fire models described in Sections 2.3.1 through 2.3.5 that may be used to support RI/PB fire protection and implementation. The results of this project were documented in NUREG-1824 (EPRI 1011999), Verification and Validation of Selected Fire Models for Nuclear Power Plant Applications.

1.5 NFPA 805 Fire Modeling Applications

The NFPA 805[4] requirements associated with fire modeling are organized in two sections, Section 4.2.4.1 and Section 2.4.1.4. Section 4.2.4.1 describes requirements for the implementation of a performance-based fire modeling analysis. Section 2.4.1.4 describes the requirements associated with the analytical fire modeling tools selected for the analysis.

1.5.1 Requirements Associated with the Implementation of a Performance Based Fire Modeling Analysis

NFPA 805 Section 4.2.4.1 describes the process to follow when using fire modeling to address variances from deterministic requirements (VFDRs). The term VFDR is currently used in the fire protection community within the commercial nuclear industry to refer to plant conditions that deviate from deterministic requirements of NFPA 805 Section 4.2.3. Section 4.2.4.1 of NFPA 805 is subdivided by process element as follows:

Identify Targets (NFPA 805 § 4.2.4.1.1): This subsection requires the description of the VFDRs and the targets (e.g., equipment or cables) and target locations (specific locations of raceways/conduits containing the cables, electrical panels, or equipment) associated with them.

Establish Damage Thresholds (NFPA 805 § 4.2.4.1.2): This subsection requires the description of damage thresholds for the equipment and cables needed to achieve the nuclear safety performance criteria. The damage threshold (i.e., target vulnerability) for cables exposed to fire is expressed in most cases in the form of an incident heat flux on the cables or the cables' surface temperature as follows:

---

[4] References to NFPA 805 in this document specifically refer to the 2001 Edition, which is the edition endorsed in 10 CFR 50.48(c).

Damage or ignition temperature: Temperature at which the target is considered damaged or ignited. In the case of cables, the damage and ignition temperatures are assumed to be the same. In the context of a Fire PRA, damage refers to the presence of a predefined cable failure mode, such as a hot short, a short to ground, etc.

Damage or ignition incident heat flux: The heat flux received by a target material with the intensity necessary to degrade the cable jacket and insulation, exposing the conductors and allowing specific cable failure modes.

Determine Limiting Conditions (NFPA 805 § 4.2.4.1.3): This subsection requires the description of the combination of equipment or required cables with the highest susceptibility to any fire environment. This determination is needed since multiple targets (or cables) may appear in the same VFDR, or multiple VFDRs may have been identified in the fire area. These targets (or cables) may be located in various parts of the fire area and may thus be exposed to various fire sources and fire-generated conditions. The above consideration may lead to the selection of more than one limiting condition.

Establish Fire Scenarios (NFPA 805 § 4.2.4.1.4): This subsection requires the description of the fire conditions for the area under consideration resulting from the identified and analyzed fire scenarios. It should be noted that the scenario definition is consistent with the requirements listed under § 2.4.1.3 of NFPA 805 as follows:

Maximum Expected Fire Scenario: The *maximum expected fire scenario* (MEFS) is defined in NFPA 805 as the scenario that "represents the most challenging fire that could be reasonably anticipated in the occupancy type and conditions in the space." The definition continues to indicate that the scenarios "can be established based on electric power industry experience with consideration for plant-specific conditions and fire experience." Establishing the MEFS involves defining the problem in sufficient detail to perform calculations and to ensure that the input parameter set represents reasonable conditions.

Limiting Fire Scenario: The *limiting fire scenario* (LFS) is defined in NFPA 805 as the scenario in which "one or more of the inputs to the fire modeling calculation are varied to the point that the performance criteria are not met." Development of the LFS essentially involves a sensitivity analysis that identifies which combinations of input parameters or variables are critical to the analysis. The intent of LFS development is to determine if there is a reasonable margin between the MEFS and the point of failure.

For each fire scenario, the environmental conditions resulting from each MEFS are compared to the damage thresholds for the targets in the fire area. If damage thresholds are not exceeded, the targets associated with the VFDR in the fire area can be considered free of fire damage under the conditions of the postulated MEFS.

By definition, the effects of the LFS include damage to the targets in the fire area under consideration. Fire modeling parameters that have been varied to establish the LFS conditions are identified and described.

Protection of Required Nuclear Safety Success Paths (NFPA 805 § 4.2.4.1.5): This section requires the description of the effectiveness of fire protection systems and features in protecting and maintaining the operation of the circuits and components associated with the VFDRs.

Introduction

Operations Guidance (NFPA 805 § 4.2.4.1.6): This section requires the description of any operational guidance to plant personnel, including the performance of recovery actions based on the fire modeling analysis assumptions, inputs and results in the corresponding fire area.

1.5.2 Requirements Associated with the Selected Analytical Fire Models

Section 2.4.1.2 describes the requirements for the use of fire models, which include:

- The use of fire models acceptable to the authority having jurisdiction (i.e., the US Nuclear Regulatory Commission)

- The application of fire models within their range and limitations. Section 2 of this document provides guidance on ensuring the model is within the range of limitations and what steps are necessary if the application is outside existing V&V data ranges

NFPA 805 stipulates that the fire models used shall be verified and validated. In the context of this application, the specific analytical capabilities within the fire model need to be verified and validated. Model capabilities not invoked in specific calculation are outside the scope of this requirement. NUREG-1824 (EPRI 1011999) is an example of a verification and validation study for fire models specifically developed for NPP applications. Refer to Section 2 of this document for guidance on ensuring specific fire model applications are within the scope of existing V&V studies or what steps should be taken if they are not.

1.6 Fire Modeling in Support of Fire PRA

The Fire PRA primarily applies fire modeling in the fire scenario development and analysis process. A fire scenario in a Fire PRA is often modeled as a progression of damage states over time, which is initiated by a postulated fire involving an ignition source. Each damage state is characterized by a time and a set of targets damaged within that time. Fire modeling is used to determine the targets affected in each damage state and the associated time at which this occurs. The first damage state usually consists of damage only to the ignition source itself. Depending on the characteristics and configuration of the scenario, the last damage state may consist of an HGL formation that leads to a full room burnout. Damage states between the first and final states capture target sets compromised as the fire propagates through intervening combustibles. Figure 1-4 depicts an example of scenario progression through five damage states.

Ignition	Damage State 1 (Ignition Source Only)	Damage State 2	Damage State 3	Damage State 4 (Hot Gas Layer)

No additional damage outside the ignition source

t = t₁

No damage outside target set 1

t = t₂

No damage outside target set 2

t = t₃

No damage outside target set 3

t = t₄
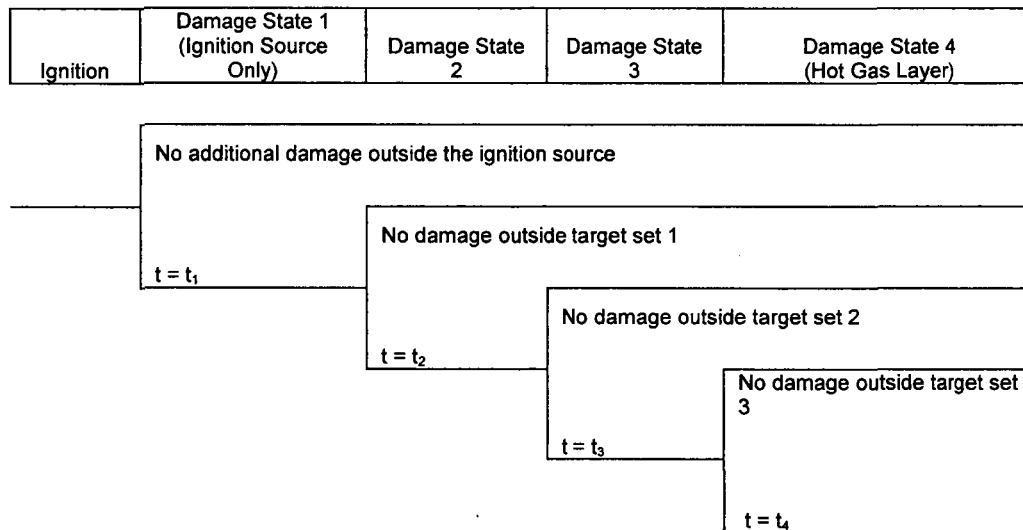
Figure 1-4: Event tree depicting scenario progression modeled in a Fire PRA

The initiating event (ignition) is characterized by the ignition source frequency. The first damage state captures the event in which damage is limited to the ignition source itself. The time t_1 (as well as any subsequent time milestones in the progression) at which this damage is postulated can be determined using fire modeling tools. Fire modeling tools are also used to determine which targets are damaged. The second and third damage states capture additional targets as the fire continues to grow or propagate through intervening combustibles. In this example, the fourth damage state is associated with HGL formation (i.e., compartment-wide damage or full room burnout).

Each scenario progression postulated in a Fire PRA is quantified to determine its contribution to fire risk. The fire risk metrics are Core Damage Frequency (CDF) and Large Early Release Frequency (LERF). The CDF is quantified using the following equation:

$$CDF_i = \lambda_i \cdot \sum_{j=1}^{n} \left(SF_j \cdot P_{NS,j} \cdot ccdp_j \right)$$ (1-1)

Where i is the fire scenario associated with the ignition source, j is the damage state postulated in the scenario (the maximum number of damage states postulated, n, equals 4 in the conceptual example presented in Figure 1-4), λ_i is the ignition frequency, SF_j is the severity factor for damage state j, $P_{NS,j}$ is the non-suppression probability for damage state j, and $ccdp_j$ is the conditional core damage probability associated with the damage state represented in that branch of the event tree. Simply stated, the equation above is used to quantify CDF of a scenario where a fire:

1. Initiates (λ_i)
2. Grows large enough to damage targets external to the ignition source (SF)
3. Is not controlled or suppressed (P_{NS})
4. Generates the potential for core damage conditions ($ccdp$)

The severity factor, SF_j, represents the fraction of fires associated with each damage state. SF_j is calculated by first determining the minimum fire size required to damage the nearest target. For example, if a target is located in the plume at a certain height above the fire source, the minimum Heat Release Rate (HRR) required to damage that target could be calculated using Heskestad's plume correlation (Heskestad, 2008). This minimum HRR can then be compared to an HRR probability distribution characterizing the ignition source to determine the fraction of fire intensities that would exceed the critical value. Figure 1-5 provides a conceptual representation of the severity factor parameter.
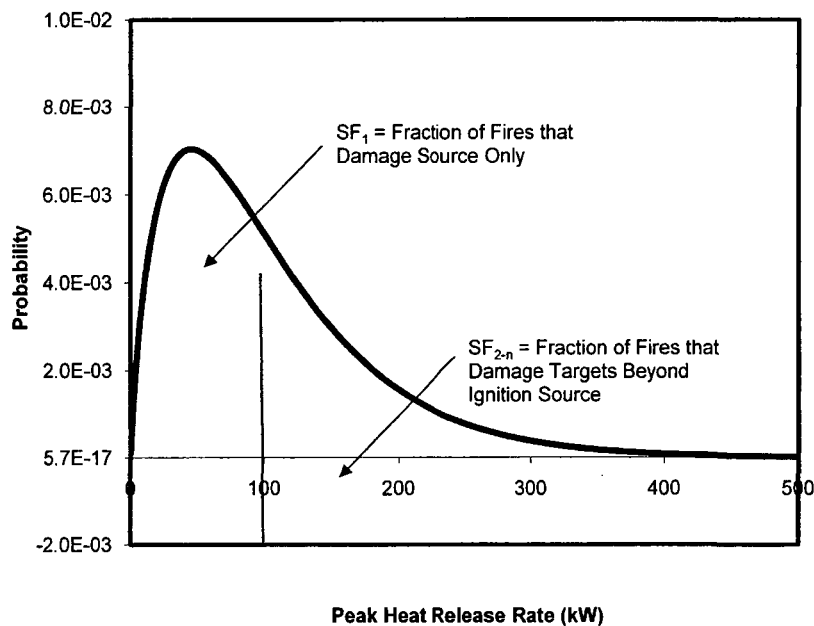
Figure 1-5: Conceptual representation of the severity factor

The non-suppression probability, P_{NS}, represents the probability of automatic and manual fire suppression systems failing to suppress the fire prior to it damaging targets within the postulated damage state. Fire modeling can lend support to the calculation of this term because target damage and the response of detection and suppression systems are functions of time.

The ccdp represents the probability of core damage given that the target damage for that damage state occurs. Fire modeling can be used in the calculation of ccdp by identifying which targets have failed within that damage state. For example, the dimensions of the physical space where damage is expected, referred to as the zone of influence of the fire, can be determined using radiation, plume, and ceiling jet correlations. The target failures can then be mapped into the plant response model (i.e., the PRA model), which is quantified to calculate scenario ccdp.

The Fire PRA standard (ASME/ANS RA-Sa-2008 and Addenda RA-Sa-2009), which lists requirements for all the technical elements associated with a Fire PRA, includes specific requirements for the use of fire models.

In terms of the models itself, the standard addresses (1) the selection of appropriate fire modeling tools for estimating fire growth and damage behavior, considering the physical behaviors relevant to the selected fire scenarios, and (2) implementation of fire models that are sufficiently capable of modeling the conditions of interest within known limits of applicability. In the case of analytical fire models, the standard requires the use of appropriate fire modeling tools with the ability to model the conditions of interest within known limits of applicability. It should be noted that the Fire PRA standard does not explicitly require fire models to be verified and validated (as is the case of Section 2.4.1.2 in NFPA 805). However, the term "known limits of applicability" from the Supporting Level Requirement FSS-D2 is intended to ensure the availability of appropriate technical justification for the use of the model in specific applications. In this context, V&V results as discussed and applied in this guide can serve as appropriate justification, but the standard does not limit analytical fire model applications to specific verification and validation ranges.

In terms of input parameters, the standard requires a technical basis for fire modeling tool input values used in the analysis, given the context of the fire scenarios being analyzed.

The requirements listed above not only apply to analytical fire models (which are the primary scope of this report) but also apply to any empirical or statistical model that may be used in the Fire PRA to assess the extent and timing of fire conditions. Requirements associated with these types of models include (1) establishing a technical basis for any applied statistical models in the context of the fire scenarios being analyzed, and (2) establishing a technical basis for any applied algebraic models in the context of the fire scenarios being analyzed.

1.7 MSO Fire Modeling Applications

The disposition of specific Multiple Spurious Operation (MSO) interactions is another type of fire modeling application frequently encountered in commercial NPPs. MSOs involve one or more fire-induced component failures that include spurious operation due to hot shorts as a result of fire damage to electrical control cables. The consideration of MSOs arises from the post-fire safe shutdown circuit analysis. MSOs are divided into two categories: those involving components necessary for safe shutdown ("green box") and those involving components that could adversely affect the shutdown capability or cause safe shutdown systems to fail ("orange box") (NEI 00-01, Rev. 2). Because MSOs are induced by circuit damage, the threshold conditions under which an MSO is postulated are typically those associated with cable failure; however, there may be situations involving a sensitive component with a lower damage threshold, such as a transmitter or a relay.

Green box MSOs need to be addressed by means other than fire modeling (NEI 00-01, Rev. 2; RG 1.189, Rev. 2). Orange box MSOs may be evaluated using fire modeling tools (NEI 00-01, Rev. 2; RG 1.189, Rev. 2). When two or more circuits are involved, the fire modeling objective is to demonstrate that at least one circuit remains free of damage for the postulated fire

Introduction

scenario. If the MSO is successfully dispositioned using fire modeling tools, it would show that the damage necessary to cause the MSO would not occur for the postulated fire scenario while there is a reasonable margin of safety.

Orange box MSO fire modeling is similar to the deterministic fire modeling described in NFPA 805. NEI 00-01, Section 4.5.2.2 outlines a process that should be followed when attempting to disposition orange box MSO interactions. Key aspects of the analysis process are as follows:

- Ignition sources are characterized by the 98th percentile severity fire as defined in NUREG/CR-6850 (EPRI 1011989)

- Transient combustible materials are assumed anywhere in the plant unless it is physically impossible

- Fire modeling tools should be verified and validated for the application

- Fire modeling should be performed in a manner consistent with the methods described in NUREG/CR-6850 (EPRI 1011989). Consideration of process enhancements in NFPA 805 is encouraged

- The analysis should include an assessment of model sensitivity to uncertainty

RG 1.189 (2009) emphasizes the need for a V&V basis for the selected fire model. Section 5.3.1.4 of RG 1.189 recommends demonstrating a reasonable safety margin (which assists in the uncertainty and sensitivity analysis) or providing fixed automatic suppression. A reasonable safety margin is left undefined, but it should at least be larger than the results sensitivity to the model uncertainties. Section 2 of this guide addresses the means by which a V&V basis is demonstrated for a fire model application.

In the simplest applications, a fire modeling analysis would be used to show that at least one circuit in the MSO interaction remains free of damage for a set of fire scenarios postulated in the area of interest. As a minimum, when two or more circuits are involved in the MSO interaction, the fixed or transient fuel package fire that is nearest to all circuits involved (i.e., the "pinch point") is evaluated. As with other fire modeling applications, care is necessary in selecting the most appropriate location and the model that captures all relevant exposure mechanisms. The analysis can become complicated when it is found that the MSO could occur, given the postulated fire. MSO interactions frequently have a time component, especially if there is an operator action taken elsewhere that mitigates the MSO but a specific amount of time is needed to perform the action. In this case, the timing of the MSO event becomes a significant aspect of the analysis and a successful outcome could be predicted if failure occurs after the operator action has taken place, provided there is a reasonable margin of safety.

The process described in NEI 00-01, Rev. 2 is fairly specific in terms of the types of fires and their location to postulate. NE 00-01, Draft Rev. 3 provides additional guidance on the selection of fires and the ability to credit existing fire protection features, such as combustible free zones or spaces that normally would not contain combustible material. If a specific feature were credited, the postulated fire size would reflect the conditions present and would not necessarily

be equal to a generic 98th percentile. In this regard, the fire selection process is analogous to the NFPA 805 MEFS.

Passive fire protection systems, such as fire-rated barriers, Electrical Raceway Fire Barrier Systems (ERFBS), and thermal insulation, may be credited, though the performance of these systems would need to be demonstrated under the postulated conditions. There is no specific guidance on the means by which active systems may be credited, including fixed suppression or manual intervention, in either version of NEI 00-01; however, it would be consistent with the original intent to credit these features if the potential for success is in the 98th percentile. It should be noted, however, that at this writing NEI 00-01 Draft Rev. 3 has not yet been endorsed by the NRC, but that its methods and guidance are consistent with NFPA 805.

1.8 Organization of the Guide

The guidance material provided in this document is divided into four chapters and a number of appendices, as outlined below.

- Chapter 2 presents a qualitative overview of the process for conducting fire modeling, including the basic principles of fire simulation, advantages and limitations of the technology, and brief descriptions of the five models
- Chapter 3 provides specific guidance on selecting models to address typical scenarios in commercial nuclear power plants
- Chapter 4 contains information on determining the sensitivity and uncertainty associated with fire modeling calculations
- Chapter 5 contains the list of references identified throughout this document
- Appendices A through H provide detailed examples of fire modeling analyses of typical NPP scenarios:
  - o Appendix A – Cabinet Fire in Main Control Room
  - o Appendix B – Cabinet Fire in Switchgear Room
  - o Appendix C – Lubricating Oil Fire in Pump Compartment
  - o Appendix D – Motor Control Center Fire in Switchgear Room
  - o Appendix E – Trash Fire in Cable Spreading Room
  - o Appendix F – Lubricating Oil Fire in Turbine Room
  - o Appendix G – Transient Fire in Multi-Compartment Corridor
  - o Appendix H – Cable Tray Fire in Annulus

2
THE FIRE MODELING PROCESS

This chapter provides a general step-by-step process for modeling fires in commercial nuclear power plants. The recommended methodology comprises six steps: (1) define fire modeling goals, (2) characterize the fire scenarios, (3) select fire models, (4) calculate fire-generated conditions, (5) conduct sensitivity and uncertainty analyses,, and (6) document the analysis. A simplified process involving the six steps is shown in Figure 2-1.
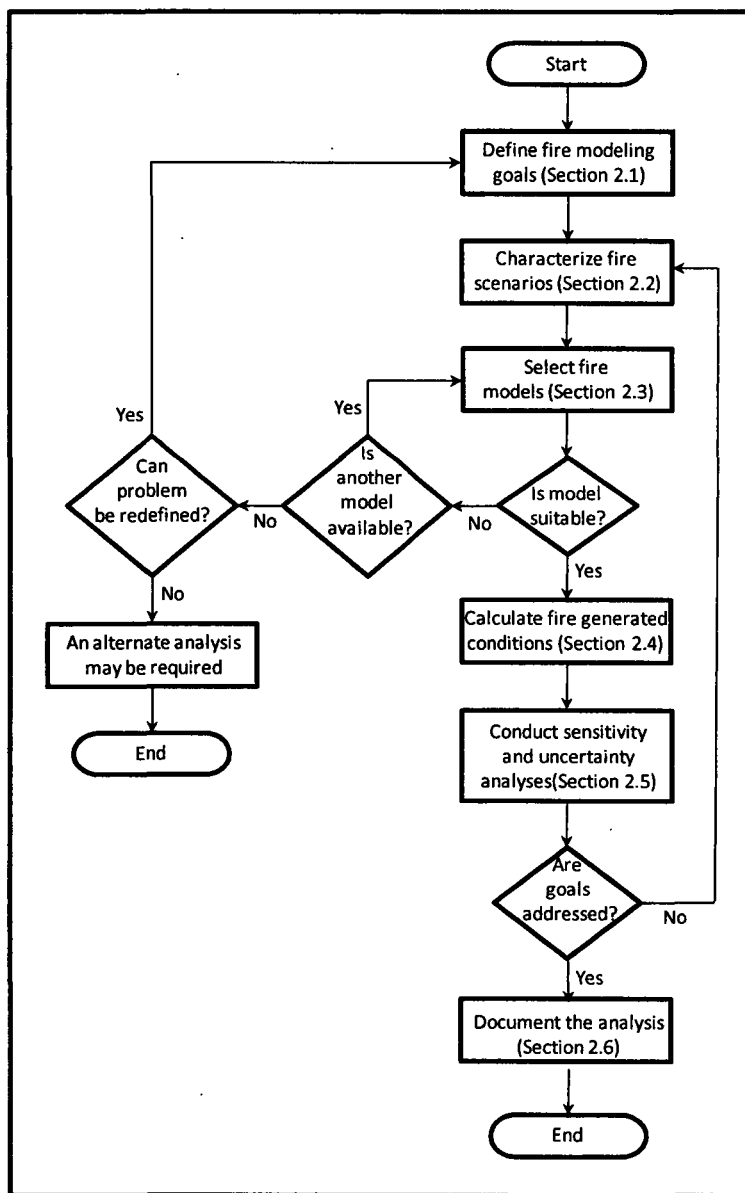
Figure 2-1. Fire Modeling Process

2.1 Step 1: Define Fire Modeling Goals

The first step in a fire model analysis is to identify and state the fire modeling goals. A clearly defined goal provides focus and is needed to correctly select the fire scenarios that will be evaluated and the fire modeling tools that will be used. The goal should be specific, and it should describe the end result in engineering terms. This implies some understanding of the conditions by which success or failure are measured (i.e., the performance criteria) at the analysis outset. The goal(s) should also identify whether the analysis results are intended to help resolve a deterministic issue or are intended as input for a probabilistic risk assessment (PRA). This distinction can affect the types of fire scenarios that would be evaluated, as well as the treatment of uncertainty in the analysis.

Any fire modeling goal may thus be viewed as a statement defining what needs to be accomplished, which criteria will be used to define success or failure, and which analysis process will be followed (e.g., probabilistic or deterministic). The criteria should be stated in terms that can be achieved by the fire modeling analysis. Some common situations in commercial nuclear power plants where fire modeling may be used include:

- Evaluating whether or when a fire could damage a single electrical cable or component

- Evaluating whether or when a fire could damage multiple electrical cables or components

- Evaluating whether conditions are habitable in an enclosure

- Evaluating the potential for fire propagation through or across a fire barrier

- Evaluating detection or sprinkler actuation

- Evaluating the potential for fire propagation between fire zones or fire areas, or to secondary combustibles

The performance criteria will be specific to the fire modeling application, but will often include one or more of the following:

- Maximum acceptable surface temperature for a cable, component, secondary combustible, structural element, or fire-rated construction

- Maximum acceptable incident heat flux for a cable, component, structural element, or secondary combustible

- Maximum acceptable exposure temperature for a cable, component, structural element, or secondary combustible

- Maximum acceptable enclosure temperature

- Maximum smoke concentration or minimum visibility

- Maximum or minimum concentration of one or more gas constituents, such as carbon monoxide, oxygen, hydrogen cyanide, etc.

The performance criteria may also involve sequences of events, such as "detection or sprinkler actuation before cable damage, which occurs when the surface temperature reaches 330 °C (625 °F)." NUREG/CR-6850 (EPRI 1011989) provides some performance thresholds for common nuclear power plant targets (see, for example, Appendix H) as well as for habitability (for example, Section 11.5.2.11).

A few simple examples will illustrate the various ways in which a fire modeling goal may be stated. In many nuclear power plant fire modeling applications, the motivation for a fire modeling analysis is a need to know whether or not an electrical cable or a component remains free of damage from a fire. This could be very specific (i.e., a particular exposure fire exposing a particular cable) or general (i.e., the maximum distance from which a particular type of fire could damage cables). In addition, it may only be necessary for a single fire to damage a single cable, or it may be necessary to simultaneously damage two particular cables with a known separation. If the particular cable or cables in the area of interest are physically damaged when the surface temperature exceeds 330 °C (625 °F), the following goals could apply:

- "Deterministically evaluate whether a fire in Fire Area "X" involving Panel "Y" could cause the surface temperature of Cable "Z" to exceed 330 °C (625 °F)."

- "Evaluate the maximum distance from any surface of an electrical panel that a 98th percentile heat release rate fire in Fire Zone "X" could cause a cable surface temperature to exceed 330 °C (625 °F) for use in screening ignition sources in the PRA."

- "Deterministically evaluate whether a fire in Fire Area "X" involving a transient fuel package could cause the surface temperature of both Cables "Y" and "Z" to exceed 330 °C (625 °F)."

- "Determine for PRA input if any ignition sources in Fire Zone "X" could damage cables in Raceway "Y" before the sprinkler system actuates."

Each of the goals explicitly state the purpose of the analysis and the means by which success is determined in terms that can be achieved by a fire modeling analysis.

2.2 Step 2: Characterize Fire Scenarios

The second step in the fire modeling process is to characterize the relevant fire scenarios that capture those technical elements necessary to address the goals. A fire scenario is defined within this guide as a set of elements needed to describe a fire event. These elements usually include the following:

- the enclosure details (i.e., compartment)
- the fire location within the enclosure
- the fire protection features that will be credited
- the ventilation conditions
- the target locations
- the secondary combustibles
- the fire, which is sometimes referred to as the "ignition source"

A number of the fire scenario elements may also be viewed as fire model input. Section 3 provides additional guidance on specific fire scenario elements as they apply to various fire modeling goals evaluated with a particular fire model. This section provides a broad perspective on the considerations that apply when formulating the appropriate fire scenario, given a fire modeling goal.

Note that when characterizing the fire scenarios, preliminary consideration should also be given to how many scenarios are needed to address a particular goal and which specific fire event characteristics each scenario should capture (i.e., which scenarios are needed). In general, at least one fire scenario would be necessary to assess the effects for a single ignition source-target set pair. The analyst should become familiar with the information necessary to develop input files for the fire modeling tools. In practice, this information should be collected during the process of selecting and describing fire scenarios to minimize the number of walkdowns and document/drawing reviews.

2.2.1 General Considerations

Various documents provide guidance for describing fire scenarios from a technical and regulatory perspective. Most of these documents are "application"-specific; for instance, NFPA 805 defines two general categories of fire scenarios, limiting fire scenarios (LFSs) and maximum expected fire scenarios (MEFSs). The input values necessary to determine the MEFS should be best estimates of the actual parameter values. The input values for the LFS can exceed those which are probable or even possible. The margin between the LFSs and the MEFSs can be used to identify those weaknesses in the analysis that could result in unacceptable effects.

In a Fire PRA, for example, the goal is to quantify the risk contribution from individual scenarios and to identify potential risk-contributing scenarios (e.g., fires impacting important targets in the compartment). Although specific elements in the scenario selection process are "standardized" for guidance and completeness purposes, a certain degree of fire protection engineering judgment is also necessary. NUREG/CR-6850 (EPRI 1011989) contains information on fire frequency, cable (target) selection, heat release rate (HRR), damage criteria, and other information that would be useful in developing fire scenarios.

Selected scenarios should represent a complete set of fire conditions that are important to the fire modeling goal. For example, if the goal of the fire modeling analysis is to estimate whether specific cable(s) will remain free of fire damage, the analyst should examine consider exposures that are close to the cables as well as exposures that are farther away. A small, localized fire exposure could be a greater challenge than a larger fire that is farther away, or vice versa. It may not always be appropriate to select, or at times even possible to define, the worst case fire scenario prior to conducting the analysis, due to the different exposure mechanisms associated with various ignition sources. In large enclosures with a limited number of targets to protect, such as a turbine building in a Pressurized Water Reactor (PWR) when the protection of a safety-related circuit is the fire modeling goal, it is easier to locate the targets of interest and then identify those fire sources capable of affecting that target.

When attempting to characterize the fire scenario, plant walkdowns should be an essential aspect of the scenario selection. Many key decisions relevant to fire modeling, including those related to model selection and input parameters, are influenced by observations made during walkdowns. The occupants, the access level to a particular area, and the fire brigade/fire department access should be observed during the walkdowns, as applicable.

It should also be noted that not all the elements associated with a commercial nuclear plant fire scenario can be directly modeled using the tools within the scope of this guide (e.g., the effect of suppression activities by the fire brigade or the conditions in a space after a sprinkler system has actuated). It is important, however, not to limit the scenario selection and description to those elements that can be modeled.

2.2.2 Enclosure Details

The enclosure details include the identity of the enclosures that belong in the fire model analysis, the physical dimensions of the enclosures included in the fire model, and the boundary materials of each enclosure. The enclosure(s) that belong in the fire model may depend on the fire modeling goal, the complexity and connectivity of the spaces in the general area of interest, the type of analysis conducted (deterministic or probabilistic), and the type of fire model selected. It is possible that no enclosure may be involved, as would be the case for an exterior transformer fire. As a minimum, the space containing the fire would normally be included in the fire model, though treatments involving empirical plume temperature or flame height correlations would not model the enclosure effects per se. Multiple enclosures might be necessary if there are flow connections (natural or forced) to adjacent areas and if the conditions in both areas could affect the analysis results or are of interest. Care should be taken to consider the potential effects of fires in adjacent areas on the targets of interest. In some cases, an HVAC recirculation system may involve areas that are fairly remote from the area of interest. Depending on the type of analysis conducted, the conditions within either or both areas may be of interest, and the fire model would thus include both spaces.

The physical dimensions of the enclosure and the boundary materials are model input and should be determined once the fire model has been selected, since the level of detail varies considerably among the fire models. One-zone models may only require a volume and boundary area; two-zone models will typically require the length, width, and height; and CFD-type models will require details commensurate with the model grid resolution. The determination of the correct physical dimensions and boundary materials are described in Chapter 3 for various types of nuclear power plant fire scenarios.

2.2.3 Fire Location

The location of the fire will depend strongly on the fire modeling goal, the target location, and the fire modeling tool selected. For example, when evaluating the performance of a fire barrier system, fire scenarios challenging the barriers are of interest; when conducting a risk analysis, fire scenarios impacting safety-related circuits may be of primary interest. The selected scenarios for these two applications may not be the same.

When selecting the fire location, the fire scenario should challenge the conditions being estimated. For example, if the goal is to evaluate flame radiation to a target, locating the ignition source relatively far from the target may not provide the best representation of the fire hazards. If the goal is to determine whether a fire can cause two circuits in different raceways to fail, it may be appropriate to locate the fire between the two raceways. There will be situations in which the target location is fixed within the plan area of a space, but there is some flexibility in the vertical placement. A good example of this is an electrical panel fire. For a given electrical panel, the floor position is fixed; however, the base of the fire is not. Depending on the type of panel, it may be appropriate to locate the fire base at the panel floor (e.g., open back and containing thermoplastic cables), at the top (open top and no side vents), or somewhere in

between. EPRI 1019259 (2009) recommends a fire elevation equal to the top of the upper vent or 0.3 m (1 ft) below the panel top for panels meeting certain physical constraints.

In the case of transient fuel package fires or other types of fires that are not fixed, some consideration of the effects of the wall or corner on the upper gas layer temperature is necessary. If the primary exposure mechanism is the Hot Gas Layer (HGL), assuming the fire is located in a corner or near a vertical boundary will produce higher HGL temperatures. However, if the analysis is performed in support of a PRA, then multiple locations should be postulated and the results weighted accordingly. Other features that affect the fire location could include the presence or slope of a floor, particularly when a melting plastic or liquid hydrocarbon fuel is considered and transient fuel packages may be staged on mezzanine levels, scaffolding, or platforms.

The following general guidelines and considerations for locating the fire for different fire exposure mechanisms may be followed as applicable:

- Targets in the fire plume or ceiling jet. Locating a source on top of a cabinet ignition source usually results in the most severe fire conditions, since it assumes that cabinet walls will not affect fire-generated conditions. Furthermore, since the fire is located in the highest possible position, flames are expected to be higher, and temperatures in the plume and ceiling jet will also be high. The user should judge whether this is a conservative assumption based on the goal of the analysis. For example, this would not necessarily be a conservative assumption if detection of the fire was a critical aspect of the analysis.

- Targets affected by flame radiation. Combustible materials that are not fixed, such as transient fuel packages and unconfined liquid spills, should be located so that there is an unobstructed (assuming that no passive fire protection system is credited) view between the source and the target. A horizontal path between flame and target provides the highest heat flux to the target.

- Targets engulfed in flames. Flame height calculations should be performed to determine whether the selected location will result in targets engulfed in flames. Proper justification should be provided as to the location of the fire to ensure that the target is out of the flames. For example, consider the case where the analyst locates the fire on top of an enclosed cabinet, resulting in a cable tray engulfed in flames. This would represent the most severe exposure for the cable tray since the fire is expected to start somewhere inside the cabinet. The analyst may choose to lower the fire's position and ignore the cabinet walls after a visual examination identifies the actual location of the combustibles.

- Targets immersed in the Hot Gas Layer. The fire's elevation may influence how far down the Hot Gas Layer will develop as predicted by some fire models, although other important scenario characteristics will also be influential.

2.2.4 Credited Fire Protection

The fire protection features that will be credited in a fire modeling analysis usually require a fire protection engineering evaluation of the system's effectiveness in performing its design objectives. This may include both an assessment of the system compliance with applicable codes, including maintenance and inspection, and an assessment of the system performance against the particular fire scenario considered. The evaluation should determine whether the

detection, suppression, and/or passive systems can protect the selected target from fire-generated conditions. Once the decision to credit a fire protection system is made, the analyst should specify the type of system selected for the scenario.

There are several common fire protection features that may be present in a typical nuclear power plant area:

- <u>Fire detection systems</u>. These include smoke, heat detectors, or high sensitivity detection systems

- <u>Fire suppression systems</u>. These include automatic or manually activated fixed systems, fire extinguishers, and fire brigades

- <u>Passive fire protection systems</u>. These include structural fire barriers, fire doors, ERFBS's, radiant shields, and fire stops

- <u>Administrative controls</u>. These include combustible or transient-free zones, combustible fuel load limits, and hotwork procedures

When assessing the performance of a system against the postulated fire hazard, it is necessary to consider the conditions under which the system is designed (fire size, fuel load, exposure temperature, plant operation mode, etc.). For example, an ordinary hazard sprinkler system may not have a sufficient water spray delivery to protect against a large hydrocarbon pool fire. Another example would be passive fire protection systems that are rated against an ASTM E119 (2008) fire exposure. Such systems may not provide sufficient fire resistance for a flame impingement fire exposure or a hydrocarbon pool fire scenario. In addition, for active fire protection systems, a valid set of response characteristics of the system are needed.

When crediting a manually actuated fixed suppression system or manual intervention, additional information relating to the occupants, the fire brigade, and the fire department are usually necessary. This may include the means of access to the area considered, the presence of a fire watch, the potential for plant personnel to be in the area, etc.

Notice that the fire modeling tools within the scope of this guide may not have the capability to model the impact of some of the fire protection features that may be credited in a given scenario. Nevertheless, fire protection features are designed to impact the outcome of a scenario, so their effects should be included in the analysis.

2.2.5 Ventilation Conditions

Ventilation conditions collectively refer to the operation of the mechanical ventilation system (e.g., the system will continue in normal operational mode, the system will transfer to smoke purge mode, the system will transfer off with close dampers, etc.) and the position of doors or other openings during the fire event (e.g., doors closed, doors open, doors opening at fire brigade arrival, etc.). Typically, both normal and off-normal ventilation conditions are considered. Spaces in which doors are normally closed may have the doors propped open or opened during the fire by plant personnel, or damaged during the fire. HVAC flows that are normally present in a space may change during the fire due to dampers closing, activation of purge modes, filter plugging, or fan damage by the hot gases. Characterization of the flow field from mechanical devices may be important in some scenarios, especially if the inlet or outlet of the mechanical system is in close proximity to the fire or target.

2.2.6 Target Locations

The target location refers to the physical dimensions of the target relative to the source fire or the fire model coordinate system. These could include the horizontal and vertical distance from the ignition source or source fire or the spatial position within the room itself. It may be necessary to further specify the location of a vulnerable portion of a target, such as the junction box on a service water pump motor. The orientation of the target with respect to the exposure fire may be of interest as well. An elevated target that is exposed only in the vertically upward direction may be susceptible to thermal radiation from an HGL, but possibly shielded from thermal radiation from the source fire itself. Note that in some types of analyses (e.g., a control room abandonment calculation), occupants may be a target.

The fire exposure mechanisms should also be assessed when quantifying the target location. Fire exposure mechanisms, such as flame impingement, fire plume, ceiling jets, HGLs, and/or flame radiation, should be considered based on the relative location of the ignition source, intervening combustibles, and the targets. The subsequent fire model analysis should quantify relevant fire conditions and include a discussion of the proper disposition of those that are not expected to affect the target.

2.2.7 Secondary Combustibles

Secondary combustibles include any combustible materials that, if ignited, could affect the exposure conditions to the target set considered. Intervening combustibles, which are classically assumed to be those combustibles that are located between the ignition source or source fire and the target, are examples of secondary combustibles. However, secondary combustibles would also include combustible materials that are not between the fire and the target but are exposed to the fire effects. In this case, if the secondary combustibles were to ignite, the total heat release rate in the enclosure (if applicable) would increase, resulting in a hotter gas layer, and the radiant energy from the burning secondary combustible would augment the exposure from the initial source fire, regardless of its location.

Secondary combustibles would include both fixed and transient materials. Typical fixed combustibles include exposed cable jackets or cable insulation, combustible thermal insulation, and combustible wall lining materials. Transient combustibles vary considerably from plant to plant and plant area to plant area, but they may include trash containers, waste accumulations, hoses, hand tools, cleaners and solvents, protective clothing, plastic containers, and so on. It is essential to perform a visual survey of an area to obtain an understanding of the types of combustibles present and the activities in the space, which can provide insight into the types of combustibles that may be present from time to time. The combustible load calculations, fire protection procedures, and fire hazards analysis could provide additional details on the nature of fixed and transient fuel packages in a particular plant area.

Combustible materials in sealed or rated containers may be excluded from consideration if the container is capable of resisting the effects of the fire. Some examples include cabinets containing flammable liquids, solid bottom cable trays with fixed top covers, and bus ducts.

Secondary combustibles will take on the characteristics of a target prior to their ignition (see Section 2.2.6). In this regard, the physical location and orientation of the secondary combustibles with respect to both the ignition source and the target set are determined. The performance criterion for a secondary combustible target is the ignition condition, which will

usually be a critical radiant heat flux or exposure temperature or an integrated heat flux. Unlike a true target, once the performance criterion has been met, the secondary combustible is assumed to ignite and then takes on the characteristics of a second source fire (see Section 2.2.8).

2.2.8 Source Fire

The source fire is the forcing function for the fire scenario. As all fire effects are directly related to the characterization of the source fire, great care must be taken in characterizing it. A source fire is often described as the "ignition source," which introduces the concept of having both a fuel package and a credible ignition mechanism. There are many ignition mechanisms in a nuclear power plant; however, ignition sources are typically grouped into electrical panels, transient fuel packages, self-ignited cable trays, hotwork-ignited cable fires, and overheated motors. A deterministic analysis will typically assume that an ignition source is present and treat any combustible material as potentially ignited.

Common fuel packages include electrical panels and transformers, cables, transient combustible material, lubricant reservoirs, and motors. Transient combustibles can vary considerably and may include trash containers, waste accumulations, hoses, hand tools, cleaners and solvents, protective clothing, plastic containers, and so on. It is essential to perform a visual survey of an area to obtain an understanding of the types of combustibles present and the activities in the space, which can provide insight into the types of combustibles that may be present from time to time. The combustible load calculations, fire protection procedures, and the fire hazards analysis could provide additional details on the nature of fixed and transient fuel packages in a particular plant area.

The source fire is typically characterized by a heat release rate, though other important aspects include the physical dimensions of the burning object, its composition, and its behavior when burning. The heat release rate may be specified as a continuous function of time (e.g., a t^2 fire), or it may be an array of heat release rate and time data. Algebraic models may only permit a constant heat release rate. There may be situations in which the heat release rate is a function of the ventilation rather than the object burning. Burning behaviors that may need consideration include whether the material can melt and form a liquid pool, whether it can spread by dripping, and where a liquid could pool.

When fire modeling is used to support a fire PRA, the heat release rate for a source fire may be represented as a frequency distribution. In this case, depending on the type of analysis, a conservative screening value may be selected (e.g., a 98th percentile peak heat release rate), or the effects may be represented using multiple points on the frequency distribution.

As was the case with secondary combustibles, combustible materials in sealed or rated containers may be excluded from consideration if the container is capable of resisting the effects of the fire. In addition, self-ignited cable fires are generally postulated only for non-IEEE-383 qualified power cables (NUREG/CR-6850/ EPRI 1011989).

2.3 Step 3: Select Fire Models

A number of models are available for performing fire simulations. These models range from algebraic models to sophisticated computational fluid dynamics (CFD) computer codes that require days to set up a scenario and perform the associated calculations. Given the availability of different models, the analyst is responsible for understanding the advantages and limitations of a particular model in a specific situation in order to achieve the established goals. In general,

fire models can be classified into three groups: (1) algebraic models, (2) zone models, and (3) CFD models. The level of effort required to describe a scenario and the computational time consumed by each group increase in the order in which they are listed. Table 2-1 provides a summary of the three groups of models, their advantages and disadvantages, and typical applications.

In practical fire modeling applications, it is likely that a combination of all three types of models would be useful for analyzing a specific problem. For example, algebraic models might be used to estimate the radiative flux to a target for determination of a zone of influence or minimum separation distance. A zone model would provide the temperature of the HGL and height as a function of time for evaluating cable temperatures. CFD model calculations could be used to provide more detailed information on fire-induced conditions in areas where the algebraic models and zone models are not conclusive. Complex models can also be used as a means of estimating the degree of conservatism in a simple model analysis.

The first step in selecting a model is to determine whether the scenario can be analyzed using algebraic models, zone models, or CFD models. This guide focuses on the models: FDT^s (NUREG-1805, 2004), FIVE-Rev1 (EPRI 1002981, 2002), CFAST (Jones et al., 2004), MAGIC (Gay et al., 2005), and FDS (McGrattan et al., 2009). The FDT^s and FIVE-Rev1 are a set of relatively simple algebraic models codified in the form of electronic spreadsheets. CFAST and MAGIC represent the class of fire models commonly referred to as zone models, which divide a compartment of interest into two zones, an elevated temperature upper layer and a cool lower layer. FDS is an example of a CFD model, which divide each compartment into thousands or millions of cells. Temperatures and other quantities of interest are calculated for each cell.

Algebraic models can be performed by hand with relatively little computational effort. Karlsson and Quintiere (2000) classify algebraic models into three categories: (1) those that deal with combustion, (2) those that estimate resultant environmental conditions, and (3) those that address heat transfer. Algebraic models related to the combustion process estimate fire intensity based on the flammability characteristics of the fuel. Equations that estimate fire-generated conditions include plume, ceiling jet, and compartment temperatures. Heat transfer equations deal with target temperatures and heat fluxes in the plume, ceiling jet, and lower and upper layer regions.

Zone models are computer algorithms that solve conservation equations for energy and mass. The fundamental assumption associated with zone models is that the enclosure is divided into a limited number of distinct gas zones of uniform properties. In fire applications, the enclosure is usually divided in two zones. The HGL is the volume of smoke generated by the fire and accumulated below the ceiling of the enclosure. This layer is assumed to be homogeneous, and is therefore also assumed to have uniform density and temperature. Its temperature and depth are affected by the amount of mass and energy entering or leaving the volume in each time step during the simulation. The lower layer, which can also experience a temperature increase, is characterized by colder fresh air between the floor and the bottom of the HGL. This layer is also assumed to have uniform density and temperature.

CFD models are sophisticated algorithms that solve a simplified version of the Navier-Stokes equations. To run CFD codes, the enclosure must be divided into a large number of control volumes (perhaps several million), and the equations solved for each control volume. CFD models then provide a detailed estimate of temperature profiles because calculations are performed for each control volume specified in the enclosure. CFD models also handle turbulent gas flows. Another advantage of CFD models is their ability to simulate fire conditions in geometries other than rectangular floor compartments with flat ceilings. Some CFD models

also attempt to estimate HRR values based on flammability properties of fuels provided by the analyst. The drawback of CFD models is the computational time and the level of effort required to set up a scenario, as computational times are usually on the order of days. The time required to set up a problem usually depends on the complexity of the geometry.

Another consideration when selecting a CFD-type model is that the amount of detail supplied to the model is significantly greater than it is for the simpler empirical and zone models. These details could include ductwork, cable trays, electrical panels, and other fixed contents that may be modified, relocated, or removed. In addition, new panels, cable trays, or other fixed contents that would have been included in the fire model had they been present may be added to an area. Although these changes may be minor, at the very least they would require an assessment by a fire modeler as to whether the original analysis is still applicable or the model needs to be adapted for the change. In some situations, such as the determination of a sprinkler actuation time, such small modifications could have a significant effect on the model results.

The Fire Modeling Process

Table 2-1. Summary of Common Fire Model Tools

Fire Model Class	Examples	Typical Applications	Advantages	Disadvantages
Algebraic models	FDT^S FIVE-Rev1	Screening calculations; zone of influence; target damage by thermal radiation, Hot Gas Layer, or thermal plume acting in isolation.	Simple to use; minimal inputs; quick results; ability to do multiple parameter sensitivity studies.	Limited application range; treats phenomena in isolation; typically applicable only to steady state or simply defined transient fires (e.g., proportional to the square of time or t^2 fires).
Zone Model	CFAST MAGIC	Detailed fire modeling in simple geometries; often used to compute hot gas temperatures and target heat fluxes.	Simple to use; couples Hot Gas Layer and localized effects; quick results; ability to do multiple parameter sensitivity studies.	Error increases with increasing deviation from a rectangular enclosure; large horizontal flow paths not well treated.
Computation Fluid Dynamics Model	FDS	Detailed fire modeling in complex geometries, including computing time to target damage and habitability (MCR abandonment or manual action feasibility).	Ability to simulate fire conditions in complex geometries and with complex vent conditions.	Significant effort to create input files and post-process the results; long simulation times; difficult to model curved geometry, smoke detector performance, and conditions after sprinkler actuation.

An important consideration in the fire model selection process is the type of analysis performed. Because of the large number of potential ignition sources in a typical nuclear power plant, it is usually not practical to default to the most sophisticated tool available. Frequently, a series of screening analyses (NUREG/CR-6850/EPRI 1011989) are performed to identify a subset of fire scenarios and targets that require further analysis with greater resolution. The screening process will typically use fairly simple fire modeling tools, such as algebraic models or generic solutions. When such screening is conducted, it is important to remain within the model limitations and the verification and validation (V&V) basis for the screening model. Section 2.3.6 and Chapter 4 provide additional guidance on the significance of the fire model V&V basis and steps that the user should take to ensure that the fire model is used within acceptable limits.

2.3.1 Fire Dynamics Tools (FDT^s)

Fire Dynamics Tools (FDT^s) is a set of algebraic models preprogrammed into Microsoft® Excel® spreadsheets. The FDT^s library is documented in NUREG-1805, "Fire Dynamics Tools (FDT^s): Quantitative Fire Hazard Analysis Methods for the U.S. Nuclear Regulatory Commission Fire Protection Inspection Program" (NUREG-1805, 2004) and Supplement 1 (NUREG-1805 Supplement 1, 2011). The primary objective of the FDT^s library and the accompanying documentation is to provide a methodology for NRC fire protection inspectors to use in assessing potential fire hazards in NRC-licensed NPPs. The methodology uses simplified, quantitative fire hazard analysis techniques to evaluate the potential hazard associated with credible fire scenarios.

The FDT^s library includes a suite of spreadsheets that can be used to calculate various fire parameters under varying conditions. Documentation of the theoretical bases underlying the equations used in the FDT^s spreadsheets helps to ensure that users understand the significance of the inputs that each spreadsheet requires, and why a particular spreadsheet should (or should not) be selected for a specific analysis. The governing equations and assumptions for FDT^s are well established within the fire science community and are documented in handbooks and scientific publications, such as the *NFPA Fire Protection Handbook* (NFPA Handbook, 2008), the *SFPE Handbook of Fire Protection Engineering* (SFPE Handbook, 2008), and other fire science literature.

The complete list of spreadsheets included in the FDT^s library is shown in Table 2-2. A number of the calculation methods included in the FDT^s were part of the V&V study conducted by the NRC, EPRI, and NIST (NUREG-1824 Vol. 3, EPRI 1011999, 2007). The NRC maintains a website at http://www.nrc.gov/reading-rm/doc-collections/nuregs/staff/sr1805/final-report/index.html, where both new and updated spreadsheets are posted.

Table 2-2. Routines included in the FDT^s

Function Name	Description
02.1_Temperature_NV.xls	**Chapter 2.** Predicting Hot Gas Layer Temperature and Smoke Layer Height in a Compartment Fire with Natural Ventilation (Compartment with Thermally Thick/Thin Boundaries) Method of McCaffrey, Quintiere, and Harkleroad (MQH)
02.2_Temperature_FV.xls	**Chapter 2.** Predicting Hot Gas Layer Temperature in a Compartment Fire with Forced Ventilation (Compartment with Thermally Thick/Thin Boundaries) Method of Foote, Pagni, and Alvares (FPA) Method of Deal and Beyler
02.3_Temperature_CC.xls	**Chapter 2.** Predicting Hot Gas Layer Temperature in a Compartment Fire with Door Closed (Compartment has Sufficient Leaks to Prevent Pressure Buildup; leakage is Ignored) Method of Beyler
03_HRR_Flame_Height_Burning_Duration_Calculation.xls	**Chapter 3.** Estimating Burning Characteristics of Liquid Pool Fire, HRR, Burning Duration and Flame Height
04_Flame_Height_Calculations.xls	**Chapter 4.** Estimating Wall Fire Flame Height, Line Fire Flame Height Against the Wall, and Corner Fire Flame Height
05.1_Heat_Flux_Calculations_Wind_Free.xls	**Chapter 5.** Estimating Radiant Heat Flux from Fire to a Target Fuel *Wind-Free Condition* Point Source Radiation Model (Target at Ground Level) Solid Flame Radiation Model (Target at Ground Level) Solid Flame Radiation Model (Target Above Ground Level)
05.2_Heat_Flux_Calculations_Wind.xls	*Presence of Wind* Solid Flame Radiation Model (Target at Ground Level) Solid Flame Radiation Model (Target Above Ground Level)
05.3_Thermal_Radiation_From_Hydrocarbon_Fireballs.xls	Estimating Thermal Radiation from Hydrocarbon Fireballs
06_Ignition_Time_Calculations.xls	**Chapter 6.** Estimating the Ignition Time of a Target Fuel Exposed to a Constant Radiative Heat Flux Method of Estimating Piloted Ignition Time of Solid Materials Under Radiant Exposures Method of (1) Mikkola and Wichman, (2) Quintiere and Harkleroad, and (3) Janssens Method of Estimating Piloted Ignition Time of Solid Materials Under Radiant Exposures; Method of Toal, Silcock, and Shields Method of Estimating Piloted Ignition Time of Solid Materials Under Radiant Exposures; Method of Tewarson
07_Cable_HRR_Calculations.xls	**Chapter 7.** Estimating Full-Scale Heat Release Rate of a Cable Tray Fire
08_Burning_Duration_Soild.xls	**Chapter 8.** Estimating Burning Duration of Solid Combustibles
09_Plume_Temperature_Calculations.xls	**Chapter 9.** Estimating Centerline Temperature of a Buoyant Fire Plume

Function Name	Description
10_Detector_Activation_Time.xls	Estimating Detector Response Time **Chapter 10.** Estimating Sprinkler Response Time **Chapter 11.** Estimating Smoke Detector Response Time **Chapter 12.** Estimating Heat Detector Response Time

13_Compartment_Flashover_Calculations.xls	**Chapter 13.** Predicting Compartment Flashover
	Compartment Post-Flashover Temperature: Method of Law
	Minimum Heat Release Rate
	    Required to Compartment Flashover:
	    Method of (1) McCaffrey, Quintiere, and Harkleroad (MQH);
	    (2) Babrauskas; and (3) Thomas

14_Compartment_Over_Pressure_Calculations.xls	**Chapter 14.** Estimating Pressure Rise Attributable to a Fire in a Closed Compartment
15_Explosion_Claculations.xls	**Chapter 15.** Estimating the Pressure Increase and Explosive Energy Release Associated with Explosions
16_Battery_Compartment_Flammable_Gas_Conc.xls	**Chapter 16.** Calculating the Rate of Hydrogen Gas Generation in Battery Compartments Method of Estimating Hydrogen Gas Generation Rate in Battery Compartments Method of Estimating Flammable Gas and Vapor Concentration Buildup in Enclosed Spaces Method of Estimating Flammable Gas and Vapor Concentration Buildup Time in Enclosed Spaces

17.1_FR_Beams_Columns_Substitution_Correlation.xls
 	
17.2_FR_Beams_Columns_Quasi_Steady_State_Spray_Insulated.xls
 	
17.3_FR_Beams_Columns_Quasi_Steady_State_Board_Insulated.xls
 	
17.4_FR_Beams_Columns_Quasi_Steady_State_Uninsulated.xls
	Chapter 17. Calculating the Fire Resistance of Structural Steel Members
	
	Algebraic models:
	    Beam Substitution Correlation (Spray-Applied Materials)
	    Column Substitution Correlation (Spray-Applied Materials)
	    Heat Transfer Analysis using Numerical Methods Protected Steel Beams and Columns (Spray-Applied)
	
	Heat Transfer Analysis using Numerical Methods Protected Steel Beams and Columns (Board Materials)
	
	Heat Transfer Analysis using Numerical Methods Unprotected Steel Beams and Columns

18_Visibility_Through_Smoke.xls	**Chapter 18.** Estimating Visibility Through Smoke
19_THIEF_of_Cables_Calculation.xls	**Chapter 19.** Estimating the Thermally-Induced Electrical Failure (THIEF) of Electrical Cables

2.3.2 FIVE-Rev1

In August 2002, the Electric Power Research Institute (EPRI) published the *Fire Modeling Guide for Nuclear Power Plant Applications* (EPRI 1002981, 2002) for the first time. Since then, it has provided fire protection engineers in the commercial nuclear industry with a broad overview of fire modeling theory and applications, including representative calculations performed with various state-of-the-art fire models. With this guide, EPRI included a library of preprogrammed Microsoft® Excel® equations, which are used to estimate some aspects of fire-induced

conditions. This collection of algebraic models/algebraic models is referred to as the Fire-Induced Vulnerability Evaluation model (FIVE-Rev1). In general, the equations in the library are closed-form analytical expressions that can be solved by hand. The capabilities of the various equations in the library include predicting temperature and convective heat fluxes in the fire plume or ceiling jet, irradiated heat flux, upper-layer temperature, time to detection, and target heating, among others. Some of the equations in FIVE were included in the V&V study (NUREG-1824 vol. 4, EPRI 1011999, 2007). Like the FDT^s, several of the equations used in the examples have not been subject to V&V. Subsequent efforts will be directed at V&V of these equations and models. The calculations included in the FIVE-Rev1 are summarized in Table 2-3.

Table 2-3. Routines included in FIVE-Rev1

Function	Description
Qf	Heat release rate profile considering t^2 growth and four stages.
Firr	Estimates flame irradiation a distance r from the fire source. Point source approximation for REMOTE targets.
FHeight	Flame height based on Heskestad's flame height correlation.
TpAlpert	Plume temperature at a specific height based on Alpert plume temperature correlation.
TpMcCaffrey	Plume temperature at a specific height based on McCaffrey plume temperature correlation.
TpHeskestad	Plume temperature at a specific height based on Heskestad plume temperature correlation.
Plcflux	Estimates convective heat flux in the fire plume.
VpAlpert	Plume velocity at a specific height based on Alpert's plume temperature correlation.
VpMcCaffrey	Plume velocity at a specific height based on McCaffrey plume temperature correlation.
VpHeskestad	Plume velocity at a specific height based on Heskestad plume temperature correlation.
EpZukoski	Air entrainment into plume based on Zukoski plume entrainment correlation.
EpThomas	Air entrainment into plume based on Thomas plume entrainment correlation.
EpHeskestad	Air entrainment into plume based on Heskestad plume entrainment correlation.
PdHeskestad	Estimates plume diameter based on Heskestad's plume correlation.
TcjAlpert	Unconfined ceiling jet temperature based on Alpert ceiling jet correlation.
TcjDelichatsios	Confined ceiling jet temperature based on Delichatsios ceiling jet correlation.
Cjcflux	Estimates convective heat flux in the ceiling jet.
VcjAlpert	Unconfined ceiling jet velocity based on Alpert ceiling jet correlation.
MQHTemperature	Compartment temperature after a specified time, given a steady HRR based on MQH approach.
MQHFlashover	Heat release rate required for flashover after a specified time based on MQH approach.
FiveTemp	Estimates compartment temperature based on FIVE.
Detact	Activation time of heat detection devices based on heat release rate profiles.
Aset	Time required by Hot Gas Layer to reach a specific height based on heat release rate profiles and openings at the bottom of the enclosure.
CThrr	Estimates heat release rate from cable trays. The correlation is based on 14 experiments with a stack of 12 horizontal cable trays and 2 experiments with a combination of 12 horizontal cable trays and 3 vertical trays.
Visib	Estimates the length of a visible path in a smoke environment. The correlation applies to light-reflecting signs.
Ttar	Estimates target temperature under constant heat flux.
Ttdam	Time to target damage under constant heat flux.

2.3.3 Consolidated Fire Growth and Smoke Transport (CFAST) Model

CFAST is a two-zone computer fire model. For a given fire scenario, the model subdivides a compartment into two control volumes, which include a relatively hot upper layer (i.e., the HGL) and a relatively cool lower layer. In addition, mass and energy are transported between the layers via the fire plume and mixing at the vents. By contrast, combustion products accumulate via the plume in the HGL. Each layer has its own energy and mass balances. The most important assumption for the model is that each zone has uniform properties, that is, that the temperature and gas concentrations are constant throughout the zone, only changing as a function of time. The CFAST model describes the conditions in each zone by solving equations for conservation of mass, species, and energy, along with the ideal gas law. The Technical Reference Guide for CFAST (Jones et al., 2004) provides a detailed discussion concerning the specific derivation of these conservation laws. Documentation for CFAST also includes a User's Guide (Peacock et al., 2008b), which details the use of the model, and a Model Development and Evaluation Guide (Peacock et al., 2008a), which presents the latest model V&V results.

For some applications, including long hallways or tall shafts, the two-zone assumption may not be appropriate. To address this, CFAST includes empirical algorithms to simulate smoke flow and filling in long corridors and for a single well-mixed volume in tall shafts. CFAST also includes several correlations (as sub-models), based on experimental data that are used to calculate various physical processes during a fire scenario: smoke production, fire plume dynamics, heat transfer by radiation, convection, conduction, natural flows through openings (vertical and horizontal), forced or natural ventilation, thermal behavior of targets, heat detectors, and water spray from sprinklers.

CFAST models horizontal flow through vertical vents (doors, windows, wall vents, etc), vertical flow through horizontal vents (ceiling holes, hatches, roof vents, etc), and mechanical ventilation through fans and ductwork. Natural flow is determined by the pressure difference across a vent, using Bernoulli's law for horizontal vent flow, and by algebraic models for vertical vent flow. Mechanical ventilation is based on an analogy to electrical current flow in series and parallel paths where flow is split in parallel paths proportional to the flow resistance in each path and resistance to flow is additive for paths in series.

CFAST includes algorithms to account for radiation, convection, and conduction within a modeled structure. Radiative transfer occurs among the fire(s), gas layers, and compartment surfaces (ceiling, walls, and floor). It is a function of the temperature differences and emissivity of the gas layers, as well as the compartment surfaces. Convective heat transfer between gas layers and compartment or target surfaces is based on typical correlations available in the literature. CFAST uses a finite difference scheme that utilizes a non-uniform spatial mesh to advance the wall temperature solution consistent with the flux conducted into the wall (calculated using Fourier's law). The V&V results for CFAST are documented in Volume 5 of NUREG-1824 (EPRI 1011999). Additional validation results, particularly for plume temperature predictions that were not included in the NUREG-1824 (EPRI 1011999) results, are included in the CFAST Model Development and Evaluation Guide (Peacock et al., 2008a).

2.3.4 MAGIC

MAGIC is also a two-zone computer fire model, developed and maintained by Electricité de France (EdF) specifically for use in NPP analysis. MAGIC is supported by three EdF publications, including (1) the technical manual, which provides a mathematical description of

the model (Gay et al., 2005b); (2) the user's manual, which details how to use the graphical interface (Gay et al., 2005a); and (3) the validation studies, which compare MAGIC's results to experimental measurements (Gay et al., 2005c). These three proprietary publications are available through EPRI to EPRI members. In addition, V&V results for MAGIC are documented in Volume 6 of NUREG-1824 (EPRI 1011999).

MAGIC is fundamentally the same type of model as CFAST and thus solves the same basic set of differential equations. The combustion model and vent flow models are similar as well. Despite this, MAGIC still differs from CFAST in that it does not have the corridor or shaft sub-models, and the ceiling jet and wall jet treatments are different. The user should consult the technical manual for a complete description of the MAGIC sub-models (Gay et al., 2005b).

Once a given simulation is completed, MAGIC generates an output file with all of the solution variables. Through a "post-processor" interface, the user selects the relevant output variables for the analysis. Typical outputs include the temperatures of hot and cold zones, concentrations of oxygen and unburned gases, smoke migration into each compartment, the mass flow rates of air and smoke through the openings and vents, the pressures at the floor level of each compartment, the temperatures at the surfaces of the walls, and the thermal fluxes (radiative and total) exchanged by the targets placed by the user.

2.3.5 Fire Dynamics Simulator (FDS)

FDS (McGrattan et al., 2007) is a CFD model of fire-driven fluid flow. The model numerically solves a form of the Navier-Stokes equations appropriate for low-speed, thermally driven flow, with an emphasis on smoke and heat transport from fires. The partial derivatives of the equations for conservation of mass, momentum, and energy are approximated as finite differences, and the solution is updated in time on a three-dimensional, rectilinear grid. Thermal radiation is computed using a finite volume technique on the same grid as the flow solver. Lagrangian particles are used to simulate smoke movement and sprinkler discharge. FDS computes the temperature, density, pressure, velocity, and chemical composition within each numerical grid cell at each discrete time step. There are typically hundreds of thousands to several million grid cells, and thousands to hundreds of thousands of time steps. In addition, FDS computes the temperature, heat flux, mass loss rate, and various other quantities at solid surfaces.

Time histories of various quantities at a single point in space, or global quantities, such as the fire's HRR, are saved in simple, comma-delimited text files that can be plotted in a spreadsheet program. However, most field or surface data are visualized with a program called Smokeview, a tool specifically designed to help analyze results generated by FDS. FDS and Smokeview are used in concert to model and visualize fire phenomena. Smokeview does this by presenting animated tracer particle flow, animated contour slices of computed gas variables, and animated surface data, and also presents contours and vector plots of static data anywhere within a scene at a fixed time. The FDS User's Guide (McGrattan et al., 2007) provides a complete list of FDS output quantities and formats, while the Smokeview User's Guide (Forney, 2008) explains how to visualize the results of an FDS simulation. Volume 7 of NUREG-1824 (EPRI 1011999) contains the results of V&V efforts for FDS. Additional V&V results for FDS are contained in the FDS documentation series (McGrattan et al., 2007).

FDS solves conservation equations of mass, momentum, and energy for an expandable mixture of ideal gases in the low Mach number limit. This means that the equations do not permit acoustic waves, the result of which is that the time step for the numerical solution is bounded by the flow speed, rather than the sound speed. Situations in which this limitation may be

The Fire Modeling Process

encountered include jet fires, deflagrations, and detonations. The assumption also reduces the number of unknowns by one, as density and temperature can be related to a known background pressure. Flow turbulence is treated by large eddy simulation.

For most simulations, FDS uses a mixture fraction combustion model. The mixture fraction is a conserved scalar that represents, at a given point, the mass fraction of gases originating in the fuel stream. In short, the combustion is assumed to be controlled by the rate at which fuel and oxygen mix. Unlike versions of FDS prior to 5, the reaction of fuel and oxygen is not necessarily instantaneous and complete, and there are several optional schemes that are designed to estimate the extent of combustion in underventilated spaces. The mass fractions of all of the major reactants and products can be derived from the mixture fraction by means of "state relations," expressions arrived at by a combination of simplified analysis and measurement. The combustion model used by FDS is an area of active development. Consequently, FDS users should consult the latest code documentation for a description of new features or sub-models.

Numerical parameters play a very important role in a CFD model like FDS. A numerical parameter is any input value that is needed for the mathematical solution of the equations, but has little or no physical meaning. For example, the time step with which the numerical solution of the HGL temperature is computed does have units of seconds, but it is not a value that has meaning outside of that particular algorithm; nevertheless, these numerical parameters can affect the solution, and their sensitivity should be assessed in some way. For the spreadsheet and zone models, this procedure is relatively straightforward because the calculations run in less than a minute. One simply varies the value and ensures that the solution does not change appreciably. Specifically, one should simply demonstrate that the solution *converges* towards a particular value as the parameter is varied; for instance, using a smaller and smaller time step ought to lead to convergence of any evolution equation.

The numerical parameter in FDS that has the greatest importance is cell size. CFD models solve an approximate form of the conservation equations of mass, momentum, and energy on a numerical grid. The error associated with the discretization of the partial derivatives is a function of the size of the grid cells and the type of differencing used. FDS uses second-order accurate approximations of both the temporal and spatial derivatives of the Navier-Stokes equations, meaning that the discretization error is proportional to the square of the time step or cell size. In theory, reducing the grid cell size by a factor of 2 reduces the discretization error by a factor of 4; however, it also increases the computing time by a factor of at least 16 (a factor of 2 for the temporal and each spatial dimension). Clearly, there is a point of diminishing returns as one refines the numerical mesh. Determining which size grid cell to use in any given calculation is known as a *grid sensitivity study.*

Determining an optimal grid size in FDS is usually a matter of assessing the size of the fire. The physical diameter of the fire is not always a well-defined property; a compartment fire does not have a well-defined diameter, whereas a circular pan filled with a burning liquid fuel has an obvious diameter. Regardless, it is not the physical diameter of the fire that matters when assessing the "size" of the fire, but rather its characteristic diameter, D^*:

$$D^* = \left(\frac{\dot{Q}}{\rho_\infty c_p T_\infty \sqrt{g}}\right)^{2/5} \tag{2-1}$$

where $\dot{Q}$ is the fire heat release rate (kW), ρ_∞ is the ambient density of air (kg/m^3), c_p is the specific heat of air (kJ/kg/K), T_∞ is the ambient air temperature (K), and g is the acceleration of gravity (m/s^2).

In many instances, D^* is comparable to the physical diameter of the fire. FDS employs a numerical technique known as large eddy simulation (LES) to model the unresolvable or "sub-grid" motion of the hot gases. The effectiveness of the technique is largely a function of the ratio of the fire's characteristic diameter, D^*, to the size of a grid cell, δx. In short, the greater the ratio $D^*/\delta x$, the more the fire dynamics are resolved directly, and the more accurate the simulation. Past experience has shown that a ratio of 5 to 10 usually produces favorable results at a moderate computational cost for problems where gross smoke movement is of interest.

As an example, suppose the HRR of the fire were 700 kW. The characteristic diameter may then be calculated as follows:

$$D^* = \left(\frac{700 \text{ kW}}{1.2 \text{ kg/m}^3 \times 1.012 \text{ kJ/kg/K} \times 293 \text{ K } \sqrt{9.81 \text{ m/s}^2}} \right)^{2/5} = 0.63 \text{ m} \qquad (2\text{-}2)$$

To perform a grid sensitivity analysis, a good place to start might be 15 cm (6 in), which means that $D^*/\delta x = 5$. Then choose a grid of 10 cm (4 in), and then 5 cm (2 in). At this point, the calculation time will have increased by a factor of roughly 300, making it potentially impractical to compute; however, if it can be shown that there is little difference between the 5 cm and 10 cm grids, then the objective has been achieved. The meaning of "little difference" can be interpreted in several ways. Given that NUREG-1824 (EPRI 1011999), the fire model V&V study, lists the relative error expected of the various models for the various quantities, it is reasonable to interpret the difference in results on different grids in light of what is expected of the model accuracy.

Although the fire size and dimensions often determine the optimum grid resolution, there are other factors that can influence the selection of the grid resolution. These include the number of cells used to resolve a flow path dimension, the number of cells used to describe the fire dimension, and the number of cells used to resolve the conditions in a partially isolated volume. These considerations are related in that it is generally advisable to include at least three cells across any flow path, such as a door or a window, and fire dimension, regardless of the minimum number of cells computed using the fire characteristic diameter. In some cases, partially isolated volumes are created by various obstructions; if the temperature and flow conditions are of interest in these areas, a minimum of three cells across any dimension should be provided. Another consideration that could influence the grid resolution is the dimension of the obstructions that are expected to influence the result. For example, if it is necessary to quantitatively assess the effect that various conduits and light fixtures may have on the actuation time of a nearby sprinkler, the maximum grid resolution would be comparable to the dimensions of the smallest distinct obstruction included in the model.

FDS input files are frequently created with the assistance of preprocessing software, which may include commercial software packages that can create input files for FDS, drawings, spreadsheet tools created by a user to insert obstructions or create stair-step approximations, and curved geometry. This type of software can reduce the tediousness of creating the geometric representation of a space, but is not part of the FDS model. Any input files created by such software should be carefully checked by the user to ensure that the geometry or boundary data are exactly as intended.

2.3.6 Verification and Validation

The use of fire models to support fire protection decision making requires a good understanding of their limitations and predictive capabilities. NFPA 805 states that fire models shall only be applied within the limitations of the given model and shall be verified and validated. To support risk-informed/performance-based fire protection and implementation of the voluntary rule that adopts NFPA 805 as an RI/PB alternative, the NRC's Office of Nuclear Regulatory Research (RES) and the Electric Power Research Institute (EPRI) conducted a collaborative project for V&V of the five selected fire models described in Sections 2.3.1 through 2.3.5. The National Institute of Standards and Technology (NIST) was also an important partner in this project. The results of this project were documented in NUREG-1824 (EPRI 1011999), Verification and Validation of Selected Fire Models for Nuclear Power Plant Applications.

The parameters for which NUREG-1824 (EPRI 1011999) provide V&V information are shown in Table 2-4. Not all output parameters are available in all models. The information in Table 2-4 may be a useful element to consider when selecting the appropriate fire model tool. For example, it is clear that the libraries of algebraic models (FDT^s, FIVE-Rev1) have limited capabilities when compared to the zone and CFD models. These libraries do not have appropriate methods for estimating many of the fire scenario attributes evaluated in this study. The correlations that the libraries do contain are typically empirically deduced from a broad database of experiments; they are based on fundamental conservation laws, and have gained a considerable degree of acceptance in the fire protection engineering community. However, because of their empirical nature, they are subject to many limiting assumptions. The user must be cautious when using these tools.

CFD model predictions can be more accurate in complex scenarios; however, the time it takes to obtain and understand a prediction may also be an important consideration in the decision to use a particular model for a specific scenario. FDS is computationally expensive in all respects (preprocessing, simulation, and post-processing), and, while the two-zone models produce answers in seconds to minutes, FDS provides comparable answers in days to weeks. In general, FDS is better suited to estimate fire environments within more complex configurations.

The fire experiments selected for inclusion in the V&V were limited to high-quality, real-scale experiments with direct applicability to nuclear power plant applications. As it was not possible to consider all possible NPP applications, a method for determining the applicability of validation results to other specific NPP fire scenarios has been described in NUREG-1824 vol. 1 (EPRI 1011999). The applicability of the validation results is determined using normalized parameters traditionally used in fire modeling applications. Normalized parameters allow users to compare results from scenarios of different scales by normalizing the physical characteristics of the scenarios.

Table 2-4. Fire Modeling Attributes Included in NUREG 1824/EPRI 1011999 (2007)

Fire Modeling Attributes	Fire Model				
	FDT	FIVE-Rev1	CFAST	MAGIC	FDS
Hot Gas Layer (HGL) Temperature	YES	YES	YES	YES	YES
Hot Gas Layer (HGL) Height	NO	NO	YES	YES	YES
Ceiling Jet Temperature	NO	YES	YES	YES	YES
Plume Temperature	YES	YES	NO	YES	YES
Flame Height	YES	YES	YES	YES	YES
Radiated Heat Flux to Targets	YES	YES	YES	YES	YES
Total Heat Flux to Targets	NO	NO	YES	YES	YES
Total Heat Flux to Walls	NO	NO	YES	YES	YES
Wall Temperature	NO	NO	YES	YES	YES
Target Temperature	NO	NO	YES	YES	YES
Smoke Concentration	NO	NO	YES	YES	YES
Oxygen Concentration	NO	NO	YES	YES	YES
Room Pressure	NO	NO	YES	YES	YES

The Fire Modeling Process

Table 2-5 lists selected normalized parameters that may be used to compare NPP fire scenarios with validation experiments. This table was derived from NUREG-1824 (EPRI 1011999), Table 2-4 and is intended to provide guidance on which groups of validation experiments to consider when evaluating a certain attribute based on the validation results. These parameters may not be the only ones appropriate for evaluating the applicability of a specific experiment; Table 2-5 of NUREG-1824 (EPRI 1011999), vol. 1 lists the ranges of values for different physical characteristics and normalized parameters based on the experiments considered in the validation study.

For a given set of experiments and NPP fire scenarios, the user can calculate the relevant normalized parameters. If the fire scenario parameters fall within the ranges evaluated in the study, then the results of the study offer appropriate validation for the scenario. If they fall outside the range, then a validation determination cannot be made based on the results from the study. For any given fire scenario, more than one normalized parameter may be necessary for determining the applicability of the validation results.

The V&V study provides valuable insight into the predictive capability of the five fire models. This insight is ultimately characterized in terms of a bias and a standard deviation for a number of output parameters. The closer the bias is to unity, the more accurate the fire model is at predicting the given parameter, on average. The smaller the standard deviation, the smaller the expected scatter about the mean bias. Section 4 of this guide describes how the V&V uncertainty information can be used to assign a probability function to the output data.

NUREG-1824 (EPRI 1011999) provides verification and validation documentation for specific versions of fire models. Because the fire models considered are under active development, new releases occur and are expected. The user has the option of using the model version that has been verified and validated in NUREG-1824 (EPRI 1011999) or re-evaluating cases in NUREG-1824 (EPRI 1011999) to demonstrate that the predictive capability of the model has not decreased for the application at hand. It is expected that NUREG-1824 (EPRI 1011999) will be updated from time to time as the need arises.

Table 2-5. Selected Normalized Parameters for Application of the Validation Results to NPP Fire Scenarios (NUREG-1824/EPRI 1011999, 2007)

Quantity	Normalized Parameter	General Guidance	Validation Range
Fire Froude Number	$$\dot{Q}^* = \frac{\dot{Q}}{\rho_\infty c_p T_\infty D^2 \sqrt{gD}}$$	Ratio of characteristic velocities. A typical accidental fire has a Froude number of order 1. Momentum-driven fire plumes, like jet flares, have relatively high values. Buoyancy-driven fire plumes have relatively low values.	0.4 – 2.4
Flame Length, L_f, relative to Ceiling Height, H	$$\frac{L_f}{H}$$ $$\frac{L_f}{D} = 3.7\,\dot{Q}^{*2/5} - 1.02$$	A convenient parameter for expressing the "size" of the fire relative to the height of the compartment. A value of 1 means that the flames reach the ceiling.	0.2 – 1.0
Ceiling Jet Radial Distance,r_{cj}, relative to the Ceiling Height, H	$$\frac{r_{cj}}{H}$$	Ceiling jet temperature and velocity correlations use this ratio to express the horizontal distance from target to plume.	1.2 – 1.7
Equivalence Ratio, φ, as an indicator of the Ventilation Rate	$$\varphi = \frac{\dot{m}_F/\dot{m}_{O_2}}{r}$$ $$\dot{m}_F = \dot{Q}/\Delta H$$ $$\dot{m}_{O_2} = \begin{cases} 0.23 \times \frac{1}{2} A_0 \sqrt{H_0} & \text{(Natural)} \\ 0.23\, \rho_\infty \dot{V} & \text{(Mechanical)} \end{cases}$$	The equivalence ratio relates the mass loss rate of fuel, $\dot{m}_F$, to the mass flow rate of oxygen into the compartment, $\dot{m}_{O_2}$. The fire is considered over or underventilated based on whether φ is less than or greater than 1, respectively. The parameter, r, is the stoichiometric ratio.	0.04 – 0.6
Compartment Aspect Ratio	L/H or W/H, where L is the Length, W is the Width, and H is the Height of the compartment.	This parameter indicates the general shape of the compartment.	0.6 – 5.7
Radial Distance, r, relative to the Fire Diameter, D	$$\frac{r}{D}$$	This ratio is the relative distance from a target to the fire. It is important when calculating the radiative heat flux.	2.2 – 5.7

2.3.7 Fire Modeling Parameters Outside the Validation Range

The development of the sample problems documented in the appendices to this report suggests that many commercial nuclear power plant fire modeling applications can fall outside the range of applicability of the validation study documented in NUREG-1824 (EPRI 1011999). The primary reason for this is that the range of applicability, as defined by the dimensionless parameters, is governed by the experiments selected for the validation study. The selected experiments are representative of various types of spaces in commercial nuclear power plants but do not encompass all possible geometries or applications. There will thus be many areas or applications that will fall outside this application range. It is the consensus opinion of this guide's writing team that the predictive capabilities of the fire models in specific scenarios can extend beyond the range of applicability defined in NUREG-1824 (EPRI 1011999). Nevertheless, additional analysis would be required to address situations where some of the analysis parameters fall outside the range of applicability defined in NUREG-1824 (EPRI 1011999). This section describes the recommended strategies for addressing this situation.

2.3.7.1 Sensitivity Analysis

In the context of applicability of validation results, sensitivity analysis refers to varying selected input parameters in the "conservative" direction so that they fall within the applicability range. If the fire modeling conclusions are not affected by the variations in the parameters, the analyst may use the sensitivity analysis results to further justify the conclusions. Based on the dimensionless terms listed above, the following sensitivities could be evaluated:

1. Froude number: The two parameters that can be practically varied are the fire diameter and the heat release rate. For fire sizes (i.e., heat release rates) that are small for the postulated diameter, the resulting Froude number can fall under the low end of the applicability range. Similarly, for fire sizes that are relatively large for the postulated diameter, the Froude number can fall above the applicability range. In the former situation, the analysts may consider reducing the fire diameter and keeping the heat release rate profile unchanged. In most fire modeling tools, the fire diameter is simply used for determining heat release rates or for calculating the fire plume conditions, such as the flame height or plume temperature. Considering that the heat release rate is "fixed" in this sensitivity study, the fire diameter may not be a relevant parameter in the analysis, with the important exception of scenarios where the fire plume conditions are relevant. A similar approach could be used for the latter situation. Increasing the fire diameter can "force" the dimensionless term into range. It should be stressed that fire diameter is often a parameter that influences predicted flame height and fire plume conditions, and that the effects of diameter variations should be explicitly address in the analysis. This includes other dimensionless terms where the fire diameter is a key input (e.g., target distance to diameter (r/D), etc.).

2. Flame length relative to ceiling height: This is a convenient parameter for expressing the "size" of the fire relative to the height of the compartment. A value of 1 means that the flames reach the ceiling. The validation range extends up to a value of 1.0, which should cover most of the scenarios of interest in commercial nuclear plants. Scenarios that are expected out of the range are:
   a. Those associated with relatively short flames. Typical ceiling heights in power plant scenarios range from about 10' to 20' (excluding the containment and turbine

buildings, which have relatively large openings between elevations). Consequently, flame lengths shorter than 2' to 4' will be considered out of validation range. A sensitivity analysis increasing the heat release rate values should provide a conservative estimate of fire conditions within the validation range. In cases where the conclusion of the analysis does not change given the increased fire intensity (e.g., no damage within the flame length of fire plume), the suggested sensitivity analysis can be used as the justification for the evaluation of a compartment that falls outside the validation range.

b. Flame extensions under ceilings. In this particular case, not only are such flame lengths out of the range of validation, but also the models for predicting this phenomenon have not been verified or validated with a process similar to the one documented in NUREG-1824 (EPRI 1011999).

3. Ceiling Jet Radial Distance relative to the Ceiling Height: Ceiling jet temperature and velocity correlations use this ratio to express the horizontal distance from target to plume. Ceiling jet applications in commercial nuclear power plants should be carefully evaluated due to the numerous obstructions near the ceiling (e.g., cable trays, HVAC ducts, piping, etc.). Most of its applications include determination of time to detection and sprinkler activation, in which the ceiling jet velocity is a sub-model in the analysis. An alternative option is a sensitivity analysis consisting of moving the fire location to distances that would fall within the validation range; it is recognized, however, that in many situations the fire location cannot be altered, particularly in the case of fixed ignition sources or transient fires postulated near "pinch-points." In general, longer horizontal distances will result in longer activation time results; by contrast, shorter horizontal distances would result in "conservative" time-to-damage results.

4. Equivalence Ratio, ϕ, as an indicator of the Ventilation Rate: The validation available is for well-ventilated fires. That is, no model validation information is available for under ventilated compartment fires, including fire extinction due to lack of oxygen. In general, assuming that fires are well ventilated in the enclosure should result in bounding conditions as long as the heat release rate profile is appropriate. The underlying consideration is that conditions in the enclosure are not expected to be worse in a fire where the combustion process is affected by lack of oxygen than they would be under fire conditions where the combustion process is assumed unaffected. It should be noted that this assumption must be invoked with caution, as sudden air inflows into closed/under ventilated fire conditions could produce relatively severe fire conditions.

5. Compartment Aspect Ratio: It is expected that some compartments in the commercial nuclear plants would have geometric characteristics outside the validation range (e.g., relatively long/narrow corridors with high ceilings, etc.). These parameters are important in fire scenarios involving Hot Gas Layer calculations, as the size and configuration of the compartment are important input parameters. Clearly, these parameters should not be applicable in scenarios where the enclosure conditions are not considered, such as flame radiation calculations using the point source model and plume temperature calculations using semi-algebraic models where it has been determined that enclosure conditions are not a factor. As part of the sensitivity analysis, the analyst may consider "shortening" the length, width, or height of the compartment to values that fall within the validation range under the expectation that this will result in an elevated level of hazardous fire-generated conditions as predicted by the model (i.e., a conservative calculation). In cases where the conclusion of the analysis does not change given the "smaller" compartment (e.g., the Hot

Gas Layer temperature does not exceed damage threshold of cables in either case), the suggested sensitivity analysis can be used as the justification for the evaluation of a compartment that falls outside the validation range.

6. Radial Distance, r, relative to the Fire Diameter: This ratio is the relative distance from a target to the fire, and is important when calculating the radiative heat flux. Notice that the validation range starts at a distance approximately twice the length of the fire diameter. In practice, targets at very close distance (approximately less than two fire diameters from the fire) to the fire should be expected to fail given the relatively low damage threshold levels for cables. An alternative option is a sensitivity analysis consisting of moving the fire location to distances that would fall within the validation range; it is recognized, however, that in many situations the fire location cannot be altered, particularly in the case of fixed ignition sources or transients fires postulated near "pinch-points." In general, shorter horizontal distances will result in higher heat flux levels.

2.3.7.2 Additional Validation Studies

There are, of course, other fire model validation studies besides NUREG-1824 (EPRI 1011999) that can serve as a basis for establishing the applicability of fire modeling results. In developing the examples documented in the appendices to this report, the research team identified relevant validation studies outside of NUREG-1824 (EPRI 1011999), as summarized below:

- Scenarios involving targets within the fire plumes: A useful discussion of fire plumes is contained in Gunnar Heskestad's chapter in the *SFPE Handbook of Fire Protection Engineering* (4th ed.), "Fire Plumes, Flame Height, and Air Entrainment." The plume correlations used in the empirical and zone models are described, as well as their range of applicability. NUREG-1824 (EPRI 1011999) contains experimental measurements of fire plumes, but the range is somewhat limited. The plume correlations used by the models have a much wider range of applicability than that exercised in NUREG-1824 (EPRI 1011999).

- Scenarios involving targets within the ceiling jet: Similarly, Ronald Alpert's chapter "Ceiling Jet Flows" in the *SFPE Handbook* contains a description of the various correlations used to estimate the temperature and gas velocity of ceiling jets. There are extensive references to the original experimental test reports from which the correlations were derived.

- Scenarios involving targets exposed to flame radiation: A useful collection of techniques and validation data for thermal radiation calculations is found in the *SFPE Engineering Guide for Assessing Flame Radiation to External Targets from Pool Fires*, written by the SFPE Task Group on Engineering Practices, 1999.

- Scenarios involving Flashover/Post-Flashover conditions: A series of experiments was conducted at NIST as part of an investigation of the collapse of the World Trade Center towers. Validation calculations with FDS are described in the report NIST NCSTAR 1-5F, *Federal Building and Fire Safety Investigation of the World Trade Center Disaster: Computer Simulation of the Fires in the WTC Towers*, September 2005.

- Scenarios involving electrical failure of cables: The CAROLFIRE (Cable Response to Live FIRE) program led to the development and validation of the THIEF (Thermally-

Induced Electrical Failure) model (NUREG/CR-6931, Vol. 3). The model is used to estimate the temperature within an electrical cable that is exposed to an elevated temperature or heat flux.

- Scenarios involving cable burning: The CHRISTIFIRE (Cable Heat Release, Ignition, and Spread in Tray Installations in FIRE) program led to the development and validation of the FLASH-CAT (Flame Spread in Horizontal Cable Trays) model (NUREG/CR-7010, Vol. 1). This model addresses the growth and spread of fire within vertical stacks of horizontal, open-back cable trays.

In addition to NUREG-1824 (EPRI 1011999) and the various documents cited above, the individual model developers typically maintain a collection of validation cases that are included as part of the model documentation. The algebraic spreadsheet models, Fire Dynamics Tools and FIVE, are based directly on experimental correlations. Validation of these models is typically not part of the model documentation; rather, there are references to source material like the *SFPE Handbook* or the original test reports. Validation studies by the CFAST and FDS developers are contained within:

CFAST – Consolidated Model of Fire Growth and Smoke Transport, Software Development and Model Evaluation Guide, NIST Special Publication 1086, 2008.

Fire Dynamics Simulator, Technical Reference Guide, Volume 3, Validation, NIST Special Publication 1018, 2007.

2.4 Step 4: Calculate Fire-Generated Conditions

This step involves running the model(s) and interpreting the results. When running a computer model, the following general steps are recommended:

1. Determine the output parameters of interest. If the goal of the simulation is to estimate wall temperatures, for example, the analyst should be interested in internal and external wall temperatures. The analyst should ensure that the model will provide the output of interest, or at least the fire conditions that can help achieve the objectives of the analysis. The output file should be labeled with a distinctive file name.

2. Prepare the input file. In this step, the analyst enters the input parameters into the model. The best way to enter input parameters is to follow the same guidelines described in the scenario description section. Each model has a user's manual with instructions on creating the respective input file. These files are created either through user-friendly menus and screens or through a text editor. If a text editor is used, it is strongly recommended that the analyst start with an example case prepared by code developers, and make appropriate changes to that file.

3. Run the computer model. The running time for zone models is on the order of minutes, depending on the complexity of the scenario and the speed of the computer. Calculations using a CFD model may take up to days or weeks in complex scenarios, including multiple compartments, multiple fires, and mechanical ventilation systems.

4. Interpret the model results. Verify that the results are intuitively consistent with the input and expectations. Verify that the output results accurately reflect the desired input; common verifications would include the fire size and location, the location and status of any doors or boundary openings, and the forced ventilation flow rate and location. The

model output should be checked for indications of a solution error. For example, the pressure should be within reasonable bounds; the Hot Gas Layer temperature should be sensible; the Hot Gas Layer temperature should be greater than the lower gas layer temperature; and there should not be anomalous areas of flow acceleration or temperature change. Determine whether or not the fire scenario resulted in conditions that exceed the performance criteria, as applicable.

5. Arrange output data in a form that is suitable for the goal. If the results are used in a PRA screening analysis, this may take the form of a zone of influence (ZOI) dimension or a maximum HGL temperature. If the results are part of a deterministic analysis, the output form may be a conclusion with regard to the performance of some component and an associated safety margin if the component is predicted to be free of damage.

For the FDT^s and FIVE-Rev1, the input data is entered directly into a spreadsheet, and the results are presented in the spreadsheet. Some of the FDT^s spreadsheets include graphical and tabular results. FIVE-Rev1 typically provides a single result for a given set of input data; however, many of the calculations in FIVE-Rev1 are implemented as Microsoft Excel functions. These functions can be called from any cell in the spreadsheet. It is possible, for example, to specify a heat release rate in one cell and the plume temperature at a specific location above the fire for that heat release rate. By entering a list of heat release rates that vary with time, the analyst could obtain the plume temperature or other calculations as a function of time.

CFAST, MAGIC, and FDS can handle user-specified transient heat release rates, as they calculate the results for each zone or cell at each time step. The time step required to maintain stable calculations is typically determined by the model. The interval at which results are presented is a user-specified value. CFAST, MAGIC, and FDS can output results as text files, which can be read or plotted using commercially available spreadsheet programs; CFAST and FDS can also output their results in a form appropriate for SMOKEVIEW (Forney, 2008). SMOKEVIEW is a software tool that visualizes smoke and other attributes of the fire using traditional scientific methods, such as displaying tracer particle flow, two- or three-dimensional shaded contours of gas flow data (e.g., temperature), and flow vectors showing flow direction and magnitude. MAGIC includes its own post-processor for visually analyzing the results of a simulation. Post-processing may also be performed using other graphical or graphical animation software. If a software package other than one designed for viewing the particular fire model results is used, the user should verify that the output parameters are interpreted and displayed as intended.

2.5 Step 5: Conduct Sensitivity and Uncertainty Analyses

This guide recommends a comprehensive treatment of uncertainty and/or sensitivity analysis as part of a fire modeling analysis for the following reasons:

• Models are developed based on idealizations of the physical phenomena and simplifying assumptions, which unavoidably introduces the concept of model uncertainty (i.e., model error) into the analysis.

• A number of input parameters are based on available/generic data or on fire protection engineering judgment, which introduces the concept of parameter uncertainty into the analysis.

The concepts of model and parameter uncertainty have traditionally been addressed in fire modeling using uncertainty and/or sensitivity analysis. The uncertainty in a variable represents

the lack of knowledge about the variable, and is often represented with probability distributions. Its objective is to assess the variability in the model output, that is, how uncertain the output is given the uncertainties related to the inputs and structure of the model. By contrast, the sensitivity of a variable in a model is defined as the rate of change in the model output with respect to changes in the variable. A model may be insensitive to an uncertain variable. Conversely, a parameter to which a model is very sensitive may not be uncertain.

Details of the uncertainty and sensitivity analysis are included in Chapter 4 of this guide for both a deterministic- and a probabilistic-type evaluation.

2.6 Step 6: Document the Analysis

The amount of information required and generated by a fire modeling analysis can vary widely. Simple algebraic models may not require a large number of inputs, and the complete analysis, including output results, can be documented on a single piece of paper. On the other hand, some fire modeling exercises may require use of multiple computer models, where outputs from one are inputs to others. These cases, for the most part, will require a significant number of input parameters and will produce outputs requiring documentation. Regardless of the amount of information required or generated by the analysis, proper documentation is vital to identifying the important findings of the exercise and providing clear, focused conclusions.

Documentation of the fire scenario selection and description process should include enough information so that the final report is useful in current and future applications. This is particularly relevant in the commercial nuclear industry, where compartment and equipment layouts or processes do not change much over time. It is likely that fire scenarios analyzed for one application may be useful for other applications as well; the key, however, is to develop and maintain good documentation of the selected fire scenarios, including all the technical elements discussed in this section. The SFPE "Engineering Guide to Substantiating a Fire Model for a Given Application" (SFPE, 2011) provides general guidance on information to be included in fire modeling analyses.

It is likely that the information necessary for documenting the fire scenario selection will be gathered from a combination of observations made during engineering walkdowns and a review of existing plant documents and/or drawings. The documentation process then involves compiling the information from different sources into a well-organized package that can be used in future applications and for NRC regional inspections. The documentation package may consist of:

- Marked up plant drawings. Plant layout, detection, suppression, cable tray, Heating, Ventilation and Air-Conditioning (HVAC), and conduit drawings are often marked to highlight the location of the compartment, the ignition sources, the targets, the ventilation flow paths, and the fire protection features. The drawings also serve as sources of fire model input values, such as compartment dimensions, ventilation flow rates, and relative locations of fire protection systems or targets.

- Design basis documents (DBDs). DBDs provide in-depth assessments of plant features in various operation modes, such as the HVAC system.

- Sketches. Sketches are perhaps one of the most useful ways of documenting a fire scenario. A sketch typically consists of a drawing illustrating the ignition source, intervening combustibles, targets, and fire protection features. A first draft of the sketch is usually prepared during walkdowns. The analyst should take the opportunity to

include details such as raceways and conduit identifications (IDs), and other information relevant to the fire modeling analysis. Pictures often supplement sketches.

- Write-ups and input tables. Write-ups and input tables are used to compile the information collected from drawings and walkdowns in an organized way. The write-up should include a brief scenario description and detailed documentation supporting quantitative inputs to the fire modeling analysis, as well as any relevant sketches or pictures associated with each scenario.

- Software versions, descriptions, and input files. The documentation package should include the version numbers of any software, brief descriptions of the software, and copies of the input files.

The examples presented in Appendices A through H of this guide illustrate techniques for the proper documentation of fire modeling calculations using the format described. In conclusion, a properly documented analysis will enable the reviewer to reproduce the results from the information contained within the fire scenario analysis.

2.7 Summary

This chapter described a recommended process for conducting and documenting a fire modeling analysis. Chapter 3 provides guidance on selecting the appropriate fire modeling tool and input parameters for typical commercial nuclear power plant applications. Fire model uncertainty is addressed in Chapter 4 of this guide. Specific fire modeling examples evaluated using the process described in this Chapter are provided in Appendices A through H.

3
GUIDANCE ON FIRE MODEL SELECTION AND IMPLEMENTATION

This chapter provides guidance and recommendations for modeling fire scenarios in a commercial nuclear power plant. It can be considered a catalogue of generic fire scenarios and corresponding modeling objectives for which a modeling strategy is discussed, relevant fire modeling elements are described, and model selection recommendations are offered. The chapter begins with a description of key fire modeling elements applicable to most of the scenarios presented in the guide, which are intended to direct the analyst to the specific section in this chapter where guidance and recommendations are provided.

3.1 Model Implementation of Fire Scenario Elements

This section provides a description of fire modeling elements typically present in commercial nuclear power plant scenarios. The following fire modeling elements are described:

- Heat Release Rate
- Plant Area Configuration
- Ventilation Parameters
- Targets
- Intervening Combustibles

3.1.1 Heat Release Rate

The heat release rate (HRR) in a fire model is perhaps the most important parameter to specify. All enclosure fire models solve a conservation of energy equation (i.e., the energy released by the fire in the form of heat causes the temperature to increase and hot and cold air to flow in and out of the enclosure). The fire as a heat source is the driving parameter for all the modeled physical phenomena. The models track the energy being added to the enclosure and estimate the fire-induced temperature and flow of hot gases. Three questions usually have to be answered to adequately assess the heat release rate of a fire:

1. How fast does the fire grow? This is the time it takes for the fire to reach its peak intensity from the time of ignition. It is also equally important to define the growth profile to the peak intensity as a function of time. The t^2 growth profile (see Karlsson and Quintiere, p. 38) is a convenient mathematical structure to represent this growth. In some cases, experimental data of actual fuel commodities may be available, where the profile may or may not follow a t^2-type profile.

2. What is the peak intensity of the fire? The peak intensity, or peak heat release rate, represents the phase of the heat release rate profile where the fuel reaches its maximum burning rate, assuming that oxygen is available to support fuel-controlled burning. In practical applications, the peak intensity is obtained from experimental data. Alternatively, it can be estimated using the heat of combustion and the maximum burning rate of the fuel (perhaps considering the effective heat of combustion rather than the theoretical, maximum value). The peak heat release rate may also be dictated by the air supply available to the

fire. Estimates of the maximum heat release rate associated with a particular ventilation opening or airflow are available in fire protection engineering handbooks.

3. How long does the fire burn? The duration is a function of the amount of fuel available and the rate at which the fuel is consumed.

The HRR vs. time curve typically has four stages: incipient, growth, steady burning at peak intensity, and decay.

In the incipient stage, the fire burns at a low intensity (i.e., smoldering insulation or a small trash can fire). The duration of this stage may vary from seconds to hours, and the energy release is relatively low. Because of the uncertainty in the intensity of the fire during this stage, and the exact time that the fire will transition to a significant fire, the incipient stage is often not considered in the analysis.

Depending on the combustible and its arrangement, the growth to a fully developed stage will vary from seconds to minutes. The duration of the steady burning phase depends on the amount of fuel and the amount of oxygen available.

The following elements are also important in characterizing the fire source:

• The fire elevation: The fire elevation refers to the elevation of the base of the fire, measured from the floor. It is important because (1) in scenarios involving targets in the fire plume where the relative distance between the fire and the target strongly influences the resulting plume temperature, and/or (2) in scenarios where the position of the Hot Gas Layer is relevant, the fire elevation influences the air entrainment into the plume, and, consequently, the position of the layer as well as the actual heat release rate (since any air entrained from the Hot Gas Layer may be oxygen-depleted).

• The fire location: In scenarios where the fire is located along a wall and in the corner (i.e., the fire is postulated either flush with or at most a few inches from the wall or the corner), the plume is expected to entrain less air at ambient temperature, resulting in higher plume temperatures (see Karlsson and Quntiere, p. 72).

• Additional combustion properties are often necessary. Some of these properties include:

    • Fuel mass: The total (or initial) fuel mass, which is an important factor in determining the burning duration

    • Soot yield: The soot yield is an important factor in radiative heat transfer (e.g., targets immersed in the Hot Gas Layer), visibility calculations, and smoke detector response estimates

    • Radiated fraction: The fraction of the energy released by the fire that is radiated from the flames

    • Release Fractions (Yields): In some models, species production is calculated based on production yields prescribed by the user

3.1.2 Plant Area Configuration

The plant area configuration refers to the geometrical layout and construction of the enclosure. Each of these elements is described in detail next.

Compartment Geometry

Compartment geometry refers to the physical layout of the volume in which the fire is postulated. The length, width, and height of the room are the typical inputs required by the model. The size of a compartment is an important factor in the volume used to solve the fundamental conservation equations. Empirical and zone models employ considerable simplifications of the geometry, while CFD models attempt to replicate as much of the geometry as possible.

Compartment Boundary Materials

Boundary (e.g., wall) materials are characterized with thermophysical properties, which include the density, specific heat, and thermal conductivity of the material. In the majority of commercial nuclear power plant applications, the wall material is concrete. Other materials may include steel, gypsum board, etc. Properties for these materials are often available in "drop down" menus in the fire models or in fire protection engineering handbooks. Table 3-1 provides typical boundary material properties.

Table 3-1. Boundary Material Properties

Material	Thermal conductivity W/m/K	Density kg/m^3	Specific heat kJ/kg/K
Concrete	1.6	2400	0.75
Gypsum	1.7	960	1.1
Brick	0.8	2600	0.8
Steel	54	7850	0.465
Source: NUREG-1805			

3.1.3 Ventilation Effects

Ventilation effects include natural ventilation through vertical or horizontal openings, the effects of leakage paths, and/or the effects of mechanical ventilation. Each of these elements is described next.

Vertical Openings

Vertical openings refer for the most part to doors, though they can also comprise other openings in walls, such as open windows. In some cases, a selected compartment will have more vertical openings than the number that can be specified in a specific model; for example, the MQH model for calculating room temperature available in FDT^s and FIVE-Rev1 accept only one opening. The most important consideration in addressing the issue of vertical openings is to conserve the ventilation factor. If the number of vertical openings needs to be reduced in order to describe the scenario in a specific model, a weighted average for the vent factor needs to be estimated. The ventilation factor is defined as the product of the area of an opening and the square root of the height of the opening $\left(A_o \sqrt{H_o}\right)$ (Karlsson et al., 2000; Drysdale, 1996). The following steps can be used to determine the combined effective height, H_o, and area, A_o, of multiple vertical openings:

1. Add up the areas of the selected openings: $A_o = \sum_{i=1}^{n} A_i$

2. Divide the sum of the product of the area and height of each opening by the total area

calculated in step 1: $H_o = \dfrac{\sum\limits_{i=1}^{n} A_i \cdot h_i}{A_o}$

where A_i and h_i are the area and height of door i, respectively, and n is the total number of vertical openings that need to be combined. The effective width of the multiple vertical openings can be estimated by the ratio, A_o/H_o.

Regarding doors (and other operable openings), consideration should be given to the doors being opened (or closed) during a fire. For example, when the fire brigade arrives, they will open the doors to the fire area to gain access, which will affect the ventilation and possibly result in smoke spread.

Leakage Paths
The doors of most compartments in commercial NPPs are normally closed, but are not perfectly sealed. Consequently, the resulting pressure and the rate of pressure increase are often kept very small by gas leaks through openings in the walls and cracks around doors, or "leakage paths." Leakage paths must be specified in compartments with closed doors during the fire event unless the analysis considers a completely sealed enclosure where pressure rise is an important variable. By contrast, compartments with at least one open door or window can maintain pressure close to ambient during the fire event. Leakage paths therefore do not need to be specified, since the leakage opening area is negligible when compared with the opening areas of doors and windows.

Horizontal Openings
Horizontal openings consist of hatches or stairwells. For modeling purposes, the areas of horizontal openings can simply be added. Any zone model should provide similar answers with single or multiple horizontal openings as long as the total opening area is the same. Note that CFAST allows only a single connection between any pair of compartments included in a simulation. For a CFD model, no special provisions are necessary to describe a horizontal opening.

Mechanical Ventilation
Mechanical ventilation refers to any air injected into or extracted from a compartment by mechanical means. This has a number of practical applications, such as extracting smoke from the Hot Gas Layer (e.g., a smoke purge system). The ventilation rate and the vent position are the two most important mechanical ventilation parameters. For some applications, the velocity of the airflow may also be important. These mechanically induced flows have the potential to alter the fire-induced flows. Mechanical ventilation often consists of a supply and an exhaust system that are maintained to achieve a certain pressure level.

3.1.4 Targets

Targets refer to objects of interest than can be affected by the fire-generated conditions and typically consist of cables in conduits, cables in raceways, or plant equipment. Targets are characterized by their location, damage criteria, and thermophysical properties.

A target's location simply refers to its location relative to the fire. The location is represented by three-dimensional coordinates within the volume of the room in which the fire conditions are

simulated. Where the target faces in a particular direction, an orientation vector to indicate that direction needs to be entered.

The damage criteria refers primarily to a damage/response threshold. In general, the damage criteria for scenarios involving cable damage is expressed in terms of damage temperature or incidental heat flux. These thresholds are available in commercial nuclear industry documents such as NUREG-1805, NUREG/CR-6931, and NUREG/CR-6850 (EPRI 1011989).

The models within the scope of this guide require specification of the target's thermophysical properties, primarily the density, specific heat, and thermal conductivity, for the analysis. These parameters are used for estimating heat conducted into the targets. The predicted time for the gas temperature surrounding a target to reach a specific limit is usually less than the time it takes the target to reach the same limit because the heat conduction inside the target will delay the temperature rise at the surface during the heating process. These data are also available in documents such as NUREG-1805, NUREG/CR-6931, and NUREG/CR-6850 (EPRI 1011989).

3.1.5 Intervening Combustibles

In many cases, commercial nuclear plant PRA fire scenarios do not require burning targets to be modeled because it is sufficient to determine only when the target is damaged. This is clearly not the case with intervening combustibles, whose flammability characteristics need to be incorporated into the model so that the fire progression is considered. Therefore, the intervening combustibles should be described not only in terms of their proximity to the fire and the targets, but also in terms of their relevant thermophysical and flammability properties.

In many cases, intervening combustibles consist of cables in ladder back trays. Representing intervening combustibles like cables in fire models presents technical challenges that the analyst should also consider, including (1) obtaining the necessary geometric and thermophysical properties representing the intervening combustible and (2) the ability of the computer tools to model the fire phenomena (e.g., fire propagation). Because of these challenges, industry methodologies for applications (e.g., Fire PRAs) include a number of simplified models to estimate fire-generated conditions that are currently beyond the capabilities of the fire models described in this Guide. The simplified approach consists of determining the contribution to the heat release rate due to flame spread and fire propagation through cable trays. Appendix R of NUREG/CR-6850 (EPRI 1011989) provides guidance on the calculation of fire spread and heat release rates for cables trays. In addition, research is underway to develop improved methods for predicting the heat release rate and flame spread of electrical cables. A simple model called FLASH-CAT that predicts flame spread over cables in horizontal trays has been developed as part of the Cable Heat Release, Ignition, and Spread in Tray Installations during Fire (CHRISTIFIRE) project (NUREG/CR-7010, vol. 1), sponsored by the NRC and conducted by NIST.

3.2 Guidance on Model Selection and Analysis

This section provides guidance on model selection and analysis of specific fire scenarios. Each subsection is devoted to a specific fire scenario, as listed in Table 3-2. In addition, Figure 3-1 provides a pictorial representation of each of these scenarios. The circled numbers are intended to direct the reader to the section in which the scenario is described.

Table 3-2. Listing of generic fire scenarios described in this chapter

Number	Chapter Section	Scenario Description
1	3.2.1	Scenarios consisting of determining time to damage of cables above the ignition source located inside the flames or the fire plume.
2	3.2.2	Scenarios consisting of determining time to damage of cables located inside or outside the Hot Gas Layer. This scenario also includes a secondary fuel source (i.e., propagation to cable trays).
3	3.2.3	Scenarios consisting of determining time to damage of cables located in an adjacent room to the room of fire origin.
4	3.2.4	Scenarios consisting of determining time to damage of cables located inside or outside the Hot Gas Layer in rooms with complex geometries.
5	3.2.5	Scenarios consisting of determining time to loss of habitability of the main control room.
6	3.2.6	Scenarios consisting of determining time to smoke or heat detector activation.
7	3.2.7	Scenarios consisting of determining temperature of structural elements.

Each of the sections listed above is organized as follows:

1. A sketch capturing most of the technical elements relevant to the analysis. A legend summarizing the different elements presented in the sketches is provided in Figure 3-2.

2. A scenario objective stating the purpose of the modeling exercise in engineering terms.

3. A description of the relevant technical fire scenario elements, such as mechanical ventilation, the room geometry, etc. Recall that fire scenario elements refer to the different characteristics of the fire scenario that are relevant to the analysis, and should be properly represented in the model.

4. A modeling strategy section summarizing the recommended steps for performing the calculation.

5. A section listing fire model recommendations for the analysis.

6. A section referencing relevant detailed fire modeling examples documented in the Appendix section of this guide.
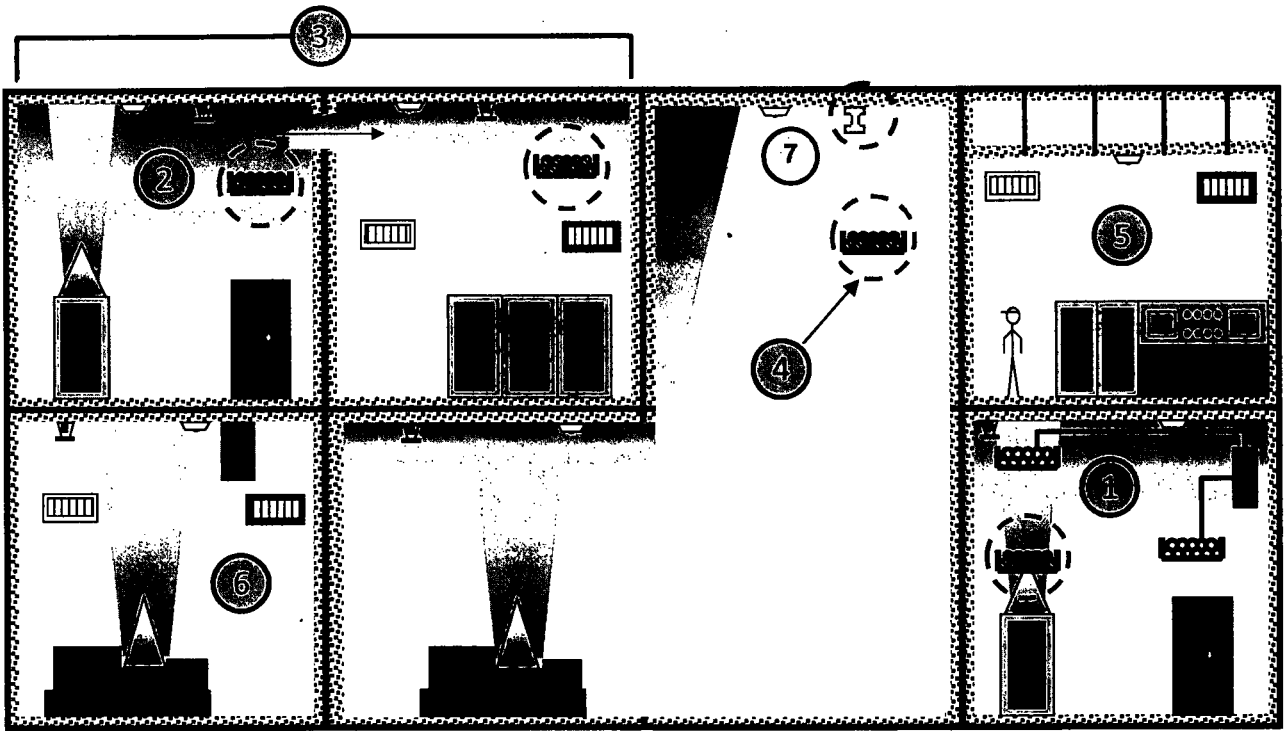
Figure 3-1. Pictorial representation of the fire scenario and corresponding technical elements described in this section.
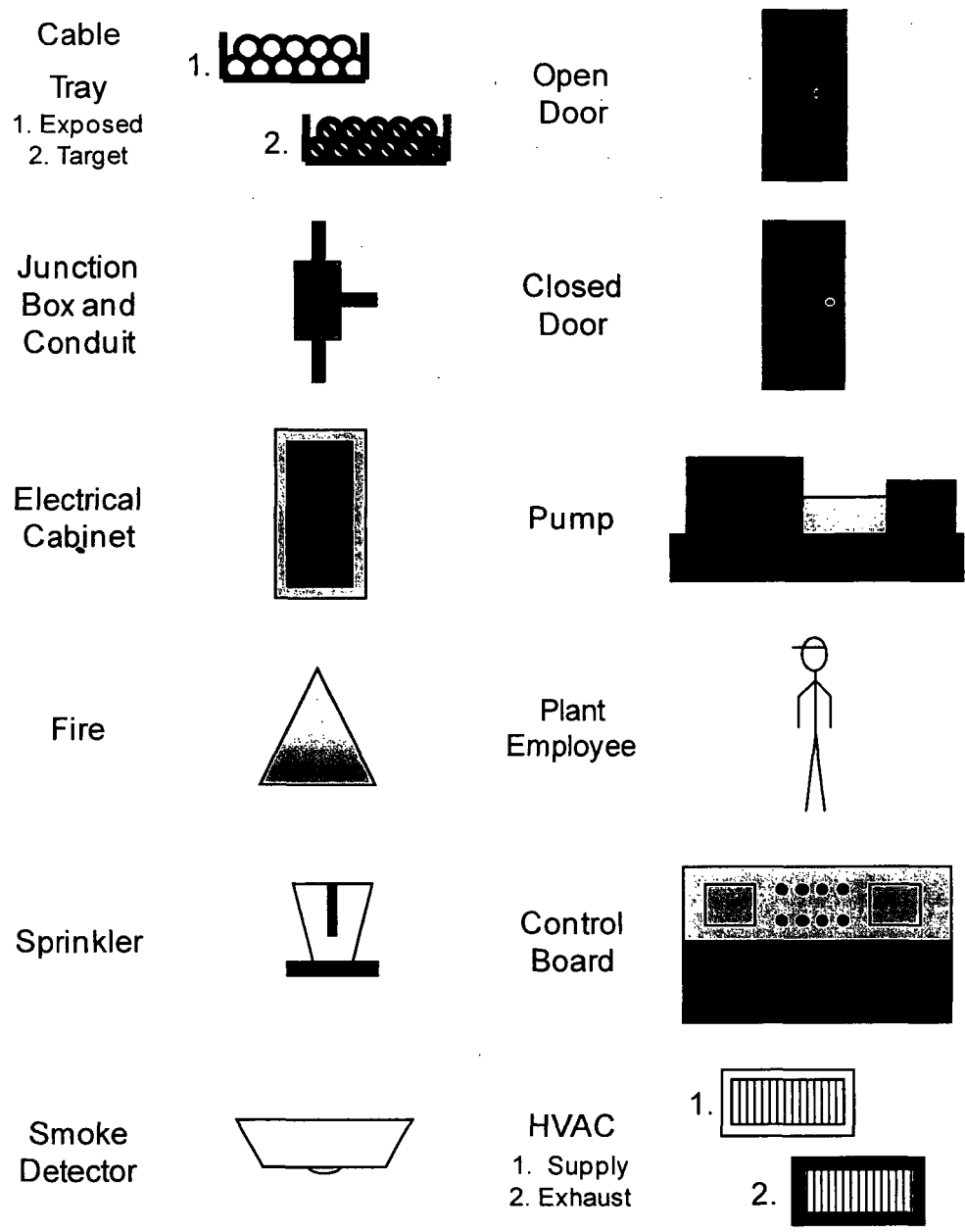
Figure 3-2. Legend for fire modeling sketches presented in this chapter.

3.2.1 Targets in the Flames or Plume

This scenario consists of a target, such as an electrical cable in a raceway immediately above an ignition source, such as an electrical cabinet. An example of this type of scenario is depicted in Figure 3-3, where the target is identified in the sketch by a dashed circle.
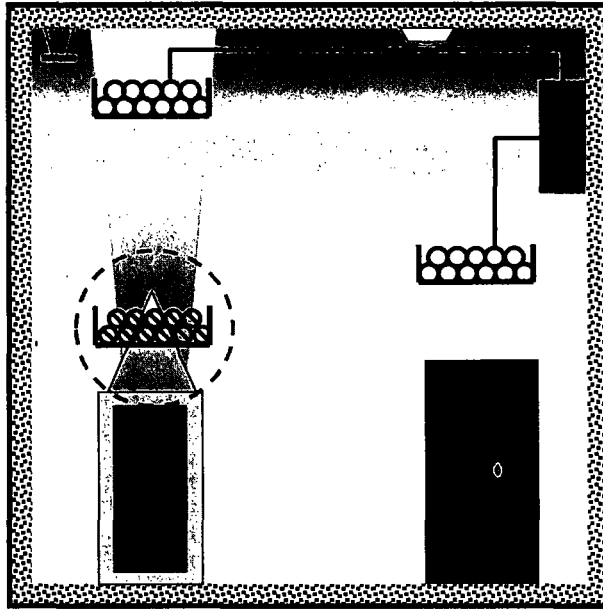
Figure 3-3. Pictorial representation of scenario 1

3.2.1.1 General Objective

The objective of this scenario is to calculate the time to damage for a target immediately above a fire. For the case shown in Figure 3-3, the target is an electrical raceway and the fire source is an electrical cabinet.

3.2.1.2 Modeling Strategy

The recommended modeling strategy is summarized in the following steps:

1. Determine whether the target cable, which is directly above the fire, is within the flame zone or within the fire plume. The target should be considered inside the flame zone if it is located directly above the base of the fire and its distance from the base of the fire is less than the flame height. If the target is above the fire but is not within the flame zone, then it is considered to be within the fire plume. It should be noted that unobstructed fire plumes will increase in diameter as a function of height. Consequently, a target may not need to be directly above the ignition source to be immersed in the fire plume.

2. Calculate the time to damage by finding the minimum of either:

    a. The time at which the flame reaches the target. This is achieved by calculating the flame height as a function of time using the heat release rate profile (e.g., heat release rate as a function of time) and fire diameter as input.

b. The time it takes the fire plume temperature to exceed the target damage temperature. This is achieved by calculating the plume temperature at the specified height as a function of time using the heat release rate profile (e.g., heat release rate as a function of time) as an input. This approach can be considered conservative, as it assumes that cable damage occurs when the gas temperature surrounding the target reaches the damage temperature (i.e., heating of the cable is ignored).

c. The surface temperature of the cable as a function of time, given a heat flux profile generated by the flame or plume.

If non-target raceways are located between the ignition source and the target, the contributions of intervening combustibles need to be considered in the analysis. For example, consider a panel fire that ignites the first of a stack of trays overhead. The fire involving the combination of the panel and first tray may then ignite the second tray in the stack, and the fire may progress to damaging the target raceway. Considerations of the intervening combustibles in the analysis include the heat release rate contribution and the corresponding effects on the target heating time. See Scenario 2 below for guidance on treatment of intervening combustibles.

In addition to the guidance provided above, the analyst should determine whether Hot Gas Layer effects are relevant in the scenario. The portion of the fire plume immersed in the Hot Gas Layer entrains air at higher temperatures (i.e., the Hot Gas Layer temperature) and is expected to have increased temperatures when compared with portions of the fire plume outside the Hot Gas Layer. In scenarios consisting of targets located relatively close to the ignition source (which is the case of the scenario discussed in this section), the Hot Gas Layer effects on the plume temperature are generally not considered, as the time to target damage is expected to be relatively short. For scenarios involving targets in the fire plume, located relatively far from the ignition source, the Hot Gas Layer effects on target heating should be considered. In the latter case, the room geometry and ventilation (both natural and mechanical) conditions should be captured by the analysis.

3.2.1.3 Recommended Models
Algebraic Models

The applicable models in the FIVE-REV1 are recommended for this scenario, provided that the configuration is within the correlation basis and that there are no significant Hot Gas Layer effects. Heskestad's flame height correlation is an alternative for determining flame height. Similarly, Heskestad's fire plume temperature correlation is an alternative for determining plume temperature and diameter (Heskestad, 2002). The FDT^s models do not allow the HRR to be input as a function of time, and, as a result, cannot be used to determine a failure time based on an HRR.

The correlations listed above are particularly applicable for scenarios consisting of targets relatively close to the ignition source, where Hot Gas Layer effects are not considered in the analysis.

As noted above, the time to damage is the minimum of either (1) the time at which the flame reaches the target or (2) the time it takes the fire plume temperature to exceed the target damage temperature. For FIVE, this is simply the time at which the HRR reaches the value required for either of the failure criteria.

Zone Models

Zone models can be used for this scenario. To do so, set up the necessary input file that includes a "target" in the location of the electrical cable of interest with the corresponding thermophysical properties so that the surface temperature of the cable can be tracked. Zone models have the ability to include Hot Gas Layer effects in their calculation of plume temperature, and are thus particularly appropriate for scenarios where the Hot Gas Layer temperature interacts with the fire plume at the location of the target.

Again, the time to damage is the minimum of either (1) the time at which the flame reaches the target or (2) the time it takes the fire plume temperature to exceed the target damage temperature. The zone models routinely calculate and report these values.

CFD Model

Although a CFD model could be used for analyzing this scenario, the level of detail and resolution offered by a CFD calculation is not necessary. On the other hand, the model would be particularly applicable if the scenario involves obstructions between the fire and the target inside the fire plume or if Hot Gas Layer effects are significant. The effects of these obstructions on the exposure conditions are not captured by algebraic models or zone models.

3.2.1.4 Detailed Examples

Readers are referred to Appendix B, which describes the analysis of an electrical cabinet fire in the switchgear room, and Appendix E, which describes the analysis of a transient fire in a cable spreading room.

3.2.2 Scenario 2: Targets Inside or Outside the Hot Gas Layer

This scenario consists of a target, such as an electrical cable in a raceway, located inside or outside the Hot Gas Layer produced by a fire involving an ignition source, such as an electrical cabinet, and a secondary fuel source, such as an electrical raceway. An example of this type of scenario is depicted in Figure 3-4.

Figure 3-4 Pictorial representation of scenario 2

3.2.2.1 General Objective

The objective of this scenario is to calculate the time to damage for a target inside or outside the Hot Gas Layer produced by a fire. Also, the time to ignition of a secondary fuel source and the resulting contribution to the total heat release rate can be determined. For the case shown in Figure 3-4, the target is a cable in an electrical raceway and the fire source is an electrical cabinet..

3.2.2.2 Modeling Strategy

Two levels of analysis can be employed: (1) algebraic models for the average room temperature as an indicator of the gas temperature surrounding the target, or (2) detailed heat transfer analysis for determining the target temperature.

The first strategy consists of determining the overall room temperature using a algebraic model (e.g., the MQH room temperature model) (McCaffrey et al., 1981). Such a calculation will indicate whether the target may be subjected to damaging temperatures and the time at which such temperatures may be observed. It should be noted that the room needs to be represented as a rectangular parallelepiped and the area of all the surfaces in the room must be conserved. In addition, if the target cable tray is relatively close, the target may be damaged by radiant heating. This can be assessed with simple point source estimates that only require the heat release rate of the fire, the separation distance between the fire and the target, and the damage criteria (i.e., critical flux for damage).

The second strategy is best addressed with a model capable of including detailed heat transfer analysis for determining the target temperature. A raceway outside the fire plume may be exposed to Hot Gas Layer conditions if the smoke accumulating in the upper part of the room (i.e., the Hot Gas Layer) descends to the location of the raceway. Consequently, targets outside the fire plume are initially exposed to "lower layer" (i.e., below the Hot Gas Layer) conditions. As the smoke continues to accumulate, the target is immersed in Hot Gas Layer conditions. As heat transfer conditions will be different for each case, a model with the capability of tracking the relevant/applicable heat transfer interaction and calculations as a function of time, such as a zone or a CFD model, should be selected to handle this scenario at the desired level of resolution.

With regard to the secondary fuel source, three distinct additional analyses must be made to determine:

- The time at which the secondary fuel source ignites,

- The heat release rate of the secondary fuel source, and

- The combined heat release rate of the primary and secondary fires.

The more detailed models, such as FDS, can handle the ignition and contribution of multiple fires, provided that the ignition criteria and source heat release rate characteristics are provided as input. Other models, especially the algebraic models, only accept the total heat release rate as a function of time, which is found by summing up the individual heat release rates.

In the present example, consider a cable tray directly above the fire. The time to ignition of the cable tray can be determined via algebraic models that estimate the flame height and plume temperature as a function of time for the initial cabinet fire (see Scenario 1 above). Once the flames from the cabinet reach the cable tray, it can be assumed to ignite. The same is true when the plume temperature at the elevation of the cable tray reaches the ignition temperature of the cables. Both calculations should be completed, and the shorter time used as the ignition time.

The heat release rate from the cable tray can be added to the heat release rate of the cabinet to determine a combined heat release rate as a function of time. This total rate can then be used in the various models as an approximation of the heat release rate as a function of time.

Appendix R of NUREG/CR-6850 (EPRI 1011989) addresses cable fires, including methods for calculating the heat release rate for a variety of cable configurations.

It should be noted that the simple summation of the two heat release rates is a simplification of a complex phenomenon and only provides a first-order approximation of the conditions created by the two separate fires.

3.2.2.3 Recommended Modeling Tools
Algebraic Models

Select the appropriate Hot Gas Layer (or room temperature) model and then collect the required inputs, including room size, opening sizes, boundary material properties, forced ventilation, and the heat release rate profiles for the initial and secondary fuel packages. For screening purposes, the use of algebraic models is recommended as long as the contributions of the first item ignited and intervening combustibles are considered. As was mentioned earlier, this approach will provide a first-order approximation of the room temperature in which the target may be immersed. The methods used by algebraic models to address the secondary fire

source are discussed above. Target damage due to radiant heating can be estimated using algebraic models; all that is required is the heat release rate of the fire (as a function of time), the separation distance between the fire and the target, and damage criteria (i.e., critical flux for damage).

Zone Models

Zone models provide a good alternative for modeling this scenario, as they provide the incident heat flux profile, the surface temperature, and the internal temperature of the target in one simulation. Set up the necessary input file with the required inputs, including room size, opening sizes, boundary material properties, heat release rate, fire diameter and a target, and fire location so that the cable's surface temperature can be predicted.

Zone models also have the benefit of being able to handle secondary fire sources as separate entities. Secondary fires can be ignited at a prescribed time, temperature, or heat flux. However, zone models have limited capabilities for handling obstructions.

Target damage due to radiant heating from the fire is easily handled by zone models, as long as there are no obstructions between the fire and the target that block radiant heat transfer. Zone models can also account for radiant heating of targets by the Hot Gas Layer.

CFD Model

The use of CFD models for this scenario is recommended for complex geometries capable of affecting the location of the Hot Gas Layer and the incident heat flux to the targets, or when greater accuracy of the ignition and contribution of secondary fires is warranted. For instance, obstructions between the ignition source and the target affect the heat balance at the surface of the target. The CFD model will require inputs similar to the ones collected for the zone models; however, the compartment geometry will need to be specified in greater detail.

Due to their detailed calculations, CFD models are best able to model secondary fire sources, including their ignition and subsequent contribution to the heat release rate within the enclosure.

Like zone models, CFD models can handle targets damaged by radiant heating from the fire and the Hot Gas Layer. CFD models can also include the effects of obstructions between the fire and the target.

3.2.2.4 Detailed Examples

Appendix C describes the analysis of a relatively large oil fire affecting a raceway in a pump room, and Appendix E describes the analysis of a transient fire in a cable spreading room.

3.2.3 Scenario 3: Targets Located in Adjacent Rooms

This scenario consists of a target, such as an electrical cable in a raceway, in a room adjacent to the room of fire origin. An opening connecting the room of origin to the adjacent room allows combustion products to enter the adjacent room. An example of this type of scenario is depicted in Figure 3-5 for the case in which there is an opening in the wall.

Figure 3-5. Pictorial representation of scenario 3

3.2.3.1 General Objective

The objective of this scenario is to calculate the time to damage for a target in the Hot Gas Layer in a room adjacent to the room of fire origin. For the case shown in Figure 3-5, the target is a cable in an electrical raceway and the fire source is an electrical cabinet.

3.2.3.2 Modeling Strategy

The recommended strategy for determining the temperature of targets located in a room adjacent to the room of fire origin consists of four basic steps:

1. Determine the following characteristics for the Hot Gas Layer in the room of fire origin and the adjacent compartment:

    a. Temperature as a function of time

    b. Depth as a function of time

2. Determine the incident heat flux surrounding the target cable.

3. Determine the surface and internal temperature of the target cable.

4. Compare the surface or internal temperature of the target with its damage temperature.

Note that this approach assumes that the effort required to model adjacent rooms is justified. One way to approach this (using algebraic models or zone models) is to first model the HGL temperature in the room of origin and the resulting effect on remote targets in the room. If this approach indicates that target damage/ignition is unlikely in the room of origin, it would be safe to assume that there would be little benefit in evaluating similar targets in adjacent spaces. However, if target damage is possible in the room of origin, the next step may be to model the

room of origin and the adjacent room as one combined volume and determine whether the resulting HGL is capable of causing damage/ignition of the target(s). If target damage in the combined volume is not likely, then it may not be worth the added effort to model the adjacent room(s) as separate volumes using more detailed modeling methods.

3.2.3.3 Recommended Modeling Tools

Algebraic Models

Generally, algebraic models are not recommended for this calculation, as a model capable of tracking fire conditions in adjacent rooms is necessary. Zone and CFD models will provide this capability. However, as an approximation, algebraic models could be used to model the HGL temperatures for determining whether damage to targets in adjacent rooms is possible. One way to approach this, using algebraic models, is to model the room of origin and the adjacent room as one combined volume to determine whether the resulting HGL is capable of causing damage to/ignition of the target(s). If this approach indicates that target damage/ignition is unlikely, it may not be worth the added effort to model the rooms as separate volumes using more detailed modeling methods, such as zone models.

Zone Models

The zone model is an appropriate tool for addressing this scenario. Zone models would provide an efficient tool for scenarios involving relatively simple geometries (i.e., geometries and openings that can be easily represented in rectangular parallelepipeds without compromising the technical elements in the analysis). Consequently, the room geometry should be represented as accurately as possible. One of the primary outputs of zone models is the height and temperature of the Hot Gas Layer versus time in each of the rooms specified in the computational domain. Zone models are also capable of determining target temperature (not just the temperature of the gases surrounding the target), given the boundary conditions generated by the fire and the thermophysical properties of the target.

CFD Model

A CFD model would be particularly appropriate for addressing targets located in adjacent rooms in scenarios with complex geometries (i.e., geometries that can't be easily represented as rectangular parallelepipeds). CFD models will be able to describe the geometry of the compartment in detail, including the opening(s) providing smoke migration paths to the adjacent room.

3.2.3.4 Detailed Examples

Readers are referred to Appendix G, which describes the analysis of targets in rooms remote from the fire room.

3.2.4 Scenario 4: Targets in Rooms with Complex Geometries

This scenario involves a room with an irregular ceiling height. Figure 3-6 provides a pictorial representation of an example of this type of scenario. The target in the example shown in Figure 3-6 is a cable tray located away from the ignition source that may eventually be immersed in the Hot Gas Layer.
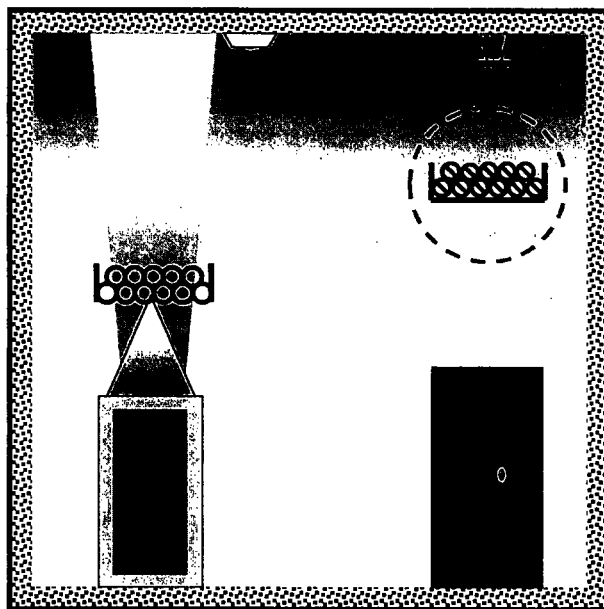

Figure 3-6. Pictorial representation of scenario 4

3.2.4.1 General Objective

The objective of this scenario is to calculate the time to damage for a target in the Hot Gas Layer in a room with a complex geometry. For the case shown in Figure 3-6, the target is a cable in an electrical raceway and the fire source is an electrical cabinet.

3.2.4.2 Modeling Strategy

Two strategies are available: (1) a first-order approximation using algebraic models and a simplification of the complex geometry for determining the room temperature as an indicator of the gas temperature surrounding the target, or (2) a detailed heat transfer analysis to determine the target's temperature while attempting to capture the details of the complex geometry.

The first strategy consists of determining the overall room temperature with an algebraic model (e.g., the MQH room temperature model), which would indicate whether the target may be subjected to damaging temperatures and the time at which such temperatures may be observed. This approach requires that the complex geometry be reduced to a single equivalent volume, which in turn requires some caution. In the case of two different ceiling heights, a correlation like MQH may underestimate the temperature of the smaller volume and overestimate the temperature of the larger. The fire's energy is conserved, but it is not expected to be uniformly distributed if the ceiling height is not uniform.

Guidance on Fire Model Selection and Implementation

The second alternative is best addressed by a model capable of capturing more than one room in a computational domain. A raceway outside the fire plume may be exposed to Hot Gas Layer conditions if the smoke accumulating in the upper part of the room eventually reaches the location of the raceway. In complex geometries, HGL development can be significantly impacted by mixing associated with spilling and venting, and these can only be modeled by zone and field models. Clearly, complex geometries will have complex heat transfer conditions, and should be handled by a model capable of tracking the relevant/applicable heat transfer interaction and calculations as a function of time, such as a zone or a field model.

3.2.4.3 Recommended Modeling Tools
Algebraic Models

Detailed analyses of complex geometries typically cannot be accomplished with algebraic models. However, for screening purposes, it is possible to use algebraic models. As mentioned earlier, this approach can provide a first-order approximation of the HGL temperature in which the target may be immersed. To utilize this approach, first select the appropriate Hot Gas Layer (or room temperature) model and then collect the required inputs, including room size, opening sizes, boundary material properties, and heat release rate. Next, the complex geometry must be reduced to a single equivalent volume while maintaining total surface area (due to the importance of energy losses through the bounding surfaces) and ceiling height, It should be noted that the more complex the space, the less ideal the equivalent volume/area approximation becomes. Based on the estimates derived using the algebraic models, more detailed modeling may be indicated.

Zone Models

Zone models should also be used with caution when modeling this scenario. If the entire space is modeled, the interface between lower and upper compartments is treated as a big door. The entrainment correlations used by the zone model to handle vertical vents were not designed for such large open "doors."

CFD Model

CFD models may be required when detailed analyses of complex geometries capable of affecting fire development and the location of the Hot Gas Layer and the incident heat flux to the target are desired. CFD models are expected to better estimate the overall compartment temperatures, both upper and lower, because there are no assumptions in the basic methodology about uniform ceilings.

3.2.4.4 Detailed Examples
Readers are referred to Appendix D, which consists of a switchgear fire in a room with a complex geometry, and Appendix H, which consists of a fire inside the containment annulus.

3.2.5 Scenario 5: Main Control Room Abandonment

This scenario consists of a fire, such as an electrical cabinet fire within the main control board, that may force operators out of the control room. A schematic diagram of an example of this type of scenario is shown in Figure 3-7. Notice the presence of a suspended ceiling in the control room in the example shown.
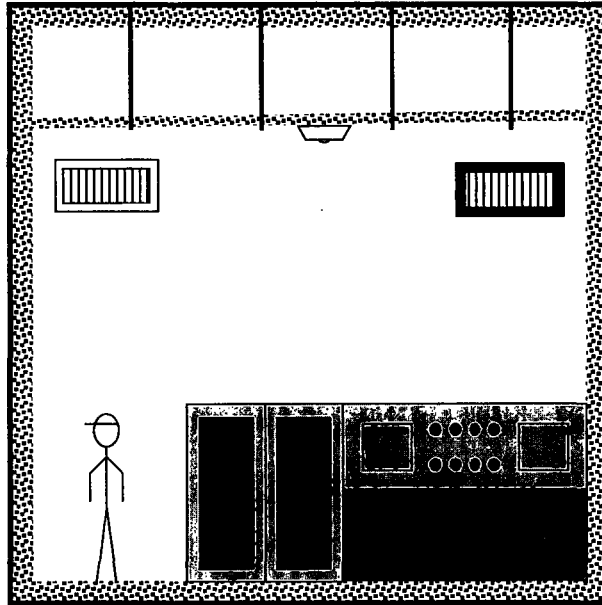
Figure 3-7. Pictorial representation of scenario 5

3.2.5.1 General Objective

The object of this scenario is to determine when control room operators will need to abandon the control room due to fire-generated conditions inside the room.

3.2.5.2 Modeling Strategy

Control room abandonment is assumed to be solely dependent on habitability conditions. As mentioned in the previous sections, control room operators are considered "targets" in this scenario, so it is necessary to establish the fire conditions that would force operators out of the control room. This can be considered as the "abandonment criteria"; for example, visibility, temperature, heat flux, and toxicity are often the habitability indicators in these scenarios. Keeping track of these conditions may suggest the time at which the operator may need to abandon the control room. Once the criteria have been established (see Chapter 11 of NUREG/CR-6850 (EPRI 1011989) for details on habitability conditions), the fire-generated conditions in the room can be calculated so that the abandonment time can be determined.

For Main Control Room analyses, two ventilation conditions should be taken into consideration: (1) the ventilation system is turned off, causing hot gases and smoke to accumulate inside the control room, and (2) the ventilation system is on smoke-purge mode.

3.2.5.3 Recommended Modeling Tools
Algebraic models

Algebraic models are not recommended for this analysis. Determining habitability and time to abandonment in a fire scenario often requires tracking numerous output variables simultaneously. Algebraic models do not provide this capability.

Zone Models

Unlike algebraic models, zone models are capable of simultaneously tracking a number of relevant output variables (i.e., habitability conditions) in this scenario, so they provide a good solution to modeling fires in main control rooms. They are also capable of modeling the impact of various ventilation configurations required for modeling control room abandonment.

CFD Model (FDS)

Field models are also a good alternative to address this scenario, particularly if complex geometries are involved. Field models have the added advantage of handling rooms with complex geometries, intervening combustibles and obstructions, and varying ventilation conditions.

3.2.5.4 Detailed Examples
Readers are referred to Appendix A, which describes the analysis of a fire in a main control room.

3.2.6 Scenario 6: Smoke Detection and Sprinkler Activation

This scenario consists of calculating smoke/heat detector or sprinkler response. In some situations, the detection devices may be shielded from the combustion products by an obstruction (e.g., beams, cable trays, HVAC ducts, etc.). Failure of a detector to respond to a fire will delay the appropriate response of either the fire brigade or an automatic suppression system. Typical scenarios are shown in Figure 3-8.
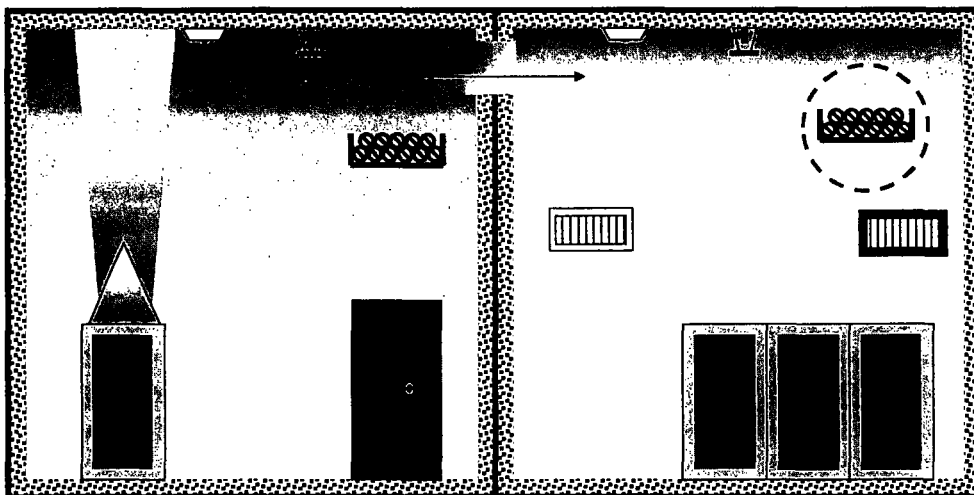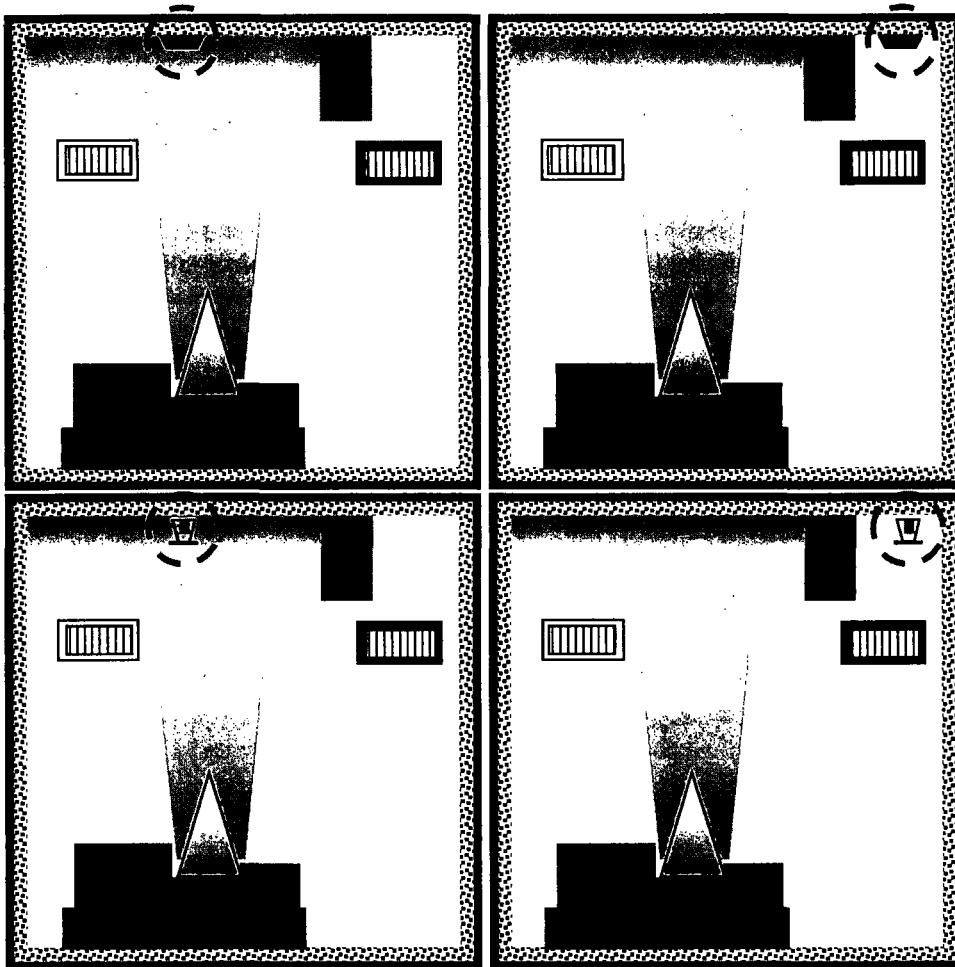

Figure 3-8. Pictorial representation of scenario 6

3.2.6.1 General Objective

The objective of this scenario is to calculate the response time of a smoke or heat detector that may be obstructed by ceiling beams, ventilation ducts, etc.

3.2.6.2 Modeling Strategy

For scenarios involving unobstructed smoke detector devices:

1. Determine the location of the detection device relative to the fire.

2. Select the detector response (activation) criteria. Chapter 11 of NUREG/CR-1805 contains guidance on estimating smoke detector response times.

3. Calculate the detection time using the appropriate model.

For scenarios involving obstructed smoke detector devices:

1. Determine the following characteristics of the Hot Gas Layer using all the necessary inputs for a Hot Gas Layer calculation, as described earlier in this chapter.

      a. Temperature as a function of time.

      b. Depth as a function of time. The smoke detector is expected to activate shortly after the Hot Gas Layer reaches the bottom of the obstruction and spills into the location of the device.

2. Select the detector response (activation) criteria. Chapter 11 of NUREG/CR-1805 contains guidance on estimating smoke detector response times.

3. Calculate the response time of the given smoke detector once the combustion products reach the detector.

For scenarios involving thermal devices (e.g., sprinklers, fusible links, or heat detectors), the process is similar. The only difference is that the thermal device needs to be characterized with relevant parameters, typically an activation temperature and the response time index (RTI). In addition, the selected model should account for the heating process of thermally thin elements (i.e., the heat detector device).

3.2.6.3 Recommended Modeling Tools

Algebraic models

Algebraic models can be used to determine time to heat or smoke detection when the fire-induced flows are not obstructed before reaching the detection device. By contrast, algebraic models are typically not recommended when fire-induced flows, such as fire plumes or ceiling jets, will be obstructed before reaching the detection device. In some cases, algebraic models that estimate the HGL temperature as a function of time may be used for rough estimates of activation times.

Zone Models

Zone Models can address the different scenario conditions presented above; for instance, CFAST and MAGIC are capable of determining time to smoke or heat detection, assuming no obstructions, and can simultaneously calculate smoke accumulation so that the time for smoke detection activation can be estimated. This would provide a first-order approximation, as zone models do not directly account for complex geometries, including obstructions. These models are not recommended for determining time to heat detection in obstructed geometries, since the velocity of the gases impacting the heat detector is not available in zone model calculations. As mentioned above, in some cases the HGL temperature alone may be used as a rough indicator of smoke and heat activation times.

CFD Model
CFD models are the best tool for estimating time to fire detection in complex geometries, including obstructions, as they can describe the compartment's complex geometries and mechanical ventilation conditions in detail.

3.2.6.4 Detailed Examples

Readers are referred to Appendices B and E, which discuss the calculation of the time to smoke and heat activation.

3.2.7 Scenario 7: Fire Impacting Structural Elements

This scenario consists of fire, such as an electrical cabinet, impacting exposed structural elements in the room. A typical example of this type of scenario is depicted in Figure 3-9.
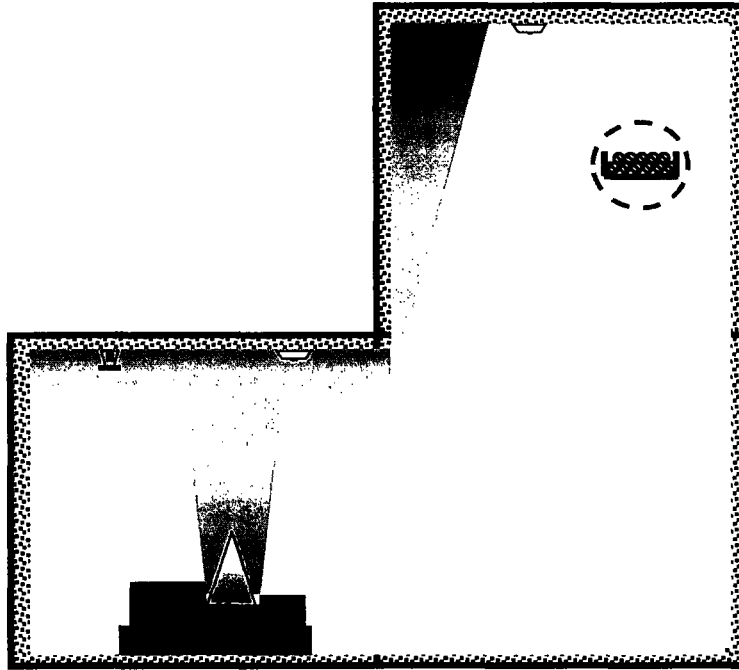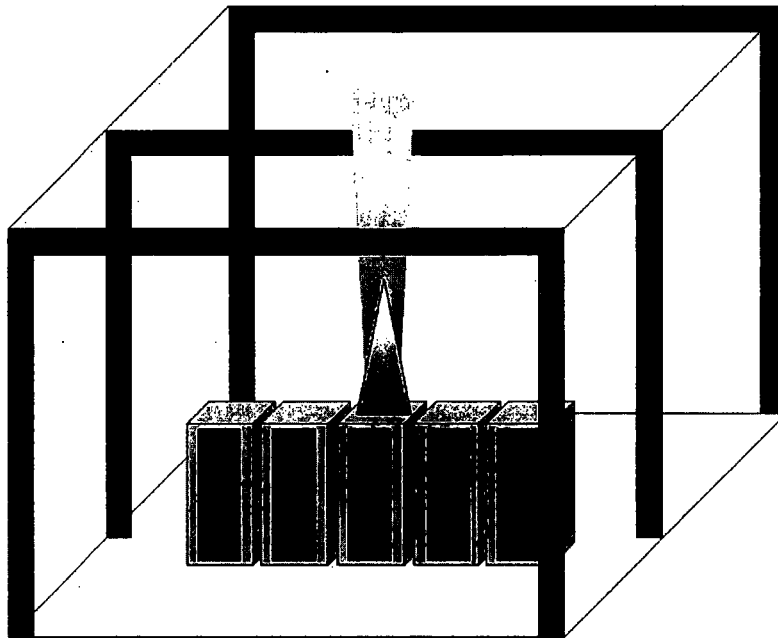

Figure 3-9. Pictorial representation of scenario 7

3.2.7.1 General Objective

The objective of this scenario is to characterize the temperature of structural elements exposed to a nearby fire source. For the case shown in Figure 3-9, the exposure fire is an electrical cabinet.

3.2.7.2 Modeling Strategy

The fire modeling tools within the scope of this guide should indicate whether the exposed structural element will reach damaging temperatures. However, this information is often not enough to determine whether the structural integrity of the compartment will be compromised by the exposing fire conditions. A more detailed structural analysis (i.e., one that involves complex temperature-dependent load-bearing calculations) may be necessary if such a determination is necessary.

Considering the limitations listed above, the following general guidance is provided:

1. Determine whether the structural element is directly above the fire, within the ceiling jet, exposed to radiant heating, or within the Hot Gas Layer. The results of this determination will suggest which model or combination of models should be used.

2. Calculate the temperature of the structural element based on the fire conditions affecting it. This will require an initial estimate of the fire-generating conditions surrounding the structural element, and, subsequently, the temperature of the element itself.

3.2.7.3 Recommended Modeling Tools

Algebraic models

Provided that the fire conditions affecting the structural element are appropriately identified (e.g., a fire plume, a ceiling jet, flame radiation, or a Hot Gas Layer exposure without significant contributions from any of the other three exposure mechanisms), algebraic models may be capable of determining whether the structural element will be exposed to damaging conditions. For example, plume temperature correlations can be used to determine the gas temperature surrounding an element inside the fire plume. MQH calculations can indicate whether compartment temperatures are near the critical temperature of structural elements; however, these may provide overly conservative estimates, as the algebraic models do not account for the heating of those structural elements that typically have large masses. Point source radiation calculations can be used to estimate the heat flux to structural elements that are not directly in the plume but close enough to the fire to become significantly heated.

Zone Models (CFAST and MAGIC)

Zone models are an appropriate tool to address this scenario, as the input file can be developed to capture the relative location of the fire and the structural element(s). Structural elements can be represented as a target, and the incident fire conditions can be tracked during the fire. Importantly, zone models are also capable of performing conduction heat transfer calculations for the structural element, resulting in a prediction of the temperature of the element itself.

CFD Model (FDS)

Field models are the best tool for estimating temperatures in structural elements in complex geometries, including obstructions, as they can handle the compartment's complex geometries, fire development, and mechanical ventilation conditions in detail, as well as the heating of the structural elements.

3.2.7.4 Detailed Examples

Readers are referred to Appendix F, which describes the analysis of a lubricating oil fire's effect on structural elements.

4
MODEL UNCERTAINTY

The fire models discussed in this Guide are classified as *deterministic* to distinguish them from *statistical* models. In essence, this means that each model takes as input a set of values, known as *input parameters*, that describe a specific fire scenario, and the model's algorithms then calculate the thermal conditions within the compartment. The output of the models usually takes the form of time histories of the various quantities of interest. In a sense, the model calculation is a virtual experiment because the design of a model simulation often involves the same thought process as the design of a physical experiment. The results of the calculation are likewise expressed in terms similar to those of an experiment, including an estimate of the uncertainty. The sources of uncertainty in a model prediction are different than those in an experimental measurement. According to NUREG-1855, Volume 1, *Guidance on the Treatment of Uncertainties Associated with PRAs in Risk-Informed Decision Making* (2009), there are three types of uncertainty associated with a model prediction:

Parameter Uncertainty: Input parameters are often chosen from statistical distributions or estimated from generic reference data. In either case, the uncertainty of these input parameters is propagated through the calculation, and the resulting uncertainty in the model prediction is known as the *parameter uncertainty*. The process of determining the extent to which the individual input parameters affect the results of the calculation is known as a *sensitivity analysis*.

Model Uncertainty: Idealizations of physical phenomena lead to simplifying assumptions in the formulation of the model equations. In addition, the numerical solution of equations that have no analytical solution can lead to inexact results. Model uncertainty is estimated via the processes of *verification* and *validation*. The first seeks to quantify the error associated with the mathematical solution of the governing equations, typically through numerical analysis, while the second seeks to quantify the error associated with the simplifying physical assumptions, typically through comparison of model predictions and full-scale experiments.

Completeness Uncertainty: This refers to the fact that a model may not be a complete description of the phenomena it is designed to predict. Some consider this a form of model uncertainty because most fire models neglect certain physical phenomena that are not considered important for a given application. For example, a model of sprinkler activation might neglect water condensation.

The focus of this chapter is <u>Model Uncertainty</u>. The issue of Parameter Uncertainty will be addressed by discussing various ways to conduct a sensitivity analysis. Completeness Uncertainty is addressed by the description of the algorithms found in the model documentation. It is addressed, indirectly, by the same process used to address the Model Uncertainty.

4.1 Validation of the Fire Models

The use of fire models to support fire protection decision making requires a good understanding of their limitations and predictive capabilities. NFPA 805 (NFPA, 2001) states that fire models shall only be applied within the limitations of the given model and shall be verified and validated. To support risk-informed/performance-based fire protection and implementation of the voluntary rule that adopts NFPA 805 as an RI/PB alternative, the NRC RES and EPRI conducted a collaborative project for the V&V of the five selected fire models described in Chapter 2. The results of this project were documented in NUREG-1824 (EPRI 1011999), *Verification and Validation of Selected Fire Models for Nuclear Power Plant Applications*.

Twenty-six full-scale fire experiments from six different test series were used to evaluate the models' ability to estimate thirteen quantities of interest for fire scenarios that were judged to be typical of those that might occur in an NPP. The results of the study are summarized in Table 4-1. An explanation of this table is to follow.

Table 4-1. Results of the V&V study, NUREG-1824 (EPRI 1011999).

Output Quantity	FDTs δ	FDTs σ_M	FIVE δ	FIVE σ_M	CFAST δ	CFAST σ_M	MAGIC δ	MAGIC σ_M	FDS δ	FDS σ_M	Exp σ_E
HGL Temperature Rise	1.44	0.25	1.56	0.32	1.06	0.12	1.01	0.07	1.03	0.07	0.07
HGL Depth	N/A		N/A		1.04	0.14	1.12	0.21	0.99	0.07	0.07
Ceiling Jet Temp. Rise	N/A		1.84	I.D.	1.15	I.D.	1.01	0.08	1.04	0.08	0.08
Plume Temperature Rise	0.73	I.D.	0.94	I.D.	1.25	0.28	1.01	0.07	1.15	I.D.	0.07
Flame Height*	I.D.	I.D.	I.D.	I.D.	I.D.	I.D.	I.D.	I.D.	I.D.	I.D.	I.D.
Oxygen Concentration	N/A		N/A		0.91	I.D.	0.90	0.18	1.08	0.14	0.05
Smoke Concentration	N/A		N/A		2.65	I.D.	2.06	I.D.	2.70	I.D.	0.17
Room Pressure Rise	N/A		N/A		1.13	0.37	0.94	0.39	0.95	0.51	0.20
Target Temperature Rise	N/A		N/A		1.00	0.27	1.19	0.27	1.02	0.13	0.07
Radiant Heat Flux	2.02	I.D.	1.42	0.55	1.32	0.54	1.07	0.36	1.10	0.17	0.10
Total Heat Flux	N/A		N/A		0.81	0.47	1.18	0.35	0.85	0.22	0.10
Wall Temperature Rise	N/A		N/A		1.25	0.48	1.38	0.45	1.13	0.20	0.07
Wall Heat Flux	N/A		N/A		1.05	0.43	1.09	0.34	1.04	0.21	0.10

I.D. indicates insufficient data for the statistical analysis.
N/A indicates that the model does not have an algorithm to compute the given Output Quantity

* All of the models except FDS use the Heskestad Flame Height Correlation (Heskestad, *SFPE Handbook*). These models were shown to be in qualitative agreement with the experimental observations, but there was not enough data to further quantify this assessment.

The Models: Five fire models were selected for the study, based on the fact that they are commonly used in fire analyses of NPPs in the U.S. Two of the models consist of simplified engineering correlations (FDTs and FIVE), two are "zone" models (CFAST and MAGIC), and one is a CFD model (FDS).

The Experiments: Six series of experiments (26 individual fire experiments in all) were selected for the NRC/EPRI fire model validation study (NUREG-1824/EPRI 1011999). Each series represented a typical fire scenario (for example, a fire in a switchgear room or turbine hall); however, the test parameters could not encompass every possible NPP fire scenario. To better understand the range of applicability of the validation study, Table 2-5 of NUREG-1824 (EPRI 1011999), Volume 1 lists various normalized parameters that may be used to compare NPP fire scenarios with the validation experiments. These parameters express, for instance, the size of the fire relative to the size of the room, or the relative distance from the fire to critical equipment. This information is important because typical fire models are not designed for fires that are very small or very large in relation to the volume of the compartment or the ceiling height.

For a given set of experiments and NPP fire scenarios, the user can calculate the relevant normalized parameters. These parameters will either be inside, outside, or on the margin of the validation parameter space. Consider each case in turn:

1   If the parameters fall within the ranges that were evaluated in the validation study, then Table 4-1 can be referenced directly.

2   If only some of the parameters fall within the range of the study, additional justification is necessary. This is a common occurrence because realistic fire scenarios involve a variety of fire phenomena, some of which are easier to estimate than others. A case in point is the burning of electrical cabinets and cables. NUREG-1824 (EPRI 1011999) does not address these fires directly, even though some of the experiments used in the study were intended as mock-ups of control or switchgear room fires. For scenarios involving these kinds of fires, the heat release rates are often taken from experiments rather than predicted by a model. It has been shown, in NUREG-1824 (EPRI 1011999) and other validation studies, that the models can estimate the transport of smoke and heat with varying degrees of accuracy, but they have not been shown (at least not in NUREG-1824 (EPRI 1011999)) to estimate the details of the fire's ignition and growth. While this does not eliminate the models from the analysis, it still restricts their applicability to only some of the phenomena.

3   If the parameters fall outside the range of the study, then a validation determination cannot be made based on the results from the study. The modeler needs to provide independent justification for using the particular model. For example, none of the experiments considered in NUREG-1824 (EPRI 1011999) were under-ventilated. However, several of the models have been independently compared to under-ventilated test data, and the results have been documented either in the literature or in the model documentation. As another example, suppose that the selected model uses a plume, ceiling jet, or flame height correlation outside the parameter space of NUREG-1824 (EPRI 1011999) but still within the parameter space for which the correlation was originally developed. In such cases, appropriate references are needed to demonstrate that the correlation is still appropriate even if not explicitly validated in NUREG-1824 (EPRI 1011999).

The Predicted Quantities: The experimental data for the validation study consisted of measurements of one or more of the 13 physical quantities listed in the table. The FDT[s] and FIVE do not possess algorithms to estimate every quantity, in which case the table cell is labeled N/A.

Model Uncertainty

The Statistics: For each model and output quantity, a summary plot of the results is presented in NUREG-1824 (EPRI 1011999). For example, Figure 4-1 compares the measured and predicted target temperatures for the model FDS. If a particular prediction and measurement are the same, the resulting point falls on the solid diagonal line. The longer-dashed off-diagonal lines indicate the experimental uncertainty. Roughly speaking, points within the longer dashed lines are said to be "within experimental uncertainty," and in such cases it is not possible to further quantify the accuracy of the prediction. Points falling outside the experimental uncertainty bounds cannot be said to be free of model uncertainty. At the time of the publication of NUREG-1824 (EPRI 1011999), the writing team decided to assign the colors Green and Yellow to indicate the degree to which the model predictions are inside or outside of the experimental uncertainty bounds. However, since the writing of NUREG-1824 (EPRI 1011999), it was decided by the authors of the Fire Model User's Guide to replace the color system with a more quantifiable metric of model accuracy.
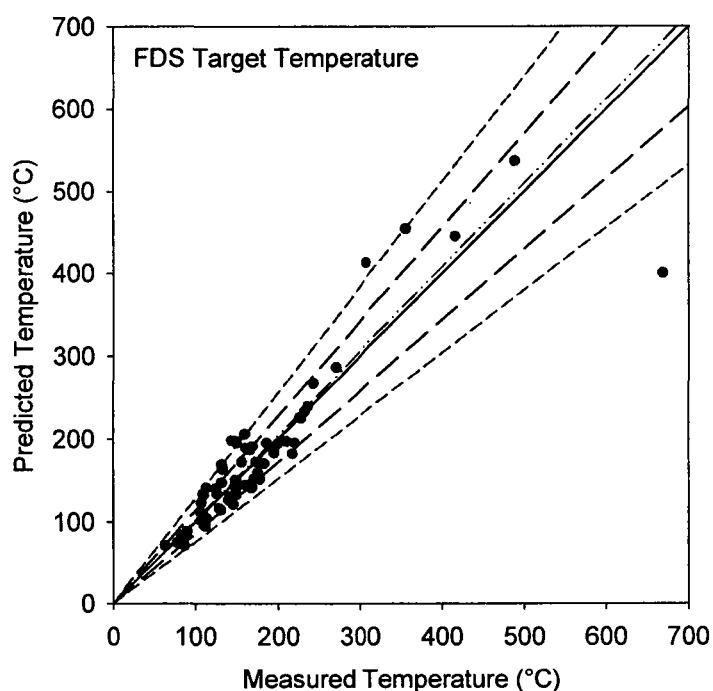
Figure 4-1. Sample set of results from NUREG-1824 (/EPRI 1011999).

Consider again Figure 4-1. To better make use of results such as these, two statistical parameters[5] have been calculated for each model and each predicted quantity. The first parameter, δ, is the *bias factor*. It indicates the extent to which the model, on average, under or overpredicts the measurements of a given quantity. For example, the bias factor for the data shown in Figure 4-1 is 1.02. This means that the model has been shown to slightly over-estimate target temperatures by 2%, on average, and this is shown graphically by the red dash-dot line just above the diagonal. The bias factor for each model and each output quantity is listed in Table 4-1.

---

[5] The statistical parameters listed in Table 4-1 are based on the versions of the fire models used in the V&V study, circa 2006. As the models are improved and new validation data introduced, these values may change.

The second statistic[6] in Table 4-1 is the relative standard deviation of the model, $\tilde{\sigma}_M$, and the experiments, $\tilde{\sigma}_E$. These indicate the uncertainty or degree of "scatter" of the model and the experiments, respectively. Referring again to Figure 4-1, there are two sets of off-diagonal lines. The first set, shown as long-dashed black lines, indicate the experimental uncertainty. The slopes of these lines are $1 \pm 2\tilde{\sigma}_E$ (it is customary to express uncertainties in the form of "2-sigma" or 95% confidence intervals). The second set of off-diagonal lines, shown as short-dashed red lines, indicates the model uncertainty. The slopes of these lines are $\delta \pm 2\tilde{\sigma}_M$. If the model is as accurate as the measurements against which it is compared, the two sets of off-diagonal lines would merge. The extent to which the data scatters outside of the experimental bounds is an indication of the degree of model uncertainty.

The derivation of the statistical parameters in Table 4-1 is provided in the next section, while their use is described here. Suppose that a model prediction is denoted M. It is assumed that the "true" value of the predicted quantity is a normally distributed random variable with a mean, $\mu = M/\delta$, and a standard deviation, $\sigma = \tilde{\sigma}_M(M/\delta)$. Using these values, the probability of exceeding a critical value, x_c, is:

$$P(x > x_c) = \frac{1}{2}\,\text{erfc}\left(\frac{x_c - \mu}{\sigma\sqrt{2}}\right) \tag{4-1}$$

Note that the *complimentary error function* is defined as follows:

$$\text{erfc}(x) = \frac{2}{\sqrt{\pi}}\int_x^\infty e^{-t^2}\,dt \tag{4-2}$$

It is a standard function in mathematical or spreadsheet programs like Microsoft Excel[7].

To summarize, the procedure for determining the probability that a quantity predicted by a model could exceed a critical value is as follows:

1. Express the model prediction as a rise above its ambient value. Call this number M. Note that the ambient value of most output quantities is zero. Temperature, oxygen concentration, and smoke layer height are exceptions. For these quantities, express the predicted value as a temperature *rise*, oxygen *decrease* below ambient, and layer *depth*.

2. Using the values of δ and $\tilde{\sigma}_M$ from Table 4-1, compute the mean, $\mu = M/\delta$, and standard deviation, $\sigma = \tilde{\sigma}_M(M/\delta)$, of the normal distribution for the quantity of interest.

3. Use the equation to compute the probability that the predicted quantity could exceed a critical value, x_c. Remember to also express this critical value as a rise above ambient in the same way as the predicted value, M.

A few examples of this procedure are included in Section 4.3.

4.2 Derivation of the Model Uncertainty Statistics

This section describes the derivation of the statistics listed in Table 4-1. These values summarize the results of the NRC/EPRI fire model validation study documented in NUREG-1824 (EPRI 1011999). This section is included for information only; there is no need for a

---

[6] For some models/quantities, there was an insufficient amount of data to calculate the relative standard deviation of the distribution, in which case I.D. is shown in the Table.

[7] Excel 2007 does not evaluate $\text{erfc}(x)$ for negative values of x, even though the function is defined for all real x. In such cases, use the identity $\text{erfc}(-x) = 2 - \text{erfc}(x)$.

Model Uncertainty

model user to perform this type of calculation. McGrattan and Toman (2011) provide additional details on the development of these uncertainty calculations.

For each of the fire models and each of the output quantities that were evaluated in the study, a plot similar to that shown in Figure 4-1 was produced. For each measurement point, a single experimental measurement was plotted against a single model prediction. The plot shows all the comparison points. The calculation of the statistics uses this set of measured and predicted values, along with an estimate of the experimental uncertainty. The purpose of the calculation is to "subtract off," in a statistical sense, the experimental uncertainty so that the model uncertainty can be estimated. Before describing the calculation, a few assumptions must be made:

1. The experimental measurements are assumed to be unbiased, and their uncertainty is assumed to be normally distributed with a constant relative standard deviation, $\tilde{\sigma}_E$ (that is, the standard deviation as a fraction of the measured value). Table 4-2 provides estimates of relative experimental uncertainties for the quantities of interest.

2. The model error is assumed to be normally distributed about the predicted value multiplied by a bias factor, δ. The relative standard deviation of the distribution is denoted as $\tilde{\sigma}_M$.

The computation of the estimated bias and scatter associated with model error proceeds as follows. Given a set of n experimental measurements, E_i, and a corresponding set of model predictions, M_i, compute the following:

$$\overline{\ln(M/E)} = \frac{1}{n}\sum_{i=1}^{n}\ln(M_i/E_i) \tag{4-3}$$

The standard deviation of the model error, $\tilde{\sigma}_M$, can be computed from the following equation:

$$\sqrt{\tilde{\sigma}_M^2 + \tilde{\sigma}_E^2} \cong \sqrt{\frac{1}{n-1}\sum_{i=1}^{n}[\ln(M_i/E_i) - \overline{\ln(M/E)}]^2} \tag{4-4}$$

The bias factor is:

$$\delta = \exp\left(\overline{\ln(M/E)} + \frac{\tilde{\sigma}_M^2 - \tilde{\sigma}_E^2}{2}\right) \tag{4-5}$$

For a given model prediction, M, the "true" value of the quantity of interest is assumed to be a normally distributed random variable with a mean of M/δ and a standard deviation of $\tilde{\sigma}_M(M/\delta)$.

There are a few issues to consider when using this procedure:

1. All values need to be positive, and each value needs to be expressed as an increase over its ambient value. For example, the oxygen concentration should be expressed as a positive number (i.e., the decrease in concentration below its ambient value).

2. If the measurement uncertainty is overestimated, the model error will be underestimated. If the model error is less than the experimental uncertainty, the latter should be reevaluated. The model cannot be shown to have less error than the uncertainty of the experiment with which it is compared

3. The procedure assumes that the quantity $\ln(M/E)$ is normally distributed. This is not necessarily true, especially in cases where there are an insufficient number of points in the sample. Figure 4-2 provides two examples in which the normality of the validation data is tested[8]. In cases where the data is not normally distributed, only the bias is reported.

Table 4-2. Experimental uncertainty of the experiments performed as part of the validation study in NUREG-1824(EPRI 1011999)

Quantity	$2\tilde{\sigma}_E$
HGL Temperature Rise	0.14
HGL Depth	0.13
Ceiling Jet Temperature Rise	0.16
Plume Temperature Rise	0.14
Gas Concentration	0.09
Smoke Concentration	0.33
Pressure (no forced ventilation)	0.40
Pressure (with forced ventilation)	0.80
Heat Flux	0.20
Surface or Target Temperature	0.14
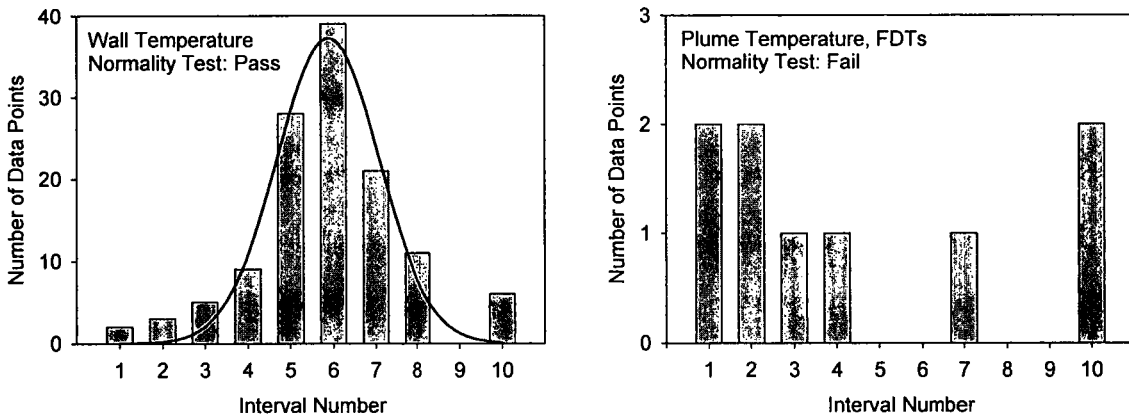
Figure 4-2. Two examples demonstrating how the validation data is tested for normality.

4.3 How to Calculate the Model Uncertainty

This section contains a few exercises to explain the procedure for calculating model uncertainty. These examples consider model uncertainty only; that is, it is assumed in each case that the input parameters are not subject to uncertainty.

---

[8] The Kolmogorov-Smirnov test for normality has been applied using the software package SigmaPlot[®]10, Systat Software, Inc. The default P value of 0.05 was used.

4.3.1 Example 1: Target Temperature

Suppose that cables within a compartment are assumed to fail if their surface temperature reaches 330 °C (625 °F). The model FDS predicts that the maximum cable temperature due to a fire in an electrical cabinet is 300 °C (570 °F). What is the probability that the cables could fail?

Step 1: Subtract the ambient value of the cable temperature, 20 °C (68 °F) to determine the predicted temperature _rise_. Refer to this value as the _model prediction_:

$$M = 300 - 20 = 280°C \tag{4-6}$$

Step 2: Refer to Table 4-1, which indicates that, on average, FDS overpredicts Target Temperatures with a bias factor, δ, of 1.02. Calculate the _adjusted model prediction_:

$$\mu = \frac{M}{\delta} = \frac{280}{1.02} = 275°C \tag{4-7}$$

Referring again to Table 4-1, calculate the standard deviation of the distribution:

$$\sigma = \tilde{\sigma}_M \left(\frac{M}{\delta}\right) = 0.13 \left(\frac{280}{1.02}\right) = 36°C \tag{4-8}$$

Step 3: Calculate the probability that the actual cable temperature would exceed 330°C:

$$P(T > 330) = \frac{1}{2} \text{erfc}\left(\frac{T - T_0 - \mu}{\sigma\sqrt{2}}\right) = \frac{1}{2} \text{erfc}\left(\frac{330 - 20 - 275}{36\sqrt{2}}\right) = 0.16 \tag{4-9}$$

The process is shown graphically in Figure 4-3. The area under the "bell curve" for temperatures higher than 330 °C (625 °F) represents the probability that the actual cable temperature would exceed that value. Note that this estimate is based only on the model uncertainty.
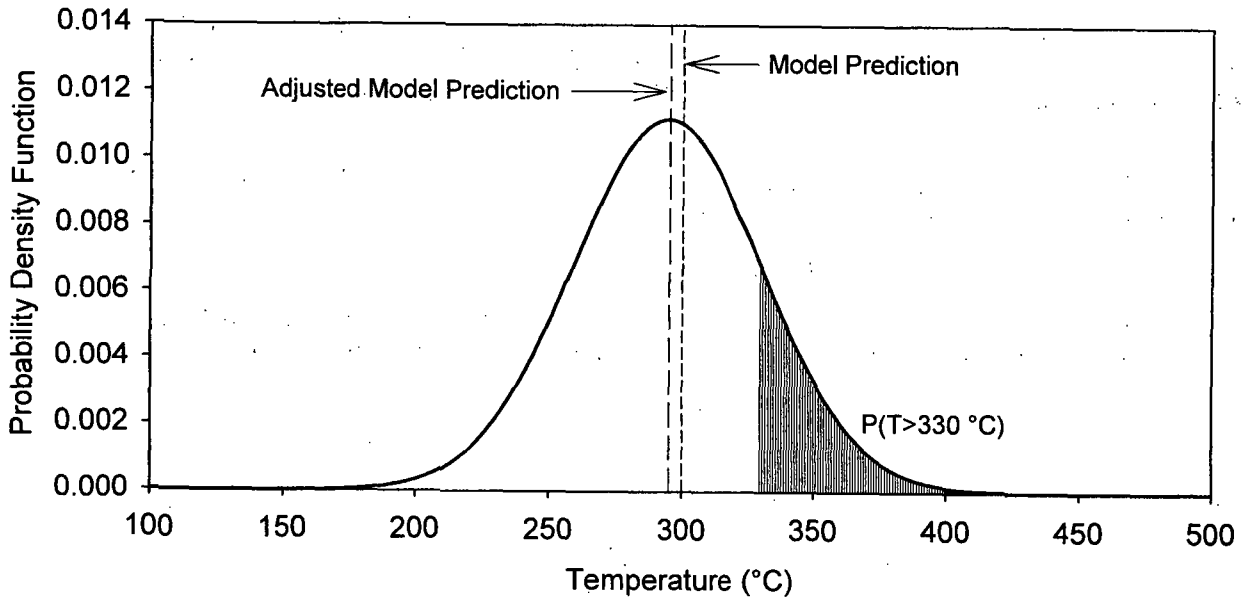
Figure 4-3. Normal distribution of the "true" value of the cable temperature in a hypothetical fire.

4.3.2 Example 2: Critical Heat Flux

As part of a screening analysis, the model MAGIC is used to estimate the radiant heat flux from a fire to a nearby group of thermoplastic cables. According to NUREG/CR-6850 (EPRI 1011989), Appendix H, one of the damage criteria for thermoplastic cables is a radiant heat flux to the target cable that exceeds 6 kW/m². The model, by coincidence, predicts a heat flux of 6 kW/m². What is the probability that the actual heat flux from a fire will be 6 kW/m² or greater? Assume for this exercise that the model input parameters are not subject to uncertainty, only the model itself.

Step 1: Unlike in the previous example, there is no need to subtract an ambient value of the heat flux (it is zero). Thus, the *model prediction* is:

$$M = 6 \text{ kW/m}^2 \tag{4-10}$$

Step 2: Refer to Table 4-1, which indicates that, on average, MAGIC overpredicts Radiant Heat Flux with a bias factor, δ, of 1.15. Calculate the *adjusted model prediction*:

$$\mu = \frac{M}{\delta} = \frac{6}{1.15} \approx 5.2 \text{ kW/m}^2 \tag{4-11}$$

Referring again to Table 4-1, calculate the standard deviation of the distribution:

$$\sigma = \tilde{\sigma}_M \left(\frac{M}{\delta}\right) = 0.36 \left(\frac{6}{1.15}\right) \approx 1.9 \text{ kW/m}^2 \tag{4-12}$$

Step 3: Calculate the probability that the actual heat flux, $\dot{q}''$, will exceed the critical value of the heat flux, $\dot{q}_c'' = 6 \text{ kW/m}^2$:

$$P(\dot{q}'' > 6) = \frac{1}{2}\,\mathrm{erfc}\left(\frac{\dot{q}''_c - \mu}{\sigma\sqrt{2}}\right) = \frac{1}{2}\,\mathrm{erfc}\left(\frac{6 - 5.2}{1.9\sqrt{2}}\right) \approx 0.34 \tag{4-13}$$

This is a somewhat surprising result. Even though the model predicts a peak radiant heat flux equal to the critical value, there is only a one in three chance that the actual heat flux would exceed this value. This is mainly due to the fact that MAGIC has been shown to over-estimate the heat flux by about 15%.

It is important to note that this calculation of model uncertainty does not take into account the input parameters, such as the heat release rate of the fire. It is only an assessment of how well the model MAGIC can estimate the radiant heat flux to a target.

4.4 Sensitivity Analysis

The previous sections describe how to express the uncertainty of a model prediction resulting from the inherent limitations of the model itself. For that discussion, it was assumed that the input parameters for the model were not subject to uncertainty. However, there will always be uncertainty associated with the model input parameters. This section suggests ways to assess the impact of this kind of uncertainty on the final prediction.

The more complex fire models discussed in this Guide may require dozens of physical and numerical input parameters for a given fire scenario. However, only a few of these parameters, when varied over their plausible range of values, will significantly impact the results. For example, the thermal conductivity of the compartment walls will not significantly affect a predicted cable surface temperature. Table 4-3 lists the input parameters whose impact on the given output quantity significantly outweighs all the other parameters. The heat release rate is almost always one of these.

In Volume 2 of NUREG-1824 (EPRI 1011999), Hamins quantifies the functional dependence of these key input parameters (see Table 4-3). These relationships are based either on the governing mathematical equations or on algebraic models. The basic mathematical form of the relationship is:

$$\text{Output Quantity} = \text{Constant} \times (\text{Input Parameter})^{\text{Power}} \tag{4-14}$$

The exact value of the Constant is not important; rather, it is the Power that matters. The larger its absolute value, the more important the Input Parameter. According to the McCaffrey, Quintiere, Harkleroad (MQH) correlation, for example, the Hot Gas Layer (HGL) temperature rise in a compartment fire is proportional to the heat release rate raised to the two-thirds power:

$$T - T_0 = C\dot{Q}^{2/3} \tag{4-15}$$

It is not the value of the constant, C, that is important here, but rather the amount that the HGL temperature, ΔT, changes due to a shift in the HRR, $\Delta\dot{Q}$. It is the two-thirds power dependence, as found in Table 4-3, that matters. To see why, take the first derivative of T with respect to $\dot{Q}$ and write the result in terms of differentials:

$$\frac{\Delta T}{T - T_0} \approx \frac{2}{3}\frac{\Delta\dot{Q}}{\dot{Q}} \tag{4-16}$$

This is a simple formula with which one can readily estimate the relative change in the model output quantity, $\Delta T/(T - T_0)$, due to the relative change in the model input parameter, $\Delta \dot{Q}/\dot{Q}$. The uncertainty in a measured quantity is often expressed in relative terms[9]. Suppose that the uncertainty in the HRR of the fire, $\Delta \dot{Q}/\dot{Q}$, is 0.15, or 15 %. The expression above indicates that a 15 % increase in the HRR should lead to a 2/3 x 15 = 10 % increase in the prediction of the HGL temperature. The result is equally valid for a reduction – if the HRR is reduced by 15 %, the HGL temperature is reduced by 10 %.

This relationship is based on an algebraic model, and has nothing to do with any particular model; however, an effective way to check a fire model is to take a simple compartment fire simulation, vary the HRR, and ensure that the change in the HGL temperature agrees with the correlation. Consider the two curves shown in Figure 4-4. For Benchmark Exercise #3 of the International Collaborative Fire Model Project (ICFMP), Test 3 was simulated with FDS, using HRR values of 1000 kW and 1150 kW. An examination of the peak values confirms that the relative change in the HGL temperature (10 %) is two-thirds the relative change in the HRR (15 %), consistent with the empirical result of the MQH correlation. Even though FDS is a much more complicated model than the simple expression shown above, it still exhibits the same functional dependence on the HRR.

Table 4-3. Sensitivity of model outputs from Volume 2 of NUREG-1824 (EPRI 1011999).

Output Quantity	Important Input Parameters	Power Dependence
HGL Temperature	HRR Surface Area Wall Conductivity Ventilation Rate Door Height	2/3 -1/3 -1/3 -1/3 -1/6
HGL Depth	Door Height	1
Gas Concentration	HRR Production Rate	1/2 1
Smoke Concentration	HRR Soot Yield	1 1
Pressure	HRR Leakage Rate Ventilation Rate	2 2 2
Heat Flux	HRR	4/3
Surface/Target Temperature	HRR	2/3

---

[9] Note that a differential relationship is only approximate. This method of relating input parameters to output quantities is valid for relative differences that are less than approximately 30% in absolute value.
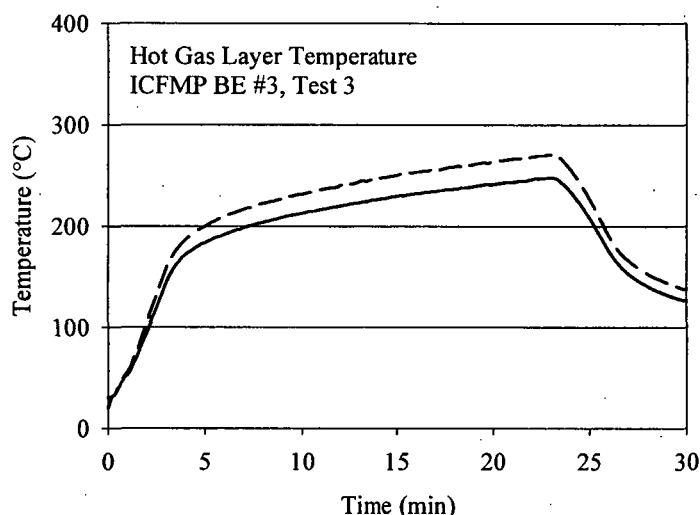
Figure 4-4. FDS predictions of HGL Temperature as a function of time due to a 1,000 kW fire (solid line) and a 1,150 kW fire (dashed).

This section describes the usefulness of sensitivity analysis. NFPA 805 uses the term "Maximum Expected Fire Scenario" to describe a severe fire that could be "reasonably anticipated" to occur within a compartment and the term "Limiting Fire Scenario" to describe a severe fire that exceeds one or more performance criteria. The analyst is often asked to determine the model inputs for both of these scenarios. For example, choosing the 98th percentile HRR from a distribution of, say, cabinet fires, along with other extreme but plausible values of the ventilation rate and material properties, produces what might be considered the Maximum Expected Fire Scenario. Determining the parameters for the Limiting Fire Scenario, however, is more difficult because it is a mathematically ill-posed problem to take a given outcome of a fire and go backwards in time and determine the conditions that might lead to it. Rather than the trial and error approach to determining parameters for a Limiting Fire Scenario, it is better to first calculate the Maximum Expected Fire Scenario and then perform a sensitivity analysis for the most important input parameters to determine which values of each will lead to the Limiting Fire Scenario.

Suppose, for example, that as part of an NFPA 805 analysis the problem is to determine the Limiting Fire Scenario for a particular compartment whose HGL temperature is not to exceed 500 °C (930 °F). Assume that the geometrical complexity of the compartment rules out the use of the empirical and zone models, and that FDS has been selected for the simulation.

Step 1: Determine an appropriate maximum expected fire heat release rate. For this example, suppose that a 98th percentile HRR for the electrical cabinet fire, 702 kW, has been determined to be the MEFS. Choose a model and calculate the peak HGL temperature.

Step 2: Assume that FDS predicts 450 °C (840 °F) for the selected fire scenario. Adjust the prediction to account for the model bias, δ (See Table 4-1):

$$T_{adj} = T_0 + \frac{T - T_0}{\delta} = 20 + \frac{450 - 20}{1.03} \approx 437°C \qquad (4\text{-}17)$$

Step 3: Calculate the change in HRR required to increase the HGL temperature to 500 °C (930 °F):

$$\Delta \dot{Q} \approx \frac{3}{2} \dot{Q} \frac{\Delta T}{T_{adj} - T_0} = \frac{3}{2} 702 \frac{500 - 437}{417} = 159 \text{ kW} \qquad (4\text{-}18)$$

This calculation suggests that adding an additional 159 kW to the original 702 kW will produce an HGL temperature in the vicinity of 500 °C (930 °F). This result can be double-checked by re-running the model with the modified input parameters.

Table 4-3 lists several other parameters besides the HRR that can affect the HGL temperature. Following the example just discussed, similar calculations can be performed in which these other parameters are varied to determine how else the LFS might be reached. For example, suppose that the surface area, A, of the compartment is 400 m² (4300 ft²). How much would the surface area have to increase or decrease to raise the HGL temperature to 500 °C (930 °F)? Or if the thermal conductivity of the walls, k, is 0.1 W/m/K, how much would it have to change? If the ventilation rate is 1 m³/s, how much would it have to change? If the door height, h, is 2 m, how much would it have to change? Following the example for the HRR, the required changes in these parameters can be calculated as follows:

$$\Delta A \approx -3A \frac{\Delta T}{T_{adj} - T_0} = -3(400) \frac{500 - 437}{417} = -181 \text{ m}^2 \qquad (4\text{-}19)$$

$$\Delta k \approx -3k \frac{\Delta T}{T_{adj} - T_0} = -3(0.1) \frac{500 - 437}{417} = -0.045 \text{ W/m/K} \qquad (4\text{-}20)$$

$$\Delta \dot{V} \approx -3\dot{V} \frac{\Delta T}{T_{adj} - T_0} = -3(1) \frac{500 - 437}{417} = -0.45 \frac{\text{m}^3}{\text{s}} \qquad (4\text{-}21)$$

$$\Delta h \approx -6h \frac{\Delta T}{T_{adj} - T_0} = -6(2) \frac{500 - 437}{417} = -1.8 \text{ m} \qquad (4\text{-}22)$$

For this example, to increase the HGL temperature by 63 °C (145 °F), one could increase the HRR by 159 kW, decrease the surface area of the compartment by 181 m² (1948 ft²), decrease the thermal conductivity of the walls by 0.045 W/m/K, decrease the ventilation rate by 0.45 m³/s, or decrease the door height by 1.8 m (5.9 ft). Of course, some of these options are not physically possible. Room dimensions and thermal properties are not subject to significant change, but the HRR and ventilation rates can vary significantly.

4.5 Chapter Summary

This chapter describes the three forms of uncertainty related to fire modeling: *parameter*, *model*, and *completeness* uncertainty. Model and completeness uncertainty are closely related, and it would be impractical to evaluate them separately. The most practical way to quantify their combined effect is to compare model predictions with as many experimental measurements as possible in order to develop a robust statistical description of the model's accuracy. The five models considered in this Guide underwent a validation study (NUREG-1824 (EPRI 1011999)) in which their predictions were compared with measurements from a variety of full-scale experiments. It is possible to take a given model's prediction of a given quantity and assume a distribution for the "true" value of this quantity. Rather than reporting the result of a calculation as a single value, it is preferable to report the probability that the true value of a predicted quantity exceeds a given critical value.

Regardless of the application, the assessment of model uncertainty is the same. However, the issue of parameter uncertainty is dependent on the application. Some analyses, PRAs for example, make use of "best estimate" input parameters. More complex forms of PRAs can involve a broad statistical sampling of input parameters from assumed distributions. Deterministic applications usually consider "worst case" or "bounding" analyses, in which extreme, yet plausible, input parameters are used. In mathematical terms, all of these applications involve selecting parameters from relatively narrow or broad regions of the parameter "space." It is impossible to consider all possible combinations of input parameters, which is why a simple form of sensitivity analysis, outlined in this chapter, can be used to extend the range of outcomes. For example, algebraic models indicate the extent to which all of the output quantities of interest are sensitive to changes in the specified HRR, reducing the need to re-run model simulations for an extensive number of values. Sensitivity analysis can help determine which input parameters are necessary to bring about the Limiting Fire Scenario in an NFPA 805 analysis.

5
REFERENCES

10 CFR 50, "Voluntary Fire Protection Requirements for Light-Water Reactors," 10 CFR Part 50, Section 50.48(c), RIN 3150-AG48, *Federal Register*, Volume 69, Number 115, U.S. Nuclear Regulatory Commission, Washington, DC, June 16, 2004.

ASME/ANS RA-Sa-2009, *Standard for Level 1/Large Early Release Frequency Probabilistic Risk Assessment for Nuclear Power Plant Applications, Addendum a*, ASME/ANS RA-S-2009, American Society of Mechanical Engineers, 2009.

ASTM E119-10a, *Standard Test Methods for Fire Tests of Building Construction Materials*, American Society for Testing and Materials, West Conshohocken, PA, 2010.

ASTM E1355–05a (2005), *ASTM Standard Guide for Evaluating the Predictive Capability of Deterministic fire Models*, American Society for Testing and Materials, West Conshohocken, PA, 2005.

Babrauskas, V., *Ignition Handbook*, Fire Science Publishers/Society of Fire Protection Engineers, Issaquah WA (2003).

Buchanan, A. H., *Structural Design for Fire Safety*, John Wiley and Sons, LTD, Chichester, England, 2001.

Drysdale, D., *An Introduction to Fire Dynamics*, John Wiley and Sons, Chichester, pp. 14, 283-284, 1996.

EPRI 1002981, *Fire Modeling Guide for Nuclear Power Plant Applications*, Electric Power Research Institute, Palo Alto, CA, August 2002.

Fire Protection Handbook, National Fire Protection Association, 20th Ed., A.E. Cote, (Editor), 2008.

Fourney, G.P., *User's Guide for Smokeview Version 5 - A Tool for Visualizing Fire Dynamics Simulation Data, Volume II: Technical Reference Guide*, NIST Special Publication 1017-2, National Institute of Standards and Technology, Gaithersburg, MD, October 2010.

Gay, L., *User Guide of MAGIC Software V4.1.1*, EdF HI82/04/022/B, Electricité de France, France, April 2005.

Gay, L., C. Epiard, and B. Gautier, *MAGIC Software Version 4.1.1: Mathematical Model*, EdF HI82/04/024/B, Electricité de France, France, November 2005.

Gay, L., J. Frezabeu, and B. Gautier, *Qualification File of Fire Code MAGIC Software Version 4.1.1: Mathematical Model*, EdF HI82/04/024/B, Electricité de France, France, November 2005.

Heskestad, G., Chapter 2, Section 2-2, "Fire Plumes," *SFPE Handbook off Fire Protection Engineering*, 2nd Edition, (P.J. DiNenno, Editor-in-Chief), National Fire Protection Association and The Society of Fire Protection Engineers, Quincy, MA, 1995.

Holman, J.P., *Heat Transfer*, 7th edition, McGraw-Hill, New York, 1990.

References

Jones, W., R. Peacock, G. Forney, and P. Reneke, *CFAST: An Engineering Tool for Estimating Fire Growth and Smoke Transport, Version 5 - Technical Reference Guide*, NIST Special Publication 1030, National Institute of Standards and Technology, Gaithersburg, MD, 2004.

Karlsson, B. and J. Quintiere, *Enclosure Fire Dynamics*, CRC Press, Boca Raton, Florida, 2000.

Köylu, U.O. and G.M. Faeth, "Carbon Monoxide and Soot Emissions from Liquid-Fueled Buoyant Turbulent Diffusion Flames," *Combustion and Flame*, 87:61-76, 1991.

McCaffrey, B.J., J.G. Quintiere, and M.F. Harkleroad, "Estimating Compartment Temperature and Likelihood of Flashover Using Fire Test Data Correlation," *Fire Technology*, Volume 17, No. 2, pp. 98-119, Quincy, MA, 1981.

McGrattan, K., et al., *Fire Dynamics Simulator (Version 5) Technical Reference, Volume 3: Validation*, NIST Special Publication 1018-5, National Institute of Standards and Technology, Gaithersburg, MD, 2010.

McGrattan, K., B. Klein, S. Hostikka and J. Floyd, *Fire Dynamics Simulator (Version 5) User's Guide*, NIST Special Publication 1019-5, National Institute of Standards and Technology, Gaithersburg, MD, 2009.

McGrattan, K., and B. Toman, "Quantifying the predictive uncertainty of complex numerical models," *Metrologia*, 48:173-180, 2011.

Mulholland, G.W., and C. Croarkin, "Specific Extinction Coefficient of Flame Generated Smoke," *Fire and Materials*, 24:227-230, 2000.

NFPA Fire Protection Handbook, 20th Edition (A.E. Cote, Editor-in-Chief), National Fire Protection Association, Quincy, MA, 1997.

NFPA 70 (NEC 2008), *National Electric Code*, National Fire Protection Association, Quincy, MA, 2008.

NFPA 805, *Performance-Based Standard for Fire Protection for Light Water Reactor Electric Generating Plants*, National Fire Protection Association, Quincy, MA, 2001.

NEI 00-01 (2009), *Guidance for Post Fire Safe Shutdown Circuit Analysis*, Revision 2, Nuclear Energy Institute, Washington, D.C., May, 2009.

NEI 00-01 (2010), *Guidance for Post Fire Safe Shutdown Circuit Analysis*, Draft Revision 3, Nuclear Energy Institute, Washington, D.C., 2010.

NEI 04-02 (2009), *Guidance for Implementing a Risk-Informed Performance-Based Fire Protection Program Under 10 CFR 50.48(c)*, Rev. 1, Nuclear Energy Institute, Washington, D.C., September, 2009.

NIST NCSTAR 1-5F, *Federal Building and Fire Safety Investigation of the World Trade Center Disaster: Computer Simulation of the Fires in the World Trade Center Towers*, National Institute of Standards and Technology, Gaithersburg, MD, 2005.

NUREG-1805, *Fire Dynamics Tools (FDT^s): Quantitative Fire Hazard Analysis Methods for the U.S. Nuclear Regulatory Commission Fire Protection Inspection Program*, U.S. Nuclear Regulatory Commission, Washington, DC, December 2004.

NUREG-1824, *Verification and Validation of Selected Fire Models for Nuclear Power Plant Applications, Volume 1: Main Report*, U.S. Nuclear Regulatory Commission, Office

of Nuclear Regulatory Research (RES), Washington, DC, 2007, and EPRI 1011999, Electric Power Research Institute (EPRI), Palo Alto, CA.

NUREG-1824, *Verification and Validation of Selected Fire Models for Nuclear Power Plant Applications, Volume 3: Fire Dynamics Tools (FDT^s)*, U.S. Nuclear Regulatory Commission, Office of Nuclear Regulatory Research (RES), Washington, DC, 2007, and EPRI 1011999, Electric Power Research Institute (EPRI), Palo Alto, CA.

NUREG-1824, *Verification and Validation of Selected Fire Models for Nuclear Power Plant Applications, Volume 4: Fire-Induced Vulnerability Evaluation (FIVE-Rev1)*, U.S. Nuclear Regulatory Commission, Office of Nuclear Regulatory Research (RES), Washington, DC, 2007, and EPRI 1011999, Electric Power Research Institute (EPRI), Palo Alto, CA.

NUREG-1824, *Verification and Validation of Selected Fire Models for Nuclear Power Plant Applications, Volume 5: Consolidated Fire Growth and Smoke Transport Model (CFAST)*, U.S. Nuclear Regulatory Commission, Office of Nuclear Regulatory Research (RES), Washington, DC, 2007, and EPRI 1011999, Electric Power Research Institute (EPRI), Palo Alto, CA.

NUREG-1824, *Verification and Validation of Selected Fire Models for Nuclear Power Plant Applications, Volume 6: MAGIC*, U.S. Nuclear Regulatory Commission, Office of Nuclear Regulatory Research (RES), Washington, DC, 2007, and EPRI 1011999, Electric Power Research Institute (EPRI), Palo Alto, CA.

NUREG-1824, *Verification and Validation of Selected Fire Models for Nuclear Power Plant Applications, Volume 7: Fire Dynamics Simulator (FDS)*, U.S. Nuclear Regulatory Commission, Office of Nuclear Regulatory Research (RES), Washington, DC, 2007, and EPRI 1011999, Electric Power Research Institute (EPRI), Palo Alto, CA.

NUREG/CR-4680, *Heat and Mass Release Rate for Some Transient Fuel Source Fires: A Test Report*, U.S. Nuclear Regulatory Commission, Washington, DC, December 2004.

NUREG/CR-6850, *EPRI/NRC-RES Fire PRA Methodology for Nuclear Power Facilities: Volume 1: Summary and Overview*, U.S. Nuclear Regulatory Commission, Office of Nuclear Regulatory Research (RES), Washington, DC: 2005 and EPRI 1011989, Electric Power Research Institute (EPRI), Palo Alto, CA.

NUREG/CR-6850, *EPRI/NRC-RES Fire PRA Methodology for Nuclear Power Facilities: Volume 2: Detailed Methodology*, U.S. Nuclear Regulatory Commission, Office of Nuclear Regulatory Research (RES), Washington, DC: 2005 and EPRI 1011989, Electric Power Research Institute (EPRI), Palo Alto, CA.

NUREG/CR-6931, *Cable Response to Live Fire (CAROLFIRE), Volume 1: Test Descriptions and Analysis of Circuit Response Data*, U.S. Nuclear Regulatory Commission, Washington, DC, 2007.

NUREG/CR-6931, *Cable Response to Live Fire (CAROLFIRE), Volume 2: Cable Fire Response Data for Fire Model Improvement*, U.S. Nuclear Regulatory Commission, Washington, DC, 2007.

NUREG/CR-6931, *Cable Response to Live Fire (CAROLFIRE), Volume 3: Thermally-Induced Electrical Failure (THIEF) Model*, U.S. Nuclear Regulatory Commission, Washington, DC, 2007.

References

NUREG/CR-7010, *Cable Heat Release, Ignition, and Spread In Tray Installations during Fire (CHRISTIFIRE), Volume 1: Horizontal Trays*, National Institute of Standards and Technology, Gaithersburg, MD, 2011.

Peacock, R., K. McGrattan, B. Klein, W. Jones, and P. Reneke, *CFAST – Consolidated Model of Fire Growth and Smoke Transport (Version 6) – Software Development and Model Evaluation Guide*, Special Publication 1086, National Institute of Standards and Technology, Gaithersburg, MD, 2008.

Peacock, R., W. Jones, P. Reneke and G. Forney, *CFAST: An Engineering Tool for Estimating Fire Growth and Smoke Transport, Version 6 – User's Guide*, Special Publication 1041, National Institute of Standards and Technology, Gaithersburg, MD, 2008.

Quintiere, J.G., *Principles of Fire Behavior*, Delmar Publishers, 1998.

Quintiere, J.G., *Fundamentals of Fire Phenomena*, John Wiley, 2006.

Regulatory Guide 1.189, *Fire Protection for Nuclear Power Plants*, U.S. Nuclear Regulatory Commission, Bethesda, MD, April, 2009.

Schiffiliti, R. and W. Pucci, *Fire Modeling, State of the Art*, Fire Detection Institute, 1996

SFPE, *SFPE Engineering Guide to Assessing Flame Radiation to External Targets from Pool Fires*, SFPE Engineering Guide, Society of Fire Protection Engineers, Bethesda, MD, March 1999.

SFPE, *SFPE Engineering Guide to Fire Exposures to Structural Elements*, SFPE Engineering Guide, Society of Fire Protection Engineers, Bethesda, MD, November, 2005.

SFPE, *SFPE Engineering Guide to Piloted Ignition of Solid Materials Under Radiant Exposure*, SFPE Engineering Guide, Society of Fire Protection Engineers, Bethesda, MD, January, 2002.

SFPE, *SFPE Engineering Guide to Predicting Room of Origin Fire Hazards*, SFPE Engineering Guide, Society of Fire Protection Engineers, Bethesda, MD, November, 2007.

SFPE, *SFPE Engineering Guide to Substantiating a Fire Model for a Given Application*, SFPE Engineering Guide, Society of Fire Protection Engineers, Bethesda, MD, June, 2010.

SFPE Handbook of Fire Protection Engineering, 4th Edition (P.J. DiNenno, Editor-in-Chief), National Fire Protection Association and The Society of Fire Protection Engineers, Quincy, MA, 2008.

Steel Construction Manual, 13th edition, American Institute of Steel Construction, New York, New York, 2006.

UL 217, *Single Station Fire Alarm Device*, Underwriters' Laboratories, Northbrook, Illinois.

Wallis, G.B., "Draft Final NUREG-1824, Verification and Validation of Selected Fire Models for Nuclear Power Plant Applications", Memorandum from Advisory Committee on Reactor Safeguards to Luis Reyes, ML062980154, US Nuclear Regulatory Commission, October 2006.

A
Cabinet Fire in Main Control Room

A.1 Modeling Objective

The purpose of the calculations described in this Appendix is to determine the length of time that the Main Control Room (MCR) remains habitable after the start of a fire within a low-voltage control cabinet. These calculations are based on the guidance provided in Chapter 11 of NUREG/CR-6850 (EPRI 1011989), Volume 2, "Detailed Fire Modeling (Task 11)." MCR fire scenarios are treated differently than fires within other compartments, mainly because of the necessity to consider forced abandonment in addition to equipment damage.

A.2 Description of the Fire Scenario

General Description: A fire ignites within a control cabinet containing XPE/neoprene cables. The door to the MCR is normally closed, and normal ventilation conditions are in place at the start of the fire. Following guidance given in Chapter 11 of NUREG/CR-6850, two scenarios are considered, one in which the ventilation system is turned off and one in which the ventilation system is switched to smoke-purge mode at the start of the fire.

Geometry: Drawings of the MCR are shown in Figure A-1 and Figure A-2. The compartment has a variety of control cabinets in addition to typical office equipment, such as computer monitors on table tops. There is an "open grate" ceiling above the floor, a photograph of which is shown in Figure A-3. One wall of the compartment is made of concrete with no additional lining material. The other exterior walls are constructed of five-eighth in gypsum board supported by steel studs. The floor is a slab of concrete covered with low-pile carpet. The ceiling is a slab of concrete with the same thickness as the floor, but with no lining material.

Materials: Nominal values for the thermal properties of various materials in the compartment have been taken from NUREG-1805, Table 2-3 and are listed in Table 3-1. Carpet is not listed in the table, but, according to NUREG-1805, Table 6-5, the thermal inertia ($k\rho c$) for "Carpet (Nylon/Wool Blend)" is 0.68 $(kW/m^2/K)^2$ s, its "Ignition Temperature" is 412°C (774°F), and its "Minimum Heat Flux for Ignition" is 18 kW/m^2.

Detection System: Smoke detectors are located as shown in Figure A-1 below the plenum space at the open grate ceiling level and on the upper concrete ceiling. However, smoke detection plays no role in the fire scenarios under consideration.

Ventilation: During normal operation, the ventilation system provides five air changes per hour. As seen in Figure A-1, ventilation is provided by six supply diffusers and two return vents of nominally the same size. The supply air to the compartment is equally distributed among the six supply vents, and the return air is drawn equally from the two returns. A 120 Pa overpressure (relative to the adjacent compartments) is maintained in the MCR. Leakage from the compartment occurs via a 2.5 cm (1 in) high crack under the 0.91 m (3 ft)-wide door on the west side of the compartment. All other penetrations are sealed.

Figure A-1. Geometry of the Main Control Room. The cabinet is at lower right.

Notes:
1. Ceiling is Concrete.
2. Floors are Concrete covered with Carpet.
3. Open Grate Drop Ceiling at 3.0 m (10 ft) above Floor.
4. Gypsum on Walls is 1.6 cm (5/8 in) thick.
5. Dimensions are in meters, 1 meter = 3.28 ft.

Left Side View

Main Control Room

1 m = 3.28 ft
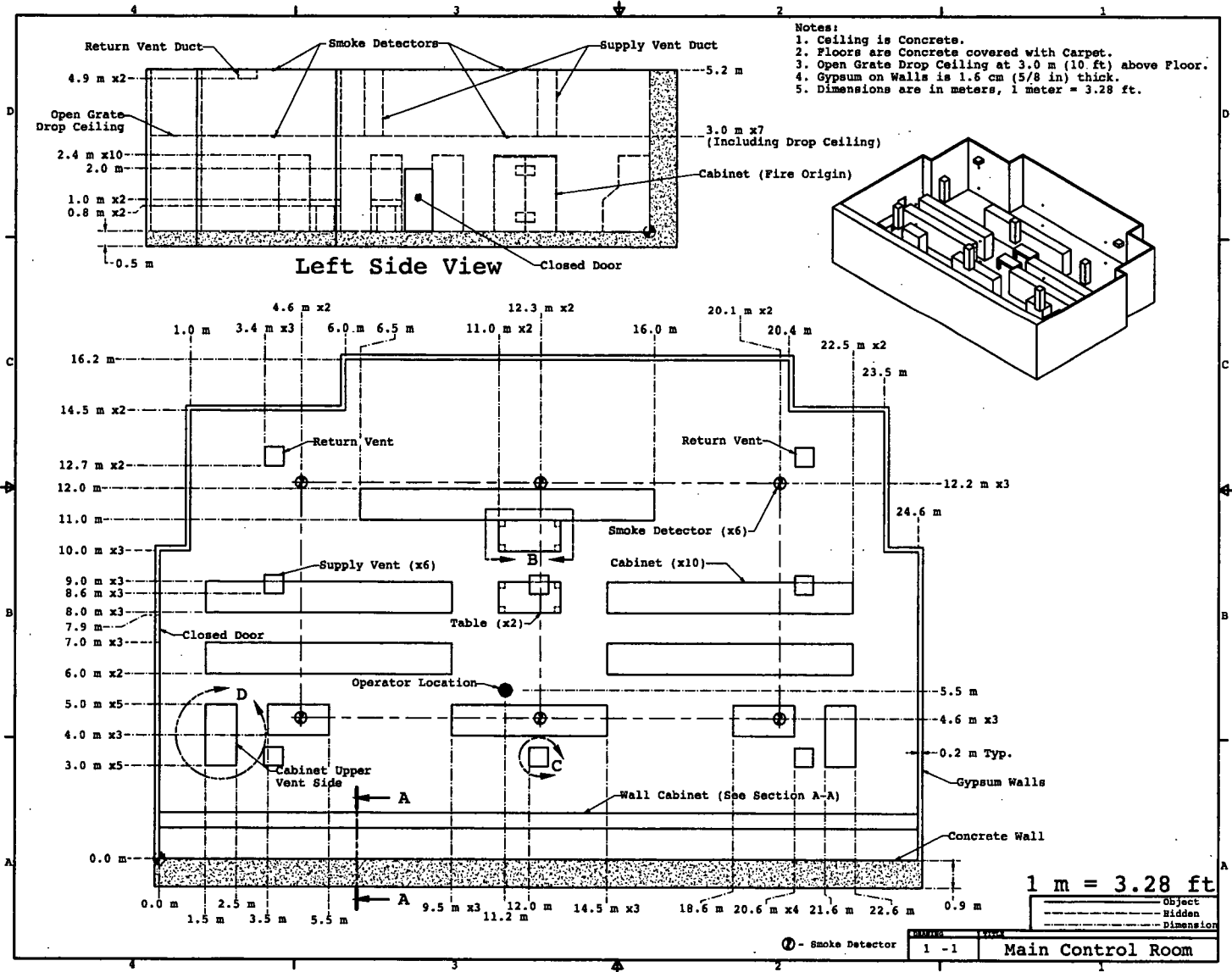
Figure A-2. Main Control Room Details.

SECTION A-A

- 1.0 m
- 2.4 m
- 1.4 m
- 1.0 m
- 1.5 m

DETAIL B
TYPICAL

- 0.2 m Typ.
- 0.2 m Typ.
- 1.0 m
- 2.0 m

DETAIL C
(Supply or Return Vent, Typ.)

- 0.6 m
- 0.6 m

DETAIL D, ISO VIEW
(Fire Origin Cabinet)

- 0.6 m
- 0.3
- 0.2 m

Upper Cabinet Opening

Lower Cabinet Opening
(Same Dimensions as Upper Vent)

Object
Hidden
Dimension
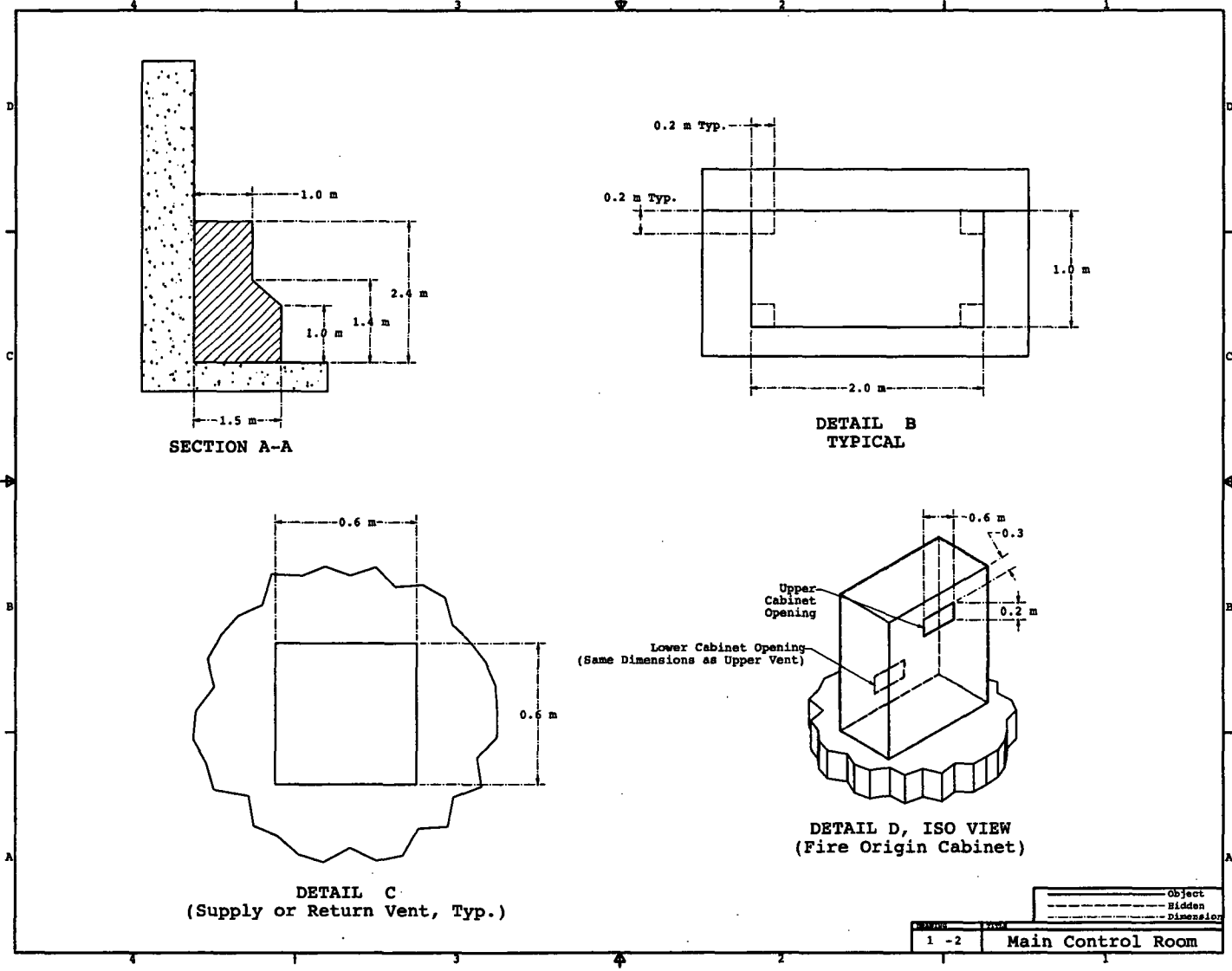
1 -2   Main Control Room
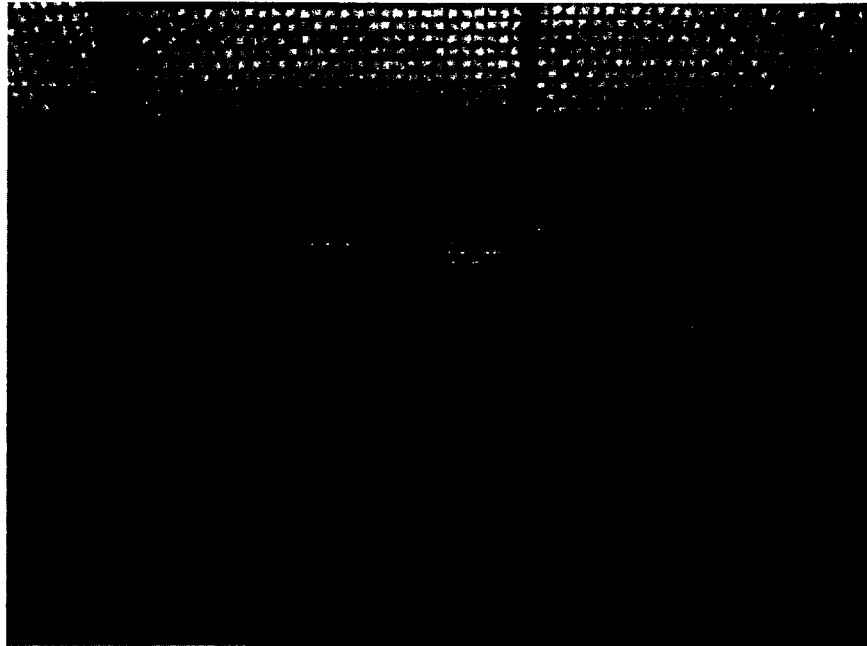
Figure A-3. Photograph of a typical "open grate" ceiling.

Figure A-4. Photograph of a typical control cabinet.

NUREG/CR-6850 (EPRI 1011989), Volume 2, Chapter 11, recommends that two possibilities be taken into consideration regarding ventilation: (1) the ventilation system is turned off, and (2) the ventilation system is in smoke-purge mode. Smoke-purge mode provides 25 air changes per hour.

Fire: The fire ignites in a control cabinet (Figure A-4), designated as the "Fire Origin" in Figure A-1, due to an electrical malfunction. The fire grows according to a "t-squared" curve to a maximum value of 702 kW in 12 min and remains steady for 8 additional minutes, consistent with NUREG/CR-6850 (EPRI 1011989), Appendix G, for a low-voltage cabinet fire involving more than one bundle of qualified cable. After 20 min, the fire's HRR decays linearly to zero in 19 min. A peak fire intensity of 702 kW represents the 98th percentile of the probability distribution for the HRR in cabinets of this general description. The heat release rate curve is shown in Figure A-5.

Heat Release Rate
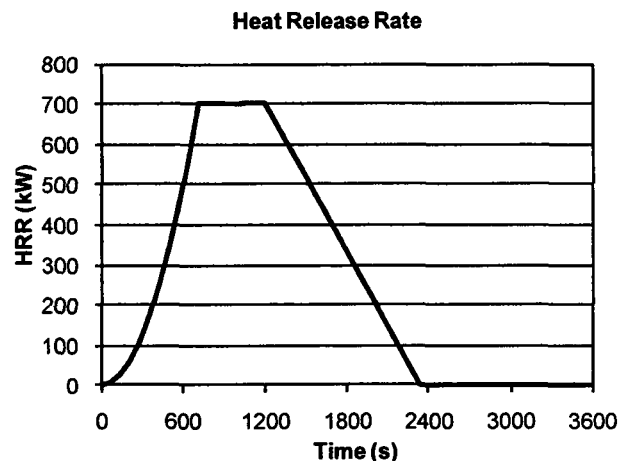
Figure A-5. Time history of the HRR used by all models in the MCR scenario.

The exterior panels of the burning cabinet do not open before or during the fire. The smoke, heat, and flames are exhausted from an air vent in the side of the cabinet. The top of the air vent is 0.3 m (1 ft) below the top of the cabinet. The air vent is 0.6 m (2 ft) wide and 0.2 m (8 in) high. The cabinet is 2.4 m (8 ft) tall.

When estimating the composition of the fire's exhaust products, the jacket and insulation material of the cable are taken as an equal-parts mixture of polyethylene (C_2H_4) and Neoprene (C_2H_5Cl), with the effective chemical formula $C_2H_{4.5}Cl_{0.5}$. The heat of combustion of the burning cables is 10.3 kJ/g (NUREG-1805, Table 2-4). This number is appropriate for cross-linked polyethelene (XLPE)/Neoprene cables. The radiative fraction[10] of the fire is 35%, consistent with typical sooty fires (Tewarson, *SFPE Handbook*, 4th ed., Table 3-4.16).

For visibility calculations, soot yield[11] is a very important parameter. According to Tewarson's chapter in the *SFPE Handbook*, the soot yield for the various combustible materials within the

---

[10] The fraction of the fire's total energy emitted as thermal radiation.

[11] The soot yield is defined as the mass of smoke particulate generated per unit mass of fuel consumed.

Cabinet Fire in Main Control Room

cabinet ranges from 0.01 to 0.20. For this scenario, the soot yield for the combustion reaction is taken to be 0.10, but the results of the calculation should be assessed in light of the wide variation in possible soot yields, and the fact that the fire could potentially be underventilated. This value of 0.10 is an estimate for a fire burning in an environment where the equivalence ratio approaches 1. The calculated optical density is directly proportional to this parameter; thus, the entire range of values can easily be assessed during post-processing of the results. The mass extinction coefficient is 8.7 m^2/g, based on measurements made by Mulholland and Croarkin (2000).

The CO yield of the fire, y_{CO}, can be estimated from the soot yield, y_s, using a correlation developed by Köylu and Faeth:

$$y_{CO} = \frac{12\,x}{M_f\,\nu_f}\,0.0014 + 0.37\,y_s \tag{A-1}$$

where x is the number of carbon atoms in a fuel molecule (two in this example), M_f is the molecular weight of the fuel (46.26 g/mol, calculated from the effective chemical formula), y_s is the soot yield, and ν_f is the stoichiometric coefficient of the fuel, here taken to be one since all species yields are taken as a ratio to the mass of fuel consumed. For this example, the CO yield (y_{CO}) is calculated from the above equation to be 0.038 kg/kg.

Based on the yields of soot and CO for the fuel considered in this example, the complete chemical reaction can be written:

$$C_2H_{4.5}Cl_{0.5} + 2.59\,O_2 \rightarrow 0.06\,CO + 0.38\,C + 1.56\,CO_2 + 2\,H_2O + 0.5\,HCl \tag{A-2}$$
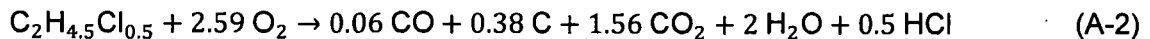
Note that the soot is treated as pure carbon, C, and that all of the chlorine produces HCl.

Habitability: The MCR is manned 24 hours per day during normal plant operations. To assess habitability of the compartment, the operator stands at the position indicated in Figure A-1. According to NUREG/CR-6850 (EPRI 1011989), Volume 2, Chapter 11, "Detailed Fire Modeling," a space is considered uninhabitable if at least one of the following occurs:

1. The incident heat flux at 1.8 m (6 ft) exceeds 1 kW/m^2. A smoke layer temperature of approximately 95°C (200°F) generates this level of heat flux.

2. The smoke layer descends below 1.8 m (6 ft) from the floor, and the optical density of the smoke is greater[12] than 3 m^{-1}.

---

[12] The original edition of NUREG/CR-6850 contains an error in the specification of the optical density (NRC ADAMS Accession Number ML061630360).

A.3 Selection and Evaluation of Fire Models

NUREG/CR-6850 (EPRI 1011989), Volume 2, Chapter 11 recommends zone and CFD models for estimating the HGL temperature, heat flux, HGL descent rate, and smoke obscuration in the MCR. Algebraic models can also provide useful estimates of various fire-generated conditions. Following is a discussion of the strengths and weaknesses of the available models.

Algebraic Models: FIVE and the FDT[s] both contain correlations to estimate the HGL temperatures within a closed, ventilated compartment. However, the FDT[s] do not allow the HRR to be input as a function of time. Because the objective of the calculation is to estimate the time to loss of habitability, FIVE is used to provide a first estimate of the compartment temperature.

FIVE and the FDT[s] both contain methods to estimate the heat flux from a fire to a target. However, the description of the scenario indicates that the fire is ignited and remains largely within a closed control cabinet. Thus, distant targets, including the operators, may not be exposed directly to the thermal radiation. It is more likely that the descending Hot Gas Layer will be responsible for most of the heat flux to which the operator is exposed. Neither FIVE nor the FDT[s] have a method to account for this source of thermal radiation.

Zone Models: The fire scenario outlined in the previous section falls within the range of applicability for a zone model. If the open grate-style ceiling below the actual concrete ceiling slab can be neglected, the overall geometry and fire size will lead to a fire environment in the control room volume that conforms to a basic two-zone approximation. For this analysis, the zone model CFAST version 6.1.1 is used. It has one advantage over MAGIC for this analysis; it computes the smoke obscuration, one of the critical parameters required to assess habitability.

CFD Models: The primary advantage of a CFD model for this fire scenario is that the CFD model can estimate habitability conditions at the specific location of the operator.

Validation: The principal source of validation data justifying the use of the fire models discussed above for this scenario is the NRC/EPRI V&V study documented in NUREG-1824 (EPRI 1011999). NIST has expanded the NRC/EPRI V&V to include the latest versions of CFAST (6.1.1) (Peacock, 2008) and FDS (5.5.3) (McGrattan, 2010). In particular, the FM/SNL (Factory Mutual/Sandia National Labs) test series was designed specifically as a mock-up of a control room in an NPP. One of these experiments (Test 21) involves a fire within a hollow steel cabinet.

Table A-1 lists various important model parameters and the ranges for which the NRC/EPRI validation study is applicable. A few parameters fall outside the validation parameter space and are addressed individually:

- The Fire Froude Number falls outside the range. This parameter is essentially a measure of the fire's heat output relative to its base area. In this example, the fire is assumed to emanate from the side of the cabinet with the vent opening serving as its "base." This assumption leads to a higher value of $\dot{Q}^*$ than would be calculated if it were not assumed that the fire burns completely outside of the cabinet. Thus, the high value of $\dot{Q}^*$ is the result of an assumption that will lead to more severe fire conditions than would be expected if the fire were assumed to burn partially within the cabinet.

Cabinet Fire in Main Control Room

- The relatively low Equivalence Ratio for the compartment is a result of the relatively large amount of air forced into the room during the smoke purge mode. Twenty-five air changes per hour is a considerable flow rate, and no validation experiment in NUREG-1824 involved such a high rate. However, the results of all the model simulations indicate that the scenario in which the ventilation is turned off is the more likely to compromise human habitability, and the presence of any level of ventilation reduces room temperature and heat flux and increases visibility.

Table A-1. Normalized parameter calculations for the MCR fire scenario.

Quantity	Normalized Parameter Calculation		Validation Range	In Range?
Fire Froude Number	$\dot{Q}^* = \dfrac{\dot{Q}}{\rho_\infty c_p T_\infty D^2 \sqrt{gD}} = \dfrac{702}{1.2 \times 1.012 \times 293 \times 0.4^2 \times \sqrt{9.8 \times 0.4}} \cong 6.2$		0.4 – 2.4	No
Flame Length, L_f, relative to the Ceiling Height, H	$\dfrac{L_f}{H_c} = \dfrac{2.7}{5.2} \cong 0.5$ $L_f = D\left(3.7\,\dot{Q}^{*2/5} - 1.02\right) = 0.4\,(3.7 \times 6.2^{0.4} - 1.02) \cong 2.7$		0.2 – 1.0	Yes
Ceiling Jet Radial Distance, r_{cj}, relative to the Ceiling Height, H	N/A – Ceiling jet targets are not included in simulation.		1.2 – 1.7	N/A
Equivalence Ratio, φ, of the Room, based on Forced Ventilation of Purge Mode	$\varphi = \dfrac{\dot{m}_F/\dot{m}_{O_2}}{r} \equiv \dfrac{\dot{Q}}{r\,\Delta H\,\dot{m}_{O_2}} = \dfrac{702}{13{,}100 \times 3.7} \cong 0.014$ $\dot{m}_{O_2} = 0.23\,\rho_\infty \dot{V} = 0.23 \times 1.2 \times 13.4 \cong 3.7$		0.04 – 0.6	No
Compartment Aspect Ratio	$\dfrac{L}{H} = \dfrac{24.6}{5.2} \cong 4.7$	$\dfrac{W}{H} = \dfrac{16.2}{5.2} \cong 3.1$	0.6 – 5.7	Yes
Target Distance, r, relative to the Fire Diameter, D	N/A – The radiation heat flux to the operator is based on the temperature of the HGL, not the fire.		2.2 – 5.7	N/A

A.4 Estimation of Fire-Generated Conditions

This section provides specific details on how each model is set up and run.

A.4.1 Algebraic Model (FIVE)

General: The forced ventilation correlation of Foote, Pagni, and Alvares (FPA) is used in FIVE to estimate the HGL temperature of the MCR, but only for the smoke purge scenario. A schematic diagram indicating the assumptions is shown in Figure A-6. None of the FIVE algorithms were evaluated for a closed, unventilated compartment in the NRC/EPRI V&V study documented in NUREG-1824 (EPRI 1011999).

Geometry: The FPA correlation requires that the room dimensions be given in terms of a length, width, and height. For this example, the selected compartment is not a rectangular parallelepiped; thus, it needs to be represented as such with an effective length, width, and height. The compartment height is taken directly as 5.2 m (17 ft) because it is important to maintain the same compartment height for the smoke filling calculation. Next, the effective length and width are calculated to maintain the same volume and surface area of the actual compartment. This is equivalent to maintaining the same floor area and perimeter. The floor area is 372 m^2 (4004 ft^2), and the perimeter is 83.4 m (274 ft). Maintaining the total floor area and perimeter yields an effective compartment size of 28.8 m (94.5 ft) by 12.9 m (42.3 ft).
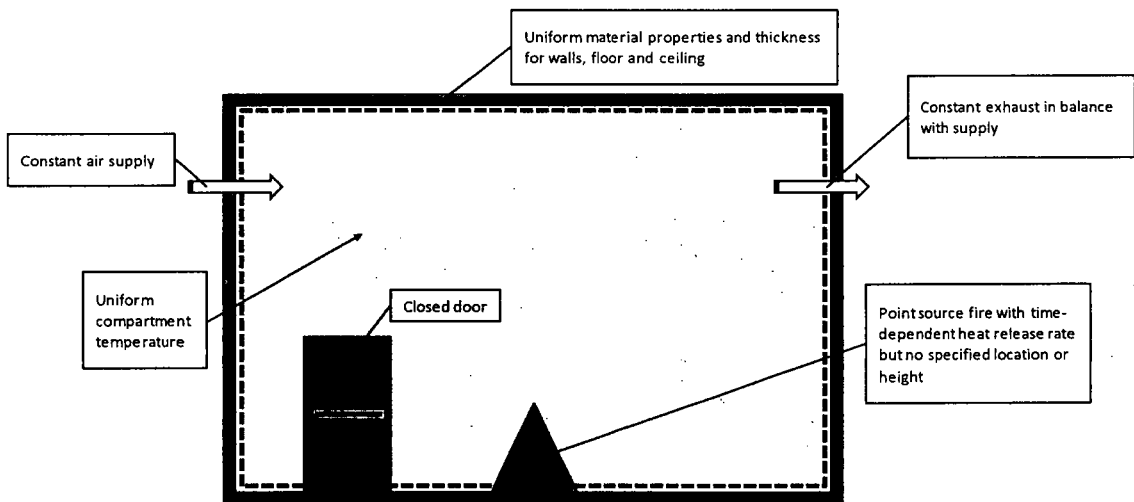
Figure A-6. Schematic diagram of the FIVE calculation.

Fire: The FPA correlation in FIVE uses the specified time-dependent HRR. It does not use the fire's elevation above the floor or any other information about the fire.

Materials: The walls, ceiling, and floor are all gypsum board rather than concrete because the FPA correlation only accounts for one type of lining material. Gypsum board was chosen because it is a better insulator and leads to a slightly higher HGL temperature, which in this scenario would more likely compromise human tenability.

Ventilation: The ventilation rate of the smoke purge mode (5700 cfm) is a direct input parameter in the FPA algorithm of FIVE.

A.4.2 Zone Model (CFAST)

Geometry: CFAST divides the geometry into one or more compartments connected by vents. For this simulation, the entire compartment is modeled as a single compartment. As with the algebraic models, zone models simulate fires in compartments with rectangular floor areas. The strategy for selecting effective room dimensions is the same as described above.

While there are numerous cabinets and tables in the compartment, most are well below the height of the fire (discussed below) and may be neglected. There are no mechanisms within CFAST to account for the open-grate ceiling. It is expected that neglecting it will lead to slightly higher HGL temperatures because there is less resistance for the rising smoke and hot gases.

Fire: In CFAST, a fire is described as a source of heat placed at a specific point within a compartment that generates combustion products according to user-specified combustion chemistry. Consistent with typical practice for the use of zone fire models for electrical cabinet fires, the fire is positioned at the top of the air vent, 0.3 m below the top of the cabinet, at the center of the cabinet. The air vent dimensions of 0.6 m wide and 0.3 m constitute the area of the burning fire. A snapshot of the CFAST simulation is shown Figure A-7.

Combustion chemistry in CFAST is described, at a minimum, by the production rates of CO, CO_2, and soot. The basic stoichiometry of the reaction is given in Eq. (A-2). The CO_2 yield is calculated:

$$y_{CO_2} = \frac{v_{CO_2} M_{CO_2}}{v_f M_f} = \frac{1.56 \times 44}{1 \times 45.26} \cong 1.52 \text{ kg/kg} \tag{A-3}$$

Direct inputs for species production rates CFAST are normalized to this CO_2 yield. Thus, the CFAST input of y_{CO}/y_{CO_2} is 0.038/1.52=0.025 and of y_s/y_{CO_2} is 0.1/1.52 = 0.066. A final input is the ratio of the mass of hydrogen to the mass of carbon in the fuel, or 0.15 kg/kg.

Materials: CFAST does not include the ability to model individual walls of different materials. For this example, the compartment walls are assumed to be entirely made of gypsum wallboard, a conservative assumption given that its thermal conductivity is the lowest of all other wall materials. The floors and ceilings are modeled as 0.5 m (1.6 ft) thick concrete.

CFAST does not use the thermal inertia, $k\rho c$, directly, but rather requires individual values of each. Based on typical thermal properties for hair, felt, and wool, the density of the carpet is 200 kg/m³, the specific heat is 2 kJ/kg/K, and the thermal conductivity is 0.68/200/2=0.0017 kW/m/K (Holman, 1990).

Ventilation: For the smoke-purge calculation, air is supplied to the MCR via the six supply vents and exhausted through the two returns. The total ventilation rate is 25 air changes per hour, 13.4 m³/s.

Fire is modeled 0.3 m below top surface of cabinet
as a 702 kW peak fire size

Compartment door is
closed throughout fire, with
a 2.5 cm crack under door to
provide normal air leakage.

MCR modeled as a rectangular compartment with an effective
size of 28.78 m x 12.91 m x 5.2 m, maintaining total compartment
volume and surface area.

Time: 1230.0
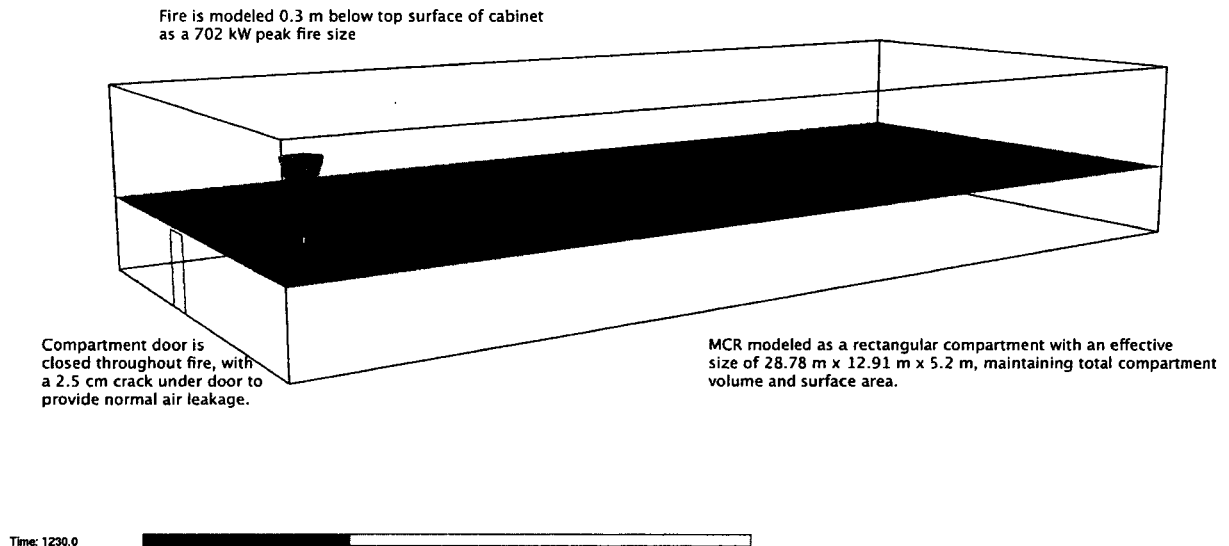
Figure A-7. Snapshot of the CFAST simulation of the MCR fire.

A.4.3 CFD Model (FDS)

Geometry: The entire compartment is included in the computational domain. The exterior concrete wall coincides with the boundary of the computational domain, meaning that the inside surface of the concrete wall is flush with the boundary of the computational domain, and the properties of concrete (including its thickness) are applied to this boundary. The tables (made out of wood) and the electrical cabinets (made out of steel) are included in the simulation. Note that the drop ceiling is not modeled because it is open and for this example provides a negligible resistance to the heat and air that go through it.

The computational mesh consists of a uniform grid of cells that are 0.2 m on a side. A simple grid resolution study demonstrates that because the details of the fire (other than its specified heat and smoke production rates) within the cabinet are not important to the question asked, there is no need to further refine the grid in the vicinity of the cabinet. An explanation related to choosing the grid sizes appropriate for use can be found in NUREG-1824 (EPRI 1011999), Vol. 7.

Fire: Following the guidance in NUREG/CR-6850 (EPRI 1011989), Supplement 1, Chapter 12, the fire is modeled as emanating from the upper vent of the burning cabinet. This assumption will result in higher HGL temperatures, as all of the fire's energy is released outside of the cabinet; in reality, a certain fraction of the fire's energy would be absorbed by the steel walls of the cabinet. An FDS/Smokeview rendering of the scenario is shown in Figure A-8.

The fuel stoichiometry is input to the model as specified above. FDS requires the designation of a single gaseous fuel molecule via the number of carbon and hydrogen atoms in the "surrogate" fuel, plus the number of "other" atoms in the molecule that play no role in the reaction. The soot yield (0.10 kg/kg) and heat of combustion (10,300 kJ/kg) are input directly.

Materials: The cabinets are represented by closed boxes with the specified properties of steel. The tables are assigned the properties of plywood that is 5 cm thick. The table legs are not modeled because they play little role in the fire or heat transfer calculation to the solids. Concrete and gypsum properties are applied to the walls and ceiling. The floor is modeled as a 1 cm-thick carpet over a 0.5 m-thick concrete slab. The concrete properties are taken directly as specified. The carpet properties are obtained in the same way as for CFAST above.

Ventilation: Air is supplied to the MCR via the six supply vents and exhausted through the two returns. Steel plates are specified beneath the supply vent openings to mimic the effect of a diffusion grill: that is, air is pushed downwards from the vent opening, but is then redirected sideways by the plate. Because of the limited resolution of the numerical grid, this is the only way to account for the more detailed flow pattern of the real vent.

The leakage from the compartment is modeled by specifying a small "vent" located at the base of the door through which air escapes at a rate determined by the pressure difference between the MCR and ambient. Note that the door crack itself is not modeled explicitly, as the numerical grid is not fine enough. Rather, the leak is spread over a slightly larger area. This assumption is justified by the fact that the volume flow through the leakage area is estimated via the equation:

$$\dot{V}_L = A_L \sqrt{\frac{2\,\Delta p}{\rho_\infty}} \tag{A-4}$$

where A_L is the *actual* leakage area (0.9 m by 0.025 m or 0.0225 m^2 in this case), Δp is the pressure difference between the inside and outside of the compartment (Pa), and ρ_∞ is the ambient air density (1.2 kg/m^3). The supply rate is divided equally among the six supply vents, and the return rate is divided equally among the two returns.
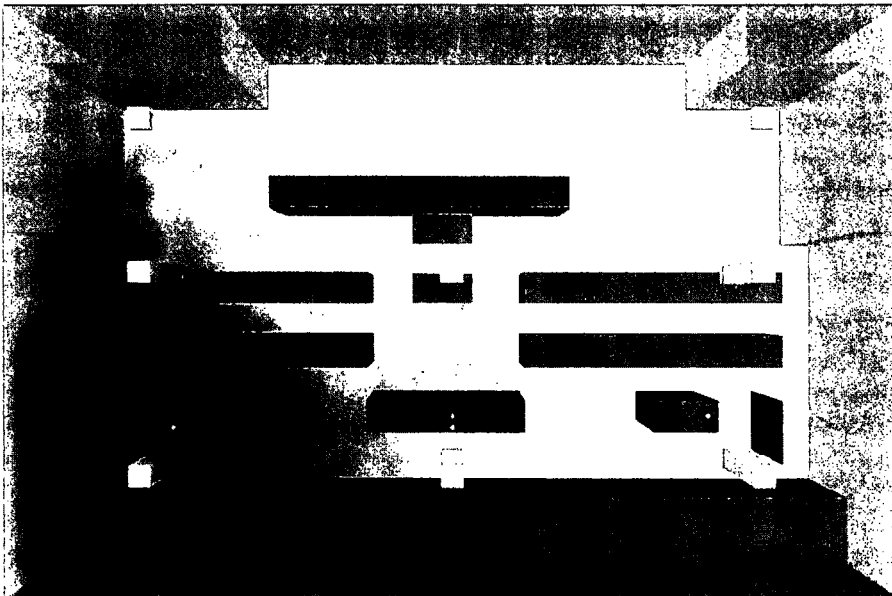
Figure A-8. FDS/Smokeview rendering of the Main Control Room, as seen from above.

A.5 Evaluation of Results

The habitability of the MCR depends on the temperature, heat flux, and smoke concentration to which the operators would be exposed. According to NUREG/CR-6850 (EPRI 1011989), Volume 2, Chapter 11, abandonment of the MCR is assumed if the gas temperature 2 m (6 ft) above the floor exceeds 95°C (200°F) or if the heat flux exceeds 1.0 kW/m^2 or if the optical density exceeds 3 m^{-1}. Each of these criteria are discussed in the following sections.

A.5.1 Temperature Criterion

One of the room habitability criteria is the temperature near the operator. However, neither FIVE nor CFAST estimate the temperature at the operator location specifically. For the purpose of assessing habitability, the HGL temperature is used to approximate the temperature to which the operator would be exposed, regardless of whether the HGL descends to the operator's height. The HGL temperature and depth predictions are shown in Figure A-9.

FIVE predicts that the temperature would exceed 95°C (200°F) in approximately 12 min when the smoke purge system is on. However, it should be noted that the FPA algorithm in FIVE overestimated the HGL temperature by an average of 83% in the NRC/EPRI V&V study documented in NUREG-1824 (EPRI 1011999). FIVE does not have an algorithm to evaluate the fire scenario when the purge system is turned off.

CFAST predicts that the HGL temperature would exceed the threshold in 15 min when the smoke purge system is off. Note that this is the HGL temperature, not the temperature in the lower layer where the operator is standing. The HGL descends to 2 m above the floor in approximately 20 min. When the smoke purge system is on, CFAST does not estimate that the temperature criterion would be reached and that the HGL would be limited to a small layer near the ceiling due to the action of the smoke exhaust system.

FDS does not predict that the temperature near the operator would ever reach 95°C (200°F), either when the ventilation is off or in smoke purge mode. The FDS's predictions of HGL temperature are lower than those of the other models because it accounts for the mixing of heat and smoke with ambient air due to the high purging flow, since it models flow within the compartment in detail. The other models are not capable of modeling the enhanced mixing of the high flow rates caused by the purging flows.

HGL Temperature

HGL Height
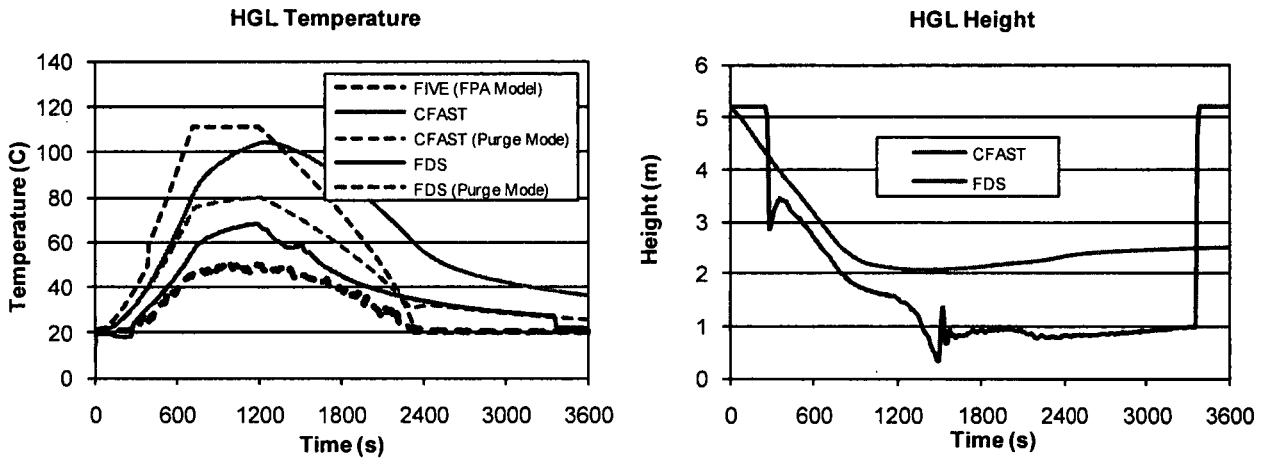
Figure A-9. Hot Gas Layer Temperature and Height for the Main Control Room scenario.

A.5.2 Heat Flux Criterion

In the fire scenario that includes the operation of the smoke purge system, neither CFAST nor FDS predict that the heat flux to the operator exceeds the tenability criterion (Figure A-10). In fact, both models estimate a peak flux of approximately 0.1 kW/m², a value that is one-tenth the critical value. However, with the smoke purge system turned off, FDS predicts a peak heat flux of 0.45 kW/m², and CFAST predicts 0.75 kW/m². The latter prediction falls within 25% of the tenability criterion. According to NUREG-1824 (EPRI 1011999), 25% is comparable to the reported accuracy of the zone models in predicting heat flux; thus, it is important to assess the CFAST prediction in greater detail. This is taken up in the section on Uncertainty.

Heat Flux to Operator
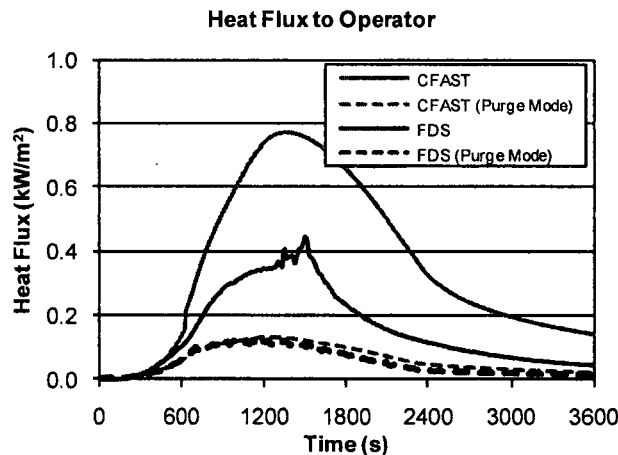
Figure A-10. Predicted heat flux at the location of the operator.

A.5.3 Visibility Criterion

The smoke optical density results are shown for CFAST and FDS in Figure A-11. The CFAST prediction is based on its upper layer smoke concentration calculation, whereas that of FDS is based on the actual operator location. Both models predict visibility that is still considerably less than the tenability criterion of 3 m^{-1} when the smoke purge system is on, but FDS predicts that the tenability criterion will be exceeded in about 12 min while CFAST predicts 18 min when the purge system is off. Such conditions could force abandonment of the MCR. It is not surprising that FDS predicts a higher smoke concentration near the operator than CFAST because FDS predicts lower gas temperatures due to increased mixing of the smoke and the heat from the fire with the surrounding air. This also demonstrates that the CFD model, FDS, does not always predict conditions that are less severe than those predicted by zone or algebraic models; in fact, a given model might estimate a more severe condition for one quantity and a less severe condition for another quantity.

Optical Density at Operator
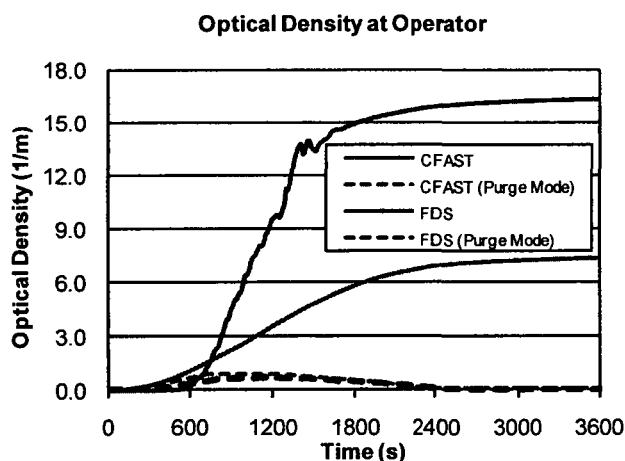
Figure A-11. Visibility criterion for the Main Control Room scenario.

A.5.4 Uncertainty

For the MCR fire scenario, the objective of the calculations is to estimate the time to abandonment; that is, the time at which the HGL temperature, heat flux, or optical density exceeds a critical value. Some of the predicted values do not exceed the critical value at any time in the simulation. To better quantify whether or not a critical value is exceeded, the uncertainty of the model predictions needs to be calculated.

As an example of how to calculate model uncertainty, consider the CFAST prediction of the total heat flux to the operator. In the NRC/EPRI V&V study (NUREG-1824(EPRI 1011999)), it was found that CFAST predictions of total heat flux are, on average, 19 % less than corresponding measurements, and the relative standard deviation of its predictions about this average value is 47 %. Following the guidance put forth in Chapter 4, this suggests that the true value of the heat flux in this scenario is normally distributed with a mean of 0.75/0.81=0.93 kW/m^2 and a

standard deviation of 0.47×0.93=0.44 kW/m². Therefore, the probability that the heat flux in the vicinity of the operator would exceed 1.0 kW/m² is:

$$P(\dot{q}'' > 1.0) = \frac{1}{2}\, \text{erfc}\left(\frac{1.0 - 0.93}{0.44\sqrt{2}}\right) \cong 0.44 \qquad \text{(A-5)}$$

In other words, there is a 44% chance of exceeding the heat flux tenability criterion when the room ventilation system is off, as calculated by CFAST.

Table A-2 lists the probability of exceeding the critical temperature and heat flux for all the models. Notice that even though some models have predicted a higher value than the critical, the fact that these models have been shown to over-estimate the given quantity lessens the likelihood that the critical threshold would be reached in an actual fire.

Table A-2. Uncertainty analysis of the model predictions of the MCR scenario.

Model	Quantity	Mode	Predicted Value	Critical Value	Probability of Exceeding
FIVE	Temperature	Purge	112 °C	95 °C	0.198
CFAST	Temperature	Purge	80 °C	95 °C	0.003
CFAST	Temperature	No Purge	105 °C	95 °C	0.705
FDS	Temperature	Purge	50 °C	95 °C	0.000
FDS	Temperature	No Purge	68 °C	95 °C	0.000
CFAST	Heat Flux	Purge	0.15 kW/m²	1.0 kW/m²	0.000
CFAST	Heat Flux	No Purge	0.75 kW/m²	1.0 kW/m²	0.432
FDS	Heat Flux	Purge	0.15 kW/m²	1.0 kW/m²	0.000
FDS	Heat Flux	No Purge	0.40 kW/m²	1.0 kW/m²	0.000

Note again that the CFAST predictions of heat flux and HGL temperature with the smoke purge system off show a dramatically greater chance of exceeding critical values than FDS. The reason has less to do with model uncertainty and more to do with model assumptions. CFAST is a two-zone model and makes the assumption that all of the smoke and heat from the fire are confined to a descending upper layer, whereas FDS, a CFD model, makes no such assumption and allows for smoke and heat transport throughout the compartment. Since both models have the same production rate of smoke and heat, the fact that the CFD model mixes these exhaust products over the entire volume means that its predicted concentration and temperature will tend to be lower.

The models show that the most likely cause of MCR abandonment is excessive smoke and loss of visibility. However, Table 4-1 indicates that both CFAST and FDS have been shown to over-estimate smoke concentration by at least a factor of 2. Because of the scarcity of experimental data, however, it is not possible to better quantify this figure. Nevertheless, an examination of Figure A-11 indicates that if one were to adjust the predicted values of smoke concentration to account for this bias, the predicted times to abandonment would increase. Further consideration of the smoke and its effect on the optical density is taken up in the next section.

A.5.5 Sensitivity

The previous section considers how model uncertainty can affect the predicted results. Model sensitivity considers how input parameter uncertainty can affect the predicted results. Recall from the discussion in Section A.2 that there is considerable uncertainty in the smoke generation rate of real fires, especially in cases where the fire might be under-ventilated inside of a cabinet. A value of 10 % was chosen for the smoke yield in the models, even though literature values range from 1 % to 20 %. In addition to the uncertainty in the specified input value of the smoke yield, the NRC/EPRI V&V study (NUREG-1824 (EPRI 1011999)) indicates that both CFAST and FDS over-estimate measured smoke concentrations, on average, by factors of 2.65 and 2.70, respectively. In light of these uncertainties in both the models and the input parameters, it is prudent to consider the sensitivity of the results of the simulations to the selected value of the smoke yield. Table 4.2 indicates that the optical density is directly proportional to the smoke yield. This means that if the smoke yield is doubled to 20 %, the predicted optical density is doubled as well. If the smoke yield is reduced by a factor of 10 to 1 %, so is the optical density. The curves in Figure A-11 can easily be adjusted to show the effect of a variation in the smoke yield. For example, if the smoke yield were doubled, the resulting FDS optical density would, too. But notice that the time to pass the threshold value of 3 m^{-1} would only slightly decrease because the optical density is increasing rapidly at this stage in the fire. However, a decrease in the smoke yield from 10 % to 1 % would result in the optical density never reaching its threshold value, at least according to the model.

A.6 Conclusion

Three models were run to assess the conditions within the MCR from a 702 kW cabinet fire. Of the three abandonment criteria, it is most likely that the operators would be forced to abandon the MCR because the optical density would surpass 3 m^{-1} approximately 12 min after the fire ignites if the smoke purge system fails to operate, according to the FDS analysis. Because FDS has been shown to over-estimate smoke concentration by more than a factor of 2, the 12 min prediction could be extended to approximately 15 min on account of the model uncertainty. A sensitivity analysis indicates that a reduction in the smoke yield from the assumed 10 % could have a similar effect of extending the time to abandonment. Increasing the assumed smoke yield would not significantly decrease the abandonment time.

If the smoke purge system does operate, removing smoke at a rate of 25 ACH, CFAST and FDS both predict that the room remains habitable, while the FPA calculation in FIVE predicts that the threshold temperature would be exceeded. However, FIVE has been shown to over-predict HGL temperature by approximately 50 %, which means that the likelihood of exceeding the critical HGL temperature, if one accounts for the model uncertainty, is approximately 20 %.

A.7 References

1. NUREG-1805, *Fire Dynamics Tools*, 2004.
2. NUREG/CR-6850 (EPRI 1011989), *Fire PRA Methodology for Nuclear Power Facilities*, 2005.
3. NUREG-1824 (EPRI 1011989, *Verification and Validation of Selected Fire Models for Nuclear Power Plant Applications*, 2007.
4. *SFPE Handbook of Fire Protection Engineering*, 4th edition, 2008.
5. NIST SP 1018-5, *Fire Dynamics Simulator (Version 5), Technical Reference Guide, Vol. 3, Experimental Validation*.

6. NIST SP 1030. *CFAST: An Engineering Tool for Estimating Fire Growth and Smoke Transport, Version 5 - Technical Reference Guide*, National Institute of Standards and Technology, Gaithersburg, Maryland, 2004.
7. G.W. Mulholland and C. Croarkin. "Specific Extinction Coefficient of Flame Generated Smoke." *Fire and Materials*, 24:227–230, 2000.
8. U.O. Köylu and G.M. Faeth. "Carbon Monoxide and Soot Emissions from Liquid-Fueled Buoyant Turbulent Diffusion Flames," *Combustion and Flame*, 87:61–76, 1991.
9. J.P. Holman, *Heat Transfer*, 7th edition, McGraw-Hill, New York, 1990.

A.8 Attachments

1. FDS input files:

    a. Main_Control_Room_No_Purge.fds
    b. Main_Control_Room_Purge.fds

2. CFAST input files:

    a. Cabinet fire in MCR No Ventilation.in
    b. Cabinet fire in MCR.in
    c. MCR 702 kW.o
    d. thermal.csv

B
Cabinet Fire in Switchgear Room

B.1 Modeling Objective

The calculations described in this appendix estimate the effects of fire in a cabinet in a Switchgear Room on nearby cable and cabinet targets. These calculations are part of a larger fire analysis described in Chapter 11 of NUREG/CR-6850 (EPRI 1011989), Volume 2, "Detailed Fire Modeling (Task 11)." The Switchgear Room contains both Train A and Train B safety-related equipment that is not separated as required by Appendix R. The lack of separation between the two has been identified as an unanalyzed condition. The purpose of the calculation is to analyze this condition and determine whether these targets fail, and, if so, at what time failure occurs. The time to smoke detector activation is also estimated. The calculation will provide information for a decision on the hazard and risk for this scenario.

B.2 Description of the Fire Scenario

General Description: The 4160 V Switchgear Room is located in the auxiliary building. The Switchgear Room contains three banks of cabinets (labeled A, B, and C in Figure B-1). The center cabinet bank (Cabinet B) serves Train A equipment necessary for safe shutdown in the event of a fire. The cabinet bank on the north side of the compartment serves both non-safety and safety-related Train A equipment. The cabinet bank on the south side of the compartment serves non-safety-related equipment. In addition to the cabinets in the compartment, there are nine cable trays, three stacks of three trays each, which run west to east, directly above each of the cabinet banks. The lower two trays above the middle bank of cabinets contain control cables for safety-related Train B equipment. The compartment is not typically manned.

Geometry: A plan and section view of the Switchgear Room is shown in Figure B-1.

Construction: The compartment floor, ceiling and walls are concrete, nominally 0.5 m (1.6 ft) thick. The cabinets and cable trays are made of steel, 1.5 mm (0.06 in) thick.

Materials: Nominal values for the thermal properties of various materials in the compartment are listed in Table 3-1 (NUREG-1805, Table 2-3). The cable trays are filled with PE-insulated, PVC-jacketed control cables, which have a diameter of approximately 15 mm (0.6 in), a jacket thickness of approximately 1.5 mm (0.06 in), and seven conductors. They are contained in nine stacked cable trays. Cables are considered damaged when the temperature reaches 205°C (400°F) or the exposure heat flux reaches 6 kW/m^2 (NUREG-1805, Appendix A). The damage criteria for the adjacent cabinet is taken to be equal to that for PVC cable since the cables inside the cabinet are unqualified.

Detection System: Two smoke detectors are located in the compartment at the locations shown in Figure B-1. The detectors are UL-listed with a nominal sensitivity of 4.9 %/m.

Ventilation: There are three supply and three return registers located near the side walls, as seen in Figure B-1. Each register has a rate of 0.472 m^3/s. The mechanical ventilation is normally on, and normal operations continue during the fire. The supply air to the compartment is equally distributed among the supply vents, and the return air is drawn equally from the

returns. The compartment has only one door, which is normally closed. The room temperature is maintained at 20°C (68°F), and the pressure is comparable to adjacent compartments. Leakage from the compartment occurs via a 2.5 cm (1 in)-high crack under the 0.91 m (3 ft)-wide door on the west side of the compartment. All other penetrations are sealed.

Fire: The fire ignites in one electrical cabinet in the middle bank of cabinets, as specified in the drawing. The cabinet door is closed, but there are vents on the top of the cabinet for air circulation. It contains more than one bundle of unqualified cable. The fire grows following a "t-squared" curve to a maximum value of 464 kW in 12 min and remains steady for 8 additional minutes, consistent with NUREG/CR-6850 (EPRI 1011989), page G-5, for a cabinet with more than one cable bundle of unqualified cable. After 20 min, the fire's HRR decays linearly to zero in 12 min. A peak fire intensity of 464 kW represents the 98th percentile of the probability distribution for HRRs in cabinets with unqualified cable in scenarios where flames propagate through cable bundles. From a cabinet configuration perspective, this selection is appropriate for control cables where cable loading is typically higher than in other types of cabinets. From an applications perspective, the use of the 98th percentile is consistent with the guidance provided in NUREG/CR-6850 (EPRI 1011989) for evaluating fire conditions with different fire intensities (including the 98th percentile) within the probability distribution range.

There is an air vent on the top the cabinet. The air vent is 0.6 m (2 ft) wide and 0.3 m (1 ft) long. The cabinet is 2.4 m (8 ft) tall. Consistent with NUREG/CR-6850 (EPRI 1011989), the fire burns within the interior of the cabinet, and the smoke, heat, and possibly flames exhaust from the air vent at the top of the cabinet.

The radiative fraction[13] of the fire is 35%, consistent with sooty fires. Burning cables in an electrical cabinet would produce a sooty fire (Tewarson, *SFPE Handbook, 4th ed.*, Table 3-4.16).

The heat of combustion of the burning cables is 24 kJ/g (Table 2-4 of NUREG-1805). This number is appropriate for PE/PVC cable. A mixture of PE (C_2H_4) and PVC (C_2H_3Cl) would have an effective chemical formula of $C_2H_{3.5}Cl_{0.5}$.

For certain smoke detector activation calculations, soot yield[14] is necessary. According to Tewarson's chapter in the *SFPE Handbook*, the soot yield for the various combustible materials within the cabinet ranges from 0.01 to 0.20. The soot yield for this scenario is taken to be 0.10, but the results of the calculation should be assessed in light of the wide variation in possible soot yields, and the fact that the fire could potentially be underventilated within the cabinet. The value of 0.10 is an estimate for a well-ventilated fire close to an equivalency ratio of 1. The calculated optical density is directly proportional to this parameter; thus, the entire range of values can easily be assessed during post-processing of the results.

The mass extinction coefficient is 8.7 m^2/g, based on measurements made by Mulholland and Croarkin [Mullholland and Croarkin, *Fire and Materials*].

The CO yield of the fire, y_{CO}, can be estimated from the soot yield, y_s, using a correlation developed by Köylu and Faeth:

---

[13] The fraction of the fire's total energy emitted as thermal radiation.
[14] The soot yield is defined as the mass of smoke particulate generated per unit mass of fuel consumed.

$$y_{CO} = \frac{12\,x}{M_f\,v_f}\,0.0014 + 0.37\,y_s \qquad (B\text{-}1)$$

where x is the number of carbon atoms in a fuel molecule (two in this example), M_f is the molecular weight of the fuel (45.26 g/mol, calculated from the effective chemical formula), y_s is the soot yield, and v_f is the stoichiometric coefficient of the fuel, here taken to be one since all species yields are taken as a ratio to the mass of fuel consumed. For this example, the CO yield (y_{CO}) is calculated from the above equation to be 0.038 kg/kg.

Based on the yields of soot and CO for the fuel considered in this example, the complete chemical reaction can be written:

$$C_2H_{3.5}Cl_{0.5} + 2.34\,O_2 \rightarrow 0.06\,CO + 0.38\,C + 1.56\,CO_2 + 1.5\,H_2O + 0.5\,HCl \qquad (B\text{-}2)$$
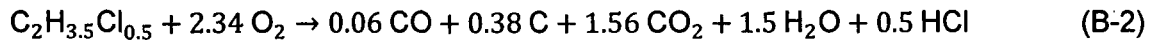
Note that the soot is treated as pure carbon, C, and that all of the chlorine produces HCl.
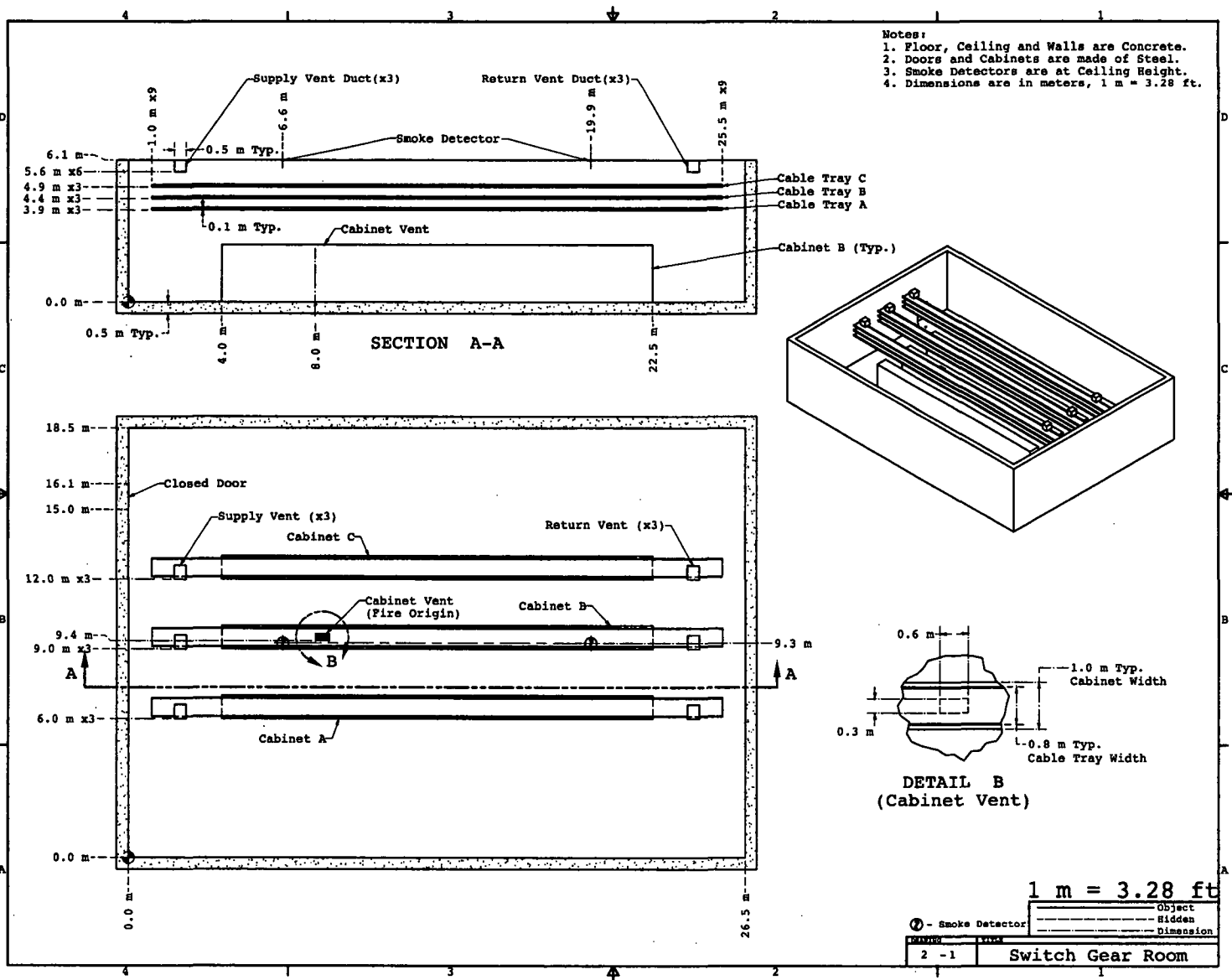
Figure B-1. Geometry of the Switchgear Room.

Notes:
1. Floor, Ceiling and Walls are Concrete.
2. Doors and Cabinets are made of Steel.
3. Smoke Detectors are at Ceiling Height.
4. Dimensions are in meters, 1 m = 3.28 ft.

Supply Vent Duct(x3) Return Vent Duct(x3)

Smoke Detector

1.0 m x9   9.9 m   19.9 m   25.5 m x9

6.1 m
5.6 m x6 — Cable Tray C
4.9 m x3 — Cable Tray B
4.4 m x3 — Cable Tray A
3.9 m x3

0.5 m Typ.

0.1 m Typ.   Cabinet Vent   Cabinet B (Typ.)

0.0 m

0.5 m Typ.   4.0 m   8.0 m   22.5 m

SECTION A-A

18.5 m

16.1 m — Closed Door

15.0 m

Supply Vent (x3)   Cabinet C   Return Vent (x3)

12.0 m x3

Cabinet Vent (Fire Origin)   Cabinet B

9.4 m
9.0 m x3   9.3 m
A   B   A

6.0 m x3

Cabinet A

0.0 m

0.0 m   26.5 m

0.6 m   1.0 m Typ. Cabinet Width

0.3 m   0.8 m Typ. Cable Tray Width

DETAIL B
(Cabinet Vent)

1 m = 3.28 ft

Object / Hidden / Dimension

- Smoke Detector

2 -1   Switch Gear Room

B.3 Selection and Evaluation of Fire Models

NUREG/CR-6850 (EPRI 1011989), Volume 2, Chapter 11 recommends empirical tools, zone models and field models for estimating the HGL temperature, heat flux, descent rate, and smoke obscuration in non-MCR fire scenarios. Following is a discussion of further strengths and weaknesses of the available models.

Algebraic Models: FIVE and the FDT^s both contain correlations to estimate the HGL Temperatures within a closed, ventilated compartment. However, the FDT^s do not allow the HRR to be input as a function of time. With a constant HRR, the FDT^s could be used by assuming an instantaneous, fully developed fire that remains at peak HRR for the duration of the fire scenario. This approach would likely estimate a shorter time to failure than tools that utilize a time-dependent HRR, but it may be useful as a screening tool. Care may be needed to ensure that such an approach would provide conservative results. In a time to failure analysis, the constant HRR may be conservative, but, for estimation of detection, a very short detection time is likely unrealistic and non-conservative.

FIVE and the FDT^s both contain methods to estimate the heat flux from a fire to a target. The FIVE analysis uses Alpert's plume temperature correlations and Heskestad's flame height correlation, whereas the FDT^s analysis uses only Heskestad's to estimate the temperature to which the cables are exposed. Neither analysis includes the effects of blockage due to the trays or the effect of thermal radiation from the Hot Gas Layer on the targets; thus, it is possible that the use of either of these models could lead to an underprediction of the heat flux.

Zone Models: The fire scenario outlined in the previous section falls within the range of applicability for a zone model. The simple compartment geometry of this scenario lends itself well to the application of zone models. Both CFAST and MAGIC include algorithms to estimate the temperature of cable targets.

In CFAST, target temperatures are calculated based on a one-dimensional heat transfer calculation that includes radiation from the fire, upper and lower gas layers, and bounding surfaces; convection from nearby gases; and conduction into the target. Radiation from the fire is modeled using a point source radiation calculation from the fire to the target.

In MAGIC, cable target temperatures are also calculated based on a one-dimensional heat transfer calculation that includes radiation exchanges between compartment surfaces, the upper and lower gas layers, and the nearby compartment fires; and convective heat transfer that involves targets heating up in the HGL, fire plume, and ceiling jet sub-layers. Each cable is divided into 20 cm (8 in.)-long segments, and the maximum surface temperature calculated on all of the segments is the criterion to cable ignition (once the ignition temperature is reached, the reported surface temperature remains constant). Thus, the relative location of the cables to the flame, plume, ceiling jet, or layers will affect the temperature calculation and the time to failure.

The relative position of the cabinet fire and cable trays may provide a challenge because the algorithms used by the zone models to assess target damage assume are based on a fire radiation point source.

For this analysis, the zone model CFAST is used.

Cabinet Fire in Switchgear Room

CFD Models: This scenario is a fairly typical application of FDS. Unlike the calculation performed for the Main Control Room scenario, however, the model is applied here in much the same way that the zone models approach it, with the fire on top of the cabinet. The primary advantage of a CFD model for this fire scenario is that the CFD model can estimate local conditions at the specific location of the target cables and adjacent cabinet. In the scenario under consideration, the fire is confined mainly within a closed cabinet. This could be modeled in FDS, and its results used to assess the effect of this detail on the overall result. For this analysis, FDS results are included as a comparison to the zone model calculations.

Validation: NUREG-1824 (EPRI 1011999) contains experimental validation results for CFAST and FDS that are appropriate for this scenario. NIST has expanded the NRC/EPRI V&V to include the latest versions of CFAST (6.1.1) (Peacock, 2008) and FDS (5.5.3) (McGrattan, 2010). In particular, the ICFMP (International Collaborative Fire Model Project) Benchmark Exercise #3 test series was designed specifically as a mock-up of a real Switchgear Room. These experiments include ventilation effects and heat fluxes to and temperatures of various targets, particularly cables. Fire sizes in these experiments bound those used in this scenario.

Although NUREG-1824 (EPRI 1011999) includes validation results for both temperature and smoke concentration, it does not include validation results specific to detector activation. CFAST predictions are based on a temperature analogy for detector activation. Available studies have reported gas temperature rises in the range of about 5 °C (41 °F) to 15 °C (59 °F) at smoke detector activation (see Davis and Notarianni 1996 or Bukowski and Averill, 1998). The FDS Validation Guide (McGrattan, 2010) includes the results of validation studies on detector activation and concludes that the model is able to estimate the smoke and gas concentrations, heat, and flow velocities at detector locations to within 15% of measurements, a value consistent with FDS predictions included in NUREG-1824 (EPRI 1011989).

Table 2-5 of Volume 1 of NUREG-1824 (EPRI 1011989) lists various important model parameters and the ranges for which the validation study is applicable. Table B-1 below lists the values of these parameters for this fire scenario, along with their ranges of applicability. The parameter, Fire Froude Number, is essentially a measure of the fire's heat output relative to its base area. In this example, the fire is assumed to attach itself to the cabinet's top vent with the vent opening serving as its "base" area. This assumption leads to a higher value of $\dot{Q}^*$ than would be calculated if it were not assumed that the fire burns completely outside of the cabinet. Thus, the high value of $\dot{Q}^*$ is the result of an assumption that will lead to more severe fire conditions than would be expected if the fire were assumed to burn partially within the cabinet. Therefore, it can be assumed that the model predictions would be valid for this scenario.

Table B-1. Key parameters and their ranges of applicability to NUREG-1824.

Quantity	Normalized Parameter Calculation	Validation Range	In Range?
Fire Froude Number	$$\dot{Q}^* = \frac{\dot{Q}}{\rho_\infty c_p T_\infty D^2 \sqrt{gD}} = \frac{464}{1.2 \times 1.012 \times 293 \times 0.48^2 \times \sqrt{9.8 \times 0.48}} \cong 2.7$$	0.4 – 2.4	No
Flame Length, L_f, relative to the Ceiling Height, H	$$\frac{L_f}{H} = \frac{2.3}{6.1} \cong 0.4$$	0.2 – 1.0	Yes
Ceiling Jet Radial Distance, r_{cj}, relative to the Ceiling Height, H	N/A – Ceiling jet targets are not included in simulation.	1.2 – 1.7	N/A
Equivalence Ratio, φ, as an indicator of the Ventilation Rate	$$\varphi = \frac{\dot{m}_F / \dot{m}_{O_2}}{r} \cong \frac{\dot{Q}}{r\,\Delta H\,\dot{m}_{O_2}} = \frac{464}{13{,}100 \times 0.4} \cong 0.09$$ $$\dot{m}_{O_2} = 0.23\,\rho_\infty \dot{V} = 0.23 \times 1.2 \times 1.42 = 0.4$$	0.04 – 0.6	Yes
Compartment Aspect Ratio	$$\frac{L}{H} = \frac{26.5}{6.1} \cong 4.3$$ $$\frac{W}{H} = \frac{18.5}{6.1} \cong 3.0$$	0.6 – 5.7	Yes
Target Distance, r, relative to the Fire Diameter, D	$$\frac{r}{D} = \frac{1.5}{0.48} \cong 3.1$$	2.2 – 5.7	Yes

Cabinet Fire in Switchgear Room

B.4 Estimation of Fire-Generated Conditions

This section provides details specific to each model.

B.4.1 Zone Model (CFAST)

Geometry: The CFAST analysis defines the compartment as a single rectangular parallelepiped with the specified dimensions. While there are a number of cable trays in the compartment, the compartment is sufficiently large that it is not considered a significant fraction of the total volume, so the compartment dimensions are taken directly from the scenario description and Figure B-1. Figure B-2 illustrates the scenario as modeled by CFAST.

Compartment size input as 26.5 m x 18.5 m x 6.1 m directly from scenario definition

Cabinets and cable trays shown for visualization only. No impact on modeled results.

Compartment leakage beneath doorway per scenario definition

Time: 1160.0
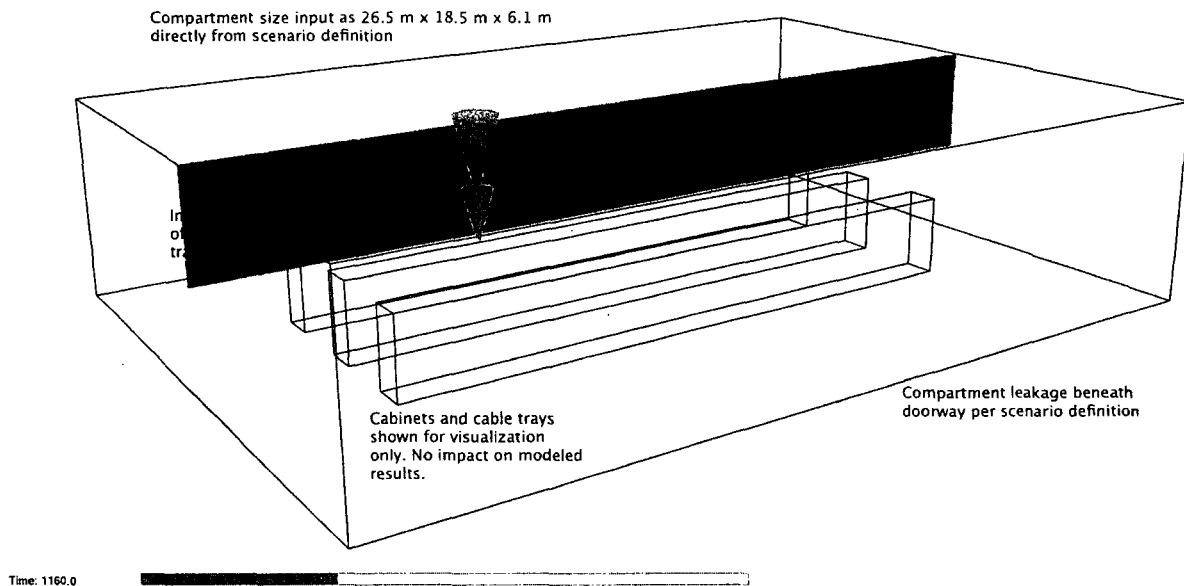
Figure B-2. CFAST/Smokeview rendering of Switchgear Room.

Fire: CFAST requires a user-specified time-dependent HRR and stoichiometry for the combustion of fuel and oxygen. For the initial fire source, the HRR is input as specified in the scenario description. For the secondary fuels, cable ignited by the initial fire, a relatively simple model for predicting the growth and spread of a fire within a vertical stack of horizontal cable trays is used. The model is referred to as FLASH-CAT, short for *Flame Spread over Horizontal Cable Trays*. The basic assumptions are taken from Appendix R of NUREG/CR-6850, with some additional information provided by the small- and intermediate-scale experiments described in NUREG/CR-7010. The FLASH-CAT model makes use of the following assumptions:

- The cable trays are horizontal and stacked vertically.
- There are no barriers separating the trays, and the tray tops and bottoms are open.
- The cables are not protected with coatings, armor shielding, or thermal blankets of any kind.
- There is a fire beneath the lowest tray.

Cabinet Fire in Switchgear Room

- Each tray has at least a single row of cables, or roughly 25% of the NEC limit.

Under these assumptions, the fire propagates upward through the array of cable trays according to an empirically determined timing sequence. In other words, the time for the fire to spread from one tray to the tray above is a function only of its order in the stack, not the thermal properties of the cables. The length of cables within a given tray that ignite initially increases as the fire spreads upwards. Lateral spread of the fire begins as soon as the cables within the tray ignite. This produces a solid V-shaped burning pattern that expands laterally with time. As the mass of combustible material within the center of the V is consumed, the V-shape becomes an expanding, open wedge of burning cable. The fires in each tray continue to spread until the end of the tray is reached. Further details are provided in NUREG/CR-7010, Volume 1.

For species yields, the fuel molecule is taken to be $C_2H_{3.5}Cl_{0.5}$ and the soot yield to be 0.1 kg/kg, as specified above. The basic stoichiometry of the reaction is given in Eq. (B-2). The CO_2 yield is calculated as follows:

$$y_{CO_2} = \frac{v_{CO_2}M_{CO_2}}{v_f M_f} = \frac{1.56 \times 44}{1 \times 45.26} \cong 1.52 \text{ kg/kg} \tag{B-3}$$

Direct inputs for production rates of CO and soot in CFAST are normalized to this CO_2 yield. Thus, CFAST input of CO/CO2 is 0.025, and C/CO2 is 0.066. HCl production is input relative to the fuel and is 0.40 kg/kg for this example. A final CFAST input is the ratio of the mass of hydrogen to the mass of carbon in the fuel, or 0.15 kg/kg.

Materials: CFAST takes the walls, floor, and ceiling as made of concrete, and uses the compartment drawing dimensions and target properties directly.

Ventilation: Mechanical ventilation and leakage are specified as input to CFAST directly from the scenario description. CFAST uses three inlet and three outlet vents for the mechanical ventilation at the heights specified in the scenario description. Horizontal placement in the compartment does not affect the zone model calculation and is not part of the input.

Fire/Smoke Detection: In CFAST, there is no direct way of calculating smoke density for smoke detector activation. The approach recommended by the developers is to model the smoke detector as a sprinkler with a low activation temperature and RTI[15]. An activation temperature of 30 °C (a 10 °C rise above ambient) and an RTI of 5 $(m/s)^{1/2}$ was selected consistent with the recommendations in the CFAST User's Guide. A temperature-based surrogate for smoke detector activation should be used with caution, particularly in locations far removed from the fire source. Gas temperatures near the ceiling are cooled due to transfer of heat to the ceiling so that lower temperatures are to be expected further from the fire source, increasing estimates of detector activation times for temperature-based methods. Direct estimation of smoke concentration within the detector, such as that included in FDS, is not affected by heat losses to the ceiling and can be expected to provide more accurate estimates of smoke detector activation.

---

[15] The accuracy of smoke detector activation predictions was not evaluated in the NUREG-1824 (EPRI 1011999) V&V study and has been identified as an area needing additional research (NUREG/CR-6978 (SAND2008-3997P)). While this guide provides some recommendations in this area, the user should carefully evaluate the applicability of these recommendations for the specific scenario and in light of new research in the area.

Cable Targets: In CFAST, target temperatures are calculated with a one-dimensional cylindrical heat transfer calculation based on the material properties and cable diameter, as specified in the scenario description.

B.4.2 CFD Model (FDS)

Geometry: The compartment has a simple rectangular geometry that coincides with the external boundary of the computational domain. In other words, the exterior walls are not explicitly declared, but are defined by default to be the external boundaries of the domain with the surface properties of concrete, given above. The cabinets are modeled simply as boxes constructed of steel, whose properties are specified above. No attempt is made to model the interior of the cabinets because the fire has been specified as originating at or near the top of one of the cabinets. Figure B-3 shows the compartment geometry used in FDS.

The numerical mesh consists of uniform grid cells, roughly 0.2 m (8 in) on a side. This is a relatively coarse mesh for scenarios of this type.

Materials: The material properties are applied directly as specified to the walls, floor, ceiling, and cabinet. The cabinet is models as a hollow steel box that is at ambient temperature inside because details of the interior are not available and are irrelevant to the question being asked.

Fire: The initial fire source is specified via a "burner" atop the central cabinet with the specified HRR. This is meant to represent a fire burning near the top of the cabinet that exhausts through the vent. The fuel for the fire is the PE/PVC cables within the cabinet. The reaction is given in Eq. (B-2).

The FLASH-CAT model (NUREG/CR-7010, Volume 1) is used to determine the ignition, HRR, flame spread, and extinction of the cables above the original fire source. Figure B-4 shows a snapshot of the burning cable during the simulation. First, ignition of the cables in the lowest tray is assumed to occur when the internal temperature of a target cable within that tray reaches the failure temperature of 200°C. This assumption is based on guidance given in NUREG/CR-6850 (EPRI 1011989), Appendix R. The calculation of the cable's internal temperature is based on the THIEF methodology (NUREG/CR-6931, Volume 3). Following ignition, the cables in the first tray burn at a rate of 250 kW/m^2, a value appropriate for thermoplastic cables (NUREG/CR-7010, Volume 1). The area of the initial fire is bounded by the width of the tray (0.8 m) and the length of the vent in the cabinet (0.6 m). The fire in the first tray spreads laterally at a rate of 3.2 m/h (NUREG/CR-6850 (EPRI 1011989), Appendix R). The fire in the second tray ignites 4 min after the first, and the lateral extent of the initial fire in the second tray is widened based on the 35° upward spread angle described in NUREG/CR-6850 (EPRI 1011989), Appendix R. The burning and spread rates of the fire in the second tray are the same as the first. The fire in the third tray ignites 3 min after the fire in the second, and the initial lateral extent of the fire is widened yet again following the 35° spread angle. Local burnout of the fire occurs when the cable plastic is consumed.

Ventilation: The door is included in the calculation merely as a surface of different properties from the default concrete wall. The supply and return vents are specified according to the drawing and given volume flow rates. Note that because of the relative coarseness of the underlying numerical grid, the ventilation rate is input directly in terms of the volume flow rate (m^3/s) rather than as a separate vent area (m^2) and velocity (m/s). The model automatically

adjusts the dimensions of all objects to conform to the numerical mesh, and it also adjusts the velocity of the air stream to properly reflect the desired volume flow rate.
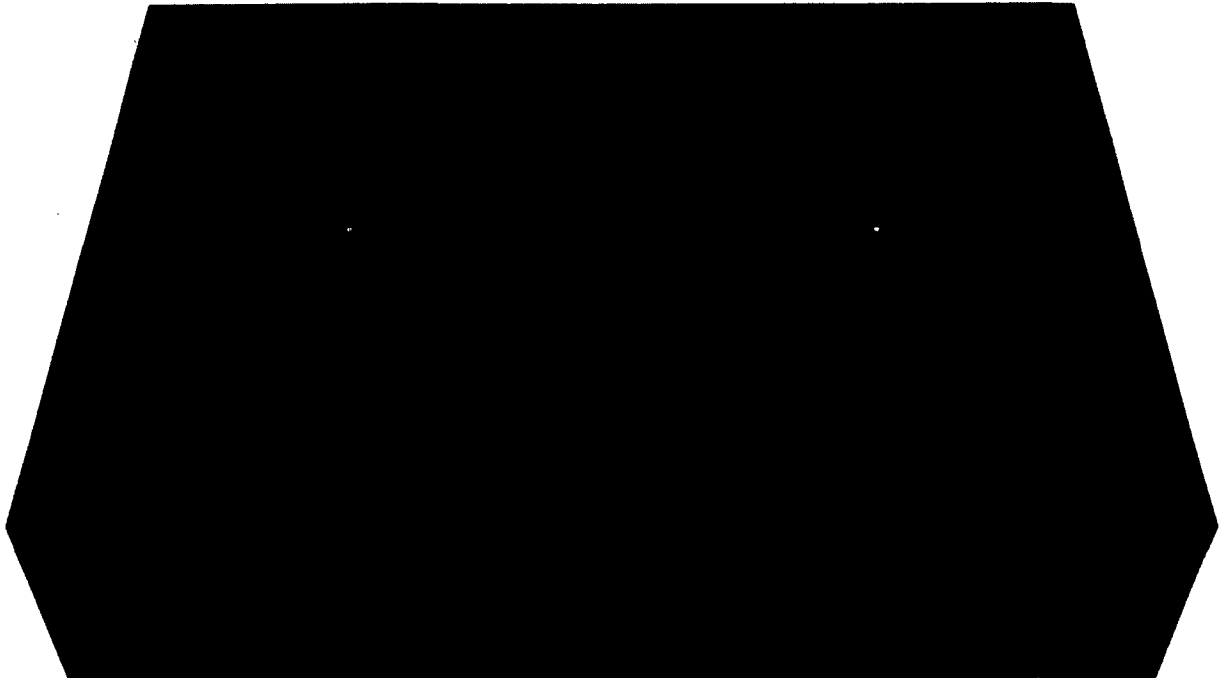
Figure B-3. FDS/Smokeview rendering of the Switchgear Room.
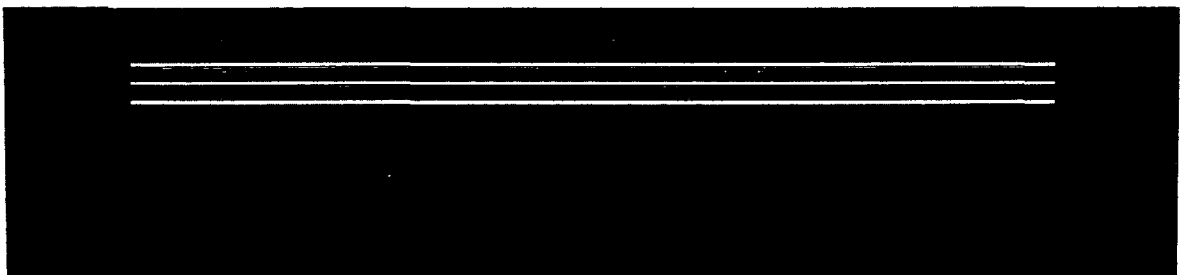
Figure B-4. FDS/Smokeview rendering of the Switchgear Room Fire showing localized ignition of extinction of secondary cable fires resulting from initial cabinet fire.

Fire/Smoke Detection: FDS includes specific algorithms to estimate the response of heat and smoke detectors to the local conditions surrounding the detectors. For smoke detectors, the inputs are the smoke obscuration (taken directly from the scenario definition) and a characteristic length (taken as the recommended default value of 1.8 m).

B.5 Evaluation of Results

The purpose of the calculations is to assess (1) the potential damage to cables in trays above an electrical cabinet fire and (2) the potential damage to adjacent cabinets. Based on the analysis detailed below, the cabinet fire is likely to fail the electrical cables just overhead in approximately 10 min, based on the analyses of both CFAST and FDS; however, it is unlikely that the fire would damage the adjacent cabinets.

B.5.1 Cable Ignition and Damage

The algebraic models cannot be used in this case to assess the damage to cables. FIVE does not have an algorithm that considers the thermal inertia of the cables. FDT^s does, but the model is only applicable when the exposing temperature is constant which is not the case for this example.

CFAST and FDS estimate the ignition and burning of the cables. NUREG/CR-6850 (EPRI 1011989) contains some guidance on modeling cable ignition, flame spread, and the fire's resulting heat release based on a limited set of fire test data. The differences in HRR between the models (Figure B-5) result from variations in the implementation of this guidance. Figure B-5(a) shows the HRR from the initial cabinet fire source only. Figure B-5(b) shows the overall HRR, including the initial cabinet fire source plus the addition of cables ignited by this initial fire.
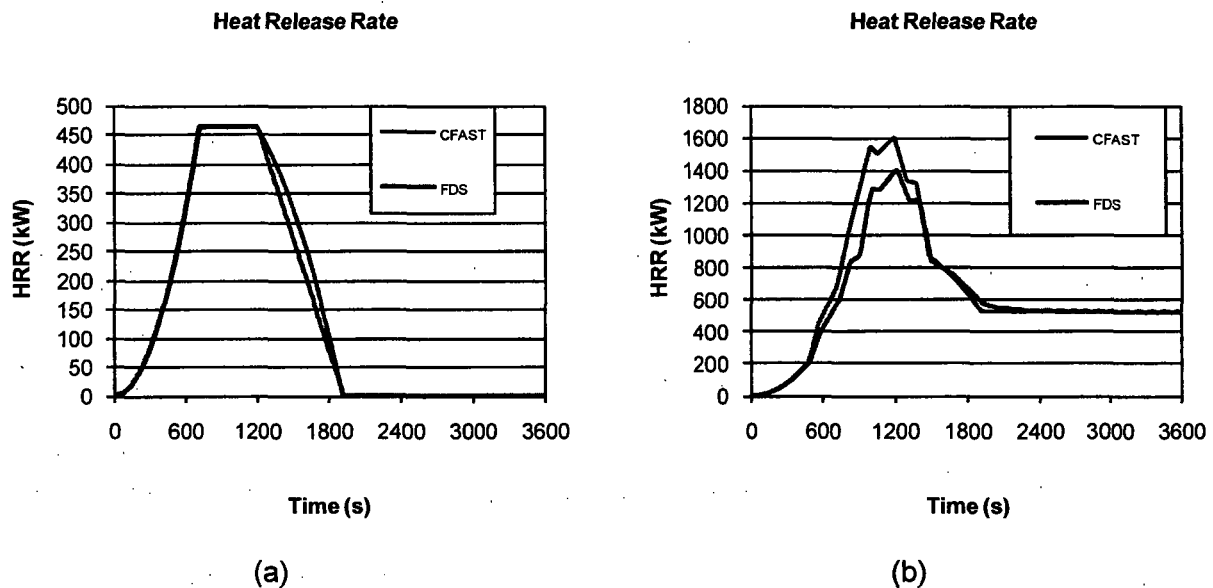
Figure B-5. Heat release rate inputs to CFAST and FDS for Switchgear Room cabinet fire scenario.

There are several possibilities that can be used to assess the potential for ignition of the lowest cable tray from the initial fire source. Cables are considered damaged when the temperature reaches 205°C (400°F) or the exposure heat flux reaches 6 kW/m^2 (NUREG-1805, Appendix A). These criteria are intended to be indicative of electrical failure, but are routinely assumed to also apply as ignition criteria. In newer studies in NUREG/CR-7010, cable ignition was not observed at fluxes below 25 kW/m^2, and most often only with direct flame impingement. Handbook values for minimum ignition flux for power and communication cables are reported in the range of 15

Cabinet Fire in Switchgear Room

kW/m^2 to 35 kW/m^2 (SFPE Handbook, Table 3-4.2). For this scenario, CFAST predicts that the flame height reaches the cable tray in approximately 490 s, quite similar to the temperature-based prediction. Table B-2 shows estimated time to ignition of the lowest cable tray for a variety of ignition criteria. For this simulation, 490 s was chosen.

Table B-2. Estimated time to ignition of lowest cable tray, CFAST, Switchgear Room cabinet fire

Ignition Criterion	Time (s)
Gas temperature ≥ 205 °C	270 s
Cable temperature ≥ 205 °C	860 s
Heat flux ≥ 6 kW/m^2	490 s
Heat flux ≥ 15 kW/m^2	740 s
Flame impingement	490 s

The CFAST and FDS temperature predictions resulting from Tray A cables are shown in Figure B-6. FDS predicts cable failure in Tray A at about 495 s, CFAST in about 500 s. Peak temperatures from both models are well above the failure criteria for the cables, so it can be

Cable Tray A Temperature
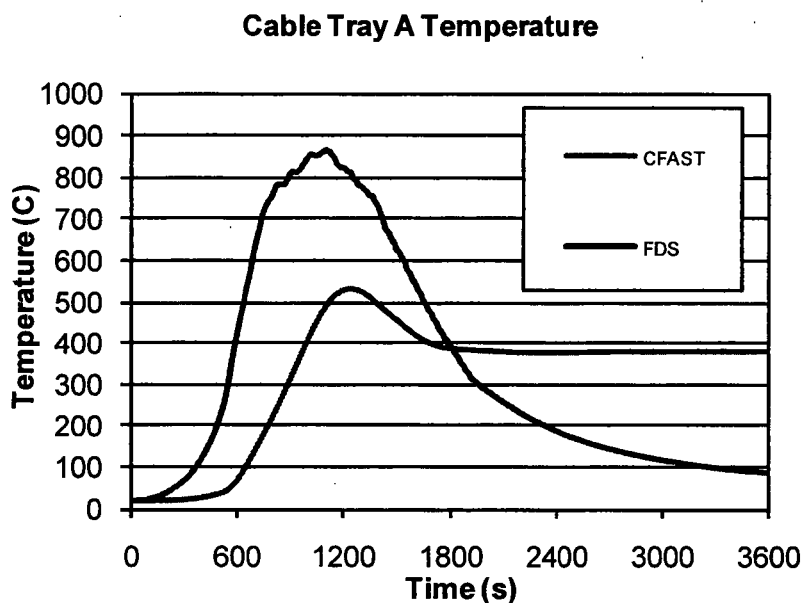
Figure B-6. Estimated temperatures for Cable Tray A directly above fire source for Switchgear Room cabinet fire scenario.

expected that the cables will ignite and provide an additional source of fire.

Qualitatively, the results of the CFAST and FDS predictions are quite different, but this is largely after flames have reached the cable tray. The radiation from the fire source in CFAST is calculated based on a point source fire positioned at the base of the fire. Thus, once the fire grows and the flame height approaches the target cable tray, the CFAST can be expected to

underestimate the local cable temperature and heat flux since the cable would actually be immersed within the flames. CFAST does include an estimate of the flame height, which can also be used as an indicator of damage to the cable. For this scenario, CFAST predicts the flame height reaches the cable tray in approximately 490 s, quite similar to the temperature-based prediction. Past this point, CFAST estimates of the local target temperature are expected to be underpredictions. FDS predictions include the impact of direct flame impingement and immersion of the target in flames. Thus, the higher temperatures predicted by FDS are expected.

Upon ignition of the bottom cable tray (Cable Tray A), the higher cable trays are ignited consistent with the FLASH-CAT model.

B.5.2 Cabinet Damage

To assess potential damage to adjacent cabinets, both the predicted temperatures and heat fluxes are evaluated. Because the two adjacent cabinets are equidistant from the fire and have similar properties, only one is considered here. The critical damage thresholds are the same for these cabinets as the cables in trays. Figure B-7 shows estimated temperature and heat flux on the cabinet surface.

The algebraic models are not capable of estimating the temperature of a target such as an electrical cabinet, whereas the other models are. CFAST and FDS all estimate similar peak temperatures below 145°C (264°F), which is well below the threshold of 205°C (424°F). The somewhat higher cabinet temperature and heat flux predicted by CFAST is consistent with the higher HRR of the fire for the CFAST simulation. CFAST and FDS both estimate an incident heat flux below about 4 kW/m^2, with the difference again caused by different HRRs.
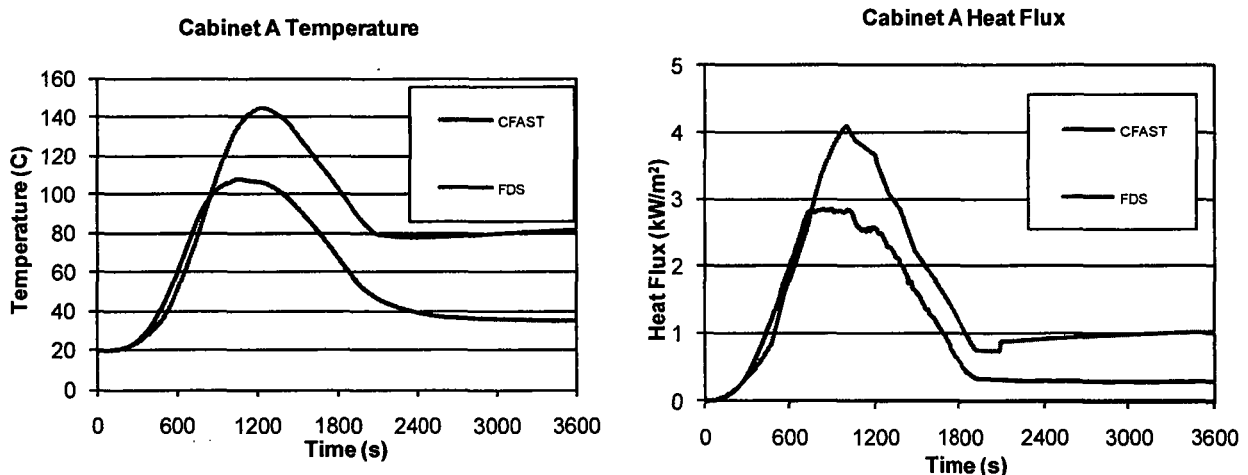
Figure B-7. Estimated temperature and heat flux on cabinet adjacent to fire source in Switchgear Room cabinet fire scenario.

B.5.3 Smoke Detector Activation

Table B-3 shows the smoke detection activation times estimated by the models. CFAST bases activation estimates on a specified temperature rise, whereas FDS bases its prediction on the

Cabinet Fire in Switchgear Room

local smoke concentration in the vicinity of the detector. The activation times based on temperature rise range from 3 to 5 min, whereas that based on smoke concentration is approximately 1 min. This is not surprising because the compartment is relatively large, and heat losses from the smoke plume to the ceiling cool the gases early in the fire, delaying the temperature-based activation estimate.

Table B-3. Smoke detector activation times, Switchgear Room cabinet fire

Model	Detector 1	Detector 2
CFAST	176 s	431 s
FDS	50 s	140 s

B.5.4 Uncertainty

In this example, the objective of the calculations is to estimate the effects of fire in a cabinet in a Switchgear Room on nearby cable and cabinet targets; that is, to determine whether and when temperatures and/or heat flux on the cable and adjacent cabinets exceed established critical values. Chapter 4, Model Uncertainty, provides guidance on how to express the uncertainty of the predictions. In the NRC/EPRI V&V study (NUREG-1824 (EPRI 1011989)), it was found that predictions of target temperatures are, on average, equal for CFAST and 2 % greater for FDS than corresponding measurements, and the relative standard deviation of its predictions about this average value is 27 % for CFAST and 13 % for FDS. For CFAST (the higher estimated temperature), this suggests that the true value of the peak cable temperature in this scenario is normally distributed with a mean of 144 °C and a standard deviation of 34 °C. Therefore, the probability that the cable temperature would exceed 205 °C is:

$$P(T > 205) = \frac{1}{2} \, \text{erfc}\left(\frac{205 - 145}{34\sqrt{2}}\right) = 0.04 \tag{B-4}$$

In other words, there is a 4 % chance of exceeding the temperature threshold for cables inside cabinet A, according to the CFAST prediction. With a lower temperature and standard deviation, the probability estimate from FDS calculations would be lower.

It should also be noted that these damage criteria are intended to be indicative of electrical failure, but are routinely assumed to also apply as ignition criteria. In newer studies in NUREG/CR-7010, cable ignition was not observed at fluxes below 25 kW/m^2, and most often only with direct flame impingement. Handbook values for minimum ignition flux for power and communication cables are reported in the range of 15 kW/m^2 to 35 kW/m^2 (*SFPE Handbook*, Table 3-4.2).

Table B-4 lists the probability of exceeding the critical temperature and heat flux for all the model calculations.

Table B-4. Uncertainty analysis of the model predictions of the cabinet fire scenario

Quantity	Location	Model	Predicted Value	Critical Value	Probability of Exceeding
Temperature	Cable Tray A	CFAST	533 °C	205	0.991
		FDS	864 °C	205	1.000
	Cabinet A	CFAST	144 °C	205	0.036
		FDS	108 °C	205	0.000
Heat Flux	Cabinet A	CFAST	4.12 kW/m²	11	0.007
		FDS	2.85 kW/m²	11	0.000

B.5.5 Sensitivity

Referring again to Table B-4, it is clear that the cables directly above the cabinet fire would be damaged by the fire and provide an additional fire source for the cables above. In addition to examining the accuracy of the models as is done in the previous section, it is also possible to estimate how large a fire would be required to damage the cables within the adjacent cabinet. Table 4-3 indicates that the temperature is proportional to the HRR to the 2/3 power. Following the methodology in Section 4.4.1, in order to increase the predicted heat flux by 7 kW/m² to reach 11 kW/m², the peak HRR, $\dot{Q}$, must increase by approximately:

$$\Delta\dot{Q} \approx \frac{3}{2}\dot{Q}\frac{\Delta T}{T-T_0} = \frac{3}{2}1600\frac{61}{124} \approx 1180 \text{ kW} \tag{B-5}$$

In other words, the peak HRR would have to be approximately 1600+1180=2880 kW to cause the cables in cabinet A to fail.

B.6 Conclusion

Based on the analysis, the cabinet fire is likely to fail the electrical cables directly overhead in approximately 10 min, based on the analyses of both CFAST and FDS. The additional cable trays directly above ignite in turn. However, it is unlikely that the fire would damage the adjacent cabinets.

B.7 References

1. NUREG-1805, *Fire Dynamics Tool*, 2004.
2. NUREG/CR-6850 (EPRI 1011989), *Fire PRA Methodology for Nuclear Power Facilities*.
3. NUREG-1824 (EPRI 1011999), *Verification and Validation of Selected Fire Models for Nuclear Power Plant Applications*, 2007.
4. *SFPE Handbook of Fire Protection Engineering*, 4th edition, 2008.
5. G.W. Mulholland and C. Croarkin. "Specific Extinction Coefficient of Flame Generated Smoke." *Fire and Materials*, 24:227–230, 2000.
6. UL 217. Underwriters Laboratories, Inc., Single Station Fire Alarm Device.
7. U.O. Köylu and G.M. Faeth, Carbon Monoxide and Soot Emissions from Liquid-Fueled Buoyant Turbulent Diffusion Flames. Combustion and Flame, 87:61–76, 1991.

Cabinet Fire in Switchgear Room

8. Jones, W., R. Peacock, G. Forney, and P. Reneke, "CFAST: An Engineering Tool for Estimating Fire Growth and Smoke Transport, Version 5 - Technical Reference Guide," SP 1030, National Institute of Standards and Technology, Gaithersburg, MD, 2004.
9. Gay, L., C. Epiard, and B. Gautier, "MAGIC Software Version 4.1.1: Mathematical Model," EdF HI82/04/024/B, Electricité de France, France, November 2005.
10. NIST SP 1018-5, *Fire Dynamics Simulator (Version 5), Technical Reference Guide, Vol. 3, Experimental Validation.*

Attachments

1.   FDS input file: Switchgear_Room_Cabinet.fds

2.   CFAST input files:

        a. Initial Fire Only.in
        b. Cabinet Fire in Switchgear.in
        c. MCC Cable Tray Secondary Fire.o
        d. Thermal.csv

C
Lubricating Oil Fire in Pump Compartment

C.1 Modeling Objective

The purpose of the calculations described in this appendix is to predict the effects of a large fire in a small compartment. Specifically, the purpose of the calculation is to determine whether important safe-shutdown cables within the compartment will fail, and, if so, at what time failure occurs. These cables are protected by an electrical raceway fire barrier system (ERFBS), but there is a concern that the existing barrier system will not provide the required protection.

C.2 Description of the Fire Scenario

General Description: The compartment is built of fire-resistive construction and contains a Train A Emergency Core Cooling System pump and a cable tray containing safe-shutdown cables and protected by an ERFBS. The pump is surrounded by a dike to contain any lube oil that may leak or spill and has a maximum capacity of 190 L of lube oil. The compartment contains one smoke detector and one sprinkler. The fire occurs when pump oil leaks into the dike area and ignites.

Geometry: The pump room comprises one rectangular room with a smaller rectangular entry area and door. Figure C-1 is a drawing of the pump compartment.

Construction: As shown in Figure C-1, the walls are 0.1 m (0.328 ft). The floor and ceiling are 0.9 m (3 ft) thick. The ASTM E-119 criteria for the temperature rise of the unexposed surface is 121 °C (250 °F); this is to guard against ignition of combustibles on the non-fire side of the wall (NUREG-1805, Section 17.4.2).

Materials: The walls, ceiling, and floor are all constructed of concrete. Nominal values for the thermal properties of various materials in the compartment are listed in Table 3-1 (NUREG-1805, Table 2-3).

Cables: The single cable tray in this compartment is filled with PVC-insulated, PE-jacketed cables. These cables have a diameter of approximately 1.5 cm (0.6 in), a jacket thickness of approximately 2 mm (0.079 in), and 7 conductors. See Figure C-1 for the location of the cable tray. Nominal values for the cable insulation thermal properties are as follows: the density is 1380 kg/m^3, the thermal conductivity is 0.192 W/m/K, and the specific heat is 1.289 kJ/kg-K. The damage criterion is taken to be when the cable temperature reaches 200°C (392°F). These values are taken from NUREG-1805, Appendix A.

ERFBS: This cable tray is protected by an ERFBS, which is two layers of 2.54 cm (1 in) thick, 128 kg/m^3 Kaowool insulation blankets, covered by 1 mil foil. The density of this material is 128 kg/m^3, the thermal conductivity is 0.06 W/m/K, the specific heat is 1.07 kJ/kg-K, and the emissivity is approximately 0.9. These values are taken from product literature.

Fire Protection Systems: As shown in Figure C-1, a smoke detector and sprinkler are located in the pump room. However, to determine if the barrier system alone will provide the required protection, the fire detection and suppression systems are not credited in the fire scenario under consideration.

Lubricating Oil Fire in Pump Compartment

Ventilation: There is one supply and one return register, each with an area of 0.5 m^2 (5.4 ft^3), providing a volume flow rate of 0.25 m^3/s. The locations are shown in Figure C-1. The ventilation system continues to operate during the fire with no changes brought about by fire-related pressure effects. This does not imply that the fire does not impact the ventilation system, but rather that there is typically limited information about the ventilation network that connects to a given compartment. The pump compartment has one door; it is 1.1 m (3.6 ft) wide and 2.1 m (6.9 ft) tall. The door is normally closed, but it is opened 10 min after ignition by the fire brigade. Before the door opens, leakage due to the doorway occurs via a 2.5 cm (1 in) gap under the door.

Fire: The fire starts following an accidental release of lube oil. The spill is contained by the dike. Using the values for transformer oil from NUREG-1805, the density is 760 kg/m^3, the heat of combustion is 46,400 kJ/kg, and the infinite-area mass loss rate of the burning oil is 0.039 kg/m^2/s. The empirical HRR reduction constant is 0.7 m^{-1}, but it is not used for this scenario because the compartment heating is expected to enhance the burning rate. Lube oil is a mixture of hydrocarbons, mostly alkanes, which have a chemical formula of the form C_nH_{2n+2} (with n ranging from 12 to 15). The radiative fraction of the fire's HRR is taken to be 35%, a typical value for sooty fires (*SFPE Handbook*).

Figure C-1. Geometry of the Pump Room.

Notes:
1. Walls are made of Concrete.
2. Door is made of Steel.
3. Smoke Detector at Ceiling Height.
4. Dimensions are in meters, 1 m = 3.28 ft.
5. ERFBS = Electrical Raceway Fire Barrier System

Cable Tray Protected By ERFBS

4.9 m
4.5 m
4.0 m x2
3.5 m x2
2.1 m x2
1.5 m
0.1 m
0.0 m

Smoke Detector
Sprinkler
4.6 m

Supply/Return Vent
Pump
Hatched Area is Door Opening
Fire Location

Supply Vent
Return Vent

Cable Tray Protected by ERFBS

4.6 m
4.1 m
3.8 m
3.0 m x2
2.3 m
2.1 m
1.5 m
1.4 m
0.0 m

Supply Vent
Pump
Return Vent
Door
Hatched Area is Space Between Pump Platform and Dike Walls

1.3 m
0.2 m

Cables
ERFBS Layer 2
0.0254 m (1 in) Thick
ERFBS Layer 1
0.0254 m (1 in) Thick
Cable Tray

SECTION A-A
DETAIL VIEW

1 m = 3.28 ft

⊘ - Smoke Detector

Object
Hidden
Dimension

3 -1   Pump Room

C.3 Selection and Evaluation of Models

This section describes the applicability of the models to this scenario.

Algebraic Models: Neither FIVE nor the FDT^s contain correlations to estimate the HGL temperatures within a flashed-over, underventilated compartment. Also, the point source radiation heat flux calculation included within FIVE and the FDT^s cannot account for the attenuation of thermal radiation by the smoke that fills the compartment. Consequently, neither model is used for this scenario.

Zone Models: This fire scenario is not a typical application of a zone model because it involves post-flashover conditions where the two layers essentially become one. Nevertheless, zone models can transition to this state when the HGL essentially descends all the way to the floor and the room becomes a well-stirred reactor. Conservation laws of mass and energy still apply within the single layer. In addition, the rules governing the heating of a target immersed in the HGL still apply, even when the HGL is the entire compartment. The zone model MAGIC has been selected for this application to demonstrate its use. There is no compelling advantage to either MAGIC or CFAST for this scenario.

CFD Models: This fire scenario is a challenging application, even for a CFD model. It involves relatively high temperatures, underventilated conditions, and flashover. The primary advantage of a CFD model for this fire scenario is that CFD models typically include combustion algorithms that estimate near- and post-flashover conditions.

Validation: This scenario falls outside the range of applicability of the NRC/EPRI V&V study documented in NUREG-1824 (EPRI 1011999) primarily because the equivalence ratio indicates that this is an underventilated fire whether the door to the compartment is open or closed (see Table C-1). The only experiment in NUREG-1824 (EPRI 1011999) that comes close to addressing the open-door phase of this scenario is Benchmark Exercise (BE) #4, a relatively large hydrocarbon fire within a relatively small compartment, with an Equivalence Ratio of 0.6.

However, two experiments were performed by EDF at CNPP in 1997 and were compared to the predictions of the zone model MAGIC. One test featured a fully-developed 1,000 kg cable fire in a two-room configuration. The size and construction of the fire room was similar to the pump room. There was good agreement between recorded and predicted Hot Gas Layer temperatures which exceeded those typically associated with flashover condition, as well as oxygen depletion. Thermal fluxes to cable targets were also recorded, but these targets were not protected. Although the fire room had an open vent, oxygen deletion within the Hot Gas Layer suggests that natural ventilation was insufficient for the large HRR of the fire. These experiments and the MAGIC simulations are described in EdF HI-82/04/022/A.

As part of the work performed at NIST for the investigation of the World Trade Center disaster, FDS has been validated against large-scale fire experiments. The experiments involved fairly large fires in a relatively small compartment, limited ventilation, a liquid fuel spray fire, and the measurement of the heat flux to and temperatures of insulated steel (similar to the cables protected by Kaowool blankets). These experiments and the FDS simulations are described in NIST NCSTAR 1-5F.

Table C-1. Normalized parameter calculations for the Pump Room fire scenario.

Quantity	Normalized Parameter Calculation	Validation Range	In Range?
Fire Froude Number	$$\dot{Q}^* = \frac{\dot{Q}}{\rho_\infty c_p T_\infty D^2 \sqrt{gD}} = \frac{4980}{1.2 \times 1.012 \times 293 \times 1.87^2 \times \sqrt{9.8 \times 1.87}} \cong 0.93$$	0.4 – 2.4	Yes
Flame Length, L_f, relative to the Ceiling Height, H	$$\frac{L_f}{H} = \frac{4.8}{4.9} \cong 0.99$$ $$L_f = D\left(3.7\,\dot{Q}^{*2/5} - 1.02\right) = 1.87\,(3.7 \times 0.93^{0.4} - 1.02) \cong 4.8$$	0.2 – 1.0	Yes
Ceiling Jet Radial Distance, r_{cj}, relative to the Ceiling Height, H	N/A	1.2 – 1.7	N/A
Equivalence Ratio, φ, as an indicator of the Ventilation Rate	$$\varphi = \frac{\dot{m}_F/\dot{m}_{O_2}}{r} \equiv \frac{\dot{Q}}{r\,\Delta H\,\dot{m}_{O_2}} = \frac{4980}{13{,}100 \times 0.07} \cong 5.5$$ $$\dot{m}_{O_2} = 0.23\,\rho_\infty \dot{V} = 0.23 \times 1.2 \times 0.25 \cong 0.07$$	0.04 – 0.6	No
Equivalence Ratio, φ, as an indicator of the Opening Ventilation	$$\varphi = \frac{\dot{m}_F/\dot{m}_{O_2}}{r} \equiv \frac{\dot{Q}}{r\,\Delta H\,\dot{m}_{O_2}} = \frac{4980}{13{,}100 \times 0.38} \cong 0.99$$ $$\dot{m}_{O_2} = 0.23 \cdot 0.5 A_o \sqrt{h_o} = 0.23 \times 0.5 \times 2.31\sqrt{2.1} \cong 0.38$$	0.04 – 0.6	No
Compartment Aspect Ratios	$$\frac{L}{H} = \frac{9.39}{4.9} \cong 1.9$$ $$\frac{W}{H} = \frac{2.81}{4.9} \cong 0.6$$	0.6 – 5.7	Yes
Target Distance, r, relative to the Fire Diameter, D	N/A	2.2 – 5.7	N/A

C.4 Estimation of Fire-Generated Conditions

This scenario was modeled using the zone model MAGIC and the CFD model FDS.

C.4.1 Zone Model (MAGIC)

The following paragraphs outline the data utilized to model the scenario using MAGIC. Figure C-2 provides an illustration of the scenario as rendered by MAGIC.

Geometry: For modeling this scenario with MAGIC, the pump compartment was initially modeled as two compartments connected by a large opening (i.e., the geometry in Figure C-1 was recreated in MAGIC). However, there were difficulties in running the simulation the full time with this configuration. Therefore, the two compartments were combined into a single compartment of the same total volume and surface area. This allows the volume in which the HGL develops, and the surface area through which energy is transferred from the compartment, to be maintained. Maintaining the total volume and surface area while leaving the ceiling height unchanged at 4.9 m (16 ft) yields an effective compartment size of 9.39 m (30.8 ft) by 2.81 m (9.2 ft). The modification to the geometry can be seen by comparing Figures C-1 and C-2. All other aspects of the geometry are relatively unchanged.

Materials: All material properties are as specified above.

Fire: The fire size is based on the surface area of the dike around the pump. For flammable/combustible liquid spills or pools, fires are typically based on surface area and a unit-area mass loss rate (see the pool fire methods in the *SFPE Handbook* chapter on *Heat Release Rates* for details). Although the dike can be thought of as four connected rectangles, the areas were reduced to a single equivalent area and the fire was modeled as a single circular area of equivalent diameter; this was found to be 1.87 m (6.1 ft). The fire immediately involves the entire surface area of the dike. Based on this area and the data in section C-2 above, an HRR of 4980 kW and a total burn time of approximately 22 minutes were calculated. The HRR is simply the mass loss rate multiplied by the heat of combustion, and the burn time is simply the total mass of the fuel divided by the mass loss rate). As noted previously, a radiant heat fraction of 35% was selected. A stoichiometric ratio of 3.48 and an average specific area of 319.2 m^2/kg were taken from the MAGIC database for kerosene.

Ventilation: Mechanical ventilation is maintained constantly during the simulation, using the values provided above. MAGIC uses circular ducts, so the rectangular ducts seen in Figure C-1 were changed to their equivalent circular area. As noted above, the door is normally closed, but it is opened 10 minutes after ignition by the arriving fire brigade. Before the door opens, leakage due to the doorway occurs via a 2.5-cm gap under the door.
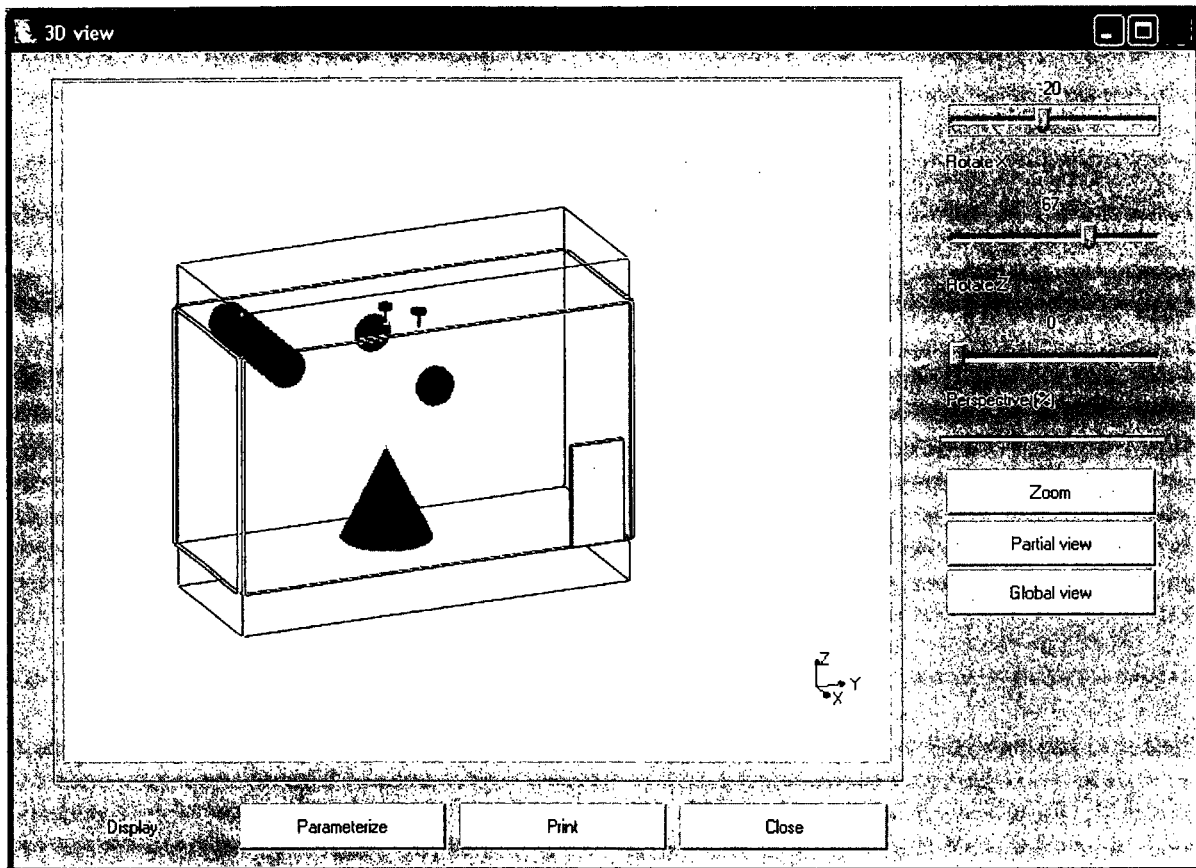
Figure C-2. MAGIC View of the Pump Room

C.4.2 CFD Model (FDS)

The following paragraphs outline the data utilized to model the scenario using FDS. Figure C-3 provides an illustration of the scenario as rendered by Smokeview.

Geometry: The compartment is modeled as shown in Figure C-1, except the pump itself is modeled as two rectangular boxes. A single uniform, rectangular mesh spans the entire compartment, plus the hallway outside the door. It is important to capture the flow in and out of the compartment following the opening of the door.

The numerical mesh employed consists of 0.2-m (0.7 ft) grid cells. A finer calculation with 0.1-m (0.3 ft) cells was performed with similar results. The latter calculation requires roughly a week of computing time on a single processor computer (2008 vintage), whereas the more coarsely gridded calculation requires about 10 hours.

Materials: All material properties are as specified above. The protected cable tray is modeled as two layers, 5 cm (2 in) of Kaowool surrounding a 2.5 cm (1 in) thick "slab" consisting of 67% copper and 33% plastic (by mass).

Fire: Due to the limited amount of validation data available for scenarios of this type and the considerable uncertainties involved, the approach taken is to *specify*, rather than attempt to *predict*, the burning rate of the fuel, even though the FDS model does provide the physical

mechanisms to estimate burning rates. The fire is specified in the diked area surrounding the pump. Although FDS has a liquid fuel burning model, it is not used here because there is not enough information about the fuel, and, more importantly, it lacks the exact geometry of the pump and diked area. FDS would assume that the oil has formed a relatively deep pool with relatively little influence by the surrounding solids. This is not the case here. Instead, the specified burning rate, 0.039 kg/m^2/s, is applied directly in the model over an area of 2.75 m^2 (29.6 ft^2) yielding a burning rate of 0.107 kg/s. The density of the oil is 0.76 kg/L, which means that the oil burns at a rate of 0.141 L/s. At this rate, 190 L will require 1,348 s to burn out. The vaporized fuel is a mixture of various hydrocarbons, but FDS uses only one fuel molecule in the combustion sub-model. For this calculation the fuel molecule is modeled as $C_{14}H_{30}$.

Ventilation: The volume flow rates are applied as specified.
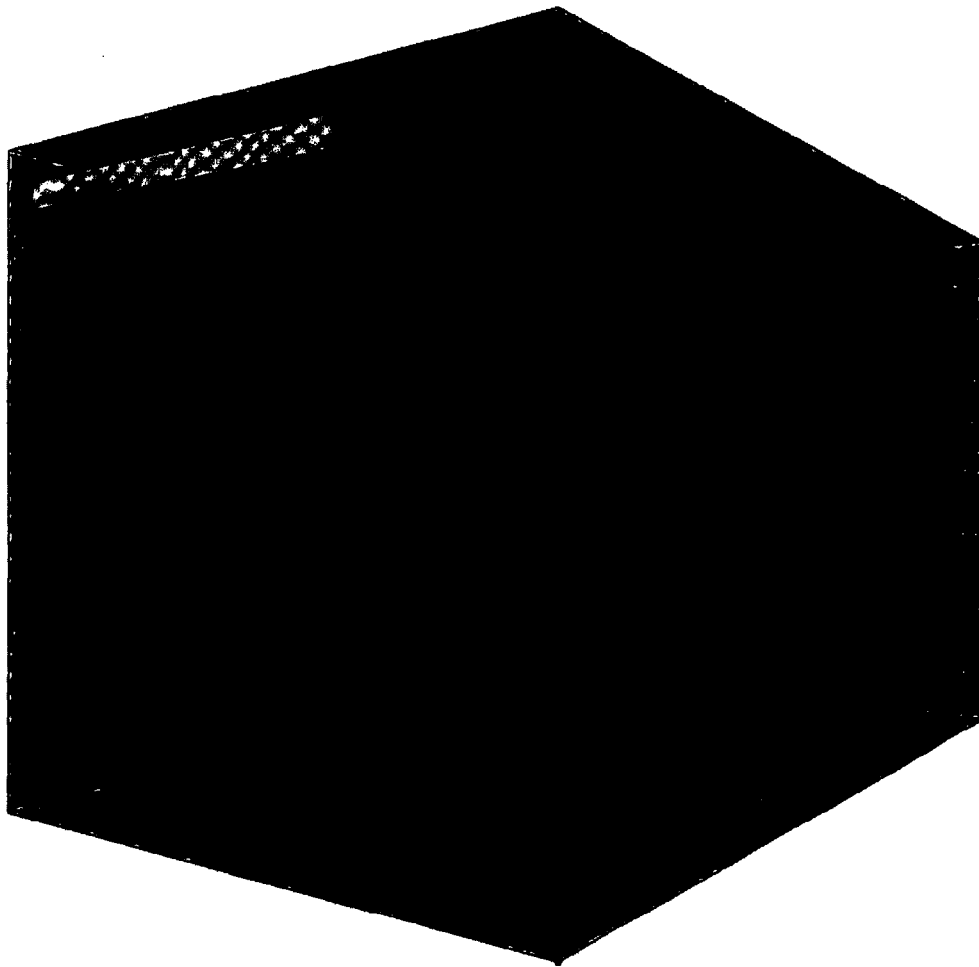
Figure C-3. FDS/Smokeview rendering of the Pump Room scenario at the early stage of the fire, before the compartment becomes underventilated.

C.5 Evaluation of Results

The primary purpose of the calculations is to assess whether critical cables within the pump room would be damaged in the event of a lube oil fire. In order to make this assessment, the gas temperatures and heat flux to the target tray, and the heating of the target cables under the protective Kaowool, need to be predicted. The results of the zone model MAGIC and the CFD model FDS are consistent, particularly the HRR. This is not surprising because the models use the same specified burning rate, the same fuel stoichiometry, and the same basic rules of gas phase flame extinction based on oxygen and temperature levels in the vicinity of the fire. The ERFBS is expected to protect the cables from reaching temperatures that would limit their functionality in the event of a fire of burning spilled lube oil. The following sections describe the results in greater detail.

C.5.1 The Fire

Although the burning rate of the lube oil spilled within a dike has been specified as input, it is clear from the results of the calculations that there would not be a sufficient amount of air (i.e., oxygen) within the compartment to sustain a large fire with the door closed for an extended period of time. The HRR curve predicted by the MAGIC and FDS models given the input heat release rate are shown in Figure C-4. The pronounced drop in the HRR immediately after the start of the fire and the subsequent low fire size lasting until the door opens at 10 minutes is evident in this figure. The sudden jump in the HRR predicted by FDS at 600 seconds is due to unburned fuel igniting as the door is opened. Note that none of the models has an algorithm capable of determining whether or not the fire would be sustained at this reduced burning rate until the door's opening time.
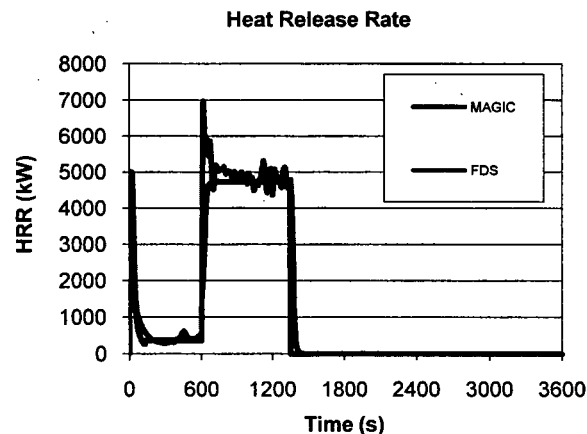
Heat Release Rate

Figure C-4. Heat Release Rate Predicted by MAGIC and FDS for the Pump Room Fire Scenario.

C.5.2 Hot Gas Layer Temperature

MAGIC and FDS estimate the temperature of the Hot Gas Layer as a function of time, as shown in Figure C-5. As expected, the Hot Gas Layer temperature changes in accordance with the altered (oxygen-starved) heat release rate. Once the door opens at 600 seconds, the increased

heat release causes the HGL temperature to rapidly increase until the fire dies out. After the fire burns out, the HGL temperature slowly drops as heat leaves the HGL through the bounding surfaces and open door.
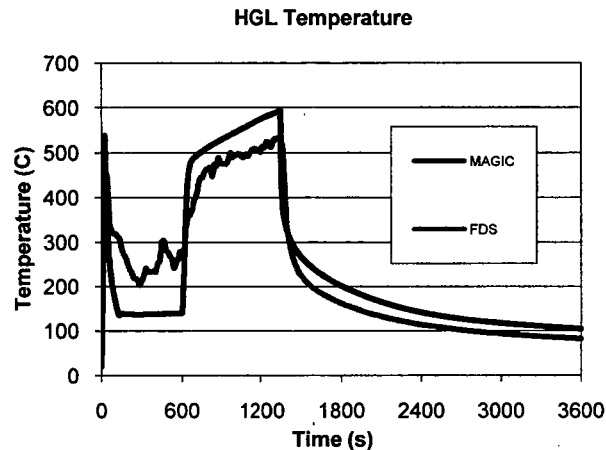
Figure C-5. Hot Gas Layer Temperature Predicted by MAGIC and FDS for the Pump Room Fire Scenario.

C.5.3 Cable Temperature

MAGIC and FDS have heat conduction algorithms to account for the multiple layers of insulation and cable materials. The surface temperature predictions of the cables protected by the ERFBS (Kaowool in this case) are shown in Figure C-6. MAGIC predicts a maximum cable surface temperature of about 55 °C (131 °F). FDS predicts a maximum cable surface temperature of about 40 °C (104 °F). These are both substantially below the 200°C (392 °F) damage threshold cited above. Note that although the HRR drops and then rises dramatically depending on ventilation, the cable temperature slowly rises. This is due to the thermal lag caused by the insulation (i.e., Kaowool).

ERFBS-Protected Cable Surface Temperature
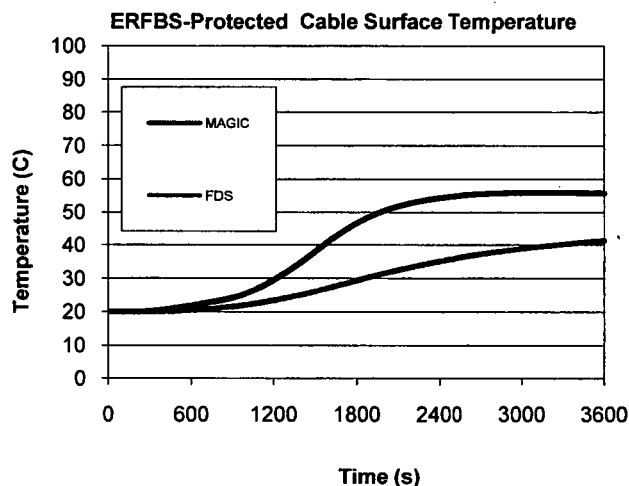
Figure C-6. Cable Surface Temperature Predicted by MAGIC and FDS for the Pump Room Fire Scenario.

C.5.4 Uncertainty

Chapter 4, Model Uncertainty, provides guidance on how to express the uncertainty of the MAGIC predictions. In the NRC/EPRI V&V study (NUREG-1824 (EPRI 1011989)), it was found that MAGIC predictions of target temperatures are, on average, 27% greater than corresponding measurements, and the relative standard deviation of its predictions about this average value is 19%. However, these values are for the surface temperature of an exposed target, not a protected (i.e., insulated) target. Since the conduction models (i.e., heat transfer equations) from the surface in are well known, the surface temperature uncertainties provide a reasonable approximation of the overall uncertainty of the protected target. This suggests that the true value of the protected cable temperature in this scenario can be approximated as being normally distributed with a mean of 46.2 °C and a standard deviation of 12.5 °C. Therefore, the probability that the protected cable temperature would exceed 200°C is:

$$P(T > 200) = \frac{1}{2} \operatorname{erfc}\left(\frac{200 - 46.2}{12.5\sqrt{2}}\right) \cong 0 \qquad \text{(C-1)}$$

In other words, there is a near-zero chance of exceeding the temperature threshold for cable damage, according to the MAGIC prediction. The same type of calculation can be performed for FDS, with similar results (i.e., a near-zero likelihood of target failure).

C.5.5 Sensitivity

There can be considerable uncertainty in the heat release rates of real fires. As a result, it is prudent to consider the sensitivity of the results of simulations to the selected heat release rates. Table 4.2 indicates that both the Hot Gas Layer temperature and target surface temperature predictions are each related to the heat release rate by a two-thirds power dependence.

Equation 16 in Chapter 4 is a simple formula that can be used to estimate the relative change in the model Hot Gas Layer temperature and target surface temperature output quantity, $\Delta T / (T - T_0)$, due to the relative change in the model heat release rate input parameter, $\Delta \dot{Q} / \dot{Q}$:

$$\frac{\Delta T}{T - T_0} \approx \frac{2}{3} \frac{\Delta \dot{Q}}{\dot{Q}} \tag{C-2}$$

The predicted cable surface temperature is only 46.2 °C (115 °F), far less than the 200 °C (392 °F) damage temperature. Based on this equation, a six-fold increase in the heat release rate of the fire would be required to cause the cable temperature to increase to the damage temperature.

C.6 Conclusion

Based on the calculations above, the ERFBS is expected to protect the cables from reaching temperatures that would limit their functionality in the event of a fire involving burning spilled lube oil. This conclusion is based on the predictions of the zone model MAGIC and the CFD model FDS, while accounting for the uncertainty in the temperature predictions of the models and the sensitivity of the predictions to variations in the heat release rate.

C.7 References

1. NUREG-1805. *Fire Dynamics Tools.*
2. NUREG/CR-6850 (EPRI 1011989), *Fire PRA Methodology for Nuclear Power Facilities.*
3. NUREG-1824 (EPRI 1011999), *Verification and Validation of Selected Fire Models for Nuclear Power Plant Applications*, 2007.
4. *SFPE Handbook of Fire Protection Engineering*, 4th edition, 2008.
5. ASTM E 119, "Standard Test Method for Fire Tests of Building Construction and Materials."
6. UL 217, Underwriters Laboratories, Inc., Single Station Fire Alarm Device.
7. NIST SP 1086, *CFAST – Consolidated Model of Fire Growth and Smoke Transport (Version 6), Software Development and Model Evaluation Guide.*
8. NIST SP 1018-5, *Fire Dynamics Simulator (Version 5), Technical Reference Guide, Vol. 3, Experimental Validation.*
9. NIST NCSTAR 1-5F, *Federal Building and Fire Safety Investigation of the World Trade Center Disaster: Computer Simulation o the Fires in the World Trade Center Towers*, 2005.
10. Gay, L., C. Epiard, and B. Gautier, "*MAGIC Software Version 4.1.1: Mathematical Model*," EdF HI82/04/024/B, Electricité de France, France, November 2005.
11. Gay, L., Frezabeu, J., "*Qualification File of Fire Code MAGIC version 4.1.1*" EdF HI-82/04/022/A, Electricité de France, France, December 2004.

C.8 Attachments

1. FDS input file: Pump_Room.fds

2. MAGIC input file: Pump_Room.cas

D
Motor Control Center Fire in Switchgear Room

D.1 Modeling Objective

The calculations described in this example estimate the effects of a fire in a Motor Control Cabinet (MCC) in a Switchgear Room on nearby cable and cabinet targets. The purpose of the calculation is to determine whether these targets will fail, and, if so, at what time failure occurs.

D.2 Description of the Fire Scenario

General Description: The Switchgear Room is located in the reactor building. The compartment contains multiple motor control centers and some other switchgear cabinets.

Geometry: The layout of the compartment is shown in Figure D-1. Figure D-2 shows the equipment typically contained in the compartment, and Figure D-3 shows the significant elevation change between the "high" and "low" ceilings.

Materials: Property values for the relevant materials are listed in Table 3-1. The cabinet housing is 1.5 mm thick steel.

Cables: The cable trays are filled with cross-linked polyethylene (XPE or XLPE) insulated cables with a Neoprene jacket. These cables have a diameter of approximately 1.5 cm (0.6 in), a jacket thickness of approximately 2 mm (0.79 in), 7 conductors, and a mass per unit length of 0.4 kg/m. Tray locations are shown in the compartment drawing. XLPE cables fail when the internal temperature just underneath the jacket reaches approximately 400°C (750 °F) (NUREG/CR-6931, Vol. 2, Table 5.10) or the exposure heat flux exceeds 11 kW/m^2 (NUREG-1805, Appendix A). Damage criteria for the adjacent cabinets are equivalent to that for the cable trays because the cables within the cabinet are subjected to a similar thermal exposure as the steel cabinet housing.

Fire: A fire starts within a motor control center cabinet. The cabinet is closed and contains more than one bundle of qualified cable. The fire grows following a "t-squared" curve to a maximum value of 702 kW in 12 min and remains steady for 8 additional minutes, consistent with NUREG/CR-6850 (EPRI 1011989), Appendix G, for a cabinet with more than one cable bundle of qualified cable. After 20 min, the HRR decays linearly to zero in 19 min. A peak fire intensity of 702 kW represents the 98th percentile of the probability distribution for HRR in cabinets of this general description.

The top of the cabinet contains a louvered air vent, 0.6 m (2 ft) wide and 0.3 m (1 ft) long. The cabinet is 2.4 m (8 ft) tall. The fire burns within the interior of the cabinet, and the smoke, heat, and possibly flames exhaust from the air vent at the top of the cabinet.

Ventilation: The compartment is normally supplied with three air changes per hour. The supply and return vents are indicated on the drawing. The two doors are normally closed. Normal HVAC operations continue during the fire, and the doors remain closed. The volume of the compartment is 882 m^3 (31,150 ft^3), meaning that three air changes per hour requires a volume flow rate of 0.735 m^3/s.
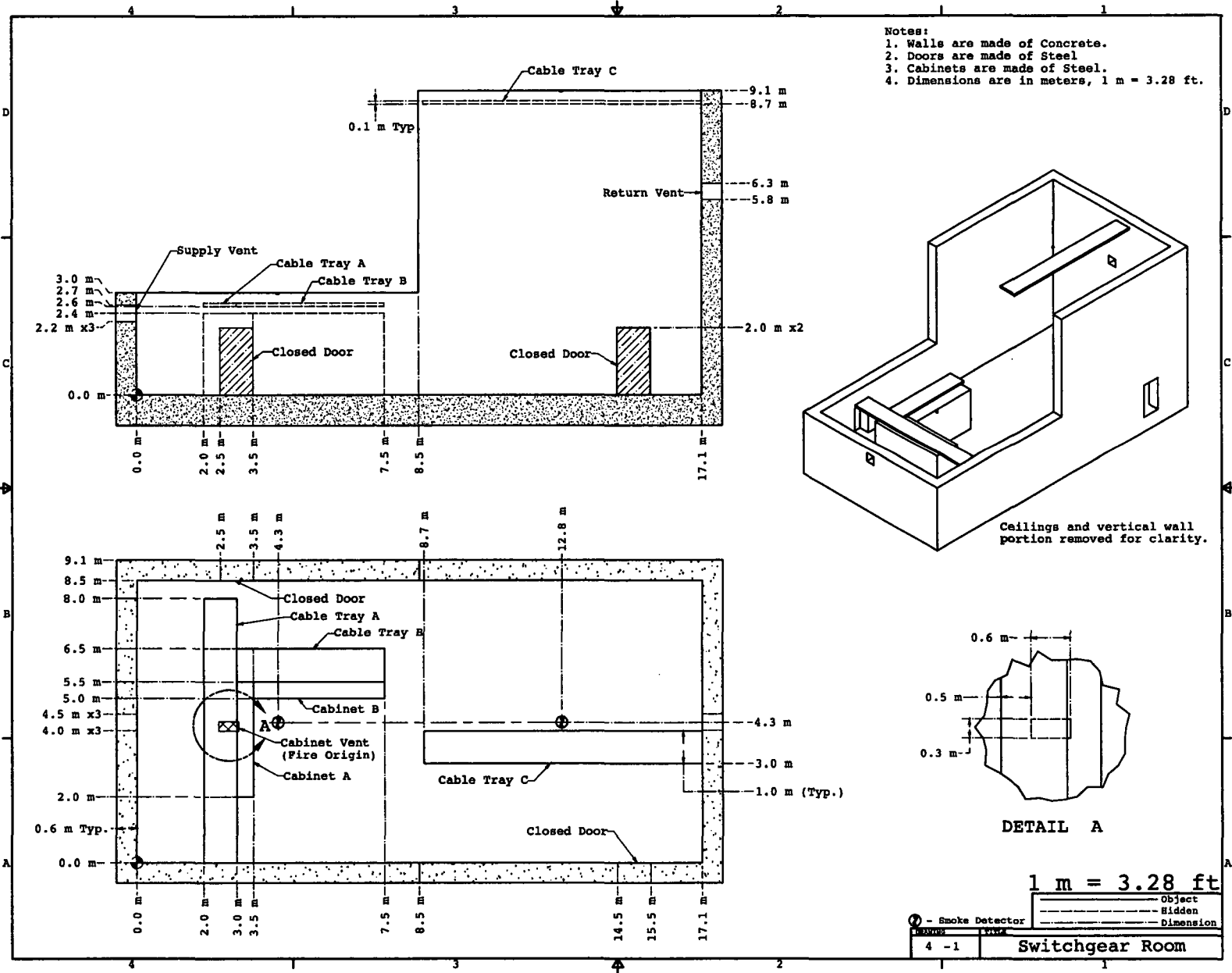
Figure D-1. Geometry of the MCC/Switchgear Room.

Notes:
1. Walls are made of Concrete.
2. Doors are made of Steel
3. Cabinets are made of Steel.
4. Dimensions are in meters, 1 m = 3.28 ft.

Cable Tray C

9.1 m
8.7 m

0.1 m Typ

6.3 m
5.8 m

Return Vent

Supply Vent

Cable Tray A
Cable Tray B

3.0 m
2.7 m
2.6 m
2.4 m
2.2 m x3

2.0 m x2

Closed Door

Closed Door

0.0 m

0.0   2.0 2.5   3.5   7.5 8.5   17.1 m

Ceilings and vertical wall
portion removed for clarity.

2.5 m 3.5 m 4.3 m   8.7 m   12.8 m

9.1 m
8.5 m
8.0 m

Closed Door
Cable Tray A
Cable Tray B

6.5 m

5.5 m
5.0 m
4.5 m x3
4.0 m x3

Cabinet B

A

4.3 m

Cabinet Vent
(Fire Origin)

Cabinet A

3.0 m

Cable Tray C

1.0 m (Typ.)

2.0 m

0.6 m Typ.

Closed Door

0.0 m

0.0   2.0   3.0 3.5   7.5 8.5   14.5 15.5   17.1 m

DETAIL   A

0.6 m

0.5 m

0.3 m

1 m = 3.28 ft

Object
Hidden
Dimension

⊘ – Smoke Detector

DRAWING	TITLE	
4 -1		Switchgear Room

Figure D-2. Typical electrical cabinet in the lower part of the Switchgear Room.
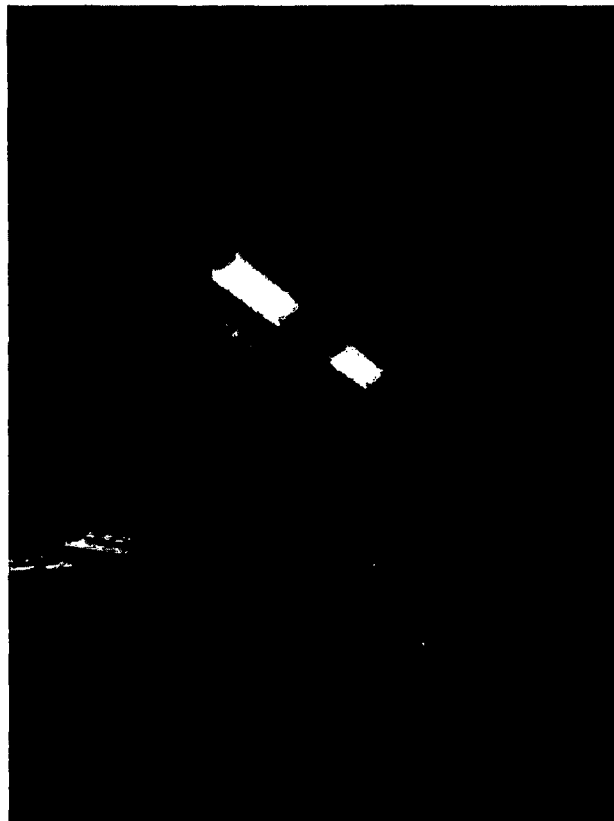
Figure D-3. View of the high ceiling space.

D.3 Selection and Evaluation of Fire Models

The fire scenario described above is challenging primarily because it involves a single large compartment with two very different ceiling heights, and the empirical and zone models are based on the assumption that the compartment is fairly uniform in height.

Algebraic Models: The correlations used in the FDT^s and FIVE to estimate HGL temperature are based on compartment fire experiments with relatively uniform ceiling height. However, these calculation methods can be used to estimate the flame height and the radiation heat flux to various targets. For this scenario, the FDT^s are selected, but FIVE would be appropriate as well for these calculations.

Zone Models: This scenario is challenging for a zone model because of the non-uniform ceiling height. Typically, the geometry is modeled as two connected compartments. Alternatively, CFAST can model the space as a single compartment with a variable cross-sectional area to account for the extra volume of the high-ceiling space. For this reason, CFAST is used in the analysis.

CFD Models: This scenario is a fairly typical application of a CFD fire model. The fact that there are two ceiling heights is not an issue, as the compartment geometry is input as is, with no need for further assumptions. In fact, it is very convenient in a case like this to use two rectangular meshes instead of one. Not only does it conform nicely to the actual geometry, but it also enables the calculation to be run in parallel on two processors instead of one. Figure D-5 is an FDS/Smokeview depiction of the scenario.

Validation: The principal source of validation data justifying the use of the above-listed fire models for this scenario is the NRC/EPRI V&V study documented in NUREG-1824 (EPRI 1011999). NIST has expanded the NRC/EPRI V&V to include the latest versions of CFAST (6.1.1) (Peacock, 2008) and FDS (5.5.3) (McGrattan, 2010). Table D-1 lists various important model parameters and the ranges for which the validation study is applicable. All but one parameter, the Fire Froude Number, fall within the ranges. This parameter is essentially a measure of the fire's heat output relative to its base area. In this example, the fire is assumed to "sit" atop the cabinet with the vent opening serving as its "base." This assumption leads to a higher value of Q^* than would be calculated if it were not assumed that the fire burns completely outside of the cabinet. Thus, the high value of Q^* is the result of an assumption that will lead to more severe fire conditions than would be expected if the fire were assumed to burn partially within the cabinet

The second important issue in regard to model validation is the two-tiered ceiling. None of the experiments used in the NRC/EPRI validation study have a similar ceiling configuration. For this reason, the algebraic models are limited only to "open" fire predictions, such as flame height and radiation heat flux, for which the compartment geometry is irrelevant. CFAST is to be used in a way that was not validated in NUREG-1824 (EPRI 1011999), but still conforms with the basic physical assumptions of the model. A CFD model makes no particular assumptions based on ceiling geometry; in fact, the set of experiments used in the NRC/EPRI study referred to as Benchmark Exercise #2 provides validation data to evaluate the models' ability to estimate the plume and HGL temperature/depth of smoke and hot gases filling a fairly large, open hall with an angled roof.

Table D-1. Normalized parameter calculations for the MCC fire scenario.

Quantity	Normalized Parameter Calculation		Validation Range	In Range?
Fire Froude Number	$\dot{Q}^* = \dfrac{\dot{Q}}{\rho_\infty c_p T_\infty D^2 \sqrt{gD}} = \dfrac{702}{1.2 \times 1.012 \times 293 \times 0.5^2 \times \sqrt{9.8 \times 0.5}} \cong 3.6$		0.4 – 2.4	No
Flame Length, L_f, relative to the Ceiling Height, H	$\dfrac{L_f}{H} = \dfrac{2.6}{5.2} = 0.5$ $L_f = D\left(3.7\,\dot{Q}^{*2/5} - 1.02\right) = 0.5\,(3.7 \times 3.6^{0.4} - 1.02) \cong 2.6$		0.2 – 1.0	Yes
Ceiling Jet Radial Distance, r_{cj}, relative to the Ceiling Height, H	N/A – There are no targets like sprinklers or smoke detectors under consideration in this example.		1.2 – 1.7	N/A
Equivalence Ratio, φ, as an indicator of the Ventilation Rate	$\varphi = \dfrac{\dot{m}_F/\dot{m}_{O_2}}{r} \equiv \dfrac{\dot{Q}}{r\,\Delta H\,\dot{m}_{O_2}} = \dfrac{702}{13,100 \times 0.2} \cong 0.27$ $\dot{m}_{O_2} = 0.23\,\rho_\infty \dot{V} = 0.23 \times 1.2 \times 0.735 \cong 0.2$ kg/s		0.04 – 0.6	Yes
Compartment Aspect Ratio (Lower | Upper)	$\dfrac{L}{H} = \dfrac{8.5}{3.0} \cong 2.8$ $\dfrac{W}{H} = \dfrac{8.5}{3.0} \cong 2.8$	$\dfrac{L}{H} = \dfrac{8.6}{9.1} \cong 0.9$ $\dfrac{W}{H} = \dfrac{8.5}{9.1} \cong 0.9$	0.6 – 5.7	Yes
Target Distance, r, relative to the Fire Diameter, D	$\dfrac{r}{D} = \dfrac{1.4}{0.5} \cong 2.8$		2.2 – 5.7	Yes

D.4 Estimation of Fire-Generated Conditions

This section describes how each of the models is used in the analysis, including specific assumptions unique to the particular model.

D.4.1 Algebraic Models (FDT^s)

Fire: The FDT^s use a steady-state HRR in both the flame height and radiation heat flux calculation. A constant HRR of 702 kW is used for both. A fire diameter is calculated from the vent area atop the cabinet, 0.5 m (1.6 ft). The Heskestad correlation yields a flame height of 2.7 m (8.9 ft). The cables just above the cabinet would be engulfed in flame and fail.

The point source radiation model predicts the heat flux to the cabinet an estimated 1.4 m (4.6 ft) from the fire. The result indicates a peak heat flux of 9.8 kW/m^2. Note that this estimate does not include the contribution from the HGL, and that the FDT^s do not include a means to estimate the temperature of the cabinet.

D.4.2 Zone Models (CFAST)

Geometry: Zone fire models subdivide the space of interest into one or more compartments connected by vents. With CFAST, the single, large compartment is modeled as two smaller compartments stacked one atop the other, connected by a horizontal vent. The reason for this is that the fire is located completely underneath the ceiling of the lower compartment. The smoke plume does not rise directly into the upper compartment; rather, the smoke pours from beneath the lower ceiling like smoke flowing into a horizontal vent. Figure D-4 shows the geometry of the CFAST calculation. Note that two additional dummy compartments have been included in the calculation, not connected to any other compartment in the simulation, to visually represent the MCC cabinets within the Switchgear Room. These are included for visualization purposes only and have no impact on the calculation.

Fire: Following guidance in NUREG/CR-6850 (EPRI 1011989), the fire is placed near the top of the cabinet. It is positioned directly below the exposed cable tray to maximize exposure of the cable for the simulation. The specified fire area and HRR are input directly into the model.

Cables: One of the objectives of the calculation is to estimate the potential damage to the cables within three trays. CFAST uses the Thermally-Induced Electrical Failure (THIEF) methodology developed as part of the CAROLFIRE program (NUREG/CR-6931, Vol. 3). Each of the three target cables is specified directly in the model. Electrical functionality is lost when the temperature just inside of the 2 mm (0.08 in) jacket reaches 400 °C (752 °F).

Ventilation: The two compartments used to model the space are connected by a single large vent. Although the largeness of this vent relative to the compartment size is not typical of a zone model application, the simple two-compartment geometry of the space and the more dominant mechanical ventilation flow from one side of the Switchgear Room to the other should minimize any uncertainty in the calculation resulting from the large connecting vent. Mechanical ventilation is included at the specified height and with the specified volume flow applied to the single supply (in the low-ceiling space) and return (in the high-ceiling space). Additionally, since zone fire models assume that compartments are completely sealed unless otherwise specified, a typical leakage vent, 25 mm (1 in) in height, is included at the bottom of each closed doorway to reflect the fact that the doorways are not totally airtight.

Smokeview 5.1.5 - May 10 2008
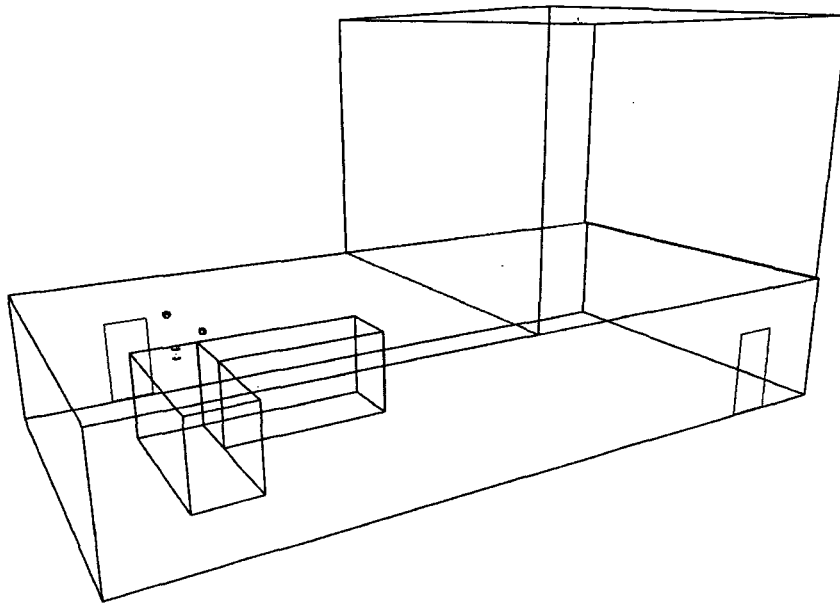
Figure D-4. Geometry of two-height ceiling Switchgear Room as modeled in CFAST.

D.4.3 CFD Model (FDS)

Geometry: The entire compartment is included in the computational domain. To avoid including a large portion of area outside the compartment, two separate meshes are used, one for the low-ceiling section and one for the high-ceiling section. The *FDS User's Guide* contains detailed instructions for running the simulation on multiple computers. The concrete walls are essentially the boundaries of these two meshes. The electrical cabinets and cables are included in the simulation as simple rectangular solids, and their dimensions have been approximated to the nearest 15 cm (5.9 in). There is no attempt to model the details of either the cable trays or cabinets because the grid resolution is not fine enough. This is an appropriate assumption because the cables and cabinets are merely "targets" for which it is sufficient to know their bulk thermal properties. An FDS/Smokeview rendering of the scenario is shown in Figure D-5.

The numerical mesh consists of uniform grid cells, roughly 15 cm (5.9 in) on a side. This is a relatively coarse mesh for a scenario of this type, but finer meshes do not produce significantly different results in this case. It should be noted, however, that there is considerable uncertainty in the exact nature of the fire relative to the cabinet and the cables just above. This uncertainty mainly has to do with the assumption that the fire originates directly atop the cabinet rather than deep within. With a model like FDS, it is possible to compare the results of different fire configurations, but it is not done here for the sake of brevity.

Fire: The fire burns over an area of 0.6 m (2 ft) by 0.3 m (1 ft) on top of the cabinet with a maximum HRR per unit area of 3,900 kW/m^2, yielding a total HRR of 702 kW.

Cables: FDS is limited to only 1-D heat transfer into either a rectangular or cylindrical obstruction. In this simulation, the cables are modeled as 1.5 cm (0.6 in) cylinders with uniform thermal properties. Following the Thermally-Induced Electrical Failure (THIEF) methodology in NUREG/CR-6931, Vol. 3, electrical functionality is lost when the temperature just inside of the 2 mm (0.08 in) jacket reaches 400 °C (752 °F). Note that no attempt is made in the simulation to predict ignition and spread of the fire over the cables, which is why the in-depth heat penetration calculation is focused on a single cable. At least one cable per tray is relatively free of its neighbors and would heat up more rapidly than those buried deeper within the pile.

Ventilation: Three air changes per hour are achieved with a volume flow of 0.735 m³/s applied to the single supply and return vents. No other penetrations are included in the model.

Figure D-5. FDS/Smokeview representation of the MCC/Switchgear Room scenario.

D.5 Evaluation of Results

The purpose of the calculations described above is to predict if and when various components within the compartment become damaged due to a fire in the MCC. XPE cables are expected to be damaged when their internal temperature surpasses 400 °C (750 °F) or the exposing heat flux surpasses 11 kW/m^2. Damage criteria for the adjacent cabinet are equivalent to that for the cables because the cables within the cabinet come in contact with the heated metal housing and, therefore, are exposed to similar thermal conditions. The targets of interest are three cable trays, labeled A, B and C, and a single electrical cabinet adjacent to the burning MCC. The following sections describe the results in detail.

D.5.1 Damage to Cabinet

The cabinet adjacent to the MCC is located approximately 1.4 m (4.5 ft) from the center of the fire. The point source radiation calculation included in the FDT^s predicts a heat flux of 9.8 kW/m^2. However, this is expected to be an overprediction because there is no direct line of sight between the cabinet and the fire. In other words, the adjacent cabinet does not "see" the entire fire. The point source radiation model used by the FDT^s was also shown to overestimate radiation heat flux by roughly a factor of two in the NRC/EPRI V&V study, NUREG-1824 (EPRI 1011999).

CFAST and FDS estimate the peak cabinet temperature to be approximately 160 °C (320 °F), with peak sustained heat fluxes in the range of 4 kW/m^2 to 6 kW/m^2. These predictions of heat flux and temperature are considerably lower than the damage criteria. The predicted heat flux to and temperatures of the exposed cabinets are shown in Figure D-6.
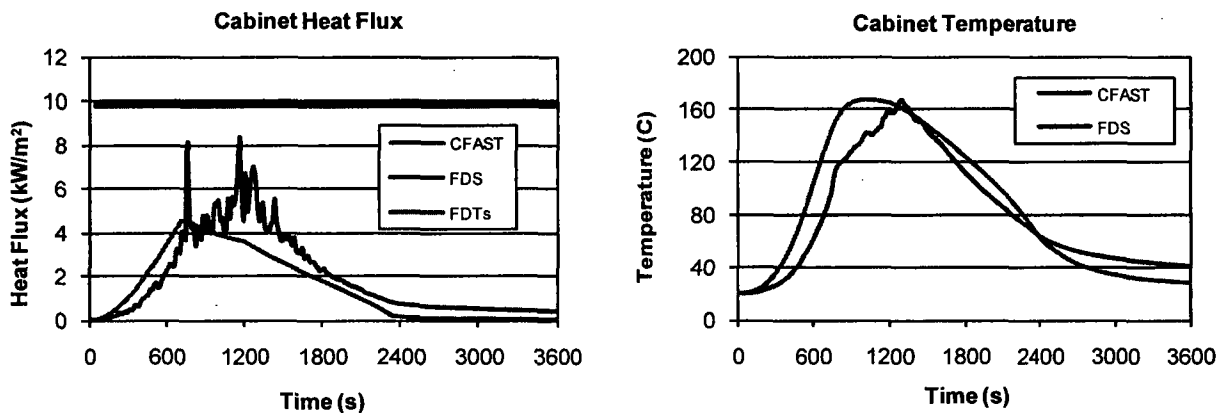
Figure D-6. Heat flux and temperature predictions for the adjacent cabinet.

D.5.2 Cable Damage Based on Temperature

The predicted heat flux to and temperatures of the cables in the three trays are shown in Figure D-7. CFAST and FDS estimate cable temperatures using the THIEF methodology (NUREG/CR-6931, Vol. 3). Both models predict that the cables in Tray A are likely to fail, but FDS predicts a failure time of approximately 8 minutes, while CFAST predicts 12 minutes. Neither model predicts that the cables in Tray B will reach the failure temperature of 400 °C

(750 °F), but both predict that these cables could reach temperatures in the neighborhood of 200 °C (392 °F). Note that these predictions are sensitive to the exact location of the target cable within the tray and its "view" of the fire. In this case, the cables in tray B are heated primarily by convection and radiation of the HGL.

The predicted cable temperatures of the cables in tray C by both FDS and CFAST indicate that they are unlikely to fail.

D.5.3 Cable Damage Based on Incident Heat Flux

The cable damage predictions discussed above require information about the thermal properties of the cables themselves. However, the cables in any given tray within a plant may have a range of sizes and thermal properties, making it impractical to estimate the temperature within each and every one. For this reason, an alternative predictor for cable damage is simply the incident heat flux to the cable surface, which does not require more detailed information about the cables themselves. In this scenario, the damage threshold has been defined to be when the heat flux exceeds 11 kW/m^2 at some point during the fire.
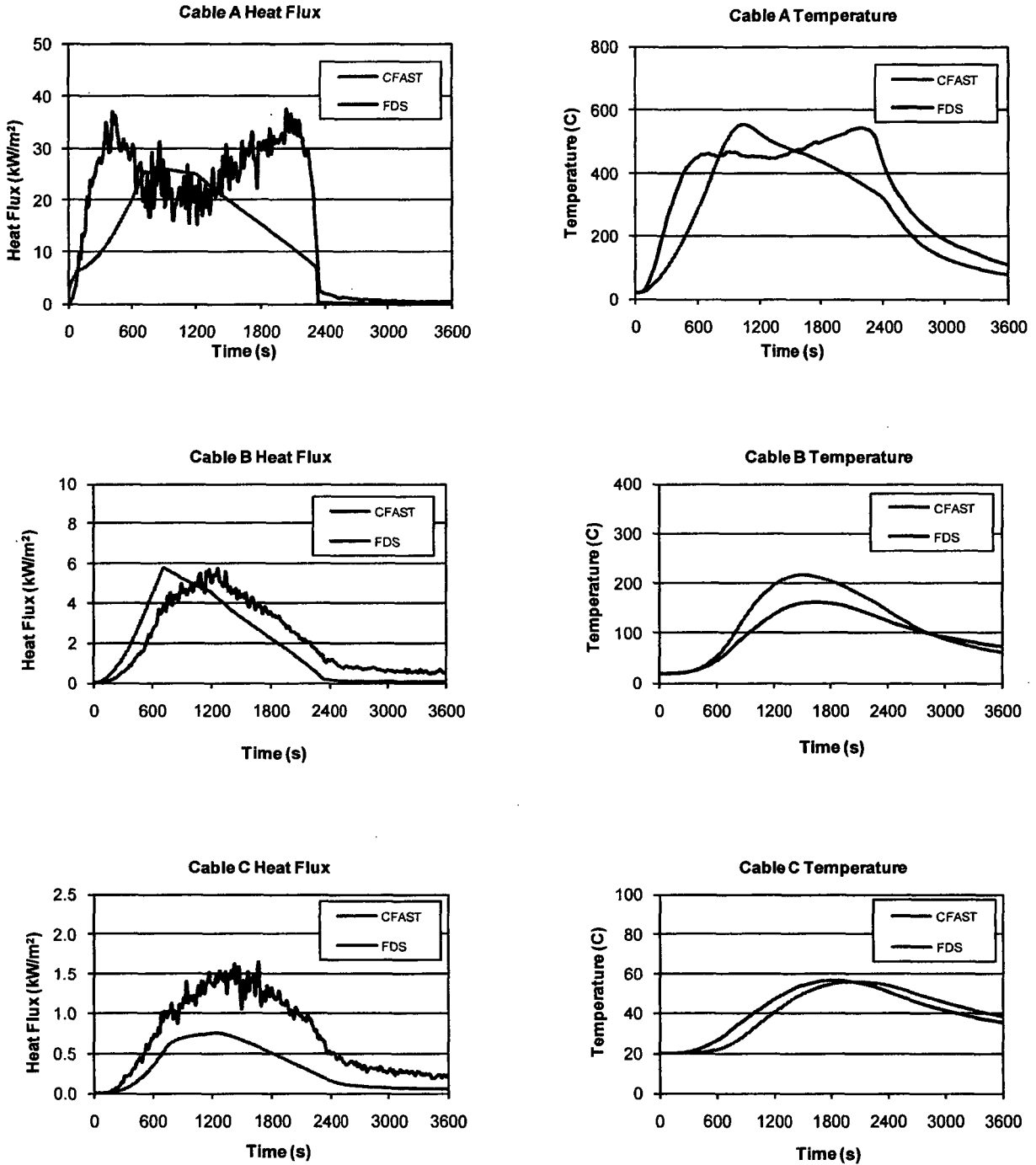
Figure D-7. Summary of cable results for the MCC/Switchgear Room.

D.5.4 Uncertainty

Chapter 4, Model Uncertainty, provides guidance on how to express the uncertainty of the model predictions. For example, consider tray B, where CFAST predicts a peak heat flux of approximately 6 kW/m^2. This value is less than the damage criterion of 11 kW/m^2, but in the NRC/EPRI V&V study (NUREG-1824 (EPRI 1011989)), it was found that CFAST predictions of total heat flux are, on average, 19 % less than corresponding measurements, and the relative standard deviation of its predictions about this average value is 47 %. This suggests that the true value of the heat flux to the cable in this scenario is normally distributed with a mean of 6/0.81=7.4 kW/m^2 and a standard deviation of 0.47×7.4=3.5 kW/m^2. Therefore, the probability that the actual heat flux to the cable would exceed 11 kW/m^2 is:

$$P(\dot{q}'' > 11) = \frac{1}{2} \, \mathrm{erfc}\left(\frac{11 - 7.4}{3.5\sqrt{2}}\right) \cong 0.151 \tag{D-1}$$

In other words, there is a 15% chance of exceeding the heat flux damage criterion for cable tray B, according to the CFAST prediction.

Table D-2 lists the model uncertainty of the temperature and heat flux predictions for CFAST and FDS. For tray A, the probabilities that the heat flux and temperature would surpass the critical value are close to 1, meaning that there is a high level of confidence that a fire would cause these cables to fail. For tray B, the probability of surpassing the critical heat flux value is much higher for the CFAST prediction than for that of FDS, even though both models estimate the same heat flux. This is because the validation data indicates that there is more uncertainty in the CFAST prediction of heat flux than FDS.

D.5.5 Sensitivity

Referring again to Table D-2, it is clear that the cables in tray A would most likely be damaged by a fire in the MCC. However, there is a chance that the cables in tray B could be damaged as well. In addition to examining the accuracy of the models, as is done in the previous section, it is also possible to consider the key input parameter and estimate the increased HRR necessary to damage the cables in tray B. Table 4-3 indicates that the heat flux is proportional to the HRR to the 4/3 power. Following the methodology in Section 4.4.1, in order to increase the predicted heat flux by 5 kW/m^2 to reach 11 kW/m^2, the peak HRR, $\dot{Q}$, must increase by approximately:

$$\Delta\dot{Q} \approx \frac{3}{4}\dot{Q}\frac{\Delta\dot{q}''}{\dot{q}''} = \frac{3}{4}702\frac{5}{6} \approx 438 \, \mathrm{kW} \tag{D-2}$$

In other words, the peak HRR of the fire would have to be approximately 702+438=1140 kW to cause the cables in tray B to fail.

Table D-2. Uncertainty analysis of the model predictions of the MCR scenario.

Model	Quantity	Target	Predicted Value	Critical Value	Probability of Exceeding
CFAST	Heat Flux	Cabinet	4.4 kW/m^2	11 kW/m^2	0.015
CFAST	Heat Flux	Cable A	26 kW/m^2	11 kW/m^2	0.919
CFAST	Heat Flux	Cable B	6 kW/m^2	11 kW/m^2	0.151
CFAST	Heat Flux	Cable C	0.75 kW/m^2	11 kW/m^2	0.000
FDS	Heat Flux	Cabinet	6 kW/m^2	11 kW/m^2	0.006
FDS	Heat Flux	Cable A	35 kW/m^2	11 kW/m^2	0.999
FDS	Heat Flux	Cable B	6 kW/m^2	11 kW/m^2	0.006
FDS	Heat Flux	Cable C	1.5 kW/m^2	11 kW/m^2	0.000
CFAST	Temperature	Cabinet	160 °C	400 °C	0.000
CFAST	Temperature	Cable A	550 °C	400 °C	0.852
CFAST	Temperature	Cable B	220 °C	400 °C	0.000
CFAST	Temperature	Cable C	55 °C	400 °C	0.000
FDS	Temperature	Cabinet	160 °C	400 °C	0.000
FDS	Temperature	Cable A	550 °C	400 °C	0.980
FDS	Temperature	Cable B	165 °C	400 °C	0.000
FDS	Temperature	Cable C	60 °C	400 °C	0.000

D.6 Conclusion

The purpose of the calculations described above is to predict if and when various components within the compartment become damaged due to a fire in the MCC. The fire model analyses performed for this scenario indicate that the fire would damage the cables in tray A because all the models (FDT^s, CFAST, FDS) predict that the flames would directly impinge on the cables themselves.

- CFAST and FDS predict that the cables in tray B are unlikely to be damaged based on the heat flux criterion. However, both models predict that the cables could reach temperatures as high as 200 °C (392 °F), a temperature that could damage thermoplastic cables.

- Neither FDS nor CFAST predicts that the cables in tray C would be damaged.

- None of the analyses indicate that the adjacent cabinet housing would be exposed to a heat flux that would cause damage.

D.7 References

1. NUREG/CR-6850 (EPRI 1011989), *Fire PRA Methodology for Nuclear Power Facilities*, 2005.
2. NUREG-1805, *Fire Dynamics Tools*, 2004.

3. NUREG-1824 (EPRI 1011989), *Verification and Validation of Selected Fire Models for Nuclear Power Plant Applications*, 2007.
4. NUREG/CR-6931, *Cable Response to Live Fire (CAROLFIRE), Volume 2: Cable Fire Response Data for Fire Model Improvement*, 2007.
5. NUREG/CR-6931, *Cable Response to Live Fire (CAROLFIRE), Volume 3: Thermally-Induced Electrical Failure (THIEF) Model*, 2007.
6. NIST SP 1086, *CFAST – Consolidated Model of Fire Growth and Smoke Transport (Version 6), Software Development and Model Evaluation Guide.*
7. NIST SP 1019, *Fire Dynamics Simulator User's Guide.*
8. NIST SP 1018, *Fire Dynamics Simulator, Technical Reference Guide, Vol. 3, Experimental Validation.*
9. *SFPE Handbook of Fire Protection Engineering*, 4th edition, 2008.

D.8 Attachments

1. FDS input file: Switchgear_Room_MCC.fds

2. CFAST input files:

        a. MCC in Switchgear.in
        b. MCC 702 kW.o
        c. thermal.csv

E
Transient Fire in Cable Spreading Room

E.1 Modeling Objective

The calculations in this appendix estimate the impact on safe-shutdown cables due to a fire in a trash bin inside a Cable Spreading Room (CSR). These calculations are part of a larger fire analysis described in Chapter 11 of NUREG/CR-6850 (EPRI 1011989), Volume 2, "Detailed Fire Modeling (Task 11)." The CSR contains a large quantity of redundant instrumentation and control cables needed for plant operation. Transient combustibles have been identified as a possible source of fire that may impact the cables. The purpose of the calculation is to analyze this condition and determine whether the cable targets will fail, and, if so, at what time failure occurs. The time to smoke detector activation is also estimated. The calculation will provide information for a decision on the hazard and risk for this scenario.

E.2 Description of the Fire Scenario

General Description: The CSR contains a large quantity of redundant instrumentation and control cables needed for plant operation. The cables are installed in either ladder-back trays or conduits.

Geometry: Figure E-1 illustrates the geometry of the CSR, and Figure E-2 shows a photograph of the CSR. In addition to cables, the CSR contains a fully enclosed computer compartment, ductwork, and large structural beams. There is no high- or medium-voltage equipment (switchgears or transformers) in the compartment. As indicated in Figure E-3, the top 2 m (6.6 ft) of the compartment is filled with cable trays containing cables, or ductwork, or large structural beams.

Construction: The walls, floor, and ceiling of the CSR are constructed of normal-weight concrete.

Materials: Nominal values for the thermal properties of various materials in the compartment have been taken from NUREG-1805 (Table 2-3) and are listed in Table 3-1. The important cables for this calculation are located in the third and sixth trays above the fire source, which are filled with PE-insulated, PVC-jacketed control cables important to safe shutdown. These cables have a diameter of approximately 1.5 cm (0.6 in), a jacket thickness of approximately 1.5 mm (0.06 in), and 7 AWG 12 conductors. These cables are damaged when the internal cable temperature reaches 205 °C (400 °F) or the exposure heat flux reaches 6 kW/m^2 (NUREG-1805, Appendix A).

The lowest cable tray contains cross-linked polyethylene (XLPE) cables. Although not important to safe shutdown of the plant, the cables in the lowest tray may ignite and provide an additional fire source to the trays above. For this reason, the bottom cable tray is protected on the lower surface by a solid metal barrier. The cables in the tray have a diameter of approximately 1.5 cm (0.6 in), a jacket thickness of approximately 1.5 mm (0.06 in), and 7 AWG 12 conductors. These cables are damaged when the temperature reaches 330°C (625°F) or the exposure heat flux reaches 11 kW/m^2 (NUREG-1805, Appendix A).

Transient Fire in Cable Spreading Room

The bottom and side surfaces of all cable trays in the CSR are of solid metal construction; top surfaces are open.

Detection System: Smoke detectors are located on the ceiling at locations shown in Figure E-1. The detectors are UL-listed with a nominal sensitivity of 4.9%/m.

Suppression System: An automatic CO_2 system is initiated by cross-zone smoke detection in the compartment or operated manually. A CO_2 discharge causes fire dampers to close and mechanical ventilation fans to stop to maintain a proper concentration of suppression agents. Activation of the CO_2 system is not modeled in this example.

Ventilation: The CSR has two doors on the east wall that are normally closed. Each door is 2 m (6.6 ft) wide by 2 m (6.6 ft) tall, with a 1 cm (0.4 in) gap along the floor. Standard procedure calls for an operator to investigate the fire within 600 s (10 min) of an alarm condition. For this reason, one of the doors is opened for this investigation.

There are two supply and two return vents for mechanical ventilation, each with an area of 0.25 m² (2.7 ft²). The total air supply rate is 1.4 m³/s. All vents are 2.4 m (8 ft) above the floor. Upon smoke detector activation, the mechanical ventilation fans stop and the dampers close.

Fire: A trash fire ignites within a cylindrical steel waste bin 0.8 m (2.6 ft) high and 0.6 m (2.0 ft) in diameter, containing 5 kg of trash. The HRR of the transient fire is estimated using NUREG/CR-4680. The heat of combustion of the trash is 20 kJ/g (*SFPE Handbook*; based on an average for various items that could be encountered in a trash can). The fire grows following a "t-squared" curve to a maximum value of 317 kW (the 98th percentile value from Table G-1 in NUREG/CR-6850 (EPRI 1011989)) in 480 s (consistent with NUREG/CR-6850 (EPRI 1011989) Supplement 1 for a transient fire growth rate contained within a trash can). The fire burns at its maximum value until the trash is consumed. The radiative fraction[16] of the fire is taken to be 35%, consistent with typical sooty fires. The soot yield of the fire is taken to be 1.5%, typical for wood and other cellulosic materials (Tewarson chapter, *SFPE Handbook*).

---

[16] The fraction of the fire's total energy emitted as thermal radiation.

Figure E-1. Geometry of Cable Spreading Room

Notes:
1. Walls are made of Concrete.
2. Doors are made of Steel.
3. Smoke Detectors are at Ceiling Height.
4. Dimensions are in meters, 1 m = 3.28 ft.

Right Side View

Cable Tray (60 Total)
See Section A-A for Details
2.8 m x4
2.2 m x4

4.0 m
3.4 m x12
2.4 m x4
2.0 m
0.0 m

0.3 m   1.5 m   3.9 m   5.2 m   6.4 m   7.6 m   10.0 m   11.2 m   12.4 m   13.6 m   16.1 m   17.3 m

0.5 m   1.5 m   0.5 m Typ.   4.8 m   5.7 m   12.8 m   13.7 m   17.0 m   18.0 m

Supply Vent Duct
Return Vent Duct
Trash Can
(Fire Origin)

NOTE: Obstructions at ceiling height are removed from Top View and Isometric View for clarity.

See Right Side View and Sheet 2 for details.

Return Vent
Smoke Detector (x14)
Trash Can
Return Vent
Computer Room
Supply Vent
Supply Vent
Closed Door
Closed Door
Concrete Wall
Cable Tray

4.0 m x3   11.9 m x3   19.8 m x2   27.7 m   33.0 m   35.7 m x3   0.7 m

18.5 m
15.5 m x2
15.0 m x2
12.0 m
6.6 m
0.5 m Typ.
3.5 m x2
3.0 m x2
0.0 m

16.3 m
16.0 m
15.5 m x5
14.0 m
12.0 m
10.0 m
9.4 m x4
8.0 m
6.0 m
4.0 m
3.3 m x5
2.0 m

0.0   3.0   5.0   7.0   10.0 m x2   10.5 m x2   16.3   23.7   29.5 m x2   30.0 m x2   33.0   35.0   37.0   40.0

Ⓩ – Smoke Detector

1 m = 3.28 ft

———— Object
———— Hidden
———— Dimension

DRAWING	TITLE
5 -1	Cable Spreading Room

Transient Fire in Cable Spreading Room

Figure E-2. Photograph of typical Cable Spreading Room
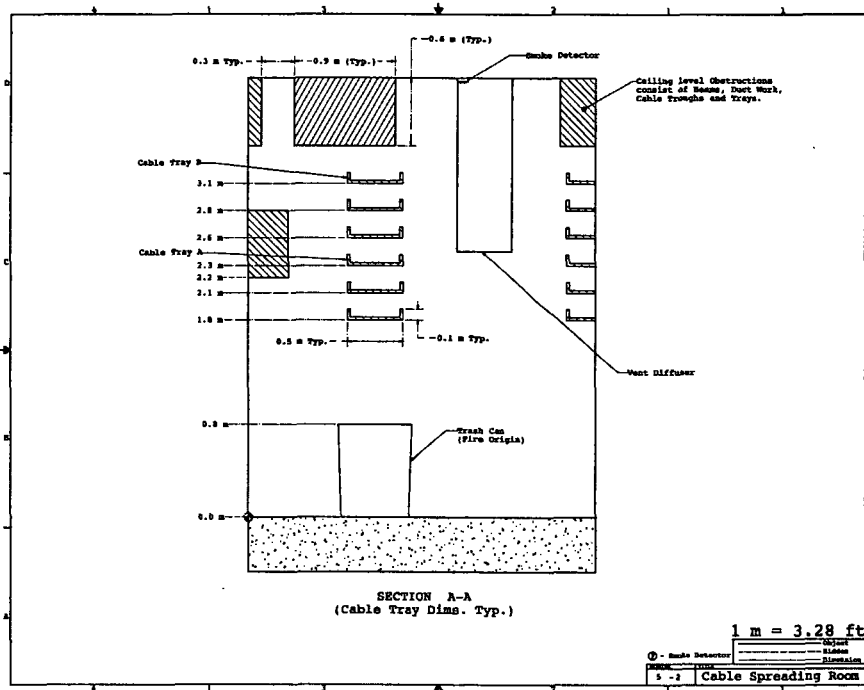
Figure E-3. Geometric detail of the Cable Spreading Room.

E.3 Selection and Evaluation of Fire Models

The fire scenario described above is a typical application of both zone models and CFD models. With a single fire contained within a rectangular compartment, the application is straightforward. Following is a discussion of further strengths and weaknesses of the available models.

Algebraic Models: FIVE and the FDT[s] both contain correlations to estimate the HGL temperatures within a closed, ventilated compartment; however, the FDT[s] do not allow the HRR to be input as a function of time. Since using the maximum HRR as a constant value will produce the highest HGL temperatures, these tools could be appropriate for screening scenarios. If necessary, additional analyses with a zone or CFD model may be appropriate.

Both algebraic models contain calculations to estimate smoke detector activation time.

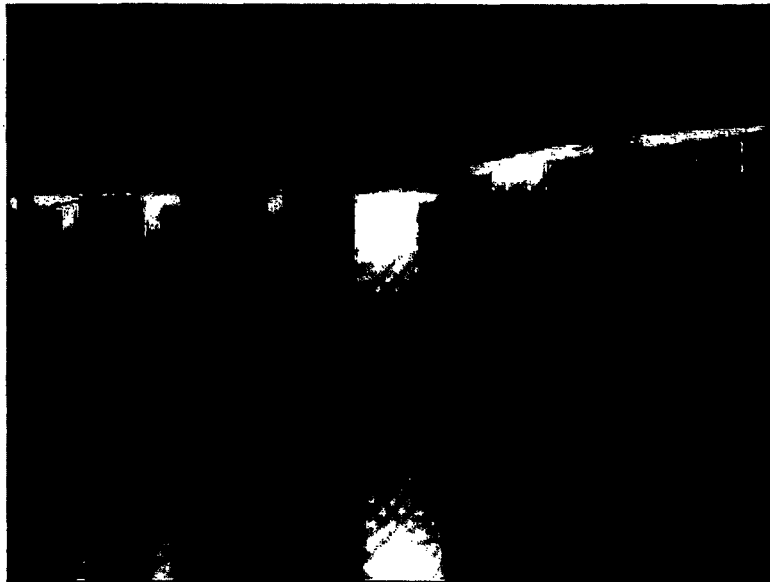FIVE and the FDT[s] also contain methods to estimate the heat flux from a fire to a target. The FIVE analysis uses Alpert's plume temperature correlations and Heskestad's flame height correlation, whereas the FDTs analysis uses only those of Heskestad to estimate the temperature to which the cables are exposed. Neither analysis included the effects of blockage due to the trays, nor the effect of thermal radiation from the Hot Gas Layer on the targets; thus, it is possible that the use of either of these models could lead to an underprediction of the heat flux.

Zone Models: The fire scenario outlined in the previous section falls within the range of applicability for a zone model. The simple compartment geometry of this scenario lends itself well to the application of zone models. Both CFAST and MAGIC include algorithms to estimate the temperature of cable targets.

In CFAST, target temperatures are calculated based on a one-dimensional heat transfer calculation that includes radiation from the fire, upper and lower gas layers, and bounding surfaces; convection from nearby gases; and conduction into the target. Radiation from the fire is modeled using a point source radiation calculation from the fire to the target.

In MAGIC, cable target temperatures are also calculated based on a one-dimensional heat transfer calculation that includes radiation exchanges between compartment surfaces, the upper and lower gas layers, and the nearby compartment fires; and convective heat transfer that involves targets heating up in the HGL, fire plume, and ceiling jet sub-layers. Each cable is divided into 20 cm (8 in.)-long segments, and the maximum surface temperature calculated on all the segments is the criterion to cable ignition (once the ignition temperature is reached, the reported surface temperature remains constant). Thus, the relative location of the cables to the flame, plume, ceiling jet or layers will affect the temperature calculation and the time to failure.

The relative position of the cabinet fire and cable trays may provide a challenge because the algorithms used by the zone models to assess target damage are based on a fire radiation point source.

For this analysis, the zone model CFAST is used.

CFD Models: This scenario is a fairly typical application of FDS. The model is applied here in much the same way that the zone models approach it, with the fire within the waste bin. The primary advantage of a CFD model for this fire scenario is that the CFD model can estimate

conditions at the specific location of the target cables, taking into account surrounding cable trays which may block radiation from the fire source. For this analysis, FDS results are included as a comparison to the zone model calculations.

Validation: NUREG-1824 (EPRI 1011999) contains experimental validation results for CFAST and FDS that are appropriate for this scenario. These experiments include ventilation effects and heat fluxes to and temperatures of various targets, particularly cables. Fire sizes in these experiments bound those used in this scenario. For CFAST, the Software Development and Model Evaluation Guide, NIST SP 1086 includes updated validation results for the newest version of the model used for this calculation. This includes all of the validation comparisons from NUREG-1824 (EPRI 1011999), plus additional comparisons for experiments not included in the NRC guide. Plume temperature calculations have been validated for a broad range of fire sizes and distances above the fire source in NIST SP 1086.

Table 2-5 of Volume 1 of NUREG-1824 (EPRI 1011999) lists various important model parameters and the ranges for which the validation study is applicable. Table E-1 below lists the values of these parameters for this fire scenario, along with their ranges of applicability.

Of these parameters, only the compartment aspect ratio is outside the range of tests included in NUREG 1824 (EPRI 1011999). In this scenario, the compartment width to height ratio is well within limits, but the length to height ratio is higher than those included in NUREG 1824 (EPRI 1011999). For a zone model, this "longer than typical" compartment is mainly a concern early in the fire development before a reasonably uniform layer has formed. Thus, prediction of events that occur early in the fire (such as smoke detection) may be expected to have a higher uncertainty if they are located distant from the fire source than those that occur later in the fire (such as ignition of cables above the initiating fire source) once the fire is more fully developed. For this scenario, smoke detectors are included throughout the compartment, but the primary ones of concern are those which would naturally respond faster, i.e., those nearest the fire.

Table E-1. Key parameters and their ranges of applicability to NUREG-1824.

Quantity	Normalized Parameter Calculation	Validation Range	In Range?
Fire Froude Number	$\dot{Q}^* = \dfrac{\dot{Q}}{\rho_\infty c_p T_\infty D^2 \sqrt{gD}} = \dfrac{130}{1.2 \times 1.012 \times 293 \times 0.82^2 \times \sqrt{9.8 \times 0.82}} = 0.5$	0.4 – 2.4	Yes
Flame Length, L_f, relative to the Ceiling Height, H	$\dfrac{L_f}{H} = \dfrac{2.6}{4.0} = 0.7$	0.2 – 1.0	Yes
Ceiling Jet Radial Distance, r_{cj}, relative to the Ceiling Height, H	N/A – Ceiling jet targets are not included in simulation.	1.2 – 1.7	N/A
Equivalence Ratio, φ, as an indicator of the Ventilation Rate	$\varphi = \dfrac{\dot{m}_F/\dot{m}_{O_2}}{r} \equiv \dfrac{\dot{Q}}{r\,\Delta H\,\dot{m}_{O_2}} = \dfrac{317}{13{,}100 \times 0.4} = 0.06$ $\dot{m}_{O_2} = 0.23\,\rho_\infty \dot{V} = 0.23 \times 1.2 \times 1.42 = 0.4$	0.04 – 0.6	Yes
Compartment Aspect Ratio	$\dfrac{L}{H} = \dfrac{40}{4.0} = 10$ $\dfrac{W}{H} = \dfrac{18.5}{4.0} = 4.6$	0.6 – 5.7	No
Target Distance, r, relative to the Fire Diameter, D	$\dfrac{r}{D} = \dfrac{2.3}{0.82} = 2.8$	2.2 – 5.7	Yes

E.4 Estimation of Fire-Generated Conditions

This section provides details specific to each model.

E.4.1 Zone Model (CFAST)

General: In CFAST, the cable spreading room is modeled as a single compartment with obstructions accounted for by modifying the cross-sectional area of the compartment as a function of height, as described in the geometry section below. Figure E-4 shows the scenario as modeled by CFAST.
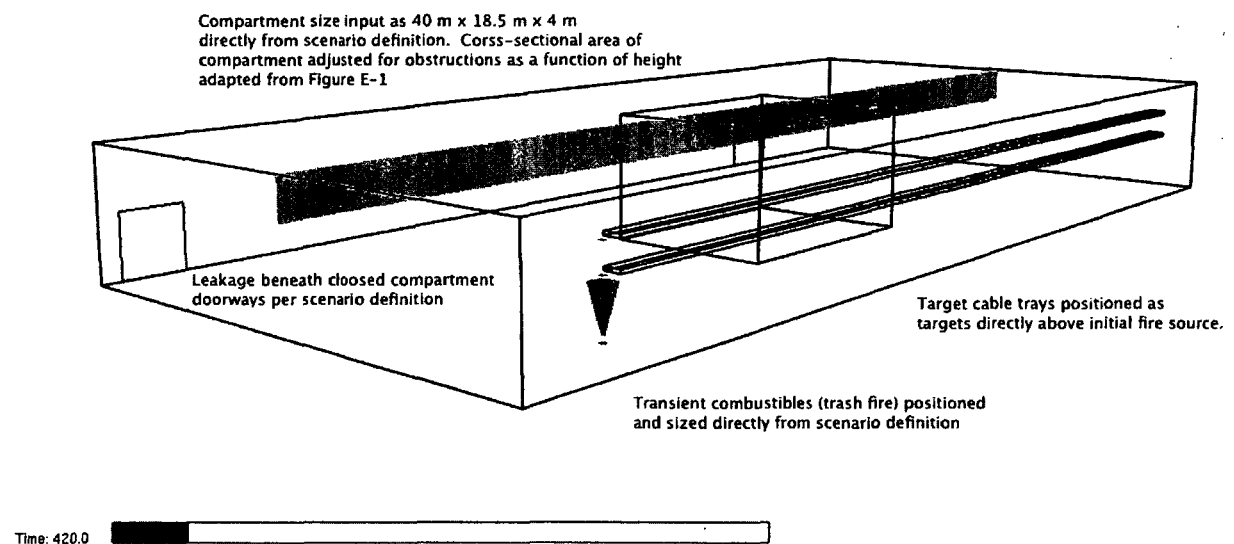
Figure E-4. CFAST rendering of the Cable Spreading Room scenario.

Geometry: Since zone models are concerned with volumes and not physical length and width, the volume of the computer compartment, as well as the numerous cable trays, ductwork, and beams, was modeled in CFAST with a cross-sectional area that varies with height. Table E-2 shows the cross-sectional area as a function of height calculated from the compartment geometry shown in Figure E-1.

Table E-2. Cross-sectional area as a function of height used for CFAST calculation

	Height (m)	Area (m²)
Floor Level	0	700.04
Bottom of Cable Trays	1.8	571.44
Bottom of Obstructions	2.2	411.44
HVAC Ductwork	2.4	410.44
Top of Obstructions	2.8	570.44
Top of Cable Trays	3.2	699.04
Ceiling Level Obstructions	3.6	267.04
Ceiling Level	4	267.04

Fire: The specified fire was input directly into CFAST. To determine the duration of the fire, the total energy of the fuel is calculated: (5 kg)×(20,000 kJ/kg) = 100,000 kJ. Conversely, the total heat release can be determined by integrating the HRR curve over time as:

$$Q = \int_0^{480} \alpha t^2 dt + \int_{480}^{t_f} 317 dt = \frac{1}{3}\alpha 480^3 + 317(t_f - 480)$$ (E-1)

where $\alpha = 317/480^2$ for a t-squared fire that grows to 317 kW in 480 s, as specified in the scenario definition. Solving for t_f yields a total burning time of 635 s. The combustibles are estimated to fill about half the volume of the waste bin (roughly consistent with the test data in Appendix G of NUREG-6850 (EPRI 1011989)).

Materials: The material properties listed above were used for the zone models.

Cables: In CFAST, target temperatures are calculated based on a one-dimensional cylindrical heat transfer calculation based on the material properties and cable diameter, as specified in the scenario description. To account for the shielding of the cables on the lower surface of the cable tray, the CFAST input for the normal vector from the cable surface is directed upwards. This effectively shields the cables from the fire below while exposing them to the surrounding gas temperature for convection and to the hot upper gas layer for radiation.

Ventilation: The supply and return air flow rates are input directly into CFAST. Upon smoke detector activation, mechanical ventilation fans stop and dampers are closed. Therefore, before a stop time for the fans could be specified, the time to smoke detector activation was needed. This requires that CFAST be run with the fans on for the entire time to find the first smoke detector activation. The model is then re-run using the smoke detector activation time as the fan-stop time.

Fire Detection: Although there are multiple smoke detectors in the space, it was assumed that the closest detector is the only one that needs to be modeled to determine time to detection. The basis for this assumption is that the nearest detector will be exposed to the greatest concentration of smoke products and the highest gas temperatures leading to the earliest response. There are no geometric or ventilation features that would prevent this from being the case in the example consider. In CFAST, there is no direct way of calculating smoke density for smoke detector activation; instead the smoke detector is modeled as a sprinkler with a low activation temperature and RTI. An activation temperature of 30 °C (86 °F) and an RTI of 5 $(m/s)^{1/2}$ were used for this scenario.

E.4.2 CFD Model (FDS)

General: This scenario is notable because it includes a considerable amount of "clutter," that is, the space has a relatively large number of obstructions. Figure E-5 illustrates the FDS simulation with all the blockages. Because the cable trays are regularly spaced in both the horizontal and vertical directions, it is easy in FDS to simply replicate a single tray as many times as necessary. Another interesting feature of the scenario is the automatic shutdown of the ventilation system at the time of any smoke detector activation. FDS models this by associating the creation or removal of obstructions or the activation/deactivation of a vent with actions taken by any number of fire protection devices.
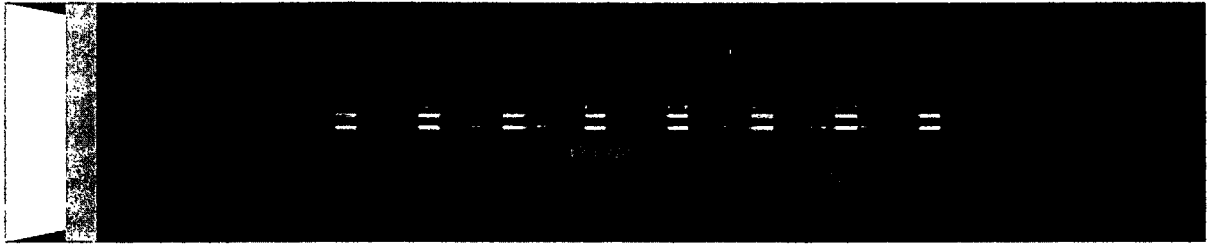
Figure E-5. FDS/Smokeview rendering of the Cable Spreading Room scenario.

Geometry: The interior of the compartment is modeled, and all obstructions have been included. To get increased resolution in the area of interest, multiple meshes are used. The finest mesh has a 10 cm (4 in) resolution and spans a volume surrounding the trash can, which is 6 m (20 ft) long, 3 m wide (10 ft), and 4 m (13 ft) high. Coarse meshes cover the remainder of the compartment and adjacent hallway with cells of 20 cm (8 in). Because the objective of the calculation is to estimate time to failure for cables within stacked trays, it is important to have at least 10 cm (4 in) resolution, the typical dimension of the rails of conventional cable trays.

Fire: The trash can is modeled with a square, rather than round, cross-section with an equivalent area to the round cross-section and a height equal to the height of the trash can. The local flow features about the fire are not a significant aspect capable of affecting the outcome of this example calculation; thus the transformed square geometry is appropriate for this application. The specified HRR is applied to the top of trash can. The duration of the fire is 635 s, as was computed for the zone model input. There is no need to model the interior of the can.

Materials: The thermal properties of the walls are applied directly as specified.

Cables: The primary objective of the calculation is to estimate the potential damage to the cables within the trays. FDS is limited to only 1-D heat transfer into either a rectangular or cylindrical obstruction. In this simulation, the cables are modeled as 1.5 cm (0.6 in) cylinders with uniform thermal properties, given above. Following the Thermally-Induced Electrical Failure (THIEF) methodology in NUREG/CR-6931, Vol. 3, electrical functionality is lost when the temperature just inside the jacket of a thermoplastic cable reaches 205°C (400°F). Note that no attempt is made in the simulation to estimate ignition and spread of the fire over the cables. The THIEF methodology does not account for the effects of bundled cables, which may reduce the overall heat-up of a single cable.

Detection: FDS has a smoke detection algorithm that predicts the smoke obscuration within the detection chamber based on the smoke concentration and air velocity in the grid cell in which the detector is located. The detector itself is not modeled, as it is merely a point within the computational domain. The two parameters needed for the model are the obscuration at alarm, which is given by the manufacturer, and an empirically determined length scale from which a smoke entry time lag is estimated from the outside air velocity. The *SFPE Handbook, 4th Edition,* provides a nominal value of 1.8 m (5.9 ft) for this length scale. The obscuration at alarm is 4.9%/m, a typical sensitivity for smoke detectors.

Ventilation: The supply and return air flow rates are input directly into FDS. The ducts are represented by rectangular obstructions with thin plates just below (one grid cell) the vent itself to represent the diffusing effect of the grill. The resolution of the grid is not fine enough to capture this effect directly. FDS is capable of stopping the ventilation system upon the activation of any smoke detector.

E.5 Evaluation of Results

The purpose of the calculations described above is to estimate smoke detector activation times and potential cable damage from a trash can fire in the Cable Spreading Room. The compartment itself is relatively large, and the relatively small fire (317 kW) does not substantially heat it up. Figure E-6 shows the heat release rate and estimated HGL temperature. Differences between the two models likely result from FDS's ability to locally account for all the blockages in the room. HGL temperature in CFAST is a spatially average value intended to represent the bulk conditions throughout the compartment, while the FDS values are a calculation based on a single vertical profile of temperature at a fixed location within the room (in this scenario placed several meters away from the fire location to eliminate local effects of the fire plume on the temperature profile).
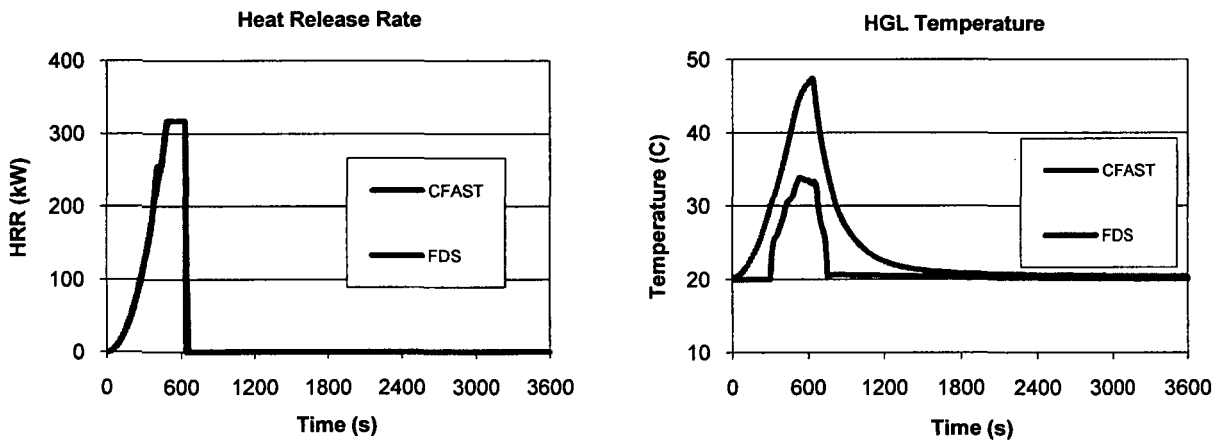
Figure E-6. Heat release rate and estimated HGL temperature for Cable Spreading Room scenario

The analysis below shows that a 317 kW waste bin fire beneath a vertical array of cable trays is unlikely to damage cables in the trays three and six levels above the fire. Both CFAST and FDS estimate peak temperatures well below 100 °C (212 °F) for cables in the third tray from the bottom. Estimated temperatures on the lowest cable tray peak at 125 °C (257 °F), still well below the ignition temperature of the cables. This is discussed in more detail below.

Because of the uncertainty in the smoke detector activation prediction of all the models and the uncertainty associated with the possible ignition of cables in the trays just above the fire, it is difficult to predict whether or not the CO_2 suppression system would be activated in time to prevent possible cable ignition. No validation results are available that address time to detector activation. Thus, the analysis makes the conservative assumption that the suppression system does not activate.

Transient Fire in Cable Spreading Room

E.5.1 Smoke Detection

Table E-3 shows the results for smoke detection activation for the models. CFAST models smoke detector actuation as a heat detector with a relatively low thermal inertia and activation temperature. However, there is no consensus in the fire literature for the appropriate RTI (Response Time Index) value and activation temperature. Given the presence of beam pockets and obstructions, even a CFD model like FDS, which uses actual smoke concentration rather than temperature in its detector algorithm, is subject to significant uncertainty.

Table E-3. Smoke detector activation times, Cable Spreading Room.

Model	Time (s)
CFAST	170 s
FDS	120 s

E.5.2 Cable Damage

Figure E-7 shows the estimated impact of the fire on the cable trays above the fire. The bottom cable is located at least 1 m (3.3 ft) above the base of the waste bin fire. With an estimated flame height of 1.7 m (5.7 ft), ignition may occur from flame impingement; however, since the bottom tray is protected by a solid metal lower surface and the heat flux to the bottom cable tray is estimated to be about 4.1 kW/m^2 (well below the critical value of 11 kW/m^2), this is unlikely.

E.5.3 Uncertainty

In this scenario, the objective of the calculations is to predict the impact of a waste bin fire on safe-shutdown cables located in cable trays directly above the fire by comparing calculated values of temperature and heat flux near the cables with critical values. In addition, calculations of smoke detector activation and flame height of the fire are also estimated. While it is estimated that none of the predicted values exceed established critical values, the uncertainty of the model calculations needs to be examined to better understand how close the predictions are to critical values.

For example, in the NRC/EPRI V&V study (NUREG-1824 (EPRI 1011999)), it was found that predictions of target heat flux are, on average, 18% lower for CFAST than corresponding measurements, and the relative standard deviation of its predictions of this average value is 47%. This suggests that the true value of the peak cable heat flux in this scenario is normally distributed with a mean of 5.1 kW/m^2 and a standard deviation of 2.4 kW/m^2. Therefore, the probability that the cable temperature would exceed 11 kW/m^2 is:

$$P(Q > 11) = \frac{1}{2}\,\text{erfc}\left(\frac{11 - 5.1}{2.4\sqrt{2}}\right) \cong 0.008 \qquad \text{(E-2)}$$

In other words, there is a less than 1% chance of exceeding the flux threshold for the lowest cable tray according to the CFAST prediction. The FDS predictions estimate temperatures even lower than CFAST.

For the upper cables, the predicted temperature and heat flux by CFAST are somewhat higher than FDS because CFAST does not account for the fact that the cable trays of interest are shielded by trays below or that the burning spreads outward from the ignition point. In any

E-12

event, neither model predicts that the upper cables will come anywhere close to the damage criteria.

Transient Fire in Cable Spreading Room

Bottom CableTemperature

Flame Height

Cable A Temperature

Cable A Heat Flux
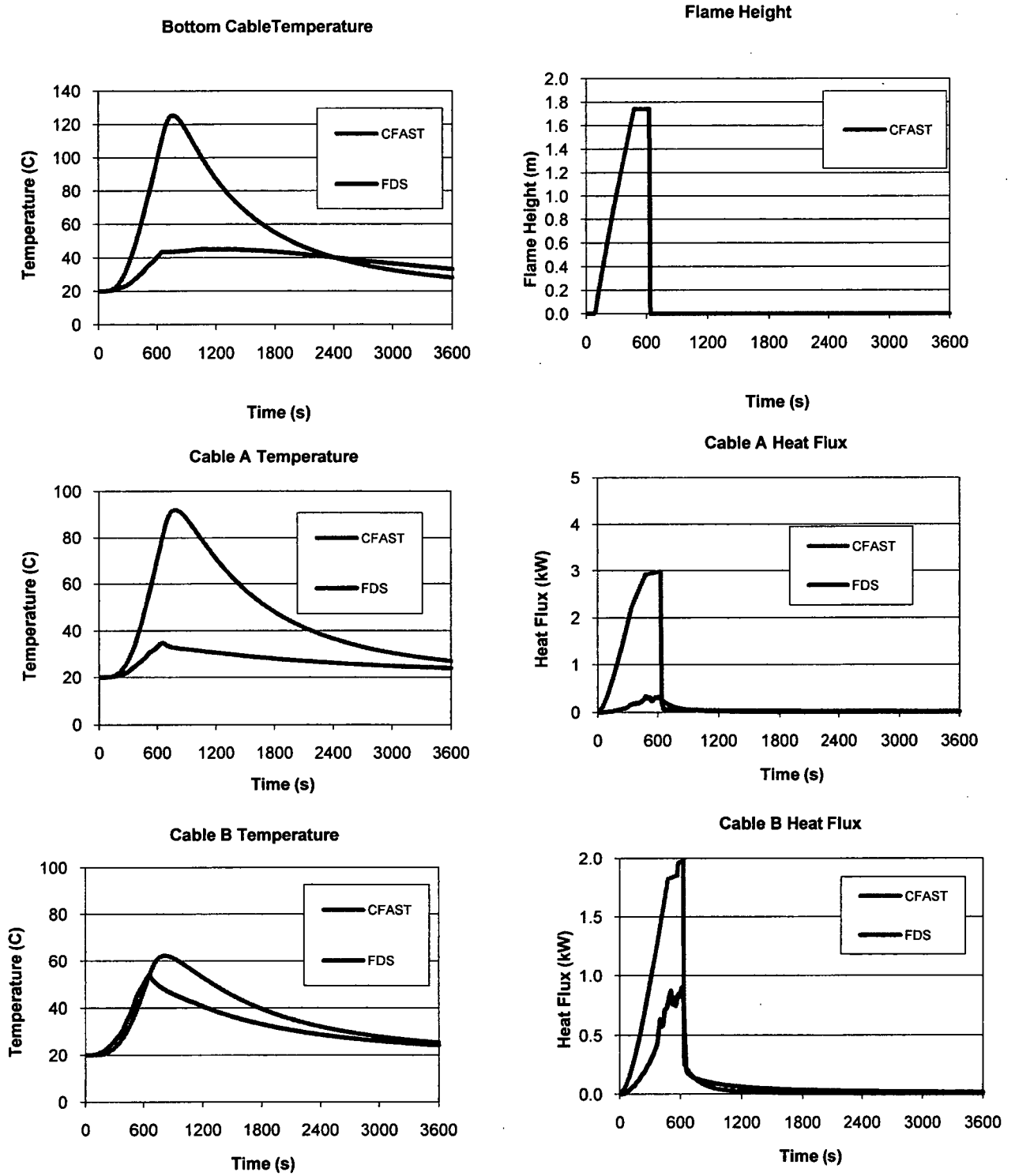

Cable B Temperature

Cable B Heat Flux

Figure E-7. Estimated cable conditions for the Cable Spreading Room.

It should also be noted that these damage criteria are intended to indicate electrical failure, but are routinely assumed to also apply as ignition criteria. In newer studies in NUREG/CR-7010, cable ignition was not observed at fluxes below 25 kW/m^2, and most often only with direct flame impingement. Handbook values for minimum ignition flux for power and communication cables are reported in the range of 15 kW/m^2 to 35 kW/m^2 (SFPE Handbook, Table 3-4.2).

Table E-4 lists the probability of exceeding the critical temperature and heat flux for all the model calculations.

Table E-4. Uncertainty analysis of the model predictions of the CSR scenario

Quantity	Location	Model	Predicted Value	Critical Value	Probability of Exceeding
Temperature	Bottom Cable	CFAST	125 °C	330 °C	0.000
		FDS	45 °C	330 °C	0.000
	Cable A	CFAST	92 °C	330 °C	0.000
		FDS	35 °C	330 °C	0.000
	Cable B	CFAST	62 °C	330 °C	0.000
		FDS	53 °C	330 °C	0.000
Heat Flux	Bottom Cable	CFAST	4.17 kW/m^2	11 kW/m^2	0.008
		FDS	--	11 kW/m^2	
	Cable A	CFAST	2.97 kW/m^2	11 kW/m^2	0.000
		FDS	0.33 kW/m^2	11 kW/m^2	0.000
	Cable B	CFAST	1.98 kW/m^2	11 kW/m^2	0.000
		FDS	0.90 kW/m^2	11 kW/m^2	0.000

E.5.4 Sensitivity

Referring again to Table E-4, it is clear that the cables directly above the waste bin fire would not be damaged by a 317 kW fire. In addition to examining the accuracy of the models as is done in the previous section, it is also possible to estimate how large a fire would be required to damage the cables. Table 4-3 indicates that the heat flux is proportional to the HRR to the 4/3 power. Following the methodology in Section 4.4.1, in order to increase the predicted heat flux by 6 kW/m^2 to reach 11 kW/m^2, the peak HRR, $\dot{Q}$, must increase by approximately:

$$\Delta \dot{Q} \approx \frac{3}{4}\dot{Q}\frac{\Delta \dot{q}''}{\dot{q}''} = \frac{3}{4}317\frac{6}{5} \approx 285 \text{ kW} \qquad \text{(E-3)}$$

In other words, the peak HRR of the fire would have to be approximately 317+285=602 kW to cause the cables in the bottom cable tray B to fail.

E.6 Conclusion

The analysis shows that a 330 kW waste bin fire beneath a vertical array of cable trays is unlikely to damage cables in the trays three and six levels above the fire. Both CFAST and FDS estimate peak temperatures well below 100 °C (212 °F) for cables in the third tray from the bottom. Estimated temperatures on the lowest cable tray peak at 125 °C (257 °F), still well below the ignition temperature of the cables.

E.7 References

1. NUREG-1805, *Fire Dynamics Tools.*
2. NUREG/CR-6850 (EPRI 1011989), *Fire PRA Methodology for Nuclear Power Facilities.*
3. NUREG-1824 (EPRI 1011999), *Verification and Validation of Selected Fire Models for Nuclear Power Plant Applications,* 2007.
4. *SFPE Handbook of Fire Protection Engineering,* 4th edition, 2008.
5. NUREG/CR-4680, *Heat and Mass Release Rate for Some Transient Fuel Source Fires: A Test Report*
6. NUREG/CR-6931, *Cable Response to Live Fire (CAROLFIRE) Volume 3: Thermally-Induced Electrical Failure (THIEF) Model.*
7. UL 217, Underwriters Laboratories, Inc., Single Station Fire Alarm Device.
8. *SFPE Engineering Guide to the Evaluation of the Computer Model DETACT-QS*
9. NIST SP 1086, *Consolidated Model of Fire Growth and Smoke Transport, CFAST (Version 6), Software Development and Model Evaluation Guide*
10. NIST SP 1018-5, *Fire Dynamics Simulator (Version 5), Technical Reference Guide, Vol. 3, Experimental Validation.*
11. Gay, L., C. Epiard, and B. Gautier, "MAGIC Software Version 4.1.1: Mathematical Model," EdF HI82/04/024/B, Electricité de France, France, November 2005.

E.8 Attachments

1. FDS input files: Cable_Spreading_Room.fds

2. CFAST input files:

   a. Trash Fire In Cable Spreading Room.in
   b. Trainsient Combustibles.o
   c. Trash Fire.o
   d. Thermal.csv

F
Lubricating Oil Fire in a Turbine Building

F.1 Modeling Objective

The calculations described in this appendix estimate the effects of a large lubricating oil fire in a Turbine Building on unprotected structural steel. This type of analysis may arise when addressing ASME/ANS RA-Sa-2009 supporting requirement FSS-F01 in a Fire Probabilistic Risk Assessment (FPRA), which requires the consideration of fire scenarios that expose structural steel. The typical scenario considered for this requirement is a catastrophic failure of the turbine itself, which would result in a large lubricating oil spill fire. The purpose of this hypothetical example is to evaluate the Turbine Building structural steel response for two potential curb locations in the Turbine Building. The calculation will provide information for a decision on the hazard posed to the structural steel for each potential fire location, thus serving as part of the basis for a plant modification.

F.2 Description of the Fire Scenario

General Description: The Turbine Building is a large structure that is approximately 100.3 m (329 ft) by 99.5 m (326 ft) by 21 m (69 ft) tall, as shown in Figure F-1. The ambient temperature in the Turbine Building is 36 °C (95 °F), which is the same temperature as the surrounding external areas. The Turbine Building often contains multiple levels; however, for this example the structure will be evaluated using two primary levels, the lower levels (collectively) and the main turbine deck. The lowest portion of the lower level floor is about 1.2 m (4 ft) below grade in the area near the fire, but most of the lower level floor elevation is at the 0 m (0 ft) elevation. The ceiling height is about 4.6 m (15 ft) above grade. The floor of the turbine deck is at the 5.6 m (18 ft) elevation, and the ceiling is at the 19.8 m elevation. The turbine deck has a somewhat smaller plan than the lower level, approximately 90 m (295 ft) by 70 m (230 ft). The building contains the turbine generators (See Figure F-1) and a Heating, Ventilation, and Air Conditioning (HVAC) room. Each turbine generator contains about 3,000 L (800 gal) in a single reservoir volume. The lubricant oil is dominated by alkanes, which have a chemical formula of C_nH_{2n+2} with n ranging from twelve to fifteen (centered about fourteen) and a soot yield of 0.1 kg soot/kg fuel consumed. The proposed curbed area is 6.1 m (20 ft) by 4.6 m (15 ft). Based on the current use of the area, the plant has identified two locations on the lower level where the curbing could be installed. The position of Curb Location 1 is as shown in Figure F-1. The south edge of Curb Location 2 is 26 m (85.3 ft) north of the south wall, and the east edge of Curb Location 2 is 21.1 m (69.2 ft) east of the west Turbine Building wall. The curbed areas will be designed to contain the entire lubricant volume from a turbine generator, or 3,000 L of lubricant.

There are forty unprotected steel support columns in a rectangular configuration (four rows of ten each) around the lube oil tank. Figure F-3 shows a typical unprotected steel column. The columns are all W14X145 standard wide flange members, as shown in Detail A of Figure F-1 (American Institute of Steel Construction [AISC], 2006). Six columns in particular are evaluated in detail and are denoted in Figure F-1 as A, B, C, D, E, and F. A plant structural analysis has revealed that the loss of any of these six columns could lead to partial collapse of the Turbine Building, which is considered an unacceptable consequence by the plant.

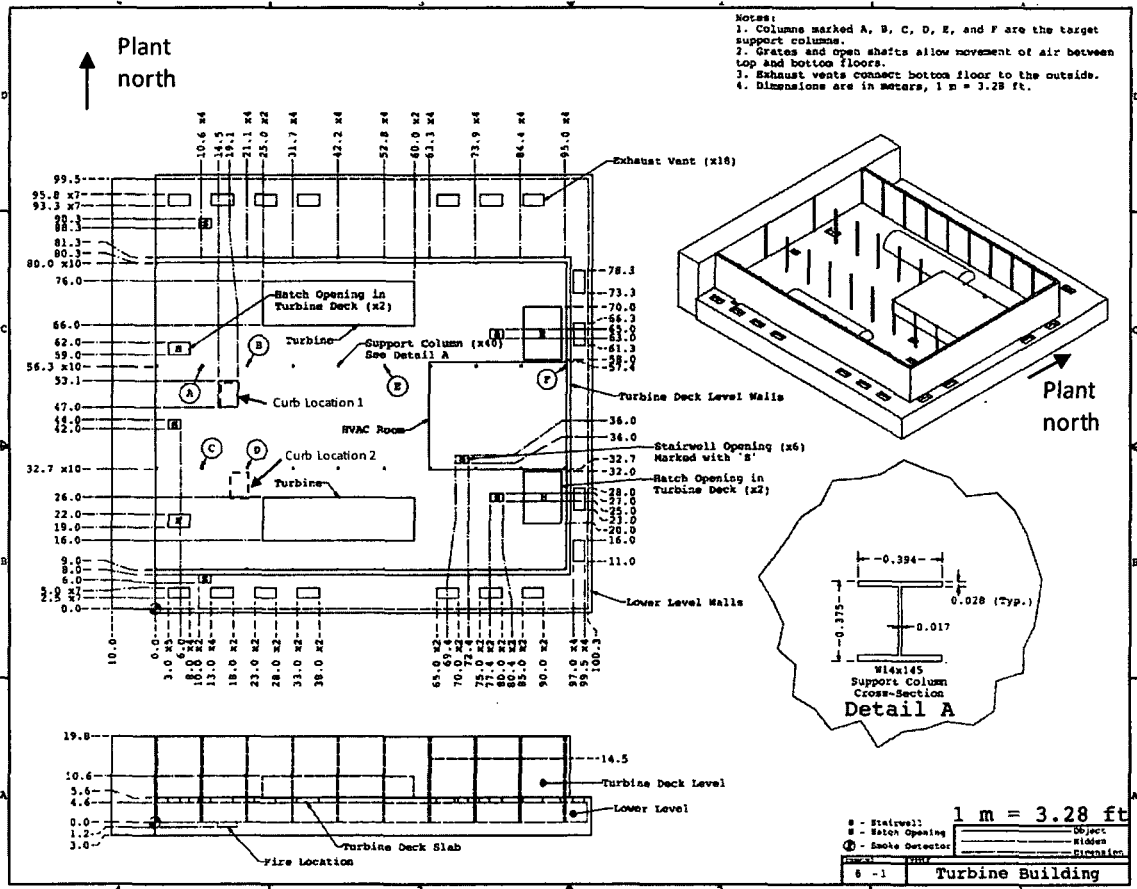**Figure F-1. Geometry of the Turbine Building.**

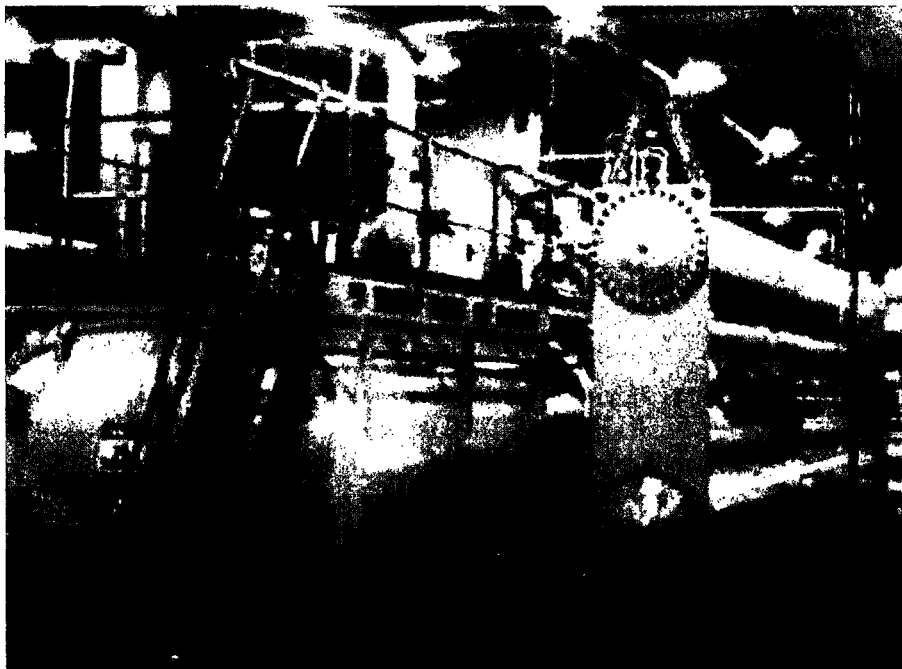**Figure F-2. Structural Steel Column in the Turbine Building.**

Figure F-3. Main Turbine Lubricating Oil Tanks in the Turbine Building.

Lubricating Oil Fire in a Turbine Building

Geometry: A plan and side view of the Turbine Building are shown in Figure F-1. The area of interest involves the two levels shown in Figure F-1, which are separated by a concrete slab. There are several stairwell, hatch, and exhaust vent penetrations throughout the slab. These penetrations are identified in Figure F-1 with the "H" symbol for a hatch and the "S" symbol for a stairwell.

Construction: The turbine deck is made of 1 m (3.3 ft) thick normal weight concrete having a density of 2,400 kg/m ^{3}). The floor and walls of the lower level are constructed of 0.3 m (1 ft) thick normal weight concrete. Numerous areas and landings in the Turbine Building are made of metal grating. The floor in the area of the lube oil tank is 1 m thick normal weight concrete. The walls and ceiling of the upper level of the Turbine Building are made of 3 mm (0.12 in) thick corrugated steel. The structural columns, steel grating, and corrugated steel are fabricated from steel containing 0.5 percent carbon.

Materials: Nominal values for the thermal properties of the normal weight concrete and steel are listed in Table F-1 (NUREG-1805, Table 2-3). The damage criteria for the structural steel are based on the acceptance criteria for an ASTM E119 (ASTM E119-10a, 2010) test and are listed in Table F-2.

Table F-1. Material Properties of Concrete and Steel in the Turbine Building

Material	Thermal Conductivity k (W/m-K)	Density ρ (kg/m³)	Specific Heat cₚ (kJ/kg-K)
Normal weight concrete	1.6	2,400	0.75
Steel (0.5% carbon)	54	7,850	0.465

Table F-2. Structural Steel Failure Criteria (ASTM E119-10a)

Member	Maximum Cross-Section Temperature (°C)	Maximum Cross-Section Average Temperature (°C)
Beam	704	593
Column	649	538

Detection System: There is no safety-related equipment in this Turbine Building, and, as such, there are no detection systems or sprinklers in the Turbine Building that are credited for this analysis. If Turbine Building underdeck sprinklers were installed, such features may be ignored when considering the potential for worst-case structural failure and the possible need for passive structural fire protection. In addition, demonstrating the suppression effectiveness for large hydrocarbon spill fires would be a significant aspect of the evaluation, but is not treated analytically with the fire modeling tools considered in this guide.

Ventilation: The Turbine Building is an open area configuration with all forced ventilation intentionally shut down at the start of the fire for reasons unrelated to the fire. There are

eighteen exhaust vents to the outside around the perimeter of the turbine deck level. There are no other internal or external openings beyond than those already noted and shown in Figure F-1.

Fire: A large, confined lubricant spill fire involving 3,000 L is postulated on the lower level. The lubricant has been preheated prior to the spill such that the growth rate of the fire would be short compared to the total time required to burn the spill volume. The total spill area is equal to 27.9 m² (300 ft²), as shown in Figure F-1, and the spill depth is thus 0.1 m (0.33 ft).

The key fuel properties for the lubricant oil are summarized in Table F-3 (NUREG-1805, Tables 3-2 and 3-4). The properties listed in NUREG-1805 actually correspond to transformer oil, but it is asserted in Table 2-6 of NUREG-1805 (2005) that the fuels are similar, and it is reasonable to use the fuel properties for transformer oil when dealing with lubricant oil.

Table F-3. Lubricant Fuel Properties (NUREG 1805, 2005)

Density, ρ (kg/m³)	Heat of combustion ΔH_c (kJ/kg)	Burning rate $\dot{m}''$ (kg/s-m²)	Empirical constant $k\beta$ (m⁻¹)
760	46,400	0.039	0.7

The peak heat release rate is computed from the plan area, the heat of combustion, and the burning rate:

$$\dot{Q}_p = \dot{m}'' \Delta H_c A \qquad \text{(F–1)}$$

which results in a peak heat release rate of 50.3 MW. The fire duration is determined using the volume, density, and burning rate:

$$\Delta t = \frac{M}{\dot{m}'' A} = \frac{V\rho}{\dot{m}'' A} \qquad \text{(F–2)}$$

which results in a fire duration of about 35 minutes.

Initial and Ambient Conditions: The ambient temperature both inside and outside the Turbine Building is 36 °C (95 °F), as noted in the General Description. The corresponding ambient density is density is 1.2 kg/m³ and the corresponding ambient air heat capacity is 1.0 kJ/kg-K, per Table B.2 in the SFPE Fire Protection Handbook (2008).

F.3 Selection and Evaluation of Fire Models

Following is a discussion of further strengths and weaknesses of the available models.

Algebraic Models: FIVE (EPRI 1002981, 2002) and the FDT^s (NUREG 1805, 2005) both contain correlations for estimating the Hot Gas Layer temperatures within a closed, ventilated compartment, the heat flux at fixed distance from the exposure fire, and the flame height, all of

Lubricating Oil Fire in a Turbine Building

which play a role to some extent in this scenario. FDT^s also contains algebraic models for predicting the fire resistance of unprotected structural steel; however, the exposure profile is limited to the ASTM E119 Standard Time-Temperature curve and is thus not applicable to this scenario.

A simple calculation of the flame height using FDT^s spreadsheet

03_HRR_Flame_Height_Burning_Duration_Calculations.xls

indicates that the predicted flame height is about 11.7 m (38 ft), which is significantly greater than the maximum ceiling height of 5.8 m (19 ft) in the area of the fuel spill. This suggests that the radiant heat flux models (point source and solid flame) would not be representative of the actual exposure conditions. The heat flux predictions using these models could be in significant error and consequently are not recommended for this application.

The geometry is also not readily modeled using the empirical Hot Gas Layer model because of the large number of horizontal vents and the large volume and boundary surface area. These models are thus not recommended for this configuration.

Zone Models: This is a particularly challenging simulation for a zone fire model, with very large compartments and numerous connections between the compartments and to the outside. With such large compartment sizes, local variations in temperatures can be expected within the lower compartment that contains the fire source. In addition, because the flame height is predicted to be greater than the ceiling height, the radiant heat flux calculations may not be representative of the conditions that would arise from the postulated fire. Results of calculations that depend on the uniform gas layer assumption inherent in all zone fire models should be evaluated with care.

In CFAST, target temperatures are calculated based on a one-dimensional heat transfer calculation that includes radiation from the fire, upper and lower gas layers, and bounding surfaces; convection from nearby gases; and conduction into the target. Radiation from the fire is calculated using a point source radiation calculation from the fire to the target.

For this analysis, the zone model CFAST is used (NIST SP 1086, 2009).

CFD Models: This scenario is challenging because it involves a very large fire in a very large space; however, the fact that the objective of the calculation is to estimate the temperature increase of steel columns that are not located within the fire itself makes it less subject to error. Predicting the heat flux to a column engulfed in fire is more difficult because it requires details of the fuel and exhaust products, including soot, within the flame region.

For this analysis, the CFD model FDS is used (NIST SP 1018-5, 2010).

Validation: The principal source of validation data justifying the use of the above-listed fire models for this scenario is the NRC/EPRI V&V study documented in NUREG-1824 (EPRI 1011999). Table 2 in Volume 1 of NUREG-1824 (EPRI 1011999) and Section 2 of this guide lists the various important model parameters and the ranges for which the validation study is applicable. Table F-4 provides a summary of the normalized parameter calculations for the Turbine Building fire scenario. In some cases, the one- and two-compartment representations yield different values, and are shown accordingly in Table F-4. Additionally, the normalized target distance to fire diameter is provided for each of the six columns.

The calculation of the equivalence ratio is not straightforward with the equations provided because of the vertical flow paths. The value listed in Table F-4 was determined from the single compartment geometry in which the horizontal vents are represented as vertical vents of equal area; as such, this value is only indicative. Nonetheless, it falls well within the validation range, and it is expected that there is adequate ventilation available, such that the equivalence ratio will be less than one.

Lubricating Oil Fire in a Turbine Building

Table F-4. Normalized Parameter Calculations for the Turbine Building Fire Scenario.

Quantity	Normalized Parameter Calculation	Validation Range	In Range?
Fire Froude Number	$$\dot{Q}^* = \frac{\dot{Q}}{\rho_\infty c_p T_\infty D^2 \sqrt{gD}} = \frac{50300}{1.2 \times 1.012 \times 293 \times 5.98^2 \times \sqrt{9.8 \times 5.98}} \cong 0.51$$	$0.4 - 2.4$	Yes
Flame length to ceiling height ratio (single enclosure model)	$$\frac{L_f}{H} = \frac{10.9}{18.8} \cong 0.58$$ $$L_f = D\left(3.7\, \dot{Q}^{*2/5} - 1.02\right) = 1.87\,(3.7 \times 0.51^{0.4} - 1.02) \cong 10.9$$	$0.2 - 1.0$	Yes
Flame length to ceiling height ratio (two enclosure model)	$$\frac{L_f}{H} = \frac{10.9}{4.6} \cong 2.4$$ $$L_f = D\left(3.7\, \dot{Q}^{*2/5} - 1.02\right) = 1.87\,(3.7 \times 0.51^{0.4} - 1.02) \cong 10.9$$	$0.2 - 1.0$	No
Ceiling jet radial distance, r_{cj}, relative to the ceiling height, H	N/A	$1.2 - 1.7$	N/A
Equivalence ratio as an indicator of the ventilation rate	N/A	$0.04 - 0.6$	N/A
Equivalence ratio as an indicator of the opening ventilation	$$\varphi = \frac{\dot{m}_F/\dot{m}_{O_2}}{r} \equiv \frac{\dot{Q}}{r\,\Delta H\,\dot{m}_{O_2}} = \frac{50300}{13{,}100 \times 14.9} \cong 0.99$$ $$\dot{m}_{O_2} = 0.23 \cdot 0.5 A_o\sqrt{h_o} = 0.23 \times 0.5 \times 113\sqrt{1.3} \cong 14.9$$	$0.04 - 0.6$	Yes

Quantity	Normalized Parameter Calculation	Validation Range	In Range?
Compartment aspect ratios (single enclosure model)	$\dfrac{L}{H} = \dfrac{86.6}{18.8} \cong 4.64$ $\dfrac{W}{H} = \dfrac{87.3}{18.8} \cong 4.64$	0.6 – 5.7	Yes
Compartment aspect ratios (two-enclosure model)	$\dfrac{L}{H} = \dfrac{100.3}{4.6} \cong 21.8$ $\dfrac{W}{H} = \dfrac{99.5}{4.6} \cong 21.6$	0.6 – 5.7	No
CURB LOCATION 1			
Target distance to fire diameter ratio (Column A)	$\dfrac{r}{D} = \dfrac{8.5}{5.98} \cong 1.42$	2.2 – 5.7	No
Target distance to fire diameter ratio (Column B)	$\dfrac{r}{D} = \dfrac{7.22}{5.98} \cong 1.21$	2.2 – 5.7	No
Target distance to fire diameter ratio (Column C)	$\dfrac{r}{D} = \dfrac{18.8}{5.98} \cong 3.15$	2.2 – 5.7	Yes
Target distance to fire diameter ratio (Column D)	$\dfrac{r}{D} = \dfrac{18.3}{5.98} \cong 3.06$	2.2 – 5.7	Yes

Lubricating Oil Fire in a Turbine Building

Quantity	Normalized Parameter Calculation	Validation Range	In Range?
Target distance to fire diameter ratio (Column E)	$\dfrac{r}{D} = \dfrac{36.5}{5.98} \cong 6.1$	2.2 – 5.7	No
Target distance to fire diameter ratio (Column F)	$\dfrac{r}{D} = \dfrac{78.4}{5.98} \cong 13.1$	2.2 – 5.7	No
CURB LOCATION 2			
Target distance to fire diameter ratio (Column A)	$\dfrac{r}{D} = \dfrac{28.03}{5.98} \cong 4.67$	2.2 – 5.7	Yes
Target distance to fire diameter ratio (Column B)	$\dfrac{r}{D} = \dfrac{26.90}{5.98} \cong 4.5$	2.2 – 5.7	Yes
Target distance to fire diameter ratio (Column C)	$\dfrac{r}{D} = \dfrac{8.8}{5.98} \cong 1.47$	2.2 – 5.7	No
Target distance to fire diameter ratio (Column D)	$\dfrac{r}{D} = \dfrac{3.94}{5.98} \cong 0.66$	2.2 – 5.7	No
Target distance to fire diameter	$\dfrac{r}{D} = \dfrac{43.3}{5.98} \cong 7.24$	2.2 – 5.7	No

Quantity	Normalized Parameter Calculation	Validation Range	In Range?
ratio (Column E)			
Target distance to fire diameter ratio (Column F)	$\dfrac{r}{D} = \dfrac{80.8}{5.98} \cong 13.5$	2.2 – 5.7	No

Lubricating Oil Fire in a Turbine Building

Table F-4 shows that the Turbine Building fire scenario falls outside of the parameter space of the NRC/EPRI V&V study, both for the single- and multiple-enclosure geometric representations (NUREG-1824 (EPRI 1011999)). It is interesting that the single compartment representation only falls out of range of the parameter space for four of the six column targets, two of them being too low (close) and two of them being too high (far). All other parameters are within the NUREG-1824 (EPRI 1011999) parameter space (NUREG-1824 (EPRI 1011999)). In the case of the multiple compartment representation applicable to both the CFAST and FDS models, the aspect ratio, the flame length to ceiling height ratio, and the four target distances fall outside the parameter space range.

A flame length to ceiling height ratio greater than one indicates that the flames would be impinging on the ceiling and spreading out under the ceiling. This configuration is beyond the model capability of CFAST and could affect the plume entrainment, the Hot Gas Layer temperature and depth, and the radiant heat flux to a target. If the Hot Gas Layer temperature is not a significant source of heat flux to a target, the significance of this parameter could decrease in the case of a target temperature calculation, provided the target distance is within the validated parameter space (i.e., not too close). The aspect ratio also plays a role in the Hot Gas Layer formation and temperature. In the case of a zone model, a large aspect ratio may suggest that there could be localized regions where the gases are significantly hotter than the average (i.e., zone temperature). This type of calculation falls within the model capability of FDS, and there is no reason to expect that the model is not applicable for these aspect ratios. Nonetheless, it is at this point necessary to provide justification either by drawing on additional data for comparison or by demonstrating that the Hot Gas Layer temperature is not a significant source of heat flux to the targets, which implies that the analysis can tolerate a significant relative error in the temperature prediction of the Hot Gas Layer.

As part of the work performed at NIST for the investigation of the World Trade Center disaster, FDS has been validated against large-scale fire experiments. The experiments involved fairly large fires in relatively small compartments, limited ventilation, a liquid fuel spray fire, and the measurement of the heat flux to and temperatures of insulated steel (similar to the cables protected by Kaowool blankets). These experiments and the FDS simulations are described in NIST NCSTAR 1-5F.

Because the target to distance ratios shown in Table F-4 are outside the validation range for four of the six column targets, it is possible that the heat flux at the nearest and farthest columns could be underpredicted. In the case of the farthest columns, this is not a serious issue because the conditions at the columns within the parameter space range are more severe but acceptable with respect to the critical steel temperature. In addition, the point source model invoked by CFAST (Jones et al., 2009) is within the model validation basis per the Society of Fire Protection Engineers's (SFPE) Engineering Guide, "Assessing Flame Radiation to External Targets from Pool Fires" (1999). In the case of the nearer columns, simple models such as CFAST are outside their intended application range. It may be prudent to investigate the potential error of using the point source model (CFAST) at such distances through the use of other radiant heat flux models (i.e., solid flame models [NUREG-1805, 2004]). Although the near and far targets are outside the NUREG-1824 parameter space for FDS, there is additional validation data for FDS for these exposure conditions. Details can be found in NIST NCSTAR 1-5F, as previously described. In addition to the temperature measurements, heat fluxes to various structural elements were calculated and compared to test data. This data can serve as the V&V basis for FDS with respect to these target columns.

F.4 Estimation of Fire-Generated Conditions

This section provides details specific to each model.

F.4.1 Zone Model (CFAST)

Geometry: The CFAST analysis defines the compartment as a single rectangular parallelepiped with the specified dimensions. Two fire model strategies are considered. First, the entire volume of the turbine generator building is represented as a single compartment. This is a simple application of the CFAST model, and the implied assumption here is that the mass transfer across the hatch and stair openings is rapid relative to the development of a Hot Gas Layer in the lower level. The horizontal openings to the exterior of the building at the 4.6 m (15 ft) elevation are treated as vertical openings centered at the 4.6 m (15 ft) elevation, which is 4.6 m (15 ft) above the floor, ignoring the depressed area near the fuel spill. The second strategy is to model the Turbine Building using two primary compartments, one for the lower deck and one for the upper turbine deck. The two compartments are connected by hatches and stairs, which are themselves modeled as sub-compartments. This represents a complex application of the CFAST model and is expected to provide a better representation of the plume entrainment in the lower level; however, CFAST does not model the entrainment from plumes originating from horizontal openings. Instead, the combustion products are directly placed in the upper hot gas zone after flowing through the horizontal opening. In addition, the gross area of the larger horizontal vents exceeds the recommended size per NIST SP 1086, indicating that there is no adequate validation data for the application. Neither geometric representation is ideal, although each configuration bounds one or more aspects of the fire scenario development and the resulting exposure to the structural steel.

The dimensions of the primary compartments and the vent characteristics for each configuration are summarized in Table F-5. The dimensions for the single compartment representation conserve the volume, aspect ratio of the lower compartment, and the total height. Another valid strategy would be to conserve the total height, the boundary surface area, and the volume. Figures F-4a and F-4b show three-dimensional views of the geometry for the two configurations. Note that the entrainment within the intermediate floor is ignored in the single compartment model; in this case the total height is 1 m (3.3 ft) lower than the height between the lower level floor and the upper level ceiling. Figures F-4a and F-4b also show the locations of the targets and the two proposed curb locations.

Table F-5. Primary Compartment Dimensions

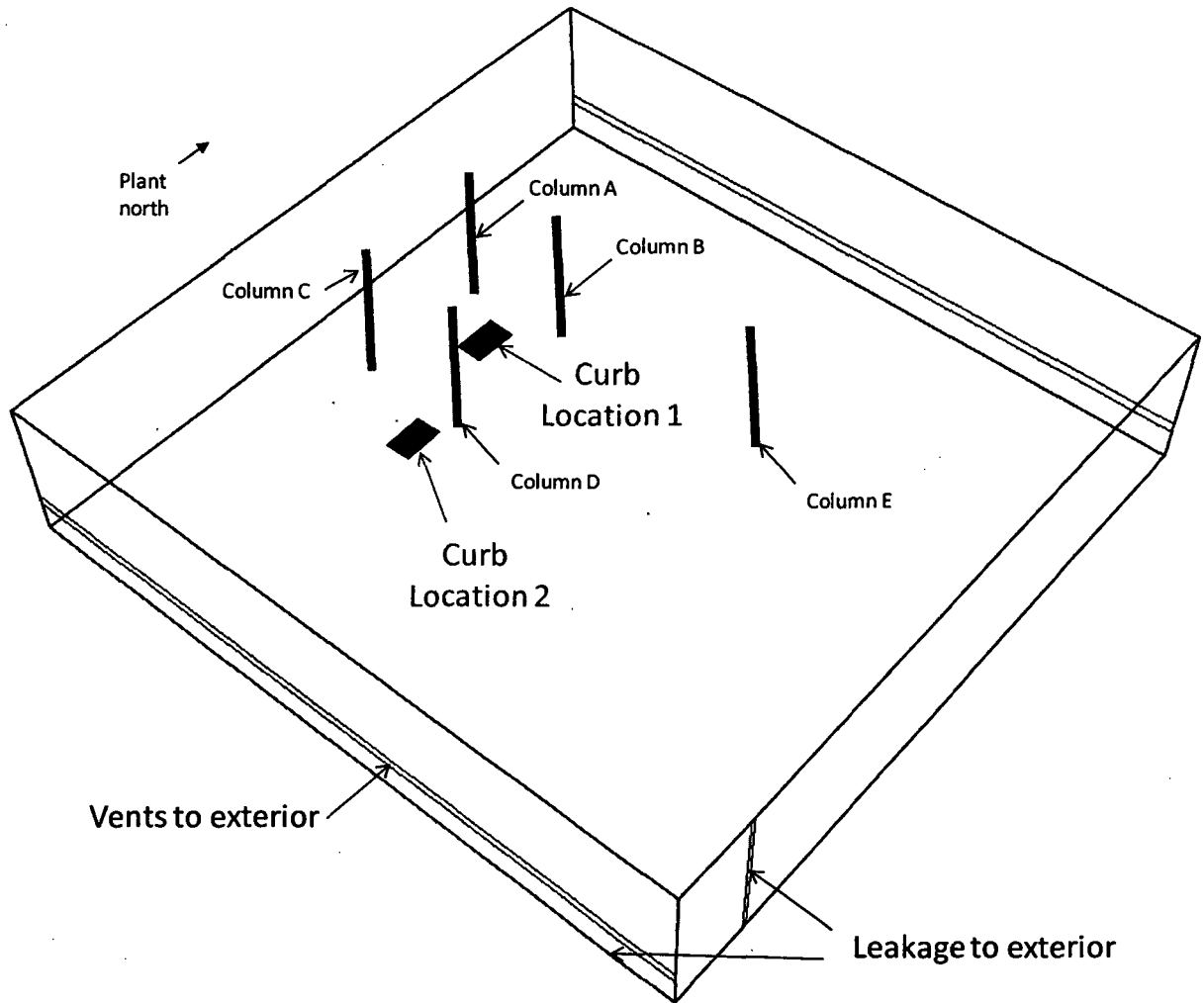| Model	Length (m)	Width (m)	Height (m)
Single Compartment	86.6	87.3	18.8
Multiple Compartments: Lower Level	100.3	99.5	4.6
Multiple Compartments: Upper Level	95	71.3	14.2

Figure F-4a. CFAST Geometry for the Single-Compartment Representation of the Turbine Building.
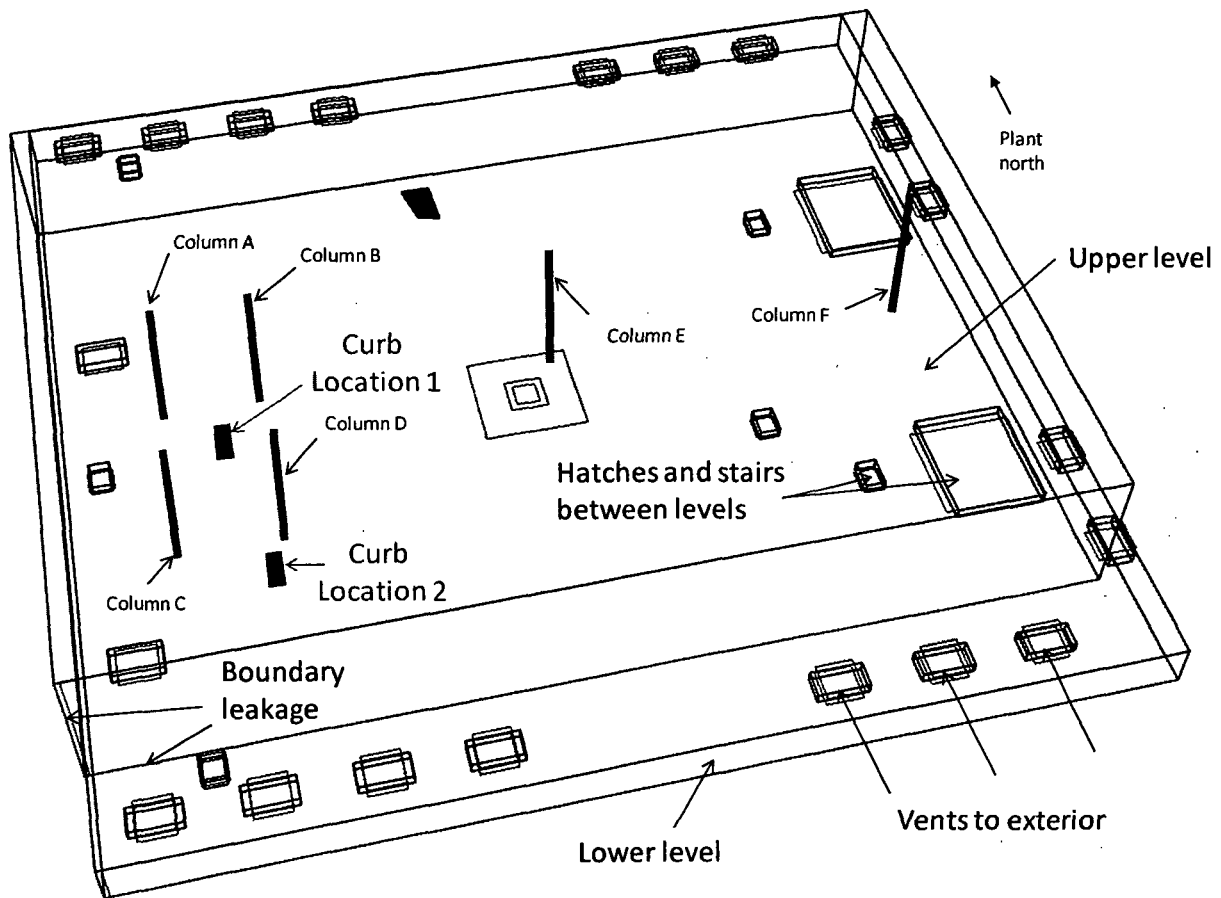
Figure F-4b. CFAST Geometry for the Two-Compartment Representation of the Turbine Building.

Note that the internal obstructions, such as the turbine generators, the condensers, and the HVAC room, as well as variations in the floor elevation, are not accounted for in the geometric definition. The total volume of these obstructions is small relative to the total volume of the Turbine Building, and ignoring them is not expected to affect the results appreciably, especially since the focus is on the heat flux to a target in the lower level. In practice, this assumption would be verified by creating another CFAST geometry that has a slightly lower volume that does not include the volume of the large obstructions. This step is not performed in this example, as it lies outside the primary focus.

Fire: The fire is specified in the curbed areas, as described in Section F.2. CFAST requires a user-specified time-dependent HRR and stoichiometry for the combustion of fuel and oxygen. As noted in Section F.2, the fuel oil is dominated by alkanes, which have a chemical formula of C_nH_{2n+2} with n ranging from 12 to 15 but centered on 14. The average fuel composition is therefore $C_{14}H_{30}$. In the absence of test results for the specific fuel oil, the gas yields needed for input to CFAST can be estimated. The CO yields are available from the work of Köylu and Faeth:

$$y_{CO} = \frac{12x}{M_f v_f} 0.0014 + 0.37 y_s \qquad \text{(F-3)}$$

where x is the number of carbon atoms in a fuel molecule (two in this example), M_f is the molecular weight of the fuel (198 g/mol, calculated from the effective chemical formula), y_s is the soot yield, and v_f is the stoichiometric coefficient of the fuel, which is equal to one since all species yields are taken as a ratio to the fuel burned. Note that this correlation is applicable to well-ventilated fires, which would be appropriate for this fire scenario given the large volumes involved and the large number of vents to the external areas. For this example, the CO yield is calculated from the above formula to be 0.037 kg CO/kg fuel. The CO_2 yield is computed using a chemical mass balance:

$$aC_{14}H_{30} + bO_2 \rightarrow cCO + dC + eCO_2 \qquad \text{(F-4)}$$

where a, b, c, d, and e are the number of moles of each reactant or product and C is the soot (unburned carbon). The number of moles of fuel required to produce 1 kg of fuel is 5.051; thus, a is equal to 5.051. The number of moles necessary to produce 0.037 kg of CO is 1.32, and the number of moles necessary to produce 0.1 kg of C is 8.33. The coefficients c and d are thus equal to 1.32 and 8.33, respectively. A mole balance on the carbon atom requires e to be 61.06. This results in a CO_2 yield of 2.69 kg CO_2/kg fuel. This is consistent with data reported by Tewarson in Table 3-4.14 of the SFPE Handbook (2008) for typical alkane fuels. The number of moles of oxidizer (b) is not an input parameter for CFAST, but may be determined from the products. It is thus equal to the number of moles of carbon dioxide plus half the number of moles of carbon monoxide, or 61.72.

Direct inputs for species production rates in CFAST are normalized to this CO_2 yield. Thus, CFAST input of CO/CO_2 is 0.014, and C/CO_2 is 0.037. A final CFAST input is the ratio of the mass of hydrogen to the mass of carbon in the fuel, or 0.178 kg H/kg C. CFAST uses the fire area directly as an input.

Materials: CFAST defines a wall, ceiling, and floor boundary using a single material, though they may be different for each of the three boundaries. In the case where the Turbine Building is modeled as two compartments, the material specification for each boundary follows from the actual geometry. Specifically, the wall and floor of the lower level are 0.3 m (1 ft) thick normal weight concrete and the ceiling is 1 m (3.3 ft) thick normal weight concrete, as is the floor of the turbine deck level. The ceiling and walls of the turbine deck level are 3 mm (0.1 in) thick corrugated steel. In the case where a single compartment is used to represent the Turbine Building, all materials are modeled using the most thermally resistive material among the different materials present. As such, the walls, floor, and ceiling are 0.3 m (1 ft) normal weight concrete.

Ventilation: There are eighteen vents from the lower level that are open to the building exterior, in addition to two stairs. In addition, there are four hatches and four stair openings connecting the lower level to the upper level. Leakage is approximated as two small vents in each primary compartment, one near the floor and one that spans the entire compartment height.

The single compartment model treats the exterior vents as vertical openings centered at the height of the vent, or 4.6 m (15 ft) above the floor. Vents between the lower and upper levels are by definition ignored (i.e., the flow between the levels is rapid relative to the development of the Hot Gas Layer). The two-compartment model approximates each horizontal flow path using additional sub-compartments having an area equal to the area of the vent and a depth equal to the floor depth, or 1 m (3.3 ft). Horizontal vents are placed at the base and top of each sub-compartment. This results in 28 additional sub-compartments and 56 horizontal vent connections.

Fire/Smoke Detection: There are no smoke or fire detector inputs for this scenario.

Steel Columns: The columns are approximated as steel plates with the given thickness of the actual columns. The orientation of the surface normal is directed toward the fire parallel to the plane of the floor since the columns' surfaces are perpendicular to the floor plane. CFAST will compute the target temperature given the predicted heat flux at the target surface. The method effectively treats the target as having an adiabatic unexposed temperature and would thus be expected to overestimate the temperature if the losses on the unexposed boundary are significant. Conversely, this model could underestimate the temperature if the surrounding temperature on the unexposed side increases significantly. To determine the location of the highest temperature, initial simulations with targets from floor to ceiling were conducted. The simple point source model for the fire led to the highest temperature on portions of the steel columns at floor level. Note that the actual height of the target in the CFAST model is slightly above the floor level, or 0.01 m (0.4 in), to ensure that the target position is not coincident with the floor position.

F.4.2 CFD Model (FDS)

Geometry: The entire turbine hall is included in the simulation. One mesh covers the lower deck, and one covers the upper turbine deck. The numerical mesh consists of uniform grid cells with a resolution of about 1 m. While this mesh appears to be fairly coarse, the fire is so large that the ratio of D^* (the characteristic fire diameter) to the cell size is about five. This is sufficient resolution to simulate the fire and its impact on the overall space, based on the range provided in Section 2 of this guide. The main focus here is the heat flux to nearby columns, not necessarily columns within the fire itself; thus, the resolution is considered adequate.

The columns cannot be resolved on the relatively coarse grid, and are approximated as steel plates with the given thickness of the actual columns. The column obstructions are one cell thick, which allows the boundary conduction on the surface opposite the fire to be exposed to the room conditions. Even though the column obstruction is one cell thick in the domain mesh, the thickness of the steel surface through which heat is transferred is equal to thickness of the column web. Note that FDS only performs a one-dimensional heat transfer calculation within solid obstructions, which is why there is little to be gained by resolving the column further. The neglect of lateral heat conduction within the solid tends to produce a slight overprediction of the average column cross-section temperature, but, because the heat flux from the fire is expected to be fairly uniform over the width of the column, a more detailed thermal conduction calculation is not warranted.
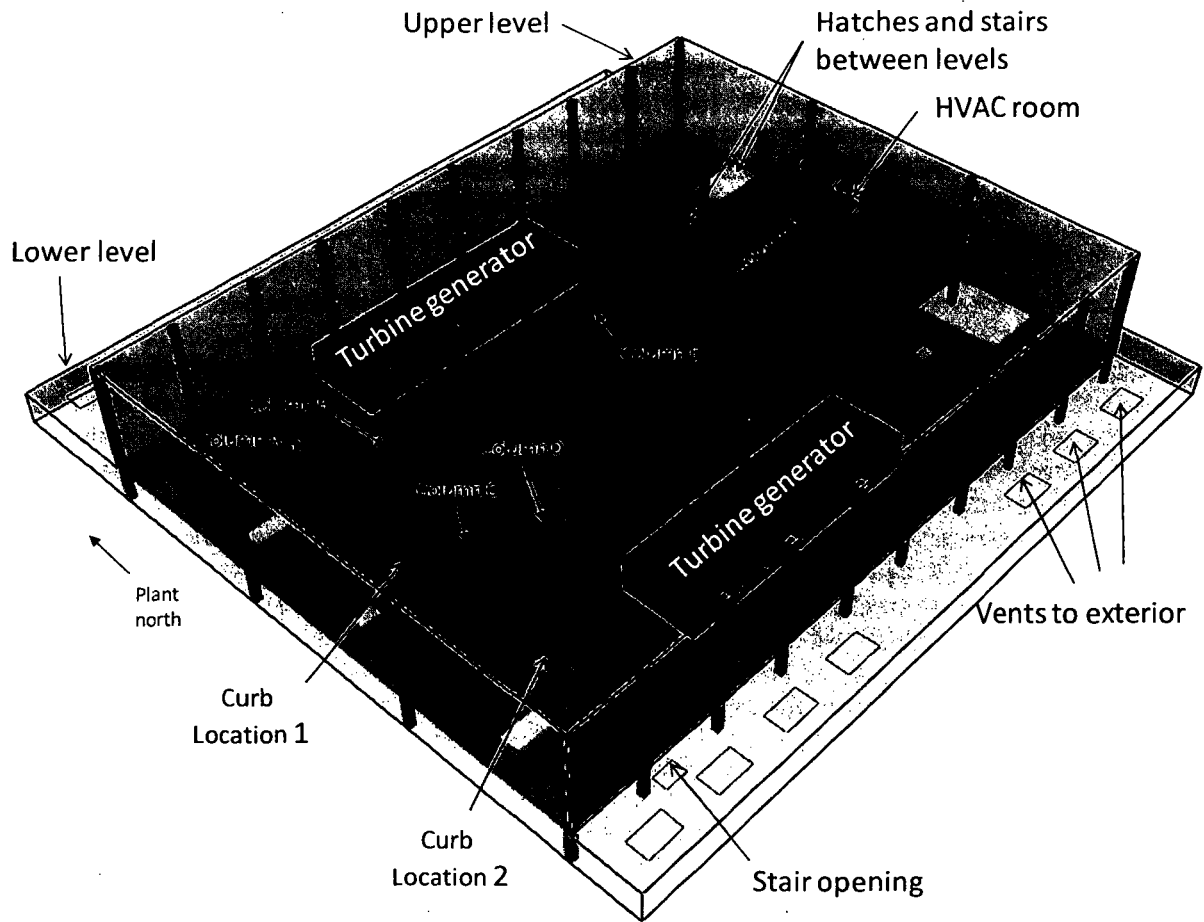
Figure F-5. FDS Geometry for the Turbine Building Fire Scenario.

Materials: The material properties are applied directly as specified to the walls, floor, ceiling and cabinet.

Fire: The fire is specified in the curbed areas, as described in Section F.2. The heat release rate, soot yield, and molecular weight are as described in Section F.2, and are provided directly as inputs to FDS. A 10-second growth rate is used to allow the flows to develop over a finite time interval.

Ventilation: The openings to the exterior and between the lower level and the upper level are modeled at the locations, as shown in Figures F-1 and F-5. It should be noted that the point of including the lower and upper levels of the Turbine Building in the simulation is to check whether there would be sufficient make-up air drawn through the various vents to sustain a steady-state 50.3 MW fire.

F.5 Evaluation of Results

The purpose of the calculations described above is to estimate the steel temperature of six large columns in the Turbine Building to determine if any would lose the ability to carry their design load in the event of a large fire in the curbed area about a tank of lubricant oil. A structural steel

column is considered to fail if the average cross section temperature of the steel exceeds 538 °C (1,000 °F), as described in Section F.2. The heat release rate profile for the lubricant oil fire in the curbed area, as modeled by CFAST and FDS, is shown in Figure F-6.
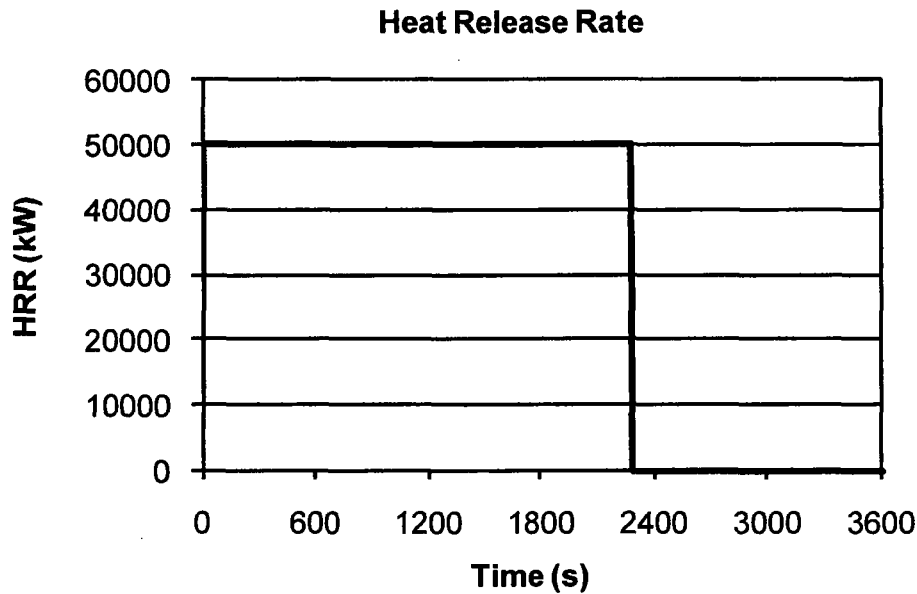
Heat Release Rate

Figure F-6. Heat Release Rates Used by CFAST and FDS for Lubricant Oil Fire Scenario.

F.5.1 Column Heat Flux and Column Temperature

The predicted heat fluxes and resulting column temperatures for the six columns shown in Figure F-2 are summarized in Figure F-7 for Curb Location 1 and Figure F-8 for Curb Location 2. Note that Column F was not included in the single-compartment CFAST model because the physical dimensions of the column exceed the enclosure dimensions. This is one drawback when using specific targets within approximated enclosure geometries.

The output quantity for FDS is the gauge heat flux relative to a 36 °C (95 °F) ambient temperature. Two locations were considered at each column, one point near the floor and comparable to the CFAST position and one point near the ceiling of the lower level. The heat flux and temperature plots are based on the point with the maximum column temperature among the two. This generally corresponds to the upper point, except for columns near the fire, where the lower point is predicted to be hotter. The output quantity for the CFAST simulations is the total heat flux, which includes the fire, boundary surface reradiation, HGL radiation, and net convective flux at the surface of the target. This quantity is comparable to the incident heat flux output by FDS.

Lubricating Oil Fire in a Turbine Building

Temperature of Column A

Heat Flux of Column A

Figure F-7a. Predicted Incident or Total Heat Flux and Column Temperature for Column A – Curb Location 1.

Temperature of Column B

Heat Flux of Column B

Figure F-7b. Predicted Incident or Total Heat Flux and Column Temperature for Column B – Curb Location 1.

Temperature of Column C

Heat Flux of Column C

Figure F-7c. Predicted Incident or Total Heat Flux and Column Temperature for Column C – Curb Location 1.

Temperature of Column D

Heat Flux of Column D

Figure F-7d. Predicted Incident or Total Heat Flux and Column Temperature for Column D – Curb Location 1.

Temperature of Column E

Heat Flux of Column E

Figure F-7e. Predicted Incident or Total Heat Flux and Column Temperature for Column E – Curb Location 1.

Temperature of Column F

Heat Flux of Column F
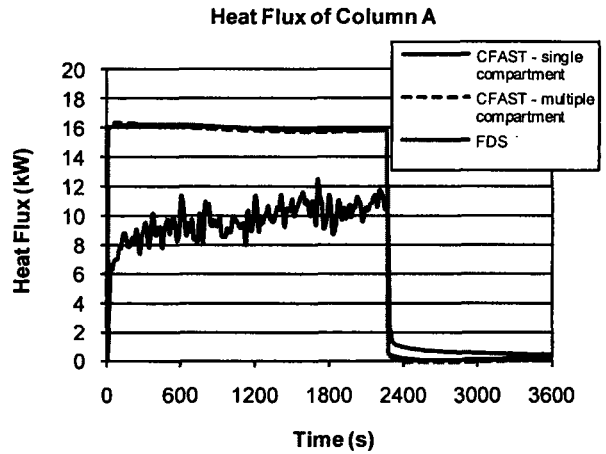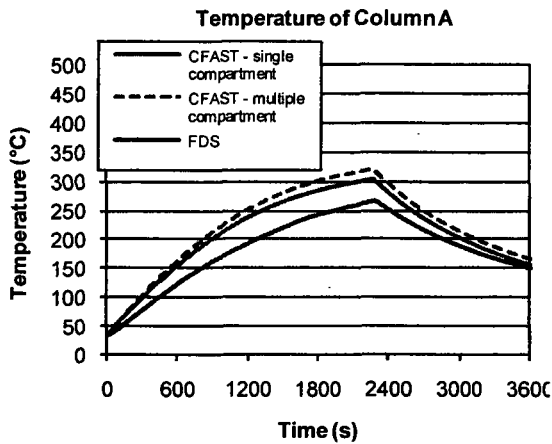

Figure F-7f. Predicted Incident or Total Heat Flux and Column Temperature for Column F – Curb Location 1.

Figure F-8a. Predicted Incident or Total Heat Flux and Column Temperature for Column A – Curb Location 2.

Figure F-8b. Predicted Incident or Total Heat Flux and Column Temperature for Column B – Curb Location 2.

Figure F-8c. Predicted Incident or Total Heat Flux and Column Temperature for Column C – Curb Location 2.
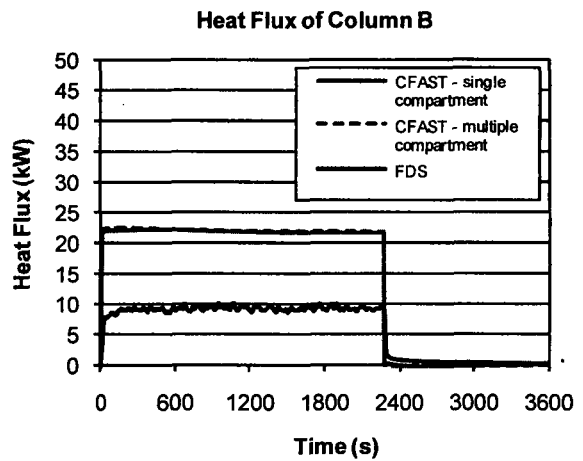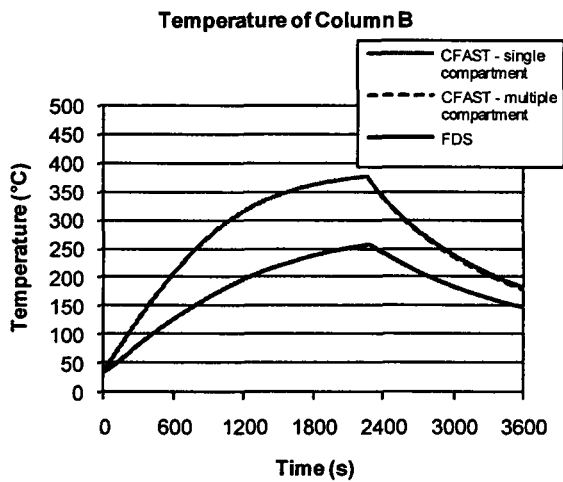
Figure F-8d. Predicted Incident or Total Heat Flux and Column Temperature for Column D – Curb Location 2.

Figure F-8e. Predicted Incident or Total Heat Flux and Column Temperature for Column E – Curb Location 2.
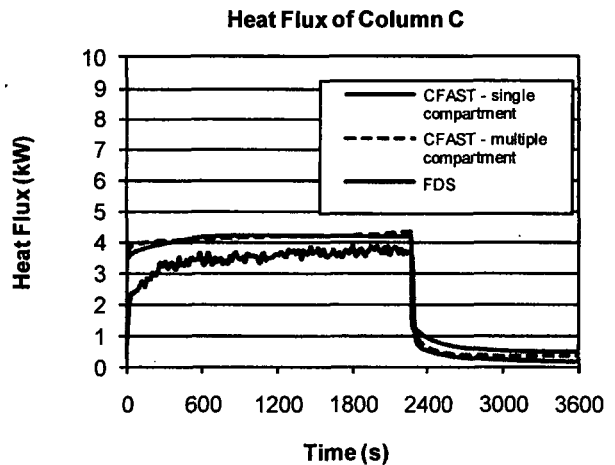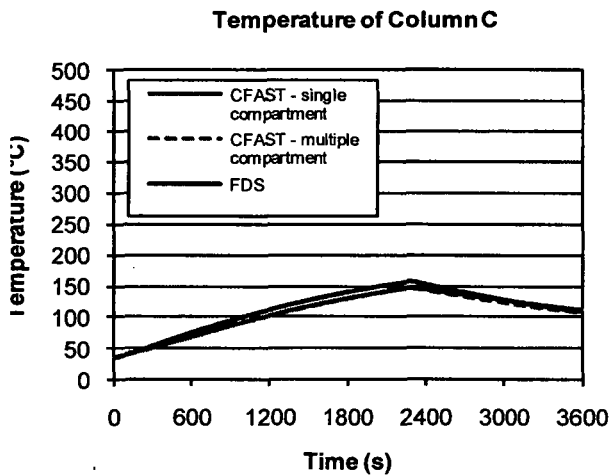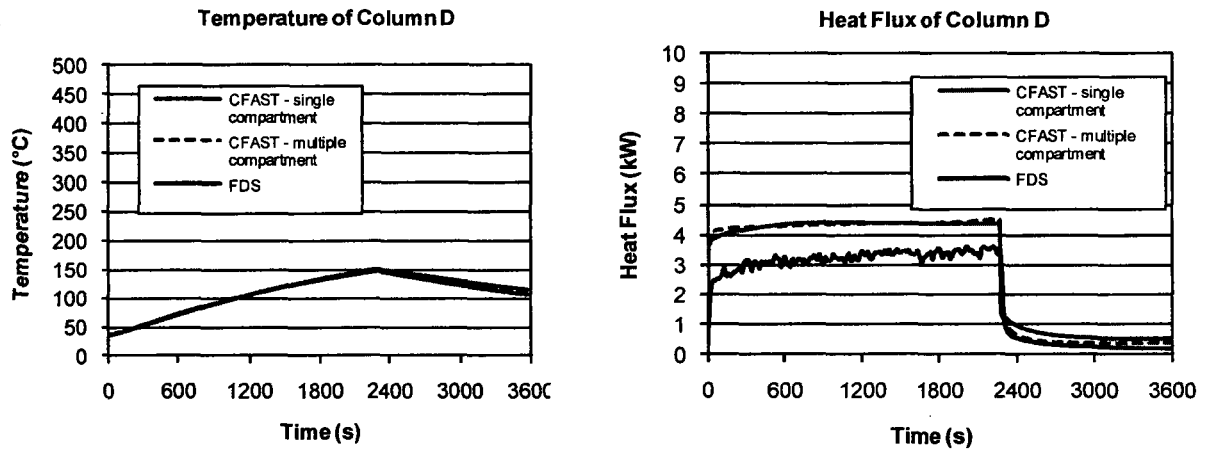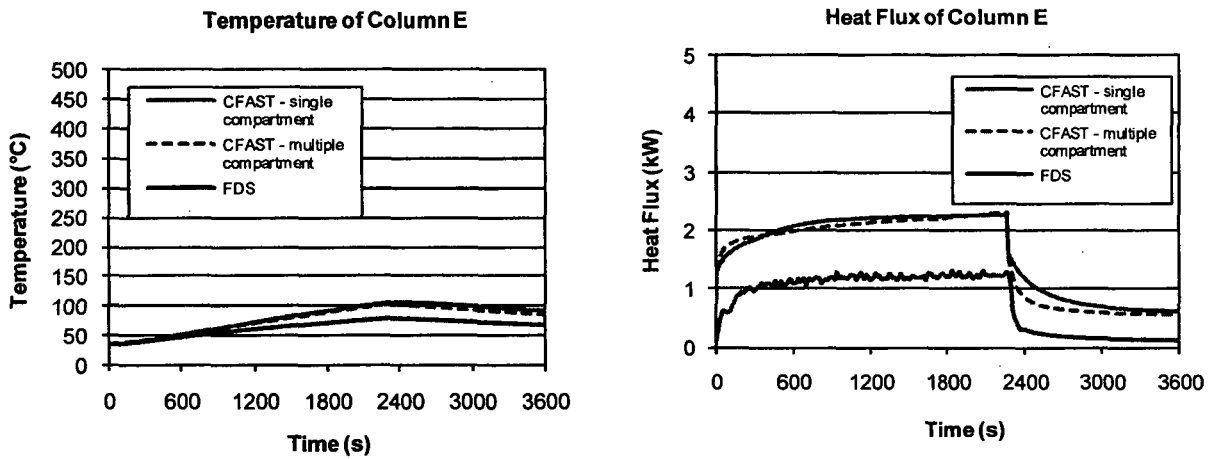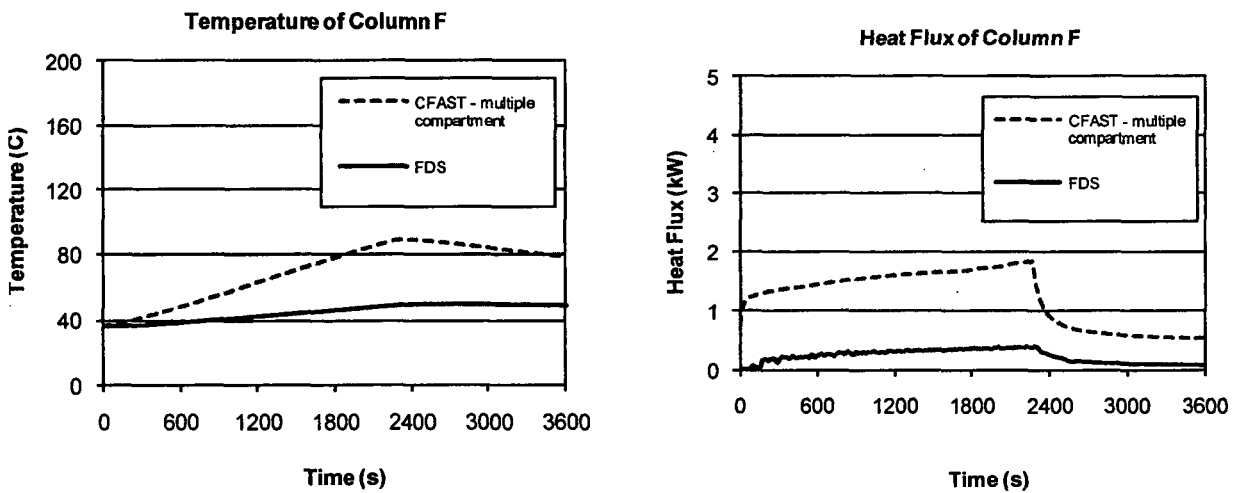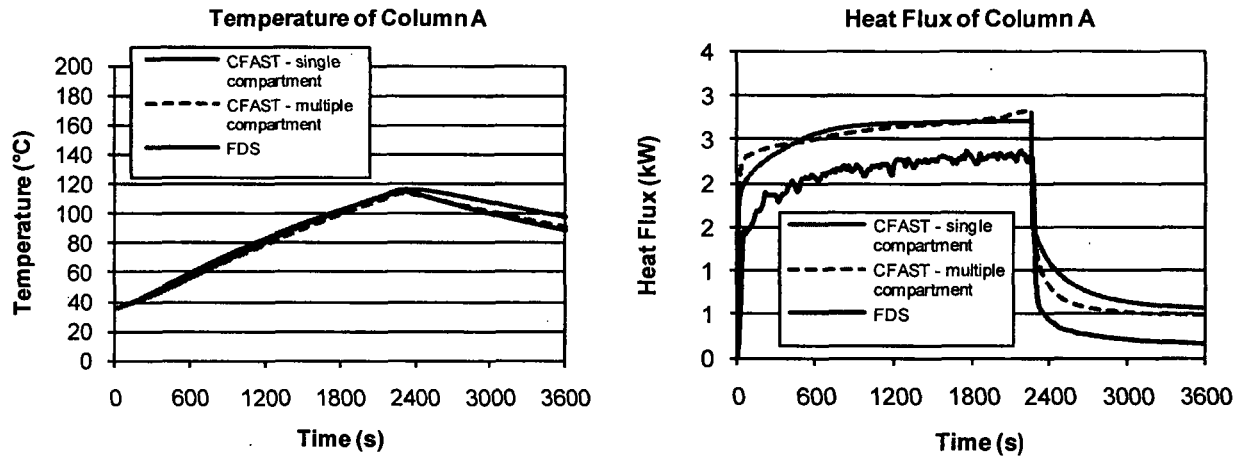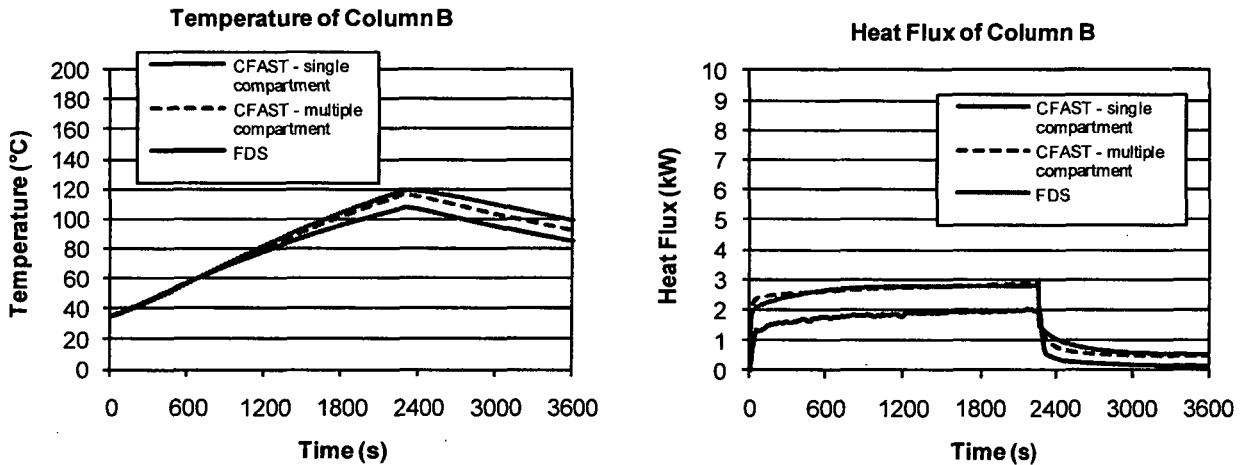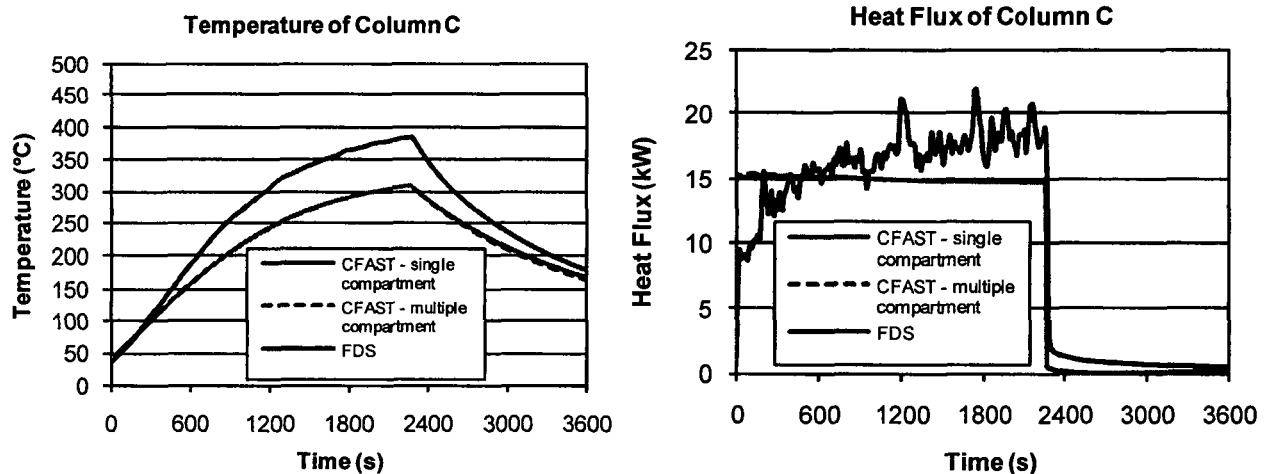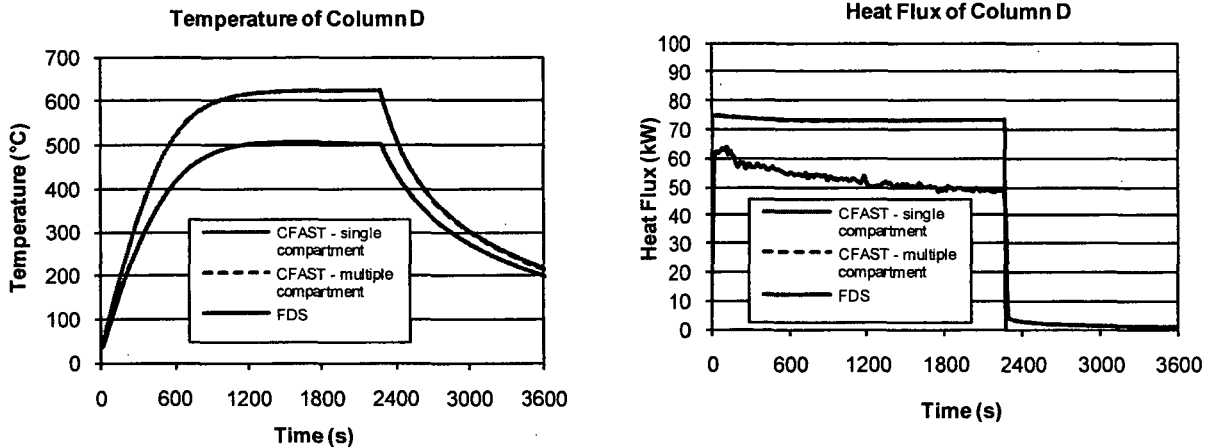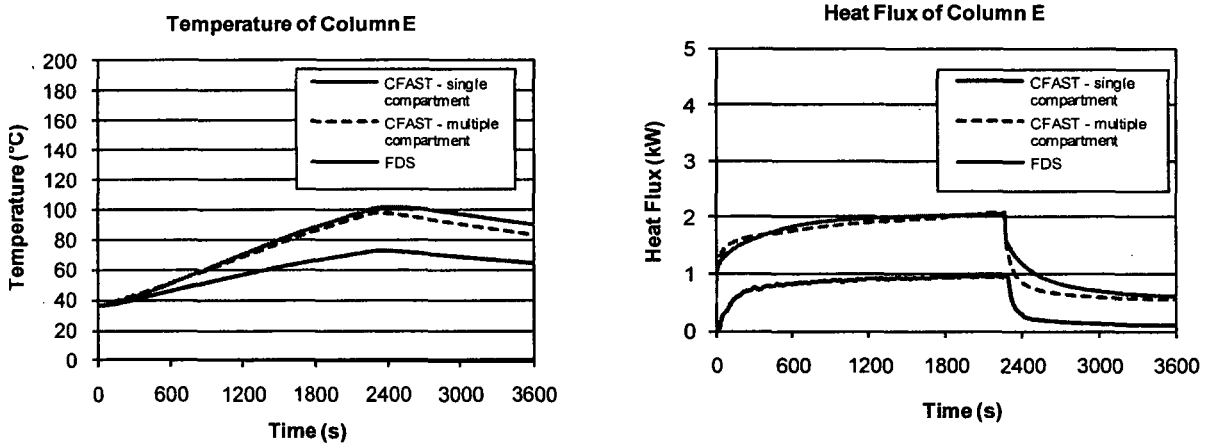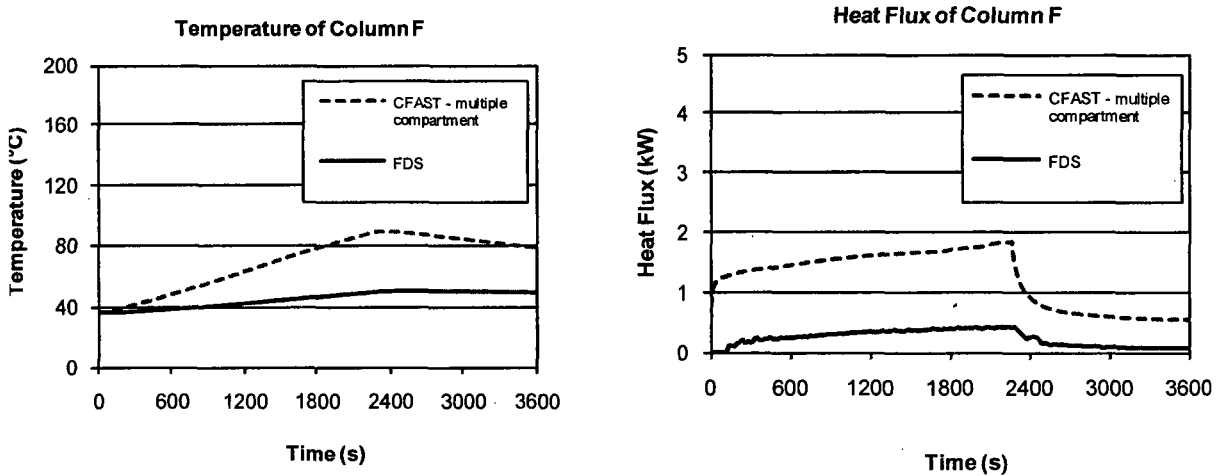

Figure F-8f. Predicted Incident or Total Heat Flux and Column Temperature for Column F – Curb Location 2.

Lubricating Oil Fire in a Turbine Building

The temperature and heat flux plots reveal several interesting aspects of the curb fire exposures to the target columns. First, the CFAST single- and multiple-compartment representations of the Turbine Building produce nearly the same result. This suggests that the exposure boundary conditions at the columns are either dominated by the flame heat flux or that the HGL temperature predictions are not strongly dependent on the presence of the intervening floor. The fraction of the boundary heat flux at the columns that comes directly from the flame actually is a function of the column position. Columns close to the fire receive about 95% of the heat flux from the flames; columns that are located far from the fire receive about 30% of their heat flux directly from the flames. This is shown in Figure F-9 for two columns in the single compartment representation of the Turbine Building. The surface heat flux in Figure F-9 refers to the heat flux radiated from the heated boundaries of the enclosure; the HGL heat flux is the heat flux radiated from the gases in the enclosure; the target convection flux is the net convective heat flux at the target surface. Both Figures F-9a and F-9b show the fractions during the time the fire is burning.
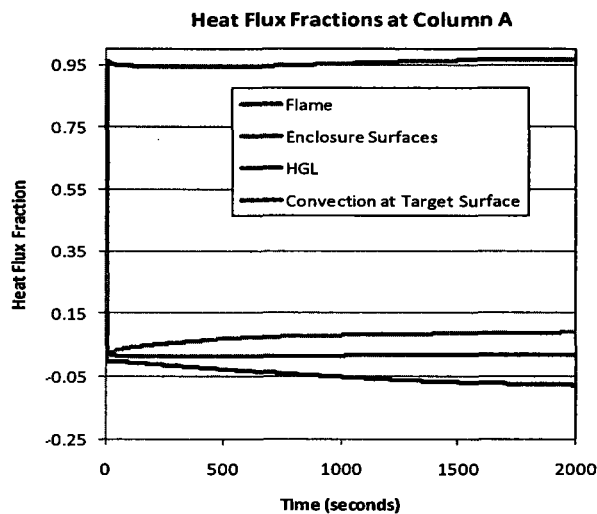
Figure F-9a. Column A Boundary Heat Flux Fractions Predicted by CFAST – Curb Location 1 in One Compartment Geometry
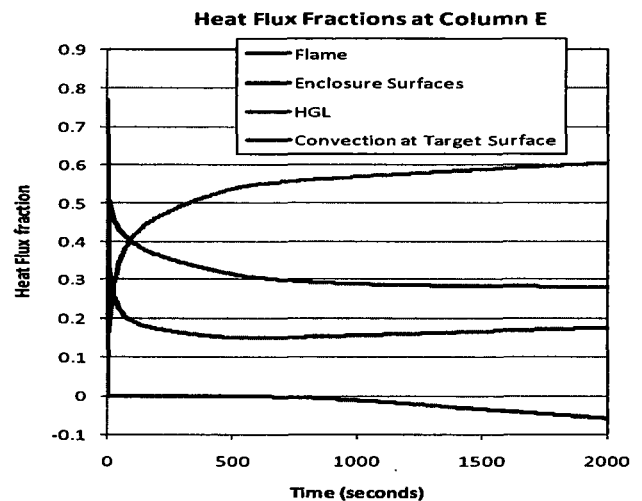
Figure F-9b. Column E Boundary Heat Flux Fractions Predicted by CFAST – Curb Location 1 in One Compartment Geometry

The Hot Gas Layer temperatures and the Hot Gas Layer heights are shown in Figures F-10a and F-10b for the single- and multiple-compartment representations. The temperatures apply to either curb location since the spatial location of the fire does not affect the HGL unless it is near a wall or in a corner. Figure F-10 indicates that the Hot Gas Layer temperatures are nearly the same for each configuration, though the layer elevation is somewhat higher in the single compartment representation. Figures F-9 and F-10 suggest that the similarity between the temperature results for the two CFAST configurations is an expected result for this application. In effect, the results do not rely on the assumptions regarding the mass flow through the horizontal vents between the lower level and the turbine deck and effectively confirm the assumption that a single-volume enclosure approximation is applicable to this application.

HGL Temperature

HGL Height
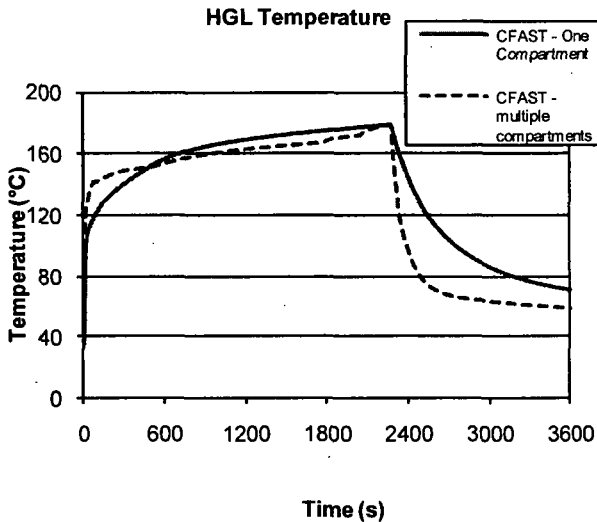
Figure F-10a. Hot Gas Layer Temperature Predicted by CFAST in the Turbine Building.
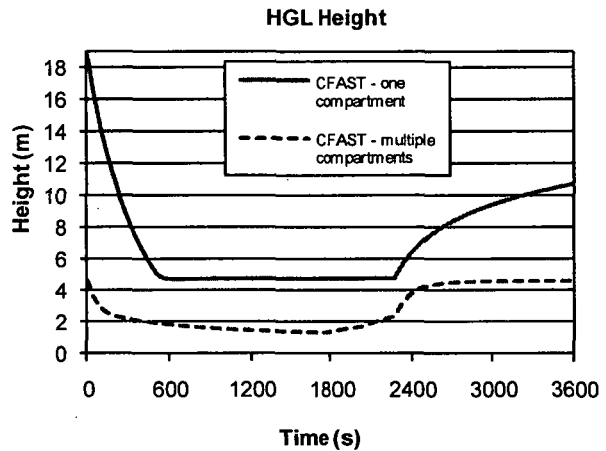
Figure F-10b. HGL Elevation Predicted by CFAST in the Turbine Building.

The CFAST and FDS predictions are generally similar with regard to the overall magnitude and trend for the target heat flux. In all cases, CFAST predicts a higher and more conservative heat flux than FDS by 50% to 100%. This is partially a result of the flame height exceeding the ceiling height by a considerable margin. In addition, the CFD model, FDS, simulates the fire with a more realistic flow field and the inclusion of blocking obstructions. The FDS predictions of heat flux are based on the solution of a three-dimensional radiation transport equation with 100 angular directions. This model accounts for both the fire and the hot smoke as sources of heat flux at the columns. FDS predicts a maximum heat flux and temperature for Column A because the simulated fire leans in the direction of this column because the large hatch nearby draws the hot gases and fire, upward.

The predicted steel temperatures for Curb Location 1 are lower than the threshold value of 538 °C (1,000 °F) at all locations by a significant margin. The maximum predicted temperature in the columns nearest the proposed curb location remains lower than 380 °C (716 °F) for the CFAST simulations and 265 °C (509 °F) for the FDS simulations. Note that the application of CFAST for predicting the temperatures at the nearest columns does not have a V&V basis; thus, more weight is assigned to the FDS results.

The predicted steel temperatures for Curb Location 2 are lower than the threshold value of 538 °C (1,000 °F) at all locations, except for Column D. CFAST predicts a steel temperature of about 620 °C (1,148 °F), while FDS predicts a steel temperature of about 508 °C (946 °F) by a significant margin. As was the case with Curb Location 1, the CFAST predictions for the nearest columns are outside the V&V basis, and more weight is assigned to the FDS results. However, in this case the FDS predictions are marginally lower than the threshold value, and, as will be seen in Section F.5.2, there is a considerable probability, based on model uncertainty alone, that the actual result would exceed the threshold margin. It is therefore concluded that Curb Location 2 is not suitable despite the plant's preference to locate it there. Curb Location 1 is preferable based on the fire modeling results.

Lubricating Oil Fire in a Turbine Building

F.5.2 Uncertainty

The results indicate that the single- and multiple-compartment representation of the Turbine Building produce nearly the same temperature, consistent with the total heat flux results. The CFAST and FDS predictions are generally similar with regard to the overall magnitude and trend for targets. The predicted steel temperature is fairly similar for Columns C and D despite the moderate differences in the total and incident heat fluxes (See Figures F-7 and F-8). This is likely due to the differences in the boundary conditions on both the exposed and unexposed faces of the steel plate. In all cases except for Column C, CFAST predicts a steel temperature greater than that of FDS. This is not surprising, since the total heat flux is greater in all cases and an adiabatic boundary condition is applied to the unexposed face.

Chapter 4, Model Uncertainty, provides guidance on how to express the uncertainty of model predictions. The uncertainty of the model predictions is considered for the columns that are predicted to have the hottest temperature, which in practice would serve as the basis for any conclusions drawn from the fire modeling results. Table F-6 summarizes the columns and hottest column temperatures for the two-zone model configurations and the FDS results.

Table F-6. Maximum Column Temperatures among the Six Columns Considered Predicted by CFAST and FDS.

Fire Model	Configuration	Curb Location	Column with Maximum Temperature	Maximum Column Temperature (°C)
CFAST	Single Compartment	1	B	377
CFAST	Two Compartment	1	B	378
FDS	Two Compartment	1	A	265
CFAST	Single Compartment	2	D	623
CFAST	Two Compartment	2	D	623
FDS	Two Compartment	2	D	508

In the NRC/EPRI V&V study (NUREG-1824 (EPRI 1011999)), it was found that CFAST predictions of target temperature increases are, on average, equal to the corresponding measurements, and the relative standard deviation of its predictions about this average value is 27%. Similarly, it was found that FDS predictions of target temperatures are, on average, 2% higher than the corresponding measurements, and the relative standard deviation of its predictions about this average value is 13%.

This suggests that the true value of the maximum steel temperature in the column for this scenario is normally distributed with a mean value and standard deviation, as summarized in Table F-7.

**Table F-7. Mean Maximum Column Temperatures and Standard Deviations among the Six
Columns Considered Based on Model Uncertainty for CFAST and FDS.**

Fire Model	Configuration	Curb Location	Mean Maximum Column Temperature Increase (°C)	Maximum Standard Deviation (°C)
CFAST	Single Compartment	1	341	92
CFAST	Two Compartment	1	342	92
FDS	Two Compartment	1	225	29
CFAST	Single Compartment	2	587	158
CFAST	Two Compartment	2	587	158
FDS	Two Compartment	2	463	60

Therefore, the probability that the steel temperature increase would exceed 518°C (932°F) at Curb Location 1 (i.e., 538 °C [1,000 °F] critical value minus the initial ambient temperature of 36 °C [95 °F]) is:

$$P(\Delta T > 518) = \frac{1}{2} \text{ erfc}\left(\frac{518 - 341}{92\sqrt{2}}\right) \cong 0.03 \tag{F-5}$$

for the single-compartment configuration in CFAST;

$$P(\Delta T > 518) = \frac{1}{2} \text{ erfc}\left(\frac{518 - 342}{92\sqrt{2}}\right) \cong 0.03 \tag{F-6}$$

for the two-compartment configuration in CFAST; and

$$P(\Delta T > 518) = \frac{1}{2} \text{ erfc}\left(\frac{518 - 225}{29\sqrt{2}}\right) \cong 0 \tag{F-7}$$

for the two-compartment configuration in FDS. In other words, there is a three or less percent chance of exceeding the temperature threshold for structural damage based only on model uncertainty, according to both CFAST predictions and the FDS prediction.

The probability that the steel temperature increase would be less than 518°C (932°F) at Curb Location 2, as predicted by CFAST, is:

$$P(\Delta T > 518) = \frac{1}{2} \text{ erfc}\left(\frac{587 - 518}{158\sqrt{2}}\right) \cong 0.33 \tag{F-8}$$

for the single-compartment configuration in CFAST and

Lubricating Oil Fire in a Turbine Building

$$P(\Delta T > 518) = \frac{1}{2} \text{ erfc}\left(\frac{587 - 518}{158\sqrt{2}}\right) \cong 0.33 \qquad (\text{F-9})$$

for the two-compartment configuration in CFAST. Similarly, the probability that the steel temperature increase would be greater than 518 °C (932 °F) at Curb Location 2, as predicted by FDS, is:

$$P(\Delta T > 518) = \frac{1}{2} \text{ erfc}\left(\frac{518 - 462}{60\sqrt{2}}\right) \cong 0.2 \qquad (\text{F-10})$$

for the two-compartment configuration in FDS. In other words, there is a three or less percent chance of exceeding the temperature threshold for structural damage based only on model uncertainty, according to both CFAST predictions and the FDS prediction.

Thus, there is at least a 20% chance that the one of the columns would exceed the temperature threshold for structural damage based only on model uncertainty, according to both CFAST predictions and the FDS prediction; however, since the FDS cases have a firmer V&V basis, they are more reliant on these results. Although FDS predicts a maximum temperature in the steel that is about 30°C (86°F) below the critical value, the model uncertainty indicates that there is a non-trivial probability that the true temperature would be greater than the threshold value. Given this insight, it is concluded that Curb Location 1 is a better option based only on fire modeling considerations.

F.5.3 Sensitivity

Heat Flux

Table 4.2 indicates that the target heat flux output parameter is primarily a function of the heat release rate. A variation in the heat release rate corresponds to a variation in the heat flux that is proportional to the heat release rate raised to the 4/3 power. Consequently, a given uncertainty in the heat flux results in a greater uncertainty in its quantity. Fortunately, the heat release rate for pool fires is fairly well defined for particular fuels. Data for the burning rate of liquid fuels provided by Babrauskas (2008) indicates that there is generally a 5% to 10% uncertainty in this input parameter, which itself is proportional to the heat release rate, though no particular uncertainty is reported for the actual fuel involved in the Turbine Building fire scenario. Consertivityly assuming a 10% uncertainty in the burning rate results in a 14% variation in the predicted heat flux. To assess whether or not this could influence the conclusions, reference is made to Figures F-7a, F-7b, and F-8d. Figures F-7a and F-7b depict the most adverse exposure fluxes to the columns, as predicted by FDS and CFAST, respectively. The maximum heat flux, as shown in Figure F-7b, is about 22.5 kW/m², and the resulting peak steel temperature is about 375 °C (707 °F). Based on the uncertainty in the fuel burning rate, one could expect the predicted heat flux to fall between 19.6 and 25.5 kW/m², based on the sensitivity of this parameter to the heat release rate alone. Figure 8d depicts a heat flux exposure condition that causes the steel to reach 500 °C (932°F) to 600 °C (1,112). In this case, the peak exposure heat flux is on the order of 50 kW/m² to 60 kW/m². This provides a strong indication that a peak heat flux of 25.5 kW/m² would not result in the steel reaching a temperature of 538 °C (1,000 °F), the failure condition for the steel in this example. Consequently, it is concluded from the parameter sensitivity information for the heat flux that the uncertainty in the heat release rate could not result in a different conclusion.

Target Temperature

Table 4.2 indicates that the target temperature output parameter is also primarily a function of the heat release rate. A variation in the heat release rate corresponds to a variation in the heat flux that is proportional to the heat release rate raised to the 2/3 power. Consequently, a given uncertainty in the heat flux results in a lower uncertainty in the target temperature quantity. As previously described, a conservative uncertainty in the heat release rate for a burning liquid fuel is about 10%, which corresponds to a variation in the predicted target temperature of 7%. To assess whether or not this could influence the conclusions, reference is made again to Figures F-7a and F-7b, which depict the most adverse steel temperatures for Curb Location 1. The maximum temperature predicted among all of the models is about 375 °C (707 °F), such that the maximum temperature increase is about 339 °C (610 °F) for an initial ambient temperature of 36 °C (95 °F). A 7% variation in this output parameter indicates that the predicted target temperature is between 351°C (664 °F) and 399°C (750 °F), which is considerably less than the failure condition of 538°C (1,000°F) for the steel in this example. Consequently, it is concluded from the parameter sensitivity information that the uncertainty in the heat release rate could not result in a different conclusion.

F.6 Conclusion

Based on the analysis above, a 50.3 MW lubricant fire in the curbed area located between Columns A, B, C, and D (Curb Location 1) is not predicted to cause the structural steel to exceed a temperature of 538 °C (1,000 °F). This is not the case for the proposed location near Column D (Curb Location 2). Consequently, the recommendation for the design package is to install the curbed area at Curb Location 1.

Overall, given the large volume of lubricant involved, it is significant that structural failure is not predicted for either the zone or the CFD fire models for Curb Location 1. Although it may seem counterintuitive, this is a direct result of the relatively small area in which the lubricant is confined. The curbing restricts the surface area of the lubricant spill, and, correspondingly, the heat release rate of the fire.

F.7 References

1. NUREG-1805, *Fire Dynamics Tool, 2004.*
2. NUREG-1824 (EPRI 1011999), *Verification and Validation of Selected Fire Models for Nuclear Power Plant Applications,* 2007.
3. *SFPE Handbook of Fire Protection Engineering,* 4th edition, 2008.
4. NIST SP 1018-5, *Fire Dynamics Simulator (Version 5), Technical Reference Guide, Vol. 3, Experimental Validation, 2010.*
5. NIST NCSTAR 1-5F, *Federal Building and Fire Safety Investigation of the World Trade Center Disaster: Computer Simulation o the Fires in the World Trade Center Towers,* 2005.
6. NIST SP 1086, *Consolidated Model of Fire Growth and Smoke Transport, CFAST (Version 6), Software Development and Model Evaluation Guide, 2009.*
7. U.O. Köylu and G.M. Faeth, Carbon Monoxide and Soot Emissions from Liquid-Fueled Buoyant Turbulent Diffusion Flames. Combustion and Flame, 87:61–76, 1991.
8. ASTM E119-10a. *Standard Test Methods for Fire Tests of Building Construction Materials,"* American Society for Testing and Materials, West Conshohocken, PA, 2010.
9. American Institute of Steel Construction, Steel Construction Manual, 13th Edition, New York, New York, 2006.

10. EPRI 1002981, *Fire Modeling Guide for Nuclear Power Plant Applications,* EPRI 1002981Electric Power Research Institute, Palo Alto, CA, August 2002.
11. SFPE, "Assessing Flame Radiation to External Targets from Pool Fires," *SFPE Engineering Guide,* Society of Fire Protection Engineers (SFPE), Bethesda, MD (1999).

F.8 Attachments

1. FDS input files:

   a. Lube_oil_fire_in_TB_Location_1.fds
   b. Lube_oil_fire_in_TB_Location_2.fds

2. CFAST input files:

   a. Lube oil fire in TB – Location 1 One compartment.in
   b. Lube oil fire in TB – Location 1 Two compartments.in
   c. Lube oil fire in TB – Location 2 One compartment.in
   d. Lube oil fire in TB – Location 2 Two compartments.in
   e. LubeOil.o
   f. thermal.csv

G
Transient Fire in a Multi-Compartment Corridor

G.1 Modeling Objective

The calculations described in this example predict the transport of smoke and heat from a stack of burning pallets through multiple compartments with different door heights and soffits. The purpose of the calculation is to determine whether important safe-shutdown equipment will fail, and, if so, at what time failure occurs. The time to smoke detector activation is also estimated.

G.2 Description of the Fire Scenario

General Description: The corridor provides access to a variety of spaces and contains support equipment. Various important cables are routed through these connecting spaces.

Geometry: This multi-compartment area consists of interconnected compartments and corridors on the same level. Figure G-1 illustrates the geometry.

Materials:

Construction: The walls, ceiling, and floor are made of concrete. The cabinets and cable trays are made of steel. All boundary surfaces are 0.5 meters thick, as shown in Figure G-1. Nominal values for the thermal properties of various materials in the compartment are listed in Table 3-1 (NUREG-1805, Table 2-3).

Cables: The cable trays contain cross-linked polyethylene (XPE or XLPE)-insulated cables with a Neoprene jacket. These cables have a diameter of approximately 1.5 cm (0.6 in), a jacket thickness of approximately 2 mm (0.079 in), and 7 conductors. The cables have a density of 1,375 kg/m^3, a specific heat of 1.39 kJ/kg/K, a thermal conductivity of 0.235 W/m/K, and an emissivity of 0.95 (NUREG/CR-6850 (EPRI 1011989)). They are considered damaged when the internal temperature just underneath the jacket reaches 330 °C (626 °F) or the exposure heat flux reaches 11 kW/m^2 (NUREG-6850 (EPRI 1011989), Table H-1). The tray locations are shown in Figure G-2.

Fire Protection Systems: There are nine smoke detectors, located as shown in Figure G-1. The detectors are UL-listed, with a nominal sensitivity of 4.9%/m. There is no automatic fire suppression.

Ventilation: The ventilation system supplies the combined space at a rate of 1.67 m^3/s (3,540 ft^3/min). The supply and return vents are shown in the drawing. There are three doors leading into the space, all of which are closed during normal operation.

Fire: The fire source, a stack of four wood pallets with two trash bags, is located in the corner, as shown in Figures G-1 and G-2.

G.3 Selection and Evaluation of Models

This section describes the applicability of each of the five fire models to this scenario. Note that a typical NPP fire modeling analysis would not require the use of all five models.

Algebraic Models: FIVE and the FDT^s are not capable of modeling fire conditions in multi-compartment scenarios, but do contain correlations that can be used for smoke detector activation estimates.

Zone Models: The fire scenario outlined in the previous section falls within the range of applicability for a zone model. Zone models can calculate the time-dependent Hot Gas Layer properties in multi-compartment scenarios, as well as the activation times of smoke detectors. Although the geometry in this scenario is somewhat complex, it can be handled by zone modeling since it is largely a group of interconnected compartments.

CFD Models: The primary advantage of a CFD model for this fire scenario is that CFD models can predict the fire more realistically. The CFD models can also provide greater accuracy when modeling smoke detector activation. The geometry of this scenario is somewhat complex due to the multiple compartments, and varying connections and these aspects can be modeled with greater accuracy using CFD models. If initial evaluations using zone modeling suggest that more detailed modeling is required, particularly in areas remote from the fire, the added input data development and model run times required for CFD models may be justified.

Validation: A source of validation data justifying the use of the fire models discussed above for this scenario is the NRC/EPRI V&V study documented in NUREG-1824 (EPRI 1011999). The National Institute of Standards and Technology (NIST) Multi-Compartment Test Series comprised 45 fire tests in a three-room suite, which consisted of two relatively small rooms connected via a relatively long corridor. The fire source, a gas burner, was located against the rear wall of one of the small compartments, and fire tests of 100 kW, 300 kW, and 500 kW were conducted. The present scenario has a larger fire in a larger, longer compartment.

Table G-1 lists various important model parameters and the ranges for which the NRC/EPRI validation study is applicable. The calculations in Table G-1 are for the fire room. The room width geometry is not within the range of validation; however, this is not a significant measure of model accuracy for this scenario, since room volume is more important for this scenario than aspect ratios. The natural ventilation parameter is just inside the range due to the large room-to-room connection, while the mechanical ventilation value is significantly out of range due to the low CFM; however, the large room-to-room opening provides more than enough ventilation for this scenario, so the mechanical ventilation parameter is also not a significant measure of model accuracy for this scenario.

Table G-1. Normalized parameter calculations for the Multi-Compartment Corridor fire scenario.

Quantity	Normalized Parameter Calculation	Validation Range	In Range?
Fire Froude Number	$$\dot{Q}^* = \frac{\dot{Q}}{\rho_\infty c_p T_\infty D^2 \sqrt{gD}} = \frac{2500}{1.2 \times 1.012 \times 293 \times 1.28^2 \times \sqrt{9.8 \times 1.28}} = 1.21$$	0.4 – 2.4	Yes
Flame Length, L_f, relative to the Ceiling Height, H	$$\frac{L_f}{H} = \frac{3.8}{6.1} = 0.62$$ $$L_f = D\left(3.7\,\dot{Q}^{*2/5} - 1.02\right) = 1.28\,(3.7 \times 1.21^{0.4} - 1.02) = 3.8$$	0.2 – 1.0	Yes
Ceiling Jet Radial Distance, r_{cj}, relative to the Ceiling Height, H	N/A	1.2 – 1.7	N/A
Equivalence Ratio, φ, as an indicator of the Ventilation Rate[1]	$$\varphi = \frac{\dot{m}_F/\dot{m}_{O_2}}{r} \equiv \frac{\dot{Q}}{r\,\Delta H\,\dot{m}_{O_2}} = \frac{2500}{13{,}100 \times 0.03} = 5.8$$ $$\dot{m}_{O_2} = 0.23\,\rho_\infty \dot{V} = 0.23 \times 1.2 \times 0.12 = 0.03$$	0.04 – 0.6	NA
Equivalence Ratio, φ, as an indicator of the Opening Ventilation	$$\varphi = \frac{\dot{m}_F/\dot{m}_{O_2}}{r} \equiv \frac{\dot{Q}}{r\,\Delta H\,\dot{m}_{O_2}} = \frac{2500}{13{,}100 \times 5.1} = 0.04$$ $$\dot{m}_{O_2} = 0.23 \cdot 0.5 A_o \sqrt{h_o} = 0.23 \times 0.5 \times 18\sqrt{6} = 5.1$$	0.04 – 0.6	Yes
Compartment Aspect Ratios	$$\frac{L}{H} = \frac{14.2}{6.1} = 2.33$$ $$\frac{W}{H} = \frac{3.0}{6.1} = 0.49$$	0.6 – 5.7	No[2]
Target Distance, r, relative to the Fire Diameter, D	N/A	2.2 – 5.7	N/A

[1] The mechanical ventilation of the fire room is prorated based on the volume fraction of the fire room to the total volume served by the mechanical ventilation system; however, for this scenario natural ventilation dominates, so mechanical ventilation does not affect the accuracy.
[2] Based on the room width to height ratio.
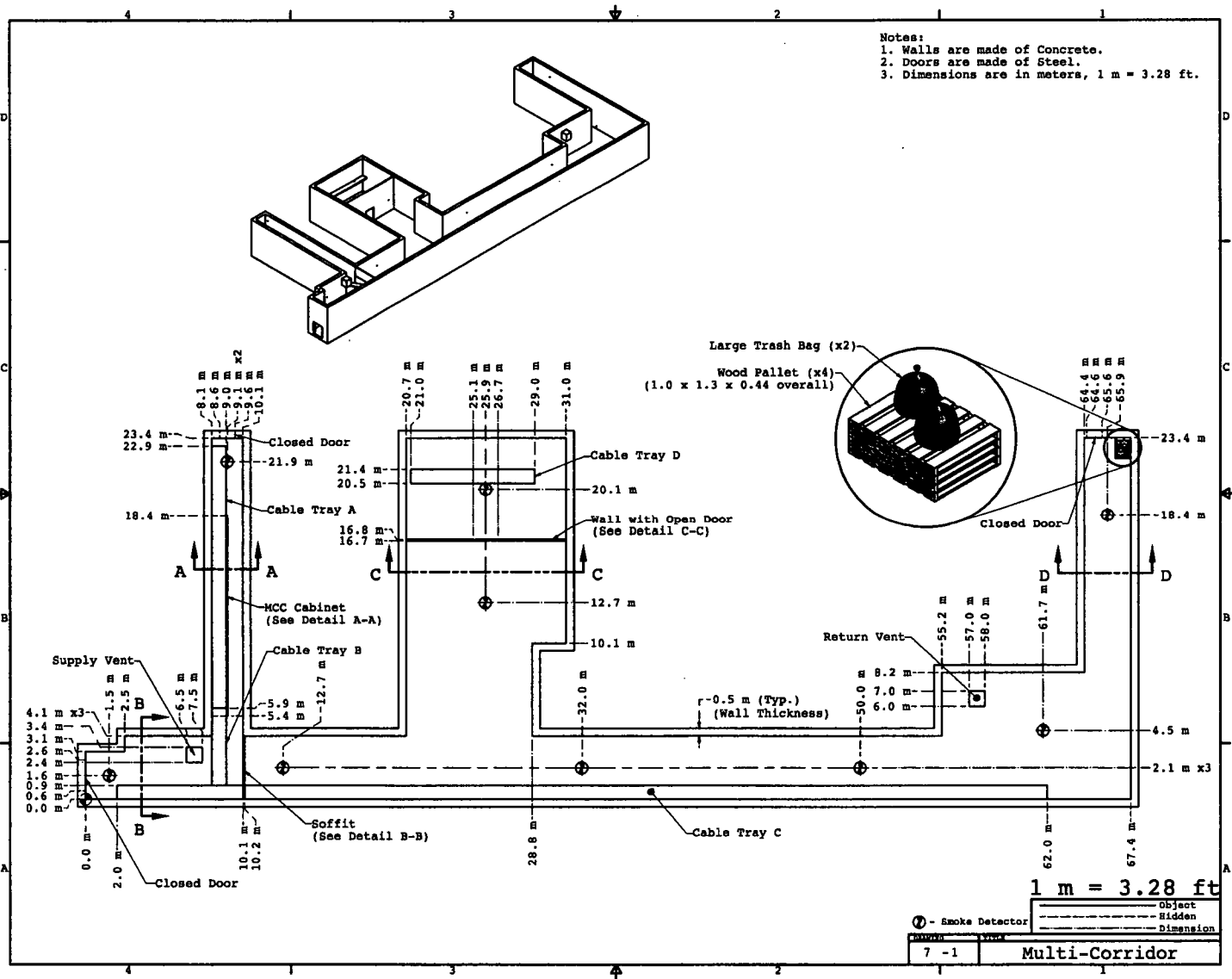
Figure G-1. Geometry of the Multi-Compartment Corridor.

Notes:
1. Walls are made of Concrete.
2. Doors are made of Steel.
3. Dimensions are in meters, 1 m = 3.28 ft.

Closed Door
21.9 m
Cable Tray A
Cable Tray D
20.1 m
Wall with Open Door
(See Detail C-C)

Large Trash Bag (x2)
Wood Pallet (x4)
(1.0 x 1.3 x 0.44 overall)
Closed Door
23.4 m
18.4 m

MCC Cabinet
(See Detail A-A)
12.7 m
10.1 m
Return Vent
Cable Tray B
Supply Vent
Soffit
(See Detail B-B)
Cable Tray C
Closed Door

4.5 m
2.1 m x3

1 m = 3.28 ft

⑦ - Smoke Detector

Object
Hidden
Dimension

7 -1   Multi-Corridor

Figure G-2. Geometry Details of the Multi-Compartment Corridor.

SECTION A-A

SECTION B-B

SECTION C-C

SECTION D-D

1 m = 3.28 ft

Object
Hidden
Dimension

☉ - Smoke Detector

DRAWING	TITLE
7 -2	Multi-Corridor

Transient Fire in a Multi-Compartment Corridor
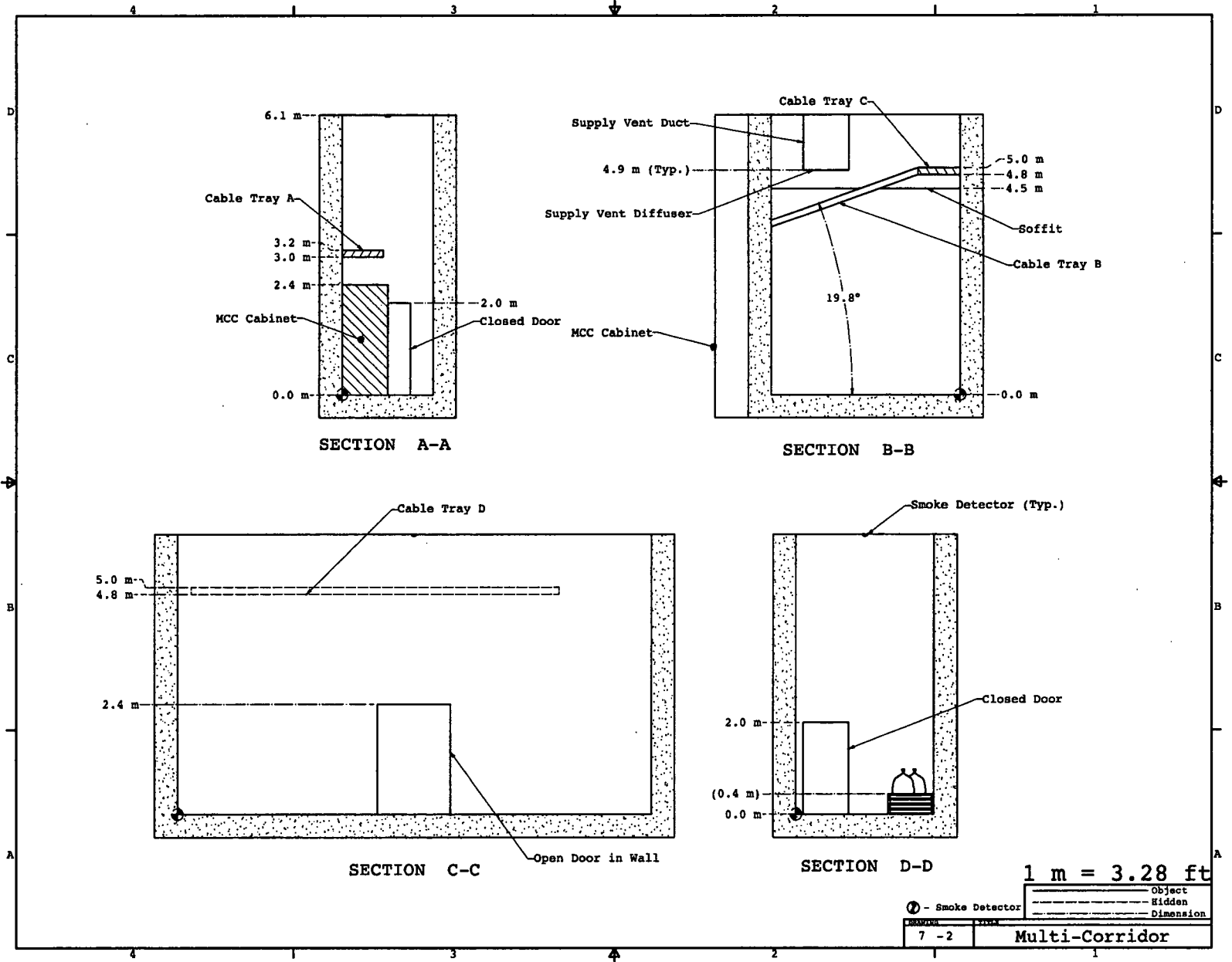
G.4 Estimation of Fire-Generated Conditions

This is a classic application of a zone fire model with a fire in one compartment connected to a number of additional compartments with doorway-like vents. Outputs of primary interest in the simulation include temperatures in the compartments, activation of smoke detectors in the compartments, and the temperature of cable targets in the compartments. This scenario was modeled using the zone model MAGIC.

Geometry: To simplify the process of modeling the multi-compartment geometry, the layout was divided into eight areas, as illustrated in Figure G-3. Note that the small indentation in compartment 1 was ignored for the MAGIC calculations. Connections between compartments was by door (compartments 5 to 6), by soffit (compartments 2 to 3), or left open by using a full-wall opening. Table G-2 summarizes the compartment dimensions used for zone modeling. A graphical depiction of the scenario, as modeled in MAGIC, is shown in Figure G-4.
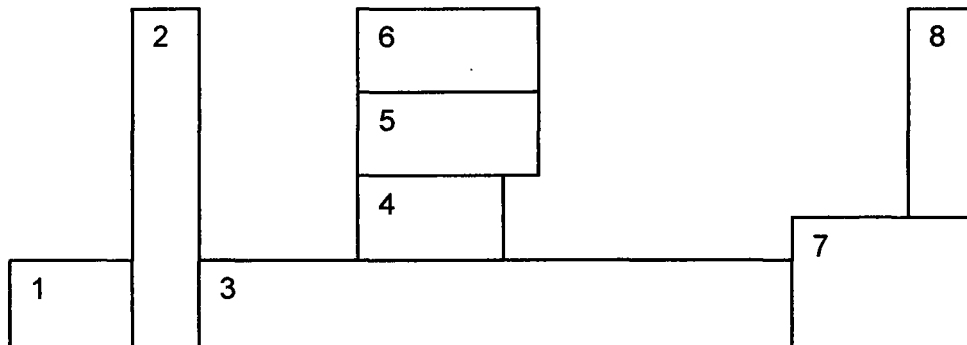
Figure G-3. Effective corridor layout for implementation in zone models (not to scale).

Table G-2. Compartment dimensions for Corridor scenario.

Comp.	Length (m)	Width (m)	Area (m²)
1	7.6	4.1	31.2
2	2.0	22.9	45.8
3	44.1	4.1	180.8
4	8.1	5	40.5
5	10.4	6.61	68.7
6	10.3	6.1	62.8
7	12.2	8.2	100.0
8	3	14.2	42.6

Fire: The fire source, a stack of four wood pallets with two trash bags, is located in the corner, as shown in Figures G-1 and G-2. As shown in the figures, the pallet stack measures 0.44 m (1.4 ft) high. The fire grows following a "t-squared" curve to a maximum value of 2,500 kW in

7 minutes and remains steady for 8 additional minutes. The HRR is estimated by combining separate estimates for a 0.44 m (1.4 ft) stack of wood pallets and 2 trash bags filled with paper and using HRR data from the *Heat Release Rates* chapter of the *SFPE Handbook*. After that, the fire's HRR decays linearly to zero in 8 minutes.

The radiative fraction of the fire is taken to be 35%, a value typical of sooty fires (*SFPE Handbook*). The soot yield is 1.5%, typical of cellulosic materials like wood and paper (*SFPE Handbook*). MAGIC uses a mass loss rate to determine the HRR; this is simply the HRR divided by the heat of combustion.

The fire was modeled as a 1.3 m^2 (14 m^2) source (equivalent diameter of 1.28 m (4.2 ft)) at an elevation of 0.44 m (1.4 ft) (see Figure G-2). For the fire, an oxygen-fuel stoichiometric ratio of 1.3 and a heat of combustion of 16.4 kJ/g were used (*SFPE Handbook*). An average specific area of 114 was calculated based on an average soot yield value for wood (*SFPE Handbook*).

Materials: The materials are as described above.

Ventilation: The ventilation rate is given above. The vents in Figure G-1 are square, but, because MAGIC uses round vents, an equivalent diameter of 1.13 m (3.7 ft) was used as input. In room-to-room connections with the same ceiling height, a shallow (0.1 m) soffit was added to allow smoother model execution. Finally, the only leakage from the space occurs via a 2.5-cm (1 in) crack under each of the three doors.

Fire Protection Systems: In MAGIC, there is no direct way of calculating smoke density for smoke detector activation. Consistent with NUREG-1805, the recommended approach given by the developers is to model the smoke detector as a sprinkler with a low activation temperature and RTI. An activation temperature of 30 °C (86 °F) and an RTI of 5 $(m/s)^{1/2}$ was selected.
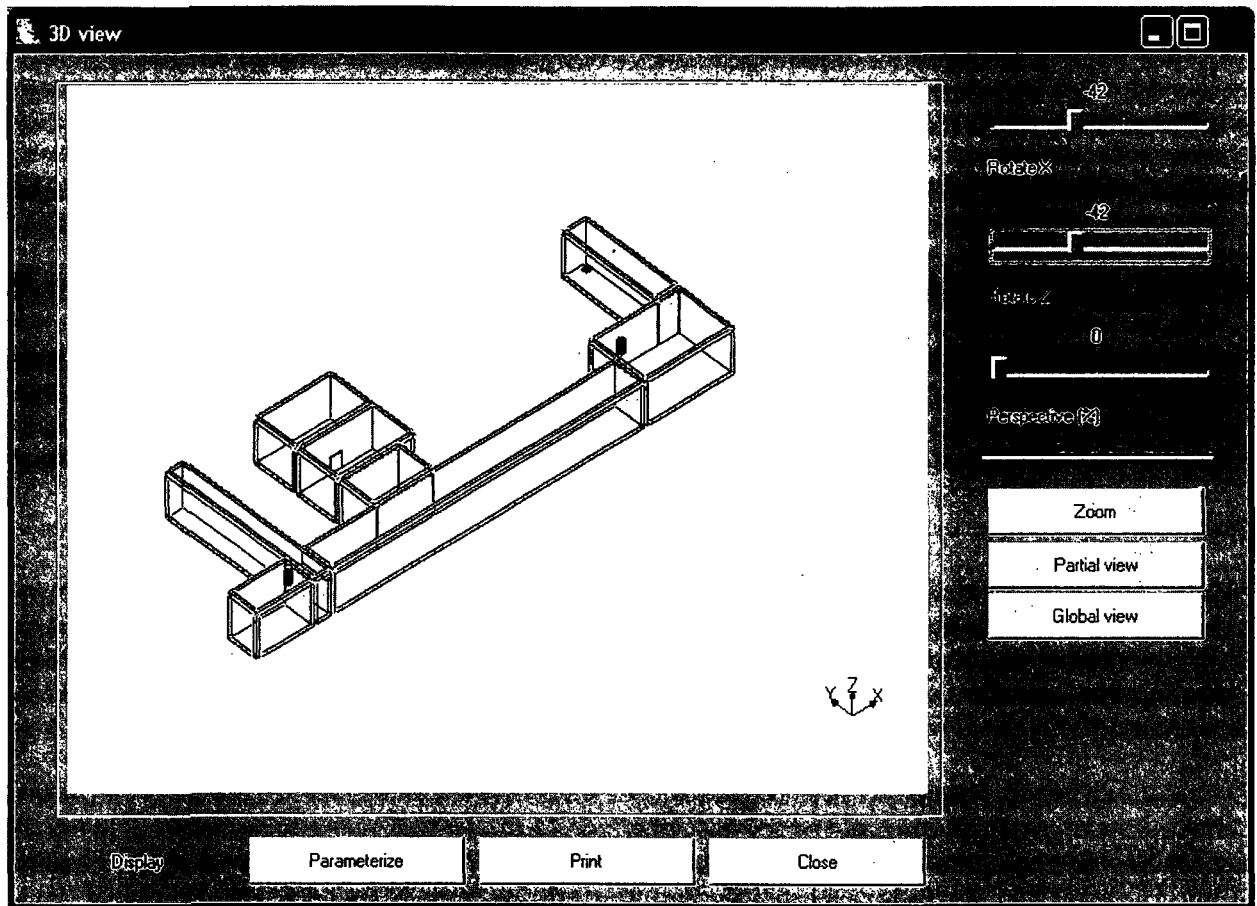
Figure G-4. MAGIC rendering of the Corridor scenario.

G.5 Evaluation of Results

The purpose of the calculations described above is to determine whether a stack of burning pallets in a corridor could generate gas temperatures in adjacent compartments that are capable of damaging cables and electrical equipment. Smoke detector activation is also estimated. Only the zone model MAGIC was used for this scenario. In general, the results demonstrate that the fire is not capable of generating damaging conditions, even in the compartment of fire origin; as a result, there is no need for detailed modeling of the targets in remote locations. However, an additional simulation was run with the fire's HRR increased by an order of magnitude, which was also found to generate HGL conditions incapable of causing damage to the cables in the remote rooms based on the failure criteria cited above. The following sections describe the results in greater detail.

G.5.1 Heat Release Rate

The heat release rate produced by MAGIC was unmodified from that based on the input (i.e., there was no oxygen starvation). The heat release rate increases as a function of t^2, has a steady burning phase, and then burns out, as shown in Figure G-5.

Heat Release Rate

Time (s)
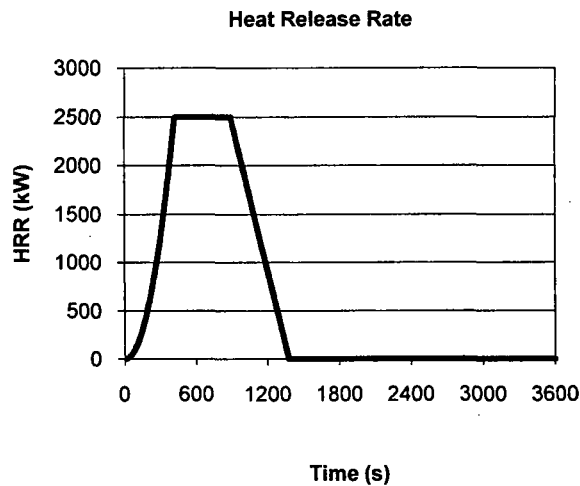
Figure G-5. Heat Release Rate produced by MAGIC for the Corridor Scenario.

G.5.2 HGL Temperature

MAGIC predicts peak temperatures of about 205 °C (400 °F) in the corridor where the fire is located (see Figure G-6). This is below the cable damage temperature threshold of 330 °C (625 °F), cited above. The HGL temperatures for the other corridors are substantially lower; for example, the center corridor is also shown in Figure G-6. A comparison of Figures G-6 and G-5 will show that the change in HGL temperature closely follows the change in the heat release rate.

HGL Temperature Fire Room

HGL Temperature Center Corridor
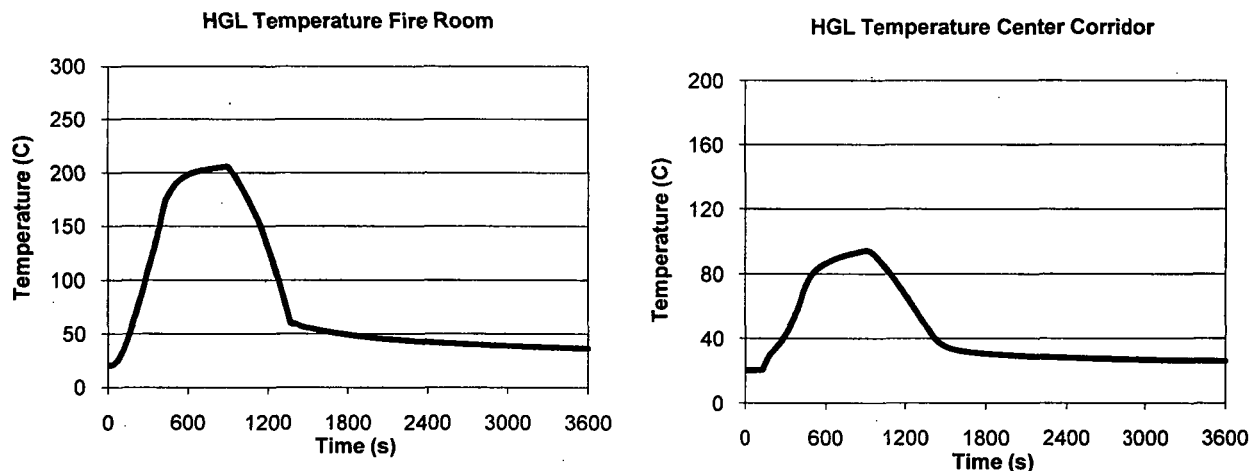
Figure G-6. Hot Gas Layer Temperature Predictions by MAGIC for the Corridor Scenario.

This scenario concerns the prediction of cable damage at a location outside the compartment of fire origin. Prior to conducting detailed analyses of cable heating in another compartment, the temperature of the Hot Gas Layer in the compartment of fire origin can be modeled as a potential screening tool. If the HGL temperature within the compartment of origin is not likely to cause damage to cables in that compartment, damage to cables outside the fire compartment is even more unlikely. As part of this approach, it is conservatively assumed that the cable surface temperature will match the HGL temperature (i.e., heat-up of the cable is assumed to be immediate).

G.5.3 Smoke Detection

The smoke detector activation time in the corridor containing the burning pallets was predicted to be 110 seconds. At this time the fire is only at 172 kW.

G.5.4 Uncertainty

Chapter 4, Model Uncertainty, provides guidance on how to express the uncertainty of the MAGIC predictions. In the NRC/EPRI V&V study (NUREG-1824 (EPRI 1011999)), it was found that MAGIC predictions of Hot Gas Layer temperatures are, on average, 1% greater than corresponding measurements, with a relative standard deviation of 7%. This suggests that the true value of the peak HGL temperature in this scenario is normally distributed with a mean of 203 °C and a standard deviation of 14.2 °C. Therefore, the probability that the cable temperature would exceed 330 °C (626 °F) is:

$$P(T > 330) = \frac{1}{2}\,\text{erfc}\left(\frac{330 - 203}{14.2\sqrt{2}}\right) \cong 0 \qquad (\text{G-1})$$

In other words, there is a near-zero probability of exceeding the damage temperature threshold for cables within the compartment of fire origin based on a surrounding HGL temperature, according to the MAGIC prediction. This demonstrates that detailed analyses of the cables outside the compartment of original are not warranted.

G.5.5 Sensitivity

There can be considerable uncertainty in the heat release rates of real fires. As a result, it is prudent to consider the sensitivity of simulation results to the selected heat release rates. Table 4.2 indicates that the Hot Gas Layer temperature prediction is related to the heat release rate by a two-thirds power dependence.

Equation 16 in Chapter 4 is a simple formula which can be used to estimate the relative change in the model Hot Gas Layer temperature output quantity, $\Delta T/(T - T_0)$, due to the relative change in the model heat release rate input parameter, $\Delta \dot{Q}/\dot{Q}$:

$$\frac{\Delta T}{T - T_0} \approx \frac{2}{3}\frac{\Delta \dot{Q}}{\dot{Q}} \tag{G-2}$$

The predicted Hot Gas Layer temperature is 203°C (397 °F), considerably less than the 330°C (625 °F) target damage temperature of interest. Based on this equation, more than twice the heat release rate of the fire would be required to cause the Hot Gas Layer temperature to increase to the damage temperature of interest.

G.6 Conclusion

The zone model MAGIC does not predict HGL temperatures capable of cable damage in any compartment or corridor, including the corridor containing the burning pallets, while accounting for uncertainty in the temperature predictions of MAGIC and the sensitivity of the predictions to variations in the heat release rate. An additional simulation was run with the fire HRR increased by an order of magnitude, which was also found to generate HGL conditions incapable of causing damage to the cables in the remote rooms. Based on a simplified method for smoke detector activation, smoke detector operation occurs at about 110 seconds.

G.7 References

1. NUREG-1805, *Fire Dynamics Tools.*
2. NUREG-1824 (EPRI 1011999), *Verification and Validation of Selected Fire Models for Nuclear Power Plant Applications*, 2007.
3. NUREG/CR-6850 (EPRI 1011999), *Fire PRA Methodology for Nuclear Power Facilities.*
4. *SFPE Handbook of Fire Protection Engineering*, 4th edition, 2008.
5. UL 217, Underwriters Laboratories, Inc., Single Station Fire Alarm Device.
6. NIST SP 1018-5, *Fire Dynamics Simulator (Version 5), Technical Reference Guide, Vol. 3, Experimental Validation.*
7. NIST SP 1086, *Consolidated Model of Fire Growth and Smoke Transport, CFAST (Version 6), Software Development and Model Evaluation Guide*
8. Gay, L., C. Epiard, and B. Gautier, "MAGIC Software Version 4.1.1: Mathematical Model," EdF HI82/04/024/B, Electricité de France, France, November 2005.

G.8 Attachments

1. MAGIC input file: Corridor.cas

H
Cable Tray Fire in Annulus

H.1 Modeling Objective

The calculations described in this Appendix examine the potential for damage to redundant safe-shutdown cables due to a fire in an adjacent tray in the annulus region of the containment building. In addition, the calculations provide information on the effectiveness of some protection strategies.

H.2 Description of the Fire Scenario

General Description: The annulus is the region between the primary containment structure and the secondary containment (shield) building. The primary and secondary containments are cylindrical with domes on top. The annulus space contains a variety of penetrations from the reactor to the external support systems. One of these penetrations contains two cable trays with cables that control systems in both trains of safety equipment. A fire starts in one tray of cables and spreads vertically and horizontally along the cables in that tray.

Geometry: The layout of the annulus is shown in Figure H-1. The exterior wall is made of concrete, while the interior wall and cable trays are made of steel. The cable tray locations are shown in Figure H-2.

Materials: Property values for the relevant materials are listed in Table 3-1. The annulus wall thicknesses are indicated in the drawing. The cable tray steel is approximately 2 mm (0.079 in) thick.

Cables: The cable trays are filled with PE-insulated, PVC-jacketed control cables. These cables have a diameter of approximately 1.5 cm (0.6 in), a jacket thickness of approximately 1.5 mm (0.06 in), and 7 conductors. There are approximately 120 cables in each tray. The mass of each cable is 0.4 kg/m. The mass fraction of copper is 0.67. These cables fail when the internal temperature just underneath the jacket reaches approximately 200 °C (390 °F) (NUREG/CR-6931, Vol. 2, Table 5.10) or the exposure heat flux exceeds 6 kW/m^2 (NUREG-1805, Appendix A).

Fire: A fire ignites at the base of the lower cable train in the vicinity of the bend at the inner wall. From the results of the CHRISTIFIRE project (NUREG/CR-7010, Vol. 1), the burning rate of the PVC cable is 250 kW/m^2. The heat of combustion of the cables is 16 MJ/kg, which is appropriate for PE/PVC cable. A mixture of PE (C_2H_4) and PVC (C_2H_3Cl) would have an effective chemical formula of $C_2H_{3.5}Cl_{0.5}$.

The fire spreads vertically at a rate of 258 mm/s and horizontally at a rate of 0.9 mm/s (NUREG/CR-6850 (EPRI 1011989), Appendix R). The peak heat release rate would be 945 kW once all of the cables in the first tray are burning.

For this scenario, the soot yield of the burning cable is 0.1; that is, 10% of the cable mass consumed is converted into smoke particulate. The radiative fraction of the fire is 35%, typical of sooty fires (Tewarson, *SFPE Handbook*, Table 3-4.16).

Cable Tray Fire in Annulus

Detection and Suppression Systems: Smoke detectors are located on the wall of the shield building 15 m (50 ft) above-grade. The detectors are UL-listed, with a nominal sensitivity of 4.9%/m. Standard response sprinklers are located on the inner wall, as shown in the drawing. The sprinklers have a response time index (RTI) of 130 $(m\ s)^{1/2}$ and activate at a temperature of 100 °C (212 °F) (NUREG-1805, Chap. 10). Each sprinkler is topped by heat collectors designed to trap heat from a fire.

Ventilation: None.

Figure H-1. Geometry of the Annulus.

90°

ø 38.4 m

ø 35.0 m

180°

0°

B

D

270°

D

SECTION   A-A

E

37.2 m

35.5 m

32.0 m

29.0 m

Concrete
Shield
Building

Steel
Containment
Liner

A

A

C

Annulus Space

Ground Level

0.0 m

8.2 m

E

Ground Level

SECTION E-E, ISO VIEW

1 m = 3.28 ft

Object
Hidden
Dimension

DRAWING   TITLE
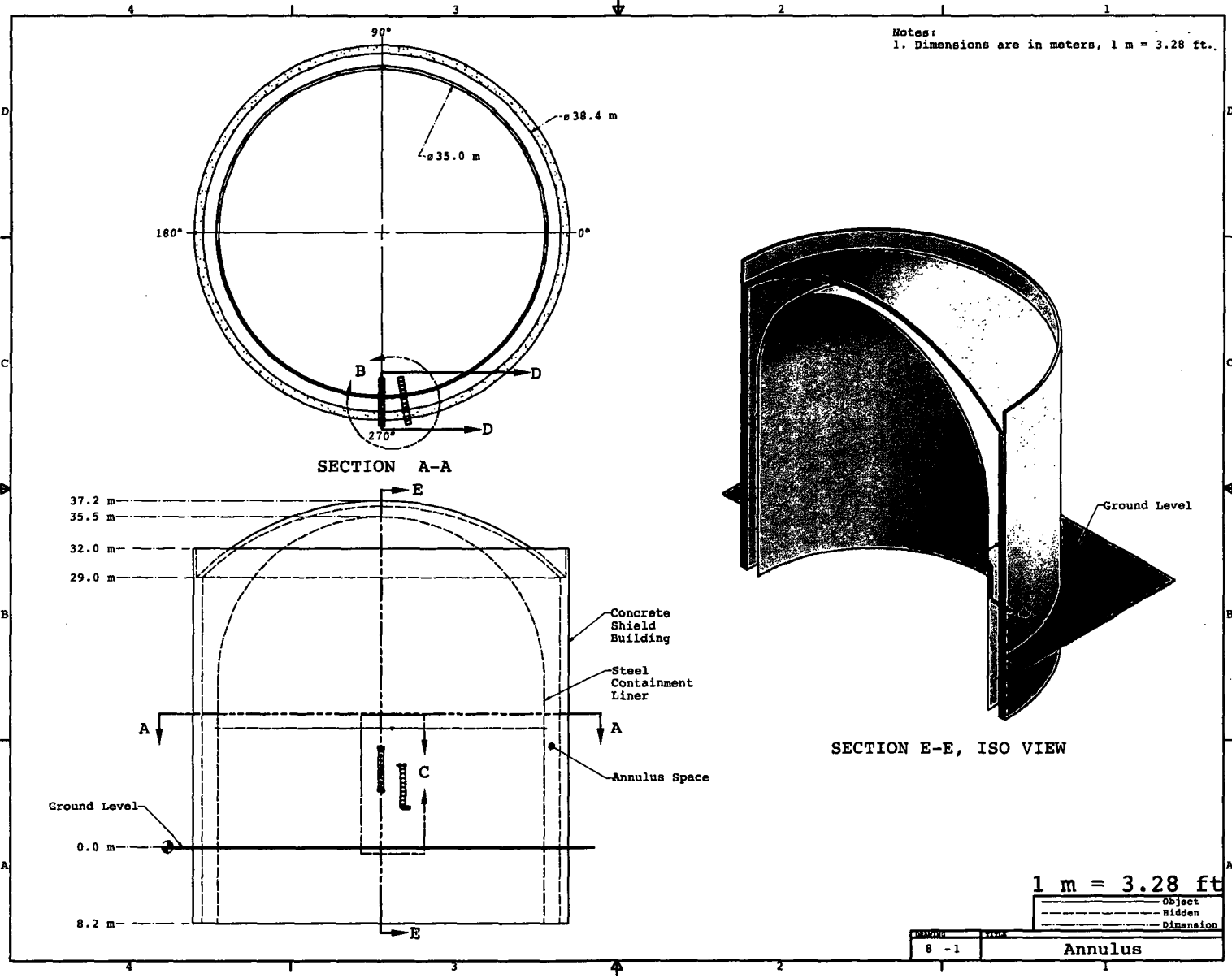
8 -1   Annulus

Figure H-2. Geometry details of the Annulus.

DETAIL B

Sprinkler
Containment Liner
Sprinkler Pipe
Shield Building

Ignition Point on
Lower Cable Tray

−0.0254 m

1.7 m

−0.9 m

(270°) 275° 280°

DETAIL C

0.6 m (Typ.)

−1.7 m

Sprinkler Pipe
Sprinkler Head

1.9 m
4.6 m
6.2 m

4.6 m
4.3 m

Ignition Point
on Cable Tray

Ground Level

SECTION D-D

Sprinkler Head

Cable Tray
Side View

Containment Liner
Penetration

Ignition Point
on Cable Tray

Shield Building
Penetration

1 m = 3.28 ft

Object
Hidden
Dimension

8 -2

Annulus

H.3 Selection and Evaluation of Fire Models

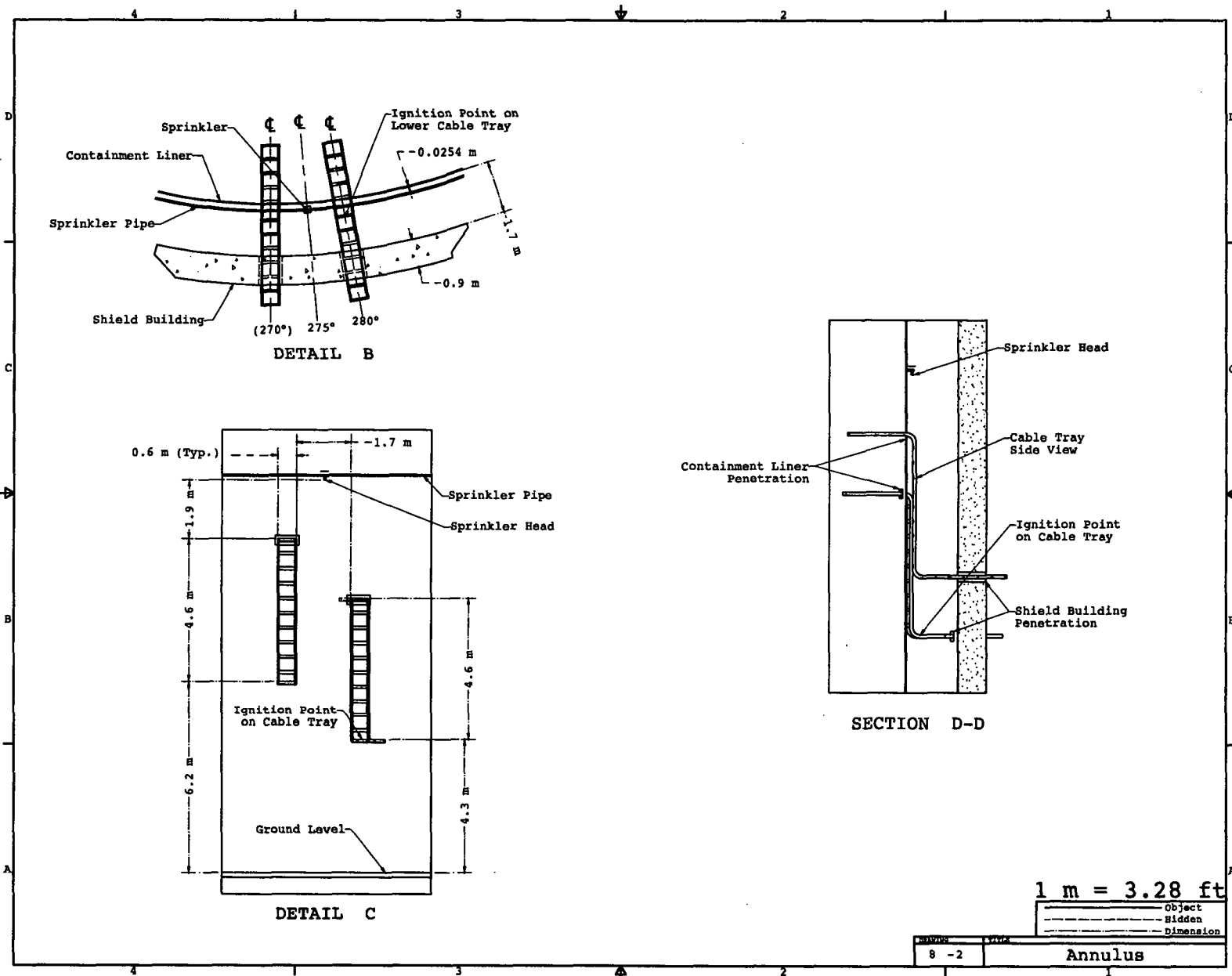The fire scenario described above can be categorized as an "open" rather than a "compartment" fire. Because of this, compartment fire models are generally inapplicable, although certain algorithms contained within these models may still apply.

Algebraic Models: The heat flux calculations in the FDT^s and FIVE can provide useful screening information for this scenario. For comparison purposes, both the point source and solid flame calculations from the FDT^s were used for this scenario. Given the proximity of the two cable trays, the solid flame model is expected to provide a more accurate estimate of the heat flux to the adjacent cable tray.

Zone Models: The geometry of this scenario is quite unique for the application of a zone model that is typically used with mostly rectangular compartments where an HGL forms from a fire source. Still, since the containment building is so large that the curvature of the walls will have little effect, a smaller compartment can be defined with a tall ceiling height and large vents so that any layer that forms will flow out into the rest of the annulus without impacting the region directly around the fire source and redundant cable tray target.

CFD Models: Although the geometry of this scenario is unlike the mostly rectangular compartments found in a nuclear power plant, it is not particularly difficult to model in FDS. In fact, the containment building is so large that the curvature of the walls has little effect on the results of the calculation. Figure H-3 is an FDS/Smokeview depiction of the scenario.

Validation: According to NUREG-1824 (EPRI 1011999), the applicability of the validation results can be determined using normalized parameters traditionally used in fire science. Normalized parameters allow users to compare results from scenarios of different scales by normalizing physical characteristics of the scenario. Table H-1 lists the parameters, and, where applicable, the values calculated for this scenario. For this scenario, only two of the parameters are applicable because the others address phenomena unique to compartment fires. The parameter that falls outside of the validation range of NUREG-1824 (EPRI 1011999), r/D, indicates that in this scenario the fire is relatively close to the target.

Only FDS was used to predict the smoke detector and sprinkler activation. The sprinkler and smoke detector activation algorithms in CFAST were developed under the assumption that the device is located in the fire plume or Hot Gas Layer. The plume would have limited impact on the devices located in the annulus, and the size of the annulus makes the accumulation of a Hot Gas Layer unlikely. In addition, smoke detector activation in CFAST is predicted based on a temperature rise above ambient rather than actual smoke obscuration. This approximation has been shown to have significant uncertainties (Schiffiliti, 1996).

Cable Tray Fire in Annulus

Table H-1. Normalized parameter calculations for the Annulus fire scenario.

Quantity	Normalized Parameter Calculation	Validation Range	In Range?
Fire Froude Number	$\dot{Q}^* = \dfrac{\dot{Q}}{\rho_\infty c_p T_\infty D^2 \sqrt{gD}} = \dfrac{945}{1.2 \times 1.012 \times 293 \times 1.1^2 \times \sqrt{9.8 \times 1.1}} \cong 0.7$	0.4 – 2.4	Yes
Flame Length, L_f, relative to the Ceiling Height, H	N/A	0.2 – 1.0	N/A
Ceiling Jet Radial Distance, r_{cj}, relative to the Ceiling Height, H	N/A	1.2 – 1.7	N/A
Equivalence Ratio, φ, as an indicator of the Ventilation Rate	N/A	0.04 – 0.6	N/A
Compartment Aspect Ratio	N/A	0.6 – 5.7	N/A
Target Distance, r, relative to the Fire Diameter, D	$\dfrac{r}{D} = \dfrac{1.7}{1.1} \cong 1.5$	2.2 – 5.7	No

Figure H-3. FDS/Smokeview rendering of the Annulus scenario.

Cable Tray Fire in Annulus

H.4 Estimation of Fire-Generated Conditions

This section provides specific details on how each model is set up and run.

H.4.1 Algebraic Models (FDT^s)

The FDT^s (NUREG 1805, 2005) contain several correlations for estimating the heat flux at a fixed distance from the exposure fire. The FDT^s spreadsheets

05.1_Heat_Flux_Calculations_Wind_Free.xls (Point Source) and

05.1_Heat_Flux_Calculations_Wind_Free.xls (Solid Flame 1)

were used in this analysis. In addition, the solid flame 1 spreadsheet calculates the equivalent diameter of the fire and the flame height to determine the size of the exposure fire.

Using the estimated peak heat release rate of 945 kW and a fire-to-target distance of 1.7 m (5.6 ft), the heat flux based on the point source model is estimated as 4.3 kW/m^2. Using the solid flame model, the heat flux is estimated as 7.1 kW/m^2 with an effective area of 1.02 m^2 (11 ft^2)and a flame height of 2.48 m (8.1 ft). As expected, the solid flame model estimate of the heat flux is significantly higher than the point source value. The spreadsheet for the solid flame calculations is shown in Figure H-4.

H-8

CHAPTER 5
ESTIMATING RADIANT HEAT FLUX FROM FIRE
TO A TARGET FUEL AT GROUND LEVEL
UNDER WIND-FREE CONDITIONS
SOLID FLAME RADIATION MODEL

Version 1805.1
(SI Units)

Parameters in YELLOW CELLS are Entered by the User.

Project / Inspection Title: Fire Model User's Guide Appendix H

INPUT PARAMETERS

Mass Burning Rate of Fuel (m″)   kg/m²-sec
Effective Heat of Combustion of Fuel ($\Delta H_{c,eff}$)   kJ/kg

Empirical Constant (kβ)   m^{-1}
Heat Release Rate (Q)   kW
Fuel Area or Dike Area (A_{dike})   1.02 m²

Distance between Fire and Target (L)   1.70 m
OPTIONAL CALCULATION FOR GIVEN HEAT RELEASE RATE
Select "User Specified Value" from Fuel Type Menu and Enter Your HRR here →   945   kW

THERMAL PROPERTIES DATA
BURNING RATE DATA FOR FUELS

Fuel	Mass Burning Rate m″ (kg/m²-sec)	Heat of Combustion ΔH_c (kJ/kg)	Constant kβ (m⁻¹)	
Methanol	0.017	20,000	100	**Select Fuel Type**
Ethanol	0.015	26,800	100	
Butane	0.078	45,700	2.7	Scroll to desired fuel type then
Benzene	0.085	40,100	2.7	Click on selection
Hexane	0.074	44,700	1.9	
Heptane	0.101	44,600	1.1	
Xylene	0.09	40,800	1.4	
Acetone	0.041	25,800	1.9	
Dioxane	0.018	26,200	5.4	
Diethy Ether	0.085	34,200	0.7	
Benzine	0.048	44,700	3.6	
Gasoline	0.055	43,700	2.1	
Kerosine	0.039	43,200	3.5	
Diesel	0.045	44,400	2.1	
JP-4	0.051	43,500	3.6	
JP-5	0.054	43,000	1.6	
Transformer Oil, Hydrocarbon	0.039	46,000	0.7	
5(0 Silicon Transformer Fluid	0.005	28,100	100	
Fuel Oil, Heavy	0.035	39,700	1.7	
Crude Oil	0.0335	42,600	2.8	
Lube Oil	0.039	46,000	0.7	
Douglas Fir Plywood	0.01082	10,900	100	
User Specified Value	Enter Value	Enter Value	Enter Value	

Reference: SFPE, Handbook of Fire Protection Engineering, 3rd Edition, 2002, Page 3-26.

Figure H-4. Screenshot showing FDTs Heat Flux Calculation using Solid Flame Approximation

CHAPTER 5
ESTIMATING RADIANT HEAT FLUX FROM FIRE
TO A TARGET FUEL AT GROUND LEVEL
UNDER WIND-FREE CONDITIONS
SOLID FLAME RADIATION MODEL

Version 1805.1
(SI Units)

ESTIMATING RADIATIVE HEAT FLUX TO A TARGET FUEL

SOLID FLAME RADIATION MODEL

$q'' = EF_{1 \rightarrow 2}$

Where

q'' = incident radiative heat flux on the target (kW/m^2)
E = emissive power of the pool fire flame (kW/m^2)
$F_{1 \rightarrow 2}$ = view factor between target and the flame

Pool Fire Diameter Calculation

$$A_{dike} = \pi D^2/4$$

$$D = \sqrt{(4A_{dike}/\pi)}$$

Where

A_{dike} = surface area of pool fire (m^2)
D = pool fire diamter (m)

D = 1.14 m

Emissive Power Calculation

E = $58 \, (10^{-0.00823 \, D})$

Where

E = emissive power of the pool fire flame (kW/m^2)
D = diameter of the pool fire (m)

E = 56.76 kW/m^2

View Factor Calculation

$F_{1 \rightarrow 2,H}$ = $(B-1/S)/\pi (B^2-1)^{1/2} \tan^{-1} ((B+1)(S-1)/(B-1)(S+1))^{1/2} - (A-1/S)/(\pi (A^2-1)^{1/2}) \tan^{-1} ((A+1)(S-1)/(A-1)(S+1))^{1/2}$
$F_{1 \rightarrow 2,V}$ = $1/(\pi S) \tan^{-1}(h/(S^2-1)^{1/2}) - (h/\pi S) \tan^{-1} ((S-1)/(S+1))^{1/2} + Ah/\pi S(A^2-1)^{1/2} \tan^{-1} ((A+1)(S-1)/(A-1)(S+1))^{1/2}$
A = $(h^2+S^2+1)/2S$
B = $(1+S^2)/2S$
S = $2R/D$
h = $2H_f/D$
$F_{1 \rightarrow 2,max}$ = $\sqrt{(F^2_{1 \rightarrow 2,H} + F^2_{1 \rightarrow 2,V})}$

Where

$F_{1 \rightarrow 2,H}$ = horizontal view factor
$F_{1 \rightarrow 2,V}$ = vertical view factor
$F_{1 \rightarrow 2,max}$ = maximum view factor
R = distance from center of the pool fire to edge of the target (m)
H_f = height of the pool fire flame (m)
D = pool fire diameter (m)

Figure H-4. Screenshot showing FDTs Heat Flux Calculation using Solid Flame Approximation (continued)

CHAPTER 5
ESTIMATING RADIANT HEAT FLUX FROM FIRE
TO A TARGET FUEL AT GROUND LEVEL
UNDER WIND-FREE CONDITIONS
SOLID FLAME RADIATION MODEL

Version 1805.1
(SI Units)

Distance from Center of the Pool Fire to Edge of the Target Calculation

R = L + D/2

Where
R = distance from center of the pool fire to edge of the target (m)
L = distance between pool fire and target (m)
D = pool fire diameter (m)

R = L+D/2 =   2.270 m

Heat Release Rate Calculation

$$Q = m''\Delta H_{c,eff} (1 - e^{-k\beta D}) A_{dike}$$

Where
Q = pool fire heat release rate (kW)
m" = mass burning rate of fuel per unit surface area (kg/m²-sec)
ΔH_c = effective heat of combustion of fuel (kJ/kg)
A_{dike} = surface area of pool fire (area involved in vaporization) (m²)
$k\beta$ = empirical constant (m⁻¹)
D = diameter of pool fire (diameter involved in vaporization, circular pool is assumed) (m)

Q =   #VALUE! kW

Pool Fire Flame Height Calculation

$$H_f = 0.235 Q^{2/5} - 1.02 D$$

Where
Hf = flame height (m)
Q = heat release rate of fire (kW)
D = fire diameter (m)

H_f =   2.479 m

S = 2R/D =   3.983
h = 2H_f/D =   4.350
A = (h²+S²+1)/2S =   4.493
B = (1+S²)/2S =   2.117

	F_{H1}	F_{H2}	F_{H3}	F_{H4}	$F_{1\to2,H}$
$F_{1\to2,H}$ = 0.053		0.318	0.912	0.308	0.770 0.053
$F_{1\to2,V}$ = 0.113	F_{V1}	F_{V2}	F_{V3}	F_{V4}	$F_{1\to2,V}$
$F_{1\to2,max} = \sqrt{(F^2_{1\to2,H} + F^2_{1\to2,V})}$ = 0.125		0.068	0.229	0.357	0.770 0.113

Figure H-4. Screenshot showing FDTs Heat Flux Calculation using Solid Flame Approximation (continued)

CHAPTER 5
ESTIMATING RADIANT HEAT FLUX FROM FIRE
TO A TARGET FUEL AT GROUND LEVEL
UNDER WIND-FREE CONDITIONS
SOLID FLAME RADIATION MODEL

Version 1805.1
(SI Units)

RADIATIVE HEAT FLUX CALCULATION

$$q'' = EF_{1\text{->}2}$$

$q'' =$	7.10 kW/m²	0.63 Btu/ft²-sec

NOTE:

Prepared by: [   ]   Date: [   ]   Organization: [   ]

Checked by: [   ]   Date: [   ]   Organization: [   ]

Additional Information:

[   ]

Figure H-4. Screenshot showing FDTs Heat Flux Calculation using Solid Flame Approximation (continued)

H.4.2 Zone Models (CFAST)

Geometry: Only the section of the annulus directly enclosing the cables and relevant targets is included in a single-compartment simulation. A taller ceiling was included to allow the HGL to form well away from the targets, since the much larger volume of the whole annulus would have to fill before any HGL would form near the fire source and targets. Horizontal vents on each side of the annulus section were included and sized to the full cross-section of the annulus to simulate flow from the simulation region to the rest of the annulus. Surfaces of this section of the annulus are constructed with concrete of the specified thickness. A screenshot of the geometry input for CFAST is shown in Figure H-5.

Fire: The fire originates near the base of the vertical portion of the cable train and quickly spreads to the entire vertical surface (4.6 m (15 ft) high by 0.6 m (2 ft) wide). With the specified HRR of 250 kW/m^2 (NUREG/CR-7010, Volume 1), this results in a peak HRR of approximately 945 kW. To determine the duration of the fire, it is calculated that 120 cables per tray multiplied by 0.4 kg/m equals 48 kg/m total mass per unit length of tray. One-third (0.33) of this mass has been determined to be combustible plastic, or 15.8 kg/m. Since the tray is 0.6 m (24 in) wide, the mass of combustibles per unit area of burning surface is 15.8/0.6=26.3 kg/m^2. The specified heat of combustion for PE/PVC is 16,000 kJ/kg (NUREG/CR-7010, Volume 1); thus, the combustible "load" is 420,800 kJ/m^2. Using the specified HRR per unit area, the duration of the fire at any particular location along the tray is 420,800/250=1,683 s. A screenshot of the fire input for CFAST is shown in Figure H-6.

Cables: One of the objectives of the calculation is to estimate the potential damage to the cables within the redundant train. CFAST calculates target temperature using a 1-D heat transfer calculation into a rectangular target. In this simulation, the cables are modeled with the uniform thermal properties given above. Following the Thermally-Induced Electrical Failure (THIEF) methodology in NUREG/CR-6931, Vol. 3, electrical functionality is lost when the temperature just inside the 1.5 mm (0.06 in) jacket reaches 200 °C (392 °F). Thus, the target thickness is specified to be 3 mm (0.12 in) so that the calculated center temperature of the target represents the temperature of the inside surface of the jacket insulation. No attempt was made in the simulation to estimate ignition and spread of the fire over the cables, which is why the in-depth heat penetration calculation is focused on a single cable.
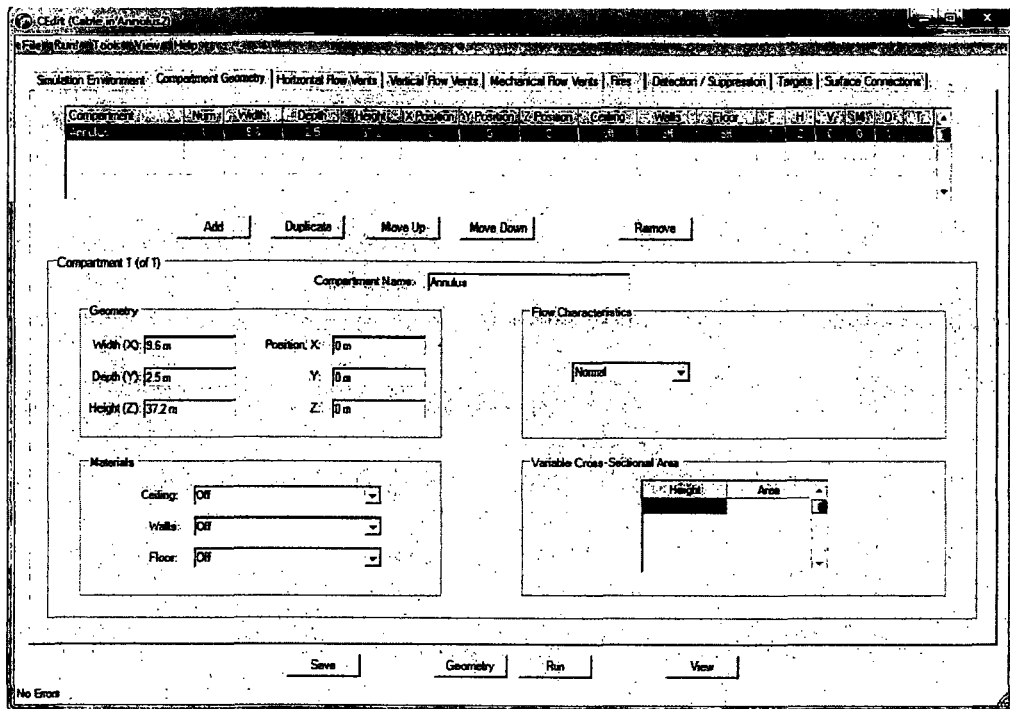
Cable Tray Fire in Annulus

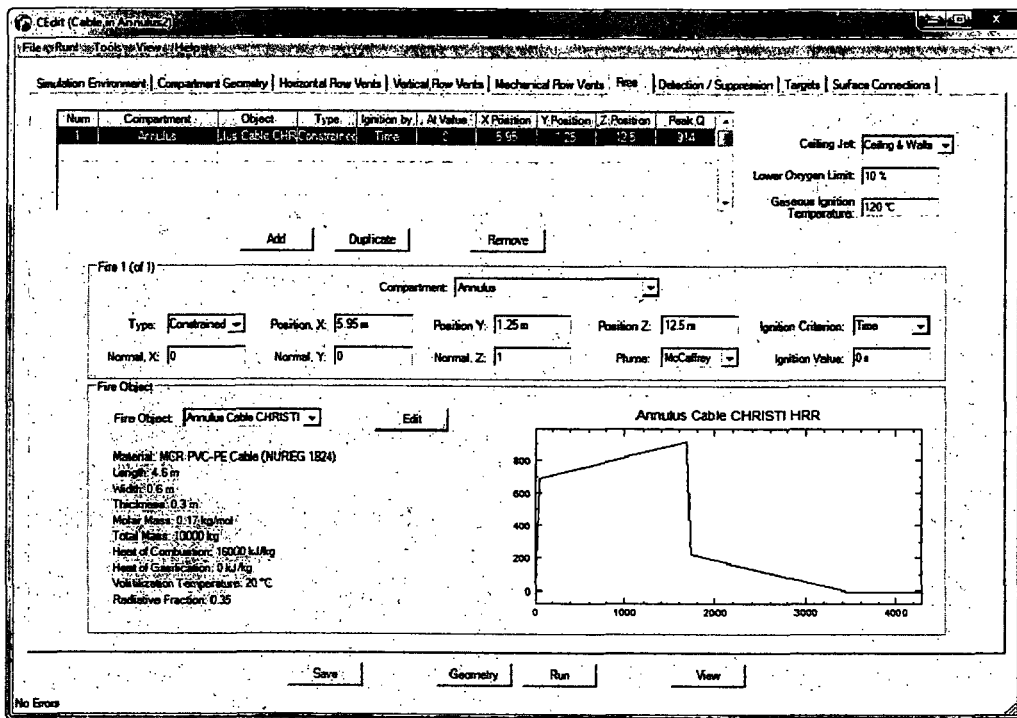**Figure H-5. Screenshot showing CFAST Geometry Input Screen.**

Figure H-6. Screenshot showing CFAST Fire Input Screen.

H.4.3 CFD Model (FDS)

Geometry: Only the section of the annulus encompassing the cables and relevant targets is included in the computational domain. This volume is 9.6 m (31.5 ft) wide, 2.5 m (8.2 ft) deep, and 12.8 m (42 ft) high. Extra depth is needed to accommodate the slight curvature of the bounding walls. The top, bottom, and sides of the computational domain are specified as "open," that is, open to an infinitely large volume. Since the volume of the annulus is very large, neither smoke build-up nor pressure effects would influence the region near the cables. Both the internal and external walls of the annulus are included in the model. Since FDS only allows rectilinear obstructions, a series of obstructions 20 cm (7.9 in) thick approximate the curved walls. The numerical grid conforms to this "stair-stepped" geometry.

Fire: The fire ignites near the base of the vertical portion of the cable train near the shielding, or inner wall. The spread rates of 25 mm/s in the vertical direction and 0.9 mm/s in the horizontal are input by using a feature of FDS whereby a surface is designated as having a fire spread over it at a designated rate. In this case, a surface is specified along the side of the vertical tray and along the top of the horizontal tray with the respective spread rates. The HRR per fire unit area is specified directly and not predicted by the model. As was previously discussed, the combustible load and duration of the fire are calculated based on the tray dimensions, number of cables per tray, cable mass per unit length, estimated combustible mass, heat of combustion for PE/PVC, and HRR per unit area. The combustible "load" is calculated as 420,800 kJ/m^2, and the duration of the fire at any particular location along the tray is 1,683 s. FDS accepts as input the combustible load as a "surface density" and computes the burn-out of fuel automatically. A Smokeview rendering of the FDS simulation is shown in Figure H-7.

Cables: One of the objectives of the calculation is to estimate the potential damage to the cables within the redundant train. FDS is limited to only 1-D heat transfer into either a rectangular or cylindrical obstruction. In this simulation, the cables are modeled as 1.5-cm cylinders. Following the Thermally-Induced Electrical Failure (THIEF) methodology in NUREG/CR-6931, Vol. 3, electrical functionality is lost when the temperature just inside the 1.5-mm (0.06 in) jacket reaches 200 °C (392 °F). Since the objective of this calculation is to estimate time to failure of the redundant cables, ignition and spread of the fire over the second set of cables is not considered. The in-depth heat penetration calculation is focused on a single cable that is relatively free of its neighbors and that would heat up more rapidly than those buried deeper within the pile.

Smoke Detection: FDS has a smoke detection algorithm that predicts the smoke obscuration within the detection chamber based on the smoke concentration and air velocity in the grid cell within which the detector is located. The detector itself is not modeled, as it is merely a point within the computational domain. The two parameters needed for the model are the obscuration at alarm, which is given by the manufacturer, and an empirically determined length scale from which a smoke entry time lag is estimated from the outside air velocity. The *SFPE Handbook* provides a nominal value of 1.8 m (5.9 ft) for this length scale. The obscuration at alarm is 4.9%/m.

Sprinkler Activation: FDS uses the conventional Response Time Index (RTI) concept to predict sprinkler activation. In this scenario, a steel plate has also been added just above the location of the sprinkler to simulate the effect of the actual deflector. Note that the sprinkler itself is just a point in the model, and its activation is determined by the time history of the temperature and velocity of hot gases within the numerical grid cell in which the sprinkler exists.
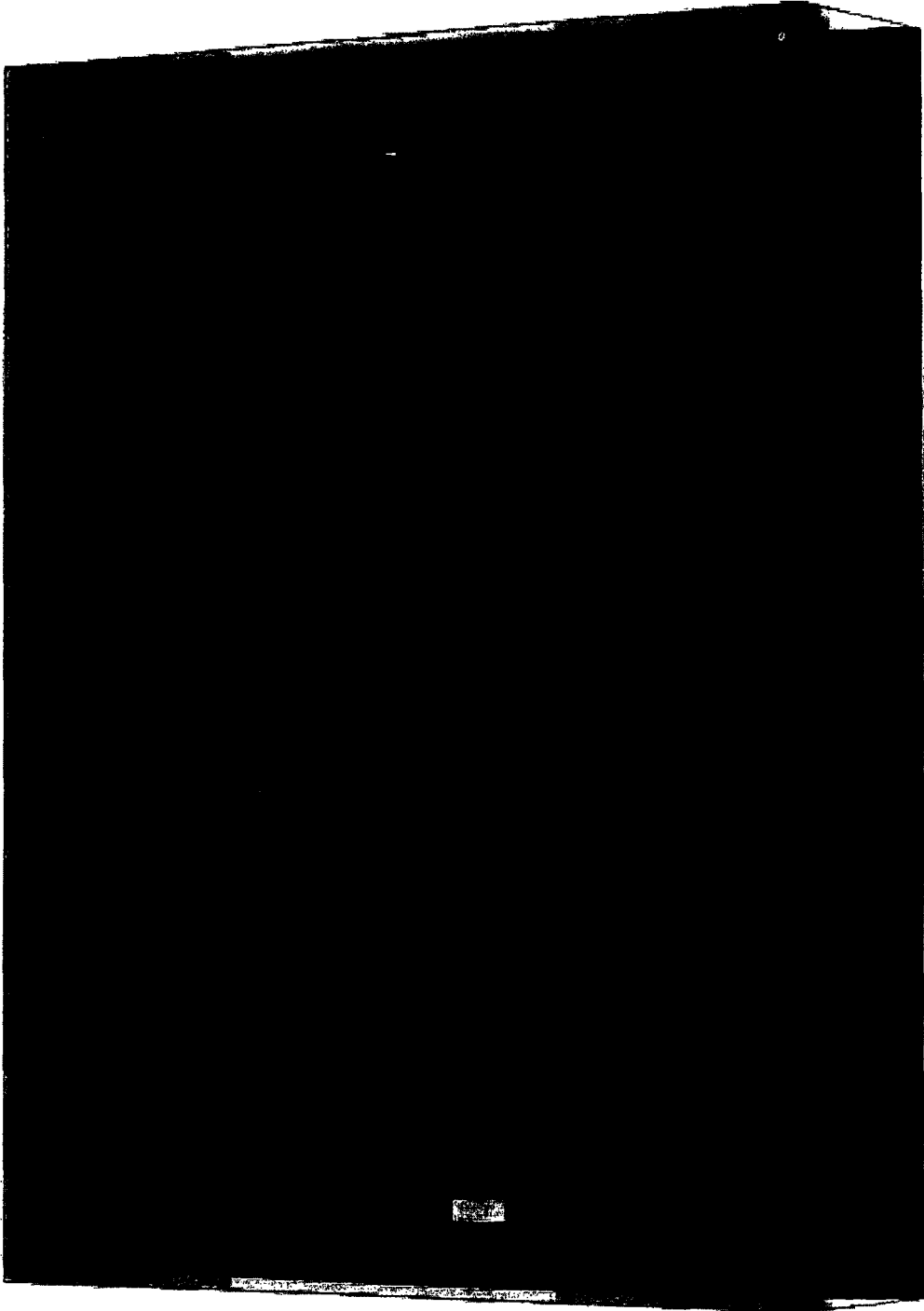
Figure H-7. FDS/Smokeview rendering of the Annulus scenario showing burning cable tray.

H.5 Evaluation of Results

The purpose of the calculations described above is to estimate the potential for damaging the redundant cables in tray B during a fire in tray A. The heat release rate profiles developed for a fire in the tray A cables are shown in Figure H-8. As previously discussed, a steady peak heat release rate is used for the FDT[s] calculations while CFAST and FDS use the same heat release rate profile.

Heat Flux and Temperature
The results of the simulations are shown in Table H-9. The heat flux calculations from the FDTs were used as a scoping analysis to determine if additional analysis was required. Using the peak heat release rate as a constant input, the solid flame model provides a worst case result for the heat flux of 7.1 kW/m^2. This value suggests a potential for damage to the redundant train of cables. A growing fire based on the estimated spread of the fire on the cables was used as input to the CFAST and FDS models. Although FDS does have an algorithm to predict flame spread, it was decided to use the specified burning and spread rates as given above. As a result, the HRR increases fairly rapidly to approximately 700 kW following ignition and the spread of the fire upwards, and it continues to increase, but not as rapidly, as the fire spreads horizontally. The peak HRR is about 945 kW.
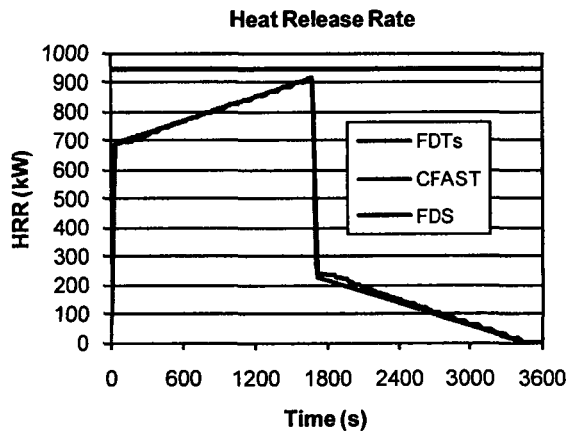
Heat Release Rate

Figure H-8 Heat Release Rates Used by the FDTs, CFAST and FDS for the Cable Tray Fire Scenario.

The heat flux from the burning cable to the redundant cable tray is predicted by CFAST to peak just above 2 kW/m^2 and for FDS just below 1.75 kW/m^2. This makes sense because the point source method of radiation heat transfer employed by CFAST would tend to over-estimate the heat flux when the target is relatively close to the fire, as in this example. The predicted interior cable temperatures predicted by both models are very similar. The temperature rises to approximately 95 °C (203 °F) in the CFAST simulation and 87 °C (189 °F) in the FDS simulation, well below the damage temperature.

H.5.1 Fire Protection Systems

FDS does not predict sprinkler activation in this scenario because the link temperature is only predicted to increase to approximately 80 °C (176 °F), less than the activation temperature of 100 °C (212 °F). FDS predicts smoke detection at about 570 s. It should be noted, however, that both the sprinkler and smoke detector are located just outside the fire plume. It is expected that for a real fire of this type, the natural air movements within such a large space as the containment annulus would almost certainly bend the plume from the vertical in a way that would be difficult to replicate with a model that is not accounting for the air movements throughout the entire facility.
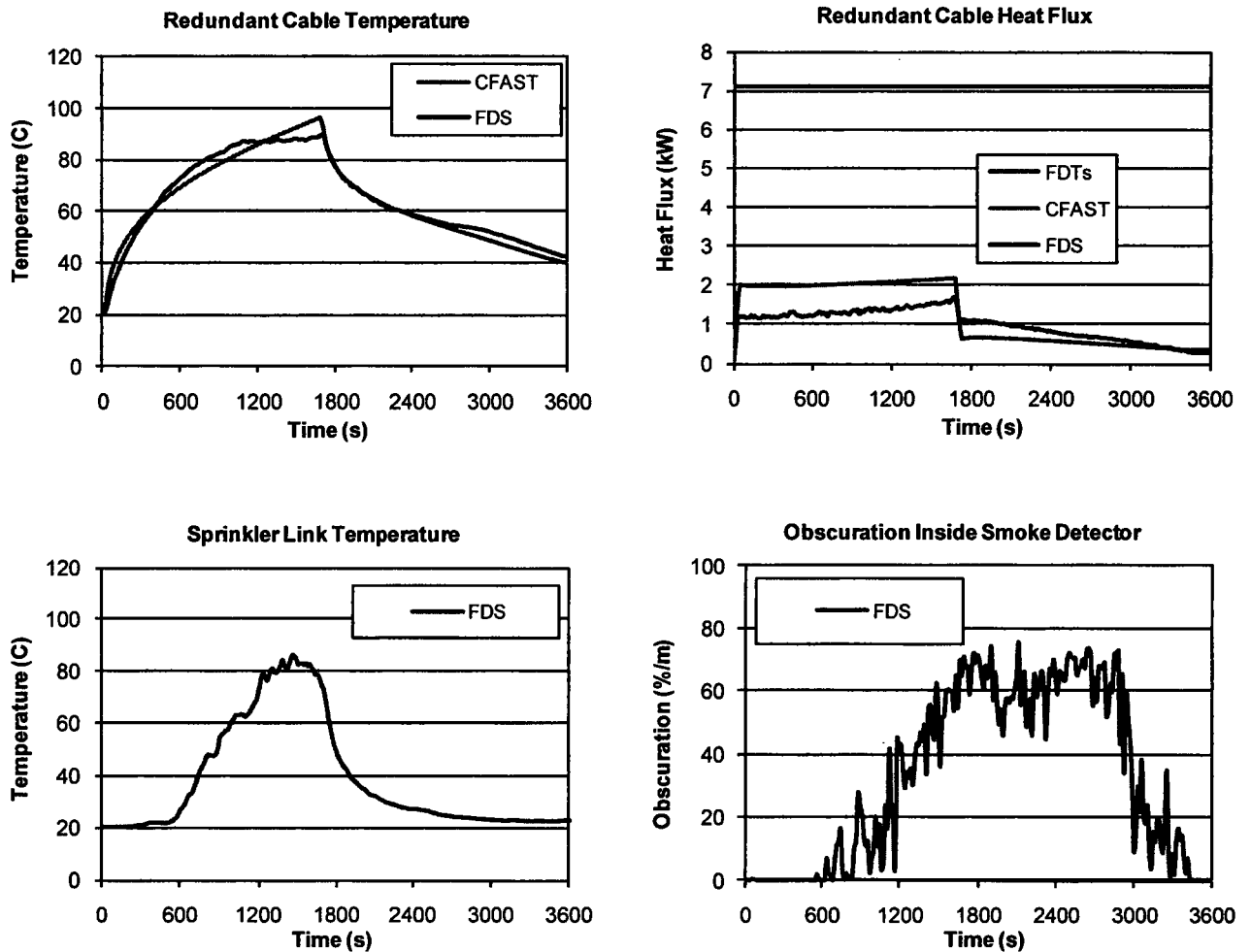
Redundant Cable Temperature

Redundant Cable Heat Flux

Sprinkler Link Temperature

Obscuration Inside Smoke Detector

Figure H-9. Summary of simulation results for the Annulus.

H.5.2 Uncertainty

For the annulus scenario, the objective is to predict the potential for damage to the redundant cables if a fire occurs in the adjacent cable tray. The predicted quantities of interest are the heat flux and temperature near the redundant cables. To better quantify whether or not the a critical value is exceeded, the uncertainty of the model predictions needs to be calculated

Chapter 4, Model Uncertainty, provides guidance on how to express the uncertainty of the model predictions. For example, consider tray B, where CFAST predicts a peak heat flux of approximately 2 kW/m². This value is less than the damage criterion of 11 kW/m², but in the NRC/EPRI V&V study (NUREG-1824 (EPRI 1011999)), it was found that CFAST predictions of total heat flux are, on average, 19 % less than corresponding measurements, and the relative standard deviation of its predictions about this average value is 47 %. This suggests that the true value of the heat flux to the cable in this scenario is normally distributed with a mean of 2/0.81=2.5 kW/m² and a standard deviation of 0.47×2.5=1.2 kW/m². Therefore, the probability that the actual heat flux to the cable would exceed 6 kW/m² is:

$$P(\dot{q}'' > 11) = \frac{1}{2} \, \mathrm{erfc}\left(\frac{6 - 2.5}{1.2\sqrt{2}}\right) \cong 0.001 \qquad \text{(H-1)}$$

In other words, there is a 0.1 % chance of exceeding the heat flux damage criterion for cable tray B, according to the CFAST prediction. Table D-2 lists the model uncertainty of the temperature and heat flux predictions for CFAST and FDS.

The uncertainty analysis can also be applied to the estimate of sprinkler activation. In the NRC/EPRI V&V study (NUREG-1824 (EPRI 1011999)), it was found that FDS predictions of target temperatures[17] are, on average, 2 % higher than the corresponding measurements, and that the relative standard deviation of its predictions about this average value is 13 %. This suggests that the true value of the link temperature is normally distributed with a mean of 79 °C and a standard deviation of 10 °C. Therefore, the probability that the link temperature would exceed 100 °C (212 °F) is:

$$P(T > 100) = \frac{1}{2} \, \mathrm{erfc}\left(\frac{100 - 79}{10\sqrt{2}}\right) \cong 0.02 \qquad \text{(H-2)}$$

H.5.3 Sensitivity

Referring again to Table D-2, it is unlikely the cables in tray B would be damaged by a fire in tray A. In addition to examining the accuracy of the models, as is done in the previous section, it is also possible to consider the key input parameter and estimate the increased HRR necessary to damage the cables in tray B. Table 4-3 indicates that the heat flux is proportional to the HRR to the 4/3 power. Following the methodology in Section 4.4.1, in order to increase the predicted heat flux by 4 kW/m² to reach 6 kW/m², the peak HRR, $\dot{Q}$, must increase by approximately:

---

[17] A sprinkler link is essentially a "target" with a thermal inertia characterized by the RTI (Response Time Index).

Cable Tray Fire in Annulus

$$\Delta \dot{Q} \approx \frac{3}{4}\dot{Q}\frac{\Delta \dot{q}''}{\dot{q}''} = \frac{3}{4}945\frac{4}{2} \approx 1417\ \text{kW} \tag{H-3}$$

In other words, the peak HRR of the fire would have to be approximately 945+1415=1339 kW to cause the cables in tray B to fail.

Table H-2. Uncertainty analysis of the model predictions for the Annulus scenario.

Model	Quantity	Target	Predicted Value	Critical Value	Probability of Exceeding
CFAST	Heat Flux	Cable B	2 kW/m^2	6 kW/m^2	0.001
FDS	Heat Flux	Cable B	1.75 kW/m^2	6 kW/m^2	0.000
CFAST	Temperature	Cable B	95 °C	200 °C	0.000
FDS	Temperature	Cable B	95 °C	200 °C	0.000

H.6 Conclusion

Using the solid flame model from the FDT^s indicates that a fire in one of the cables trays could damage the cable in the adjacent tray; however, an additional analysis using CFAST and FDS indicates that cable damage is unlikely. While it is not expected that a fire in one cable tray within the annulus region of the containment building would damage cables in the adjacent train, the models cannot conclusively predict whether a sprinkler would activate above the fire, or at what time a smoke detector might activate. These predictions are extremely sensitive to the exact locations of the devices relative to a fire plume that may be subject to unpredictable air movements throughout the entire facility. Alternative protection strategies, such as shielding between trays or other thermal barriers, should be considered to ensure the protection of the redundant cables.

H.7 References

1. NUREG/CR-6850 (EPRI 1011989), *Fire PRA Methodology for Nuclear Power Facilities.*
2. NUREG-1805, *Fire Dynamics Tools.*
3. NUREG-1824 (EPRI 1011999), *Verification and Validation of Selected Fire Models for Nuclear Power Plant Applications*, 2007.
4. SFPE Handbook, 4th edition, 2008.
5. NUREG/CR-6931, *Cable Response to Live Fire (CAROLFIRE), Volume 2: Cable Fire Response Data for Fire Model Improvement.*
6. NUREG/CR-6931, *Cable Response to Live Fire (CAROLFIRE), Volume 3: Thermally-Induced Electrical Failure (THIEF) Model.*
7. NFPA 70 (NEC 2008), *National Electric Code.*
8. UL 217,. Underwriters Laboratories, Inc., Single Station Fire Alarm Device.
9. NIST SP 1018-5,. *Fire Dynamics Simulator (Version 5), Technical Reference Guide, Vol. 3, Experimental Validation.*
10. NUREG/CR-7010, *Cable Heat Release, Ignition, and Spread In Tray Installations during Fire (CHRISTIFIRE), Volume 1: Horizontal Trays.*
11. Schiffiliti, R. and W. Pucci, *Fire Modeling, State of the Art*, Fire Detection Institute, 1996.

12. NIST NCSTAR 1-5B, *Experiments and Modeling of Structural Steel Elements Exposed to Fire.*

H.8 Attachments

1. FDS input file: Annulus.fds

2. CFAST input file:

   a. Cable in Annulus.in
   b. Annulus cable.o
   c. Thermal.csv

3. FDTs Spreadsheets:

   a. 05.1_Heat_Flux_Calculations_Wind_Free.xls (Point Source)
   b. 05.1_Heat_Flux_Calculations_Wind_Free.xls (Solid Flame 1)

NRC FORM 335 (12-2010) NRCMD 3.7	U.S. NUCLEAR REGULATORY COMMISSION	1. REPORT NUMBER (Assigned by NRC, Add Vol., Supp., Rev., and Addendum Numbers, if any.)
	BIBLIOGRAPHIC DATA SHEET *(See instructions on the reverse)*	**NUREG-1934**

2. TITLE AND SUBTITLE	3. DATE REPORT PUBLISHED	
Nuclear Power Plant Fire Modeling Application Guide (NPP FIRE MAG) Second Draft Report for Comment	MONTH	YEAR
	July	2011
	4. FIN OR GRANT NUMBER	

5. AUTHOR(S)	6. TYPE OF REPORT
D. Stroup (NRC), F. Joglar (SAIC), D. Birk (SAIC), K. McGrattan (NIST), R. Peacock (NIST), R. Wachowiak (EPRI), S. Hunt (Hughes Associates, Inc.), C. Worrell (Westinghouse), J. Milke (Univeristy of Maryland), K. Zee (ERIN)	Draft
	7. PERIOD COVERED *(Inclusive Dates)*

8. PERFORMING ORGANIZATION - NAME AND ADDRESS *(If NRC, provide Division, Office or Region, U.S. Nuclear Regulatory Commission, and mailing address; if contractor, provide name and mailing address.)*

Division of Risk Analysis
Office of Nuclear Regulatory Research
U.S. Nuclear Regulatory Commission
Washington, DC 20555-0001

9. SPONSORING ORGANIZATION - NAME AND ADDRESS *(If NRC, type "Same as above"; if contractor, provide NRC Division, Office or Region, U.S. Nuclear Regulatory Commission, and mailing address.)*

Same as above

10. SUPPLEMENTARY NOTES
   M. Salley, NRC Project Manager

11. ABSTRACT *(200 words or less)*

There is a movement to introduce risk-informed and performance-based (RI/PB) analyses into fire protection engineering practice, both domestically and worldwide. This movement exists in both the general fire protection and the nuclear power plant (NPP) fire protection communities. The U.S. Nuclear Regulatory Commission (NRC) has used risk-informed insights as a part of its regulatory decision making since the 1990s. In 2001, the National Fire Protection Association (NFPA) issued NFPA 805, *Performance-Based Standard for Fire Protection for Light-Water Reactor Electric Generating Plants, 2001 Edition.* In July 2004, the NRC amended its fire protection requirements in Title 10, section 50.48 of the *Code of Federal Regulations* (10 CFR 50.48) to permit existing reactor licensees to voluntarily adopt fire protection requirements contained in NFPA 805 as an alternative to the existing deterministic fire protection requirements. In addition, the NPP fire protection community has been using RI/PB approaches and insights to support fire protection decision making in general. One key element in RI/PB fire protection is the availability of verified and validated (V&V) fire models that can reliably estimate the effects of fires. The U.S. NRC, together with the Electric Power Research Institute (EPRI) and the National Institute of Standards and Technology (NIST), conducted a research project to verify and validate five fire models that have been used for NPP applications. The results of this effort are documented in a seven-volume NUREG report, NUREG-1824 (EPRI 1011999), *Verification and Validation of Selected Fire Models for Nuclear Power Plant Applications.* This report describes the implications of the V&V results for fire model users and reviewers. The features and limitations of the five fire models documented in NUREG-1824 are discussed relative to NPP fire hazard. Finally, the report provides information on the use of fire models in support of NFPA 805, NRC fire protection inspection oversight programs, and other commercial NPP applications.

12. KEY WORDS/DESCRIPTORS *(List words or phrases that will assist researchers in locating the report.)*	13. AVAILABILITY STATEMENT
fire, performance-based, risk-informed regulation, fire hazard analysis (FHA), fire safety, fire protection, nuclear power plant, probabilistic risk assessment (PRA), fire modeling	Unlimited
	14. SECURITY CLASSIFICATION
	(This Page) Unclassified
	(This Report) Unclassified
	15. NUMBER OF PAGES
	16. PRICE

NRC FORM 335 (12-2010)